

The Eurasia Proceedings of Science, Technology, Engineering & Mathematics

EPSTEM

VOLUME 15 ICBAST CONFERENCE

ISSN: 2602-3199

ISBN: 978-605-74825-8-7

**ICBAST 2021: International Conference on Basic Sciences and Technology
(ICBAST)**

November 04 - 07, 2021

Antalya, Turkey

Edited by: Mehmet Ozaslan (Chair), Gaziantep University, Turkey

ICBAST 2021 DECEMBER

Volume 15, Pages 1-98 (December 2021)

The Eurasia Proceedings of Science, Technology, Engineering & Mathematics
(EPSTEM)

e-ISSN: 2602-3199

©2021 Published by the ISRES Publishing

Address: Istanbul C. Cengaver S. No 2 Karatay/Konya/TURKEY

Website: www.isres.org

Contact: isrespublishing@gmail.com

Conference: ICBAST2021: International Conference on Basic Sciences and Technology
(ICBAST)

Conference website: <https://www.2021.icbast.net>

Dates: November 04 – 07, 2021

Location: Antalya, Turkey

Edited by: Mehmet Ozaslan

About Editor(s)

Prof Dr. Mehmet Ozaslan

Department of Biology, Gaziantep University, Turkey

Website: <http://mehmetozaslan.com/>

Email: ozaslanmd@gantep.edu.tr

Language Editor(s)

Assoc. Prof. Dr. Kagan Buyukkarci

Department of English Language Education, Suleyman Demirel University, Turkey

Email: kaganbuyukkarci@sdu.edu.tr

CONFERENCE PRESIDENT

Prof. Dr. Mehmet Özasan - Gaziantep University, Turkey

SCIENTIFIC BOARD

Bahar Tercan - Institute for Systems Biology, USA

Besnik Hajdari - University "isa Boletini" Mitrovica, Kosovo

Bogdan PATRUT - Alexandru Ioan Cuza Üniversitesi, Romania

Chalavadi SULOCHANA - Gulbarga University, India

Dehini RACHID -University of Bechar, Algeria

Ebba Ossiannilsson - Swedish Association for Distance Education, Swedish

Eleonora Guseinoviene - Klaipeda University, Lithuania

Elena KRELJA KURELOVIĆ - Polytechnic of Rijeka, Croatia

Eva TRNOVA - Masaryk University, Czech Republic

Farhad BALASH - Kharazmi University, Iran

Gabriel DELGADO-TORAL - Universidad Nacional Autónoma de México, Mexico
Gordana SAVIC - University of Belgrade, Serbia
Isti HIDAYAH - Semarang State University, Indonesia
Jose Manuel Lopez Guede - University of Basque Country, Spain
Marija STANIĆ - University of Kragujevac, Serbia
M. Hanefi CALP - Karadeniz Technical University, Turkey
Mohamed Ahmed - Mansoura University, Egypt
Nicu BIZON - Pitesti University, Romania
Pandian VASANT - Teknology Petronas University, Romania
Rajnalkar LAXMAN - Gulbarga University, India
Sanaa AL-DELAIMY - Mosul University, Iraq
Servet YATİN - Quincy College, United States
Shynar BAIMAGANBETOVA - Nazarbayev University, Kazakhstan
Tunde Anifowose-Kelani, Siegener Sabithos College of Health Science & Technology, Nigeria
Yiyang Chen - Soochow University (CN), China
Zipporah Pawat DUGURYIL - Federal College of Education, Nigeria

ORGANIZING COMMITTEE

Besnik Hajdari - University "isa Boletini" Mitrovica, Kosovo
Cemil Aydogdu - Hacettepe University
Danielle Gonçalves de Oliveira Prado-Federal Technological University of Paraná, Brazil
Halil SNOPE - South East European University, Macedonia
Jaya Bishnu Pradhan-Tribhuvan University, Mahendra Ratna Campus, Nepal
Mohammad Sarwar - Scialert, Dubai, United Arab Emirates
Murat Beytur - Kafkas University
M. Hanefi CALP - Karadeniz Technical University, Turkey
Resul BUTUNER - Adil Karaağac Vocational and Technical Anatolian High School, Turkey
Shaymaa Fadhel Abbas Albaayit - Baghdad University, Iraq
Tunde Anifowose-Kelani, Siegener Sabithos College of Health Science & Technology, Nigeria

Editorial Policies

ISRES Publishing follows the steps below in the proceedings book publishing process.

In the first stage, the papers sent to the conferences organized by ISRES are subject to editorial oversight. In the second stage, the papers that pass the first step are reviewed by at least two international field experts in the conference committee in terms of suitability for the content and subject area. In the third stage, it is reviewed by at least one member of the organizing committee for the suitability of references. In the fourth step, the language editor reviews the language for clarity.

Review Process

Abstracts and full-text reports uploaded to the conference system undergo a review procedure. Authors will be notified of the application results in three weeks. Submitted abstracts will be evaluated on the basis of abstracts/proposals. The conference system allows you to submit the full text if your abstract is accepted. Please upload the abstract of your article to the conference system and wait for the results of the evaluation. If your abstract is accepted, you can upload your full text. Your full text will then be sent to at least two reviewers for review. **The conference has a double-blind peer-review process.** Any paper submitted for the conference is reviewed by at least two

international reviewers with expertise in the relevant subject area. Based on the reviewers' comments, papers are accepted, rejected or accepted with revision. If the comments are not addressed well in the improved paper, then the paper is sent back to the authors to make further revisions. The accepted papers are formatted by the conference for publication in the proceedings.

Aims & Scope

Technology and basic sciences are closely related fields. Developments and innovations in one of them affect the other. Therefore, **the focus of the conference** is on studies related to these two fields. Studies in the fields of technology and basic science are accepted to the conference even if they are not associated with other field. The conference committee thinks that a study in only one field (for example, mathematics, physics, etc.) will contribute to other field (such as technology) in future studies, even if it is not associated with the presentation at the conference. In line with this perspective, studies in the following fields are accepted to the conference: Biology, Chemistry, Physics, Mathematics and Technology.

The aim of the conference is to bring together researchers and administrators from different countries, and to discuss theoretical and practical issues in all fields of technology and basic sciences.

Articles: 1-11

CONTENTS

Investigation of Theoretical and Experimental Properties of 2-[3-(n-Propyl)-4,5-dihydro-1H-1,2,4-triazol-5-one-4-yl]-Phenoxyacetic Acide / Pages: 1-9

Murat BEYTUR, Haydar YUKSEK

Quantum Chemical Calculations of 2-Methoxy-4-[(3-p-Methylbenzyl-4,5-Dihydro-1H-1,2,4-Triazol-5-One-4-YL)Azomethine] Phenyl-2-Methylbenzoate Molecule / Pages: 10-20

Gul KOTAN, Haydar YUKSEK

Synthesis of Novel ABA-Type Amphiphilic Copolymers Including 2-Hydroxypropyl Propionate and N-Isobutoxymethyl B-Alanine by Peg-Dialkoxide Initiated Hydrogen-Transfer Polymerization /

Pages: 21-27

Efkan CATIKER, Temel OZTURK, Bedrettin SAVAS, Mehmet ATAKAY, Bekir SALIH

Investigation of Conformation, Vibration and Electronic Properties of 2- Methoxythiophene Molecule by Theoretical Methods/ Pages: 28-34

Guventurk UGURLU

Theoretical and Experimental Properties of 3-Ethyl-4-(3-Acetoxy-4-Methoxy-Benzylidenamino)-4,5-Dihydro-1H-1,2,4-Triazol-5-One / Pages: 35-41

Songul ULUFER BULUT, Murat BEYTUR, Haydar YUKSEK

Theoretical (6-311G(d,p)/ 3-21G) and Spectroscopic (13C/ 1H-NMR, FT-IR) Analyses of 3-Propyl-4-[3-(2-Methylbenzoyl)-Benzylidenamino]-4,5-Dihydro-1h-1,2,4-Triazol-5-One Molecule / Pages: 42-53

Songul ULUFER-BULUT, Gul KOTAN, Haydar YUKSEK

In Silico Calculations of 2-Methoxy-6-[(3-methyl-5-oxo-4,5-dihydro-1H-1,2,4-triazol-4-yl)-iminomethyl] Phenyl Benzoate / Pages: 54-62

Murat BEYTUR, Haydar YUKSEK

Density Functional Theory Studies of Structural Nonlinear Optic and Electronic Properties of Chalcone (E)-3-(Furan-2-yl)-1-Phenylprop-2-en-1-one Molecule / Pages: 63-68

Guventurk UGURLU

Experimental (FT-IR, ¹³C/¹H-NMR) and DFT (B3LYP, B3PW91) Studies of 3-n-Propyl-4-[2-(4-Methoxybenzoxy)-3-Methoxy] Benzylidenamino-4,5-Dihydro-1h-1,2,4-Triazol-5-Ones Molecule / Pages: 69-78

Gul KOTAN, Muzaffer ALKAN, Haydar YUKSEK

The Investigation of Spectroscopic and Electronic Properties of 3-Ethyl-4-(4-cinnamoyloxybenzylidenamino)-4,5-dihydro-1H-1,2,4-triazol-5-one Compound Using Density Functional Theory and Hartree-Fock Basis Sets / Pages: 79-87

Murat BEYTUR, Haydar YUKSEK

Review on Microbial Enhanced Oil Recovery and Controlling Its Produced Hydrogen Sulfide Effects on Reservoir and Transporting Pipelines / Pages: 88-98

Ali HARATIAN, Soroosh EMAMI MEYBODI

The Eurasia Proceedings of Science, Technology, Engineering & Mathematics (EPSTEM), 2021

Volume 15, Pages 1-9

ICBAST 2021: International Conference on Basic Science and Technology

Investigation of Theoretical and Experimental Properties of 2-[3-(*n*-Propyl)-4,5-dihydro-1*H*-1,2,4-triazol-5-one-4-yl]-Phenoxyacetic Acide

Murat BEYTUR
Kafkas University

Haydar YUKSEK
Kafkas University

Abstract: In the present study, 2-[3-(*n*-propyl)-4,5-dihydro-1*H*-1,2,4-triazol-5-one-4-yl]-phenoxyacetic acide was optimized by using B3LYP/6-311+G(d,p) basis set. Firstly, IR data of the compound were calculated in gas phase by using of 6-311+G(d,p) basis set of B3LYP method and are multiplied with appropriate adjustment factors. Theoretical infrared spectrums are formed from the data obtained according to B3LYP method. In the identification of calculated IR data was used the veda4f program. Then, ¹H-NMR and ¹³C-NMR spectral data values were calculated according to the method of GIAO using the program package Gaussian G09W Software. Experimental data were obtained from the literature. Experimental and theoretical values were inserted into the graphic according to equation of $\delta_{exp}=a+b \cdot \delta_{calc}$. The standard error values were found via SigmaPlot program with regression coefficient of a and b constants. Furthermore, molecular structure, HOMO and LUMO energy analysis, electronic transitions, total static dipol moment (μ), the mean polarizability ($\langle\alpha\rangle$), the anisotropy of the polarizability ($\Delta\alpha$), the mean first-order hyperpolarizability ($\langle\beta\rangle$), electronegativity (χ), hardness (η), molecular electrostatic potential maps (MEP), and Mulliken charges of 2-[3-(*n*-propyl)-4,5-dihydro-1*H*-1,2,4-triazol-5-one-4-yl]-phenoxyacetic acide have been investigated by using B3LYP level with the 6-311+G(d,p) basis set.

Keywords: Phenoxyacetic acide, Hyperpolarizability, Theoretical.

Introduction

The development of new heterocyclic organic compounds has received considerable attention due to their potential fluorescence applications as chemosensors (Qin et al., 2015), ionic or biological probes (Mecca et al., 2016; Beytur, 2020) and lighting Technologies (Kido et al., 1995; Sun et al., 2006; Yang et al., 2015; Zhao et al., 2017). The biological activities of the Schiff bases in medicinal chemistry are attributed to the presence of groups in literature (Sztanke et al., 2013; Alkan et al., 2007; Gürsoy-Kol et al., 2010; Aktaş-Yokuş et al., 2017; Bahçeci et al., 2016; Bahçeci et al., 2017; Boy et al., 2021; Koç et al., 2019). Otherwise, Schiff bases have been used as insecticides, bacteriocides, fungicides, pesticides (Azam et al., 2007). In the last year, computational properties of Schiff bases were examined on a computer (Turhan-Irak et al., 2018; Beytur et al., 2019; Turhan-Irak et al., 2019; Uğurlu et al., 2020; Beytur et al., 2021). The optimized molecular structure, vibrational frequencies, spectroscopic parameters, atomic charges and frontier molecule orbitals (HOMO and LUMO) of the 2-[3-(*n*-propyl)-4,5-dihydro-1*H*-1,2,4-triazol-5-one-4-yl]-phenoxyacetic acide have been calculated by using DFT/B3LYP method with 6-311+G(d,p) basis set. All quantum chemical calculations were carried out by using Gaussian 09W (Frisch et al., 2009; Wolinski et al., 1990) program package and the GaussView molecular visualization program (Frisch et al., 2003). The molecular structure and vibrational calculations of the molecule were computed by using Becke-3-Lee Yang Parr (B3LYP) (Becke, 1993; Lee et al., 1988) density functional method with 6-311+G(d,p) basis set in ground state. IR absorption frequencies of analyzed molecule were

- This is an Open Access article distributed under the terms of the Creative Commons Attribution-Noncommercial 4.0 Unported License, permitting all non-commercial use, distribution, and reproduction in any medium, provided the original work is properly cited.

- Selection and peer-review under responsibility of the Organizing Committee of the Conference

calculated by two methods. Then, they were compared with experimental data (Çiftçi et al., 2018), which are shown to be accurate. Infrared spectrum was composed by using the data obtained from both methods. The assignments of fundamental vibrational modes of the title molecule were performed on the basis of total energy distribution (TED) analysis by using VEDA 4f program (Jamróz, 2004). Furthermore, molecular structure, HOMO and LUMO energy analysis, electronic transitions, total static dipole moment (μ), the mean polarizability ($\langle\alpha\rangle$), the anisotropy of the polarizability ($\Delta\alpha$), the mean first-order hyperpolarizability ($\langle\beta\rangle$), electronegativity (χ), hardness (η), molecular electrostatic potential maps (MEP), and Mulliken charges of 2-[3-(*n*-propyl)-4,5-dihydro-1*H*-1,2,4-triazol-5-one-4-yl]-phenoxyacetic acid have been investigated by using B3LYP level with the 6-311+G(d,p) basis set. The titled molecule optimized using *ab initio* Density Functional Theory (DFT/B3LYP), (Becke-3-Lee-Yang-Parr (B3LYP) hybrid density functional), and Hartree-Fock (HF) (Figure 1).

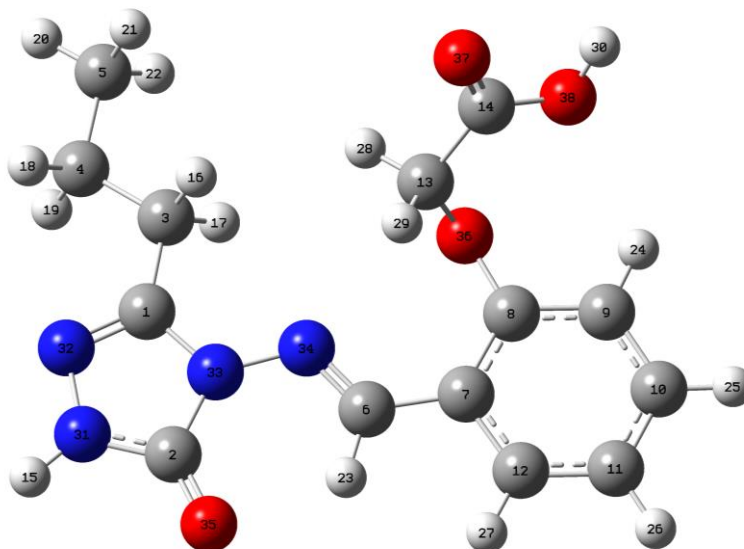


Figure 1. The optimized molecular structure of titled molecule with DFT/HF 6-311+G(d,p) level.

Method

The molecular structure of the title compound in the ground state is computed by performing both the density functional theory (DFT) and Hartree-Fock (HF) (Becke, 1993; Lee, 1998) at 6-311+G(d,p) level. Density functional for all studies reported in this paper have been in the following form

$$E_{XC} = (1 - a_0)E_X^{LSDA} + a_0E_X^{HF} + a_X\Delta E_X^{B88} + a_C E_C^{LYP} + (1 - a_C)E_C^{VWN}$$

where the energy terms are the Slater exchange, the Hartree-Fock exchange, Becke's exchange functional correction, the gradient corrected correlation functional of Lee, Yang and Parr, and the local correlation functional of Vosko, Wilk and Nusair (Vosko et al., 1980). The theoretical geometric structure of the title compound is given in Figure 1. Molecular geometry is restricted and the optimized geometrical parameters, of the title compound in this study are carried out by using Gaussian 09W program package (Frisch et al., 2009) and the visualization parts were done with GaussView program (Dennington et al., 2009) on personal computer employing 6-311+G(d,p) basis set. Additionally, harmonic vibrational frequencies for the title compound are calculated with these selected methods and then scaled by 0.9516 (Avcı et. al, 2008) and these results were compared with the experimental data (Çiftçi et al., 2018).

Results and Discussion

Vibrational Frequencies

The 2-[3-(*n*-propyl)-4,5-dihydro-1*H*-1,2,4-triazol-5-one-4-yl]-phenoxyacetic acid has 38 atoms and the number of the normal vibrations are 108. The observed and calculated vibrational frequencies, the calculated IR

intensities and assignments of selected vibrational frequencies for title compound are summarized in Table 1 and Figure 2. Experimentally (Çiftçi et al., 2018), the investigated titled compound, as expected the IR spectra data, The S-H stretching vibration at 3425 cm^{-1} , the N-H stretching vibration at 3269 cm^{-1} and two C=O peak at and 1710 cm^{-1} range was observed. In addition, C=N stretching vibration at 1652 and 1592 cm^{-1} and COO stretching vibrations at 1256 cm^{-1} are occurred.

Table 2. The calculated frequencies values of the molecule.

Selected Vibrational Types	Experimental	Scaled DFT
$\delta\text{ N}_{31}\text{N}_{32}\text{C}_1, \text{N}_{33}\text{N}_{34}\text{C}_6$ (23)	758	765
$\nu\text{ N}_{31}\text{C}_2, \text{N}_{33}\text{C}_4$ (15), $\text{N}_{31}\text{N}_{32}, \text{N}_{33}\text{N}_{34}$ (16)	758	770
$\text{O}_{38}\text{C}_{14}, \text{O}_{36}\text{C}_8$ (18)	809	799
$\delta\text{ N}_{31}\text{N}_{32}\text{C}_1, \text{N}_{33}\text{N}_{34}\text{C}_6$ (13)	957	946
$\tau\text{ C}_{14}\text{C}_{13}\text{O}_{36}\text{C}_8$ (17)	957	980
$\nu\text{ N}_{31}\text{N}_{32}, \text{N}_{33}\text{N}_{34}$ (24), $\nu\text{ N}_{31}\text{N}_{32}, \text{N}_{33}\text{N}_{34}$ (42), $\delta\text{ H}_{15}\text{N}_{31}\text{N}_{32}$ (10)	1067	1053
$\delta\text{ H}_{30}\text{O}_{38}\text{C}_{14}$ (14)	1114	1123
$\nu\text{ N}_{31}\text{C}_2, \text{N}_{33}\text{C}_4$ (19), $\text{N}_{31}\text{N}_{32}, \text{N}_{33}\text{N}_{34}$ (14)	1114	1139
$\nu\text{ O}_{38}\text{C}_{14}, \text{O}_{36}\text{C}_8$ (18)	1166	1178
$\nu\text{ N}_{31}\text{C}_2, \text{N}_{33}\text{C}_4$ (10)	1166	1180
$\nu\text{ N}_{31}\text{N}_{32}, \text{N}_{33}\text{N}_{34}$ (12)	1166	1221
$\nu\text{ N}_{31}\text{N}_{32}, \text{N}_{33}\text{N}_{34}$ (10)	1256	1234
$\delta\text{ H}_{30}\text{O}_{38}\text{C}_{14}$ (14)	1256	1304
$\delta\text{ H}_{15}\text{N}_{31}\text{N}_{32}$ (66)	1425	1330
$\nu\text{ N}_{32}\text{C}_1, \text{N}_{34}\text{C}_6$ (10)	1567	1557
$\nu\text{ N}_{32}\text{C}_1, \text{N}_{34}\text{C}_6$ (54)	1592	1565
$\nu\text{ N}_{32}\text{C}_1, \text{N}_{34}\text{C}_6$ (65)	1653	1578
$\nu\text{ O}_{35}\text{C}_2$ (73)	1710	1697
$\nu\text{ O}_{37}\text{C}_{14}$ (87)	1710	1721
$\nu\text{ C}_3\text{H}_{16}, \text{C}_{13}\text{H}_{17}, \text{C}_4\text{H}_{18}, \text{C}_4\text{H}_{19}, \text{C}_5\text{H}_{20}, \text{C}_5\text{H}_{21}, \text{C}_5\text{H}_{22}$ (71)	2870	2897
$\nu\text{ C}_9\text{H}_{24}, \text{C}_{10}\text{H}_{25}, \text{C}_{11}\text{H}_{26}, \text{C}_{12}\text{H}_{27}$ (10)	2920	2989
$\nu\text{ C}_9\text{H}_{24}, \text{C}_{10}\text{H}_{25}, \text{C}_{11}\text{H}_{26}, \text{C}_{12}\text{H}_{27}$ (100)	2965	2995
$\nu\text{ C}_9\text{H}_{24}, \text{C}_{10}\text{H}_{25}, \text{C}_{11}\text{H}_{26}, \text{C}_{12}\text{H}_{27}$ (84)	3012	3023
$\nu\text{ C}_9\text{H}_{24}, \text{C}_{10}\text{H}_{25}, \text{C}_{11}\text{H}_{26}, \text{C}_{12}\text{H}_{27}$ (98)	3025	3039
$\nu\text{ C}_9\text{H}_{24}, \text{C}_{10}\text{H}_{25}, \text{C}_{11}\text{H}_{26}, \text{C}_{12}\text{H}_{27}$ (94)	3042	3057
$\nu\text{ N}_{31}\text{H}_{15}$ (100)	3269	3498
$\nu\text{ O}_{38}\text{H}_{30}$ (100)	3425	3567

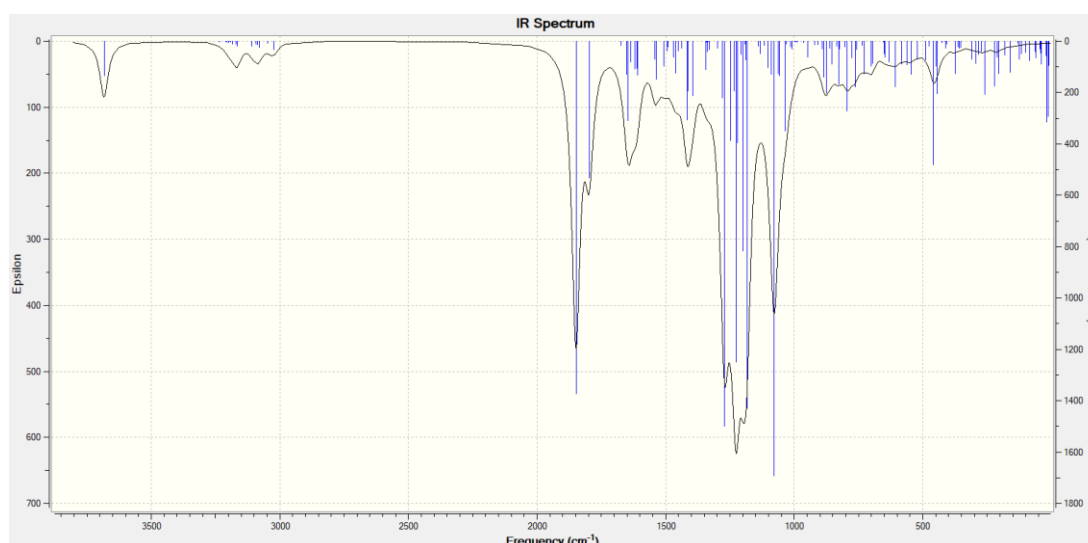


Figure 2. IR spectra simulated with DFT/B3LYP/6-311+G(d,p) level of the titled molecule

NMR Spectral Analysis

In nuclear magnetic resonance (NMR) spectroscopy, the isotropic chemical shift analysis allows us to identify relative ionic species and to calculate reliable magnetic properties which provide the accurate predictions of

molecular geometries (Rani et al., 2010; Subramanian et. al., 2010; Wade, 2006). In this framework, the optimized molecular geometry of the molecule was obtained by using B3LYP method with 6-311+G(d,p) basis level in DMSO solvent. By considering the optimized molecular geometry of the title compound the ^1H and ^{13}C NMR chemical shift values were calculated at the same level by using Gauge-Independent Atomic Orbital (GIAO) method. Theoretical and experimental (Çiftçi et al., 2016) values were plotted according to $\delta_{\text{exp}} = a \cdot \delta_{\text{calc.}} + b$, Eq. a and b constants regression coefficients with a standard error values were found using the SigmaPlot program.

The (R^2) values (DFT) for ^1H NMR (DMSO) and ^{13}C NMR (DMSO) chemical shifts in different solvents has been found as 0.9962/0.7837 for the titled compound (Table 2 and Figure 3). In our study, the ^1H -NMR spectrum of compound was observed belong to H15 proton peak at 11.85 ppm because acidic show feature (Yüksek, 1992). H23 proton was observed at 10.05 ppm. Therotically, in DMSO solvents these values for the mentioned proton atoms were found as 7.73 and 10.43 ppm, respectively (B3LYP).

Table 2. The calculated and experimental ^1H and ^{13}C NMR isotropic chemical shifts of the titled molecule.

No	Experim.	B3LYP/ DMSO	Diff. /DMSO	No	Experim.	B3LYP/ DMSO	Diff. /DMSO
1C	147,47	155,95	-8,48	15H	11,85	7,73	4,12
2C	151,78	155,87	-4,09	16H	2,65	2,70	-0,05
3C	27,24	30,89	-3,65	17H	2,65	2,81	-0,16
4C	19,41	20,06	-0,65	18H	1,69	1,77	-0,08
5C	13,96	13,99	-0,03	19H	1,69	1,54	0,15
6C	149,60	157,84	-8,24	20H	0,96	1,24	-0,28
7C	122,41	132,00	-9,59	21H	0,96	0,98	-0,02
8C	157,60	165,07	-7,47	22H	0,96	0,99	-0,03
9C	121,80	131,15	-9,35	23H	10,05	10,48	-0,43
10C	126,07	137,25	-11,18	24H	7,92	7,91	0,01
11C	113,29	130,22	-16,93	25H	7,48	7,66	-0,18
12C	133,26	141,65	-8,39	26H	7,09	7,52	-0,43
13C	65,28	73,74	-8,46	27H	7,04	7,74	-0,70
14C	170,40	179,74	-9,34	28H	4,86	5,02	-0,16
				29H	4,86	4,42	0,44
				30H	13,15	6,73	6,42

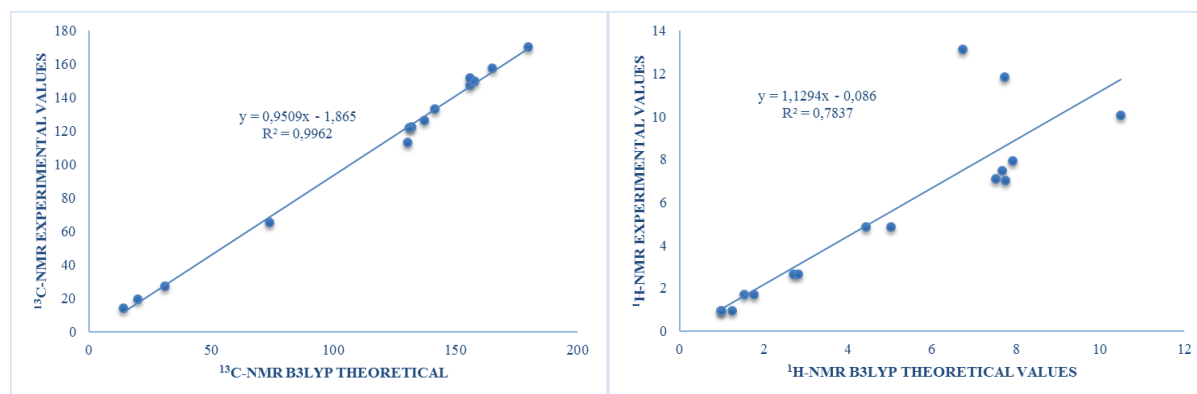


Figure 3. The correlation graphics for ^{13}C -NMR (DMSO) and ^1H -NMR (DMSO) chemical shifts of the titled molecule

Electronic and Nonlinear Optic Properties

Identifiers derived from the electronic structure of the 2-[3-(n-propyl)-4,5-dihydro-1H-1,2,4-triazol-5-one-4-yl]-phenoxyacetic acid, which are linked to the electronic structure, are called electronic structure identifiers. Some of them are, the Energy of the Highest Occupied Molecular Orbital, Energy of the Lowest Unoccupied Molecular Orbital (Figure 4), molecular hardness, chemical softness, electronegativity, chemical potential, electrophilicity index, nucleophilicity index and dipole moment (Table 3).

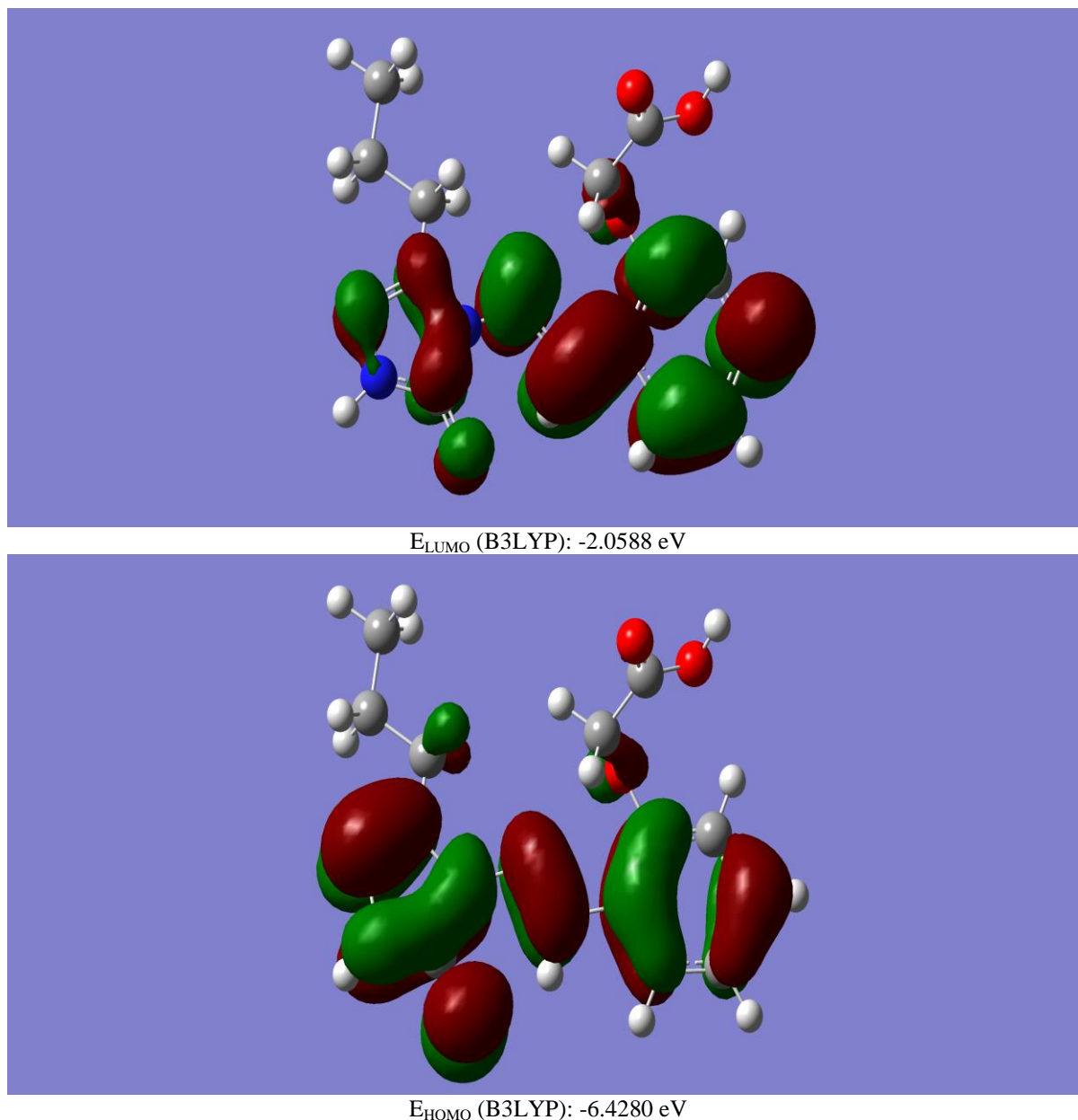


Figure 4. The calculated HOMO-LUMO energies of the molecule according to DFT/B3LYP/6-311+G(d,p) level

Table 3. Electronic properties of the molecule	
	DFT (eV)
Ionization Potential	6.4280
Electron Affinity	2.0588
Electronegativity	4.2434
electrophilic index	0.0531
Nucleophilic index	-0.6814
molecular softness	2.1846
Chemical Hardness	4.3692

The materials having nonlinear activity possess a nonlinear response to the electric fields associated with the light of a laser beam. It is well known that the higher values of dipole moment, polarizability, and hyperpolarizability are important for more active NLO properties. In this study dipole moment, polarizability and first hyperpolarizability of conformer ct of the titled molecule were investigated by using B3LYP method at 6-311+G(2d,p) basis set. The following formulas are used for calculating the magnitude of total static dipole moment (μ), polarizability (α) and first hyperpolarizability (β):

$$\mu = \left(\mu_x^2 + \mu_y^2 + \mu_z^2 \right)^{\frac{1}{2}}$$

$$\alpha = \frac{1}{3} (\alpha_{xx} + \alpha_{yy} + \alpha_{zz})$$

$$\beta = \sqrt{(\beta_{xxx} + \beta_{yyy} + \beta_{zzz})^2 + (\beta_{yyy} + \beta_{xxy} + \beta_{yzz})^2 + (\beta_{zzz} + \beta_{xxz} + \beta_{yyz})^2}$$

Where, the total static dipole moment (μ), linear polarizability (α) and the first hyperpolarizability (β) using the x , y , z components are defined. The energy gap ΔE_g , dipole moment (μ), linear polarizability (α) and the first hyperpolarizability (β) values of conformer ct of the titled molecule are investigated as a function of the two torsional angle using B3LYP/6-311+G(d,p) level of theory. The calculated results showed that behavior of dipole moment (μ), linear polarizability (α) and the first hyperpolarizability (β) values of conformer ct of the titled molecule as a function of dihedral angles have the same tendency. It means that these values are symmetric with the orthogonal conformation (90°) of the molecules (Govindarajan et al., 2012) (Table 4).

Table 4. Calculated polarization and hyperpolarizability values of the molecule (B3LYP/6-311+G(d,p))

	B3LYP
α_{xx}	44.314 a.u.
α_{yy}	33.651 a.u.
α_{zz}	20.016 a.u.
α	32.660×10^{-24} esu
$\Delta\alpha$	21.095×10^{-24} esu
β_x	6189.793 a.u.
β_y	346.476 a.u.
β_z	-591.377 a.u.
β_{xxx}	4874.76 a.u.
β_{xxy}	647.84 a.u.
β_{xyy}	667.19 a.u.
β_{yyy}	1006.03 a.u.
β_{xxz}	-515.19 a.u.
B_{xyz}	-144.36 a.u.
B_{yyz}	-321.22 a.u.
β_{xzz}	-29.81 a.u.
β_{yzz}	-240.35 a.u.
B_{zzz}	230.74 a.u.
β	6.23×10^{-30} esu

Dipole Moment and Total Energy

The energetic behavior of title molecule was investigated in vacum. Dipol moments and total energy values of title molecule were calculated by using B3LYP/6-311+G(d,p) level. The calculated dipole moments and total energy values are given in Table 5.

Table 5. The calculated dipole moment values of the molecule

Dipole Moment	B3LYP (a.u.)
μ_x	1.6261
μ_y	0.7175
μ_z	-1.1089
μ_{Toplam}	2.0949

Mulliken's Atomic Charges

The Mulliken atomic charges at the B3LYP/6-311+G(d,p) level of 2-[3-(n-propyl)-4,5-dihydro-1H-1,2,4-triazol-5-one-4-yl]-phenoxyacetic acid in gas phase are given in Table 6 (Mulliken, 1955).

Table 6. Mulliken atomic charges of the molecule

Atom	DFT	Atom	DFT	Atom	DFT	Atom	DFT
1C	-0.2816	11C	-0.2652	21H	0.1336	30H	0.2797
2C	0.4787	12C	-0.4546	22H	0.1348	31N	-0.2122
3C	0.3511	13C	-0.2777	23H	0.1766	32N	-0.1559
4C	-0.4702	14C	0.0532	24H	0.1485	33N	-0.1194
5C	-0.5218	15H	0.3325	25H	0.1343	34N	-0.0263
6C	0.0859	16H	0.1623	26H	0.1304	35O	-0.3797
7C	1.0299	17H	0.1851	27H	0.1376	36O	0.0094
8C	-0.6189	18H	0.1588	28H	0.1913	37O	-0.2885
9C	-0.2796	19H	0.1559	29H	0.1877	38O	-0.2199
10C	-0.2313	20H	0.1451				

Conclusion

In this paper, the structure of the titled compound is characterized by using FT-IR, ^1H and ^{13}C NMR spectroscopic methods. The molecular structures, vibrational frequencies, ^1H and ^{13}C NMR chemical shifts, UV-vis spectroscopies, HOMO and LUMO analyses and atomic charges of 2-[3-(n-propyl)-4,5-dihydro-1H-1,2,4-triazol-5-one-4-yl]-phenoxyacetic acid synthesized for the first time have been calculated by using DFT/B3LYP method. By considering the results of experimental works it can be easily stated that the ^1H and ^{13}C NMR chemical shifts, and vibrational frequencies spectroscopic parameters obtained theoretically are in a very good agreement with the experimental data. Also, the electronic structure of titled compound are determined electronic structure identifiers such as the Energy of the Highest Occupied Molecular Orbital, Energy of the Lowest Unoccupied Molecular Orbital, molecular hardness, chemical softness, electronegativity, chemical potential, electrophilicity index, nucleophilicity index and dipole moment. Finally, in this study, The nonlinear optical properties of the compound were calculated theoretically. It was found that the molecule concerned had a higher hyperpolarizability value than urine (0.77×10^{-30} esu).

Scientific Ethics Declaration

The authors declare that the scientific ethical and legal responsibility of this article published in EPSTEM journal belongs to the authors.

References

- Aktaş-Yokuş, Ö., Yüksek, H., Manap, S., Aytemiz, F., Alkan, M., Beytur, M., & Gürsoy-Kol, Ö. (2017). In-vitro biological activity of some new 1, 2, 4-triazole derivatives with their potentiometric titrations. *Bulgarian Chemical Communications*, 49(1), 98-106.
- Alkan, M., Yüksek, H., İslamoğlu, F., Bahçeci, S., Calapoğlu, M., Elmastaş, M., ... & Özdemir, M. (2007). A Study on 4-Acylamino-4, 5-dihydro-1H-1, 2, 4-triazol-5-ones. *Molecules*, 12(8), 1805-1816.
- Avcı, D., & Atalay, Y. (2009). Theoretical analysis of vibrational spectra and scaling- factor of 2- aryl- 1, 3, 4- oxadiazole derivatives. *International Journal of Quantum Chemistry*, 109(2), 328-341.
- Azam, F., Singh, S., Khokhra, S. L., & Prakash, O. (2007). Synthesis of Schiff bases of naphtha [1, 2-d] thiazol-2-amine and metal complexes of 2-(2'-hydroxy) benzylideneaminonaphthothiazole as potential antimicrobial agents. *Journal of Zhejiang University Science B*, 8(6), 446-452.
- Bahçeci, Ş., Yıldırım, N., Alkan, M., Gürsoy-Kol Ö., Manap, S., Beytur, M. & Yüksek, H. (2017). Investigation of Antioxidant, Biological and Acidic Properties of New 3-Alkyl(Aryl)-4-(3-acetoxy-4-methoxybenzylidenamino)-4,5-dihydro-1H-1,2,4-triazol-5-ones, *The Pharmaceutical and Chemical Journal*, 4(4), 91-101.
- Bahçeci, Ş., Yıldırım, N., Gürsoy-Kol, Ö., Manap, S., Beytur, M., & Yüksek, H. (2016). Synthesis, characterization and antioxidant properties of new 3-alkyl (aryl)-4-(3-hydroxy-4-methoxybenzylidenamino)-4, 5-dihydro-1H-1, 2, 4-triazol-5-ones. *Rasayan Journal of Chemistry*, 9(3), 494-501.
- Becke A. D. (1993). Density functional thermochemistry. III. The role of exact Exchange, *The Journal of Chemical Physics*, 98, 5648-5652.

- Beytur, M. (2020). Fabrication of platinum nanoparticle/boron nitride quantum dots/6-methyl-2-(3-hydroxy-4-methoxybenzylideneamino)-benzothiazole (ils) nanocomposite for electrocatalytic oxidation of methanol. *Journal of the Chilean Chemical Society*, 65(3), 4929-4933.
- Beytur, M., & Avinca, I. (2021). Molecular, Electronic, Nonlinear Optical and Spectroscopic Analysis of Heterocyclic 3-Substituted-4-(3-methyl-2-thienylmethyleneamino)-4, 5-dihydro-1H-1, 2, 4-triazol-5-ones: Experiment and DFT Calculations. *Heterocyclic Communications*, 27(1), 1-16.
- Beytur, M., Irak, Z. T., Manap, S., & Yüksek, H. (2019). Synthesis, characterization and theoretical determination of corrosion inhibitor activities of some new 4, 5-dihydro-1H-1, 2, 4-Triazol-5-one derivatives. *Heliyon*, 5(6), e01809.
- Boy, S. Türkan, F. Beytur, M. Aras, A. Akyıldırım O., Sedef Karaman, H., & Yüksek, H. (2021). Synthesis, design, and assessment of novel morpholine-derived Mannich bases as multifunctional agents for the potential enzyme inhibitory properties including docking study, *Bioorganic Chemistry*. 107, 104524.
- Çiftçi E., Beytur M., Calapoğlu M., Gürsoy Kol Ö., Alkan M., Toğay, V.A., Manap S., Yüksek H. (2018). Synthesis, characterization, antioxidant and antimicrobial activities and dna damage of some novel 2-[3-alkyl (aryl)-4,5-dihydro-1h-1,2,4-triazol-5-one-4-yl]-phenoxyacetic acids in human lymphocytes, *Research Journal of Pharmaceutical, Biological and Chemical Sciences*, 9(5), 1760-1771.
- Dennington, R., Keith, T., & Millam, J. (2009). *GaussView*. Shawnee Mission.
- Frisch, A., Nielson, A.B., & Holder, A.J. (2003). *Gaussview User Manual*. In *Gaussian, Inc.*, Wallingford.
- Frisch, M. J., Trucks, G., Schlegel, H. B., Scuseria, G. E., Robb, M. A., Cheeseman, J. R., Scalmani, G., Barone, V., Mennucci, B., Petersson, G. A., Nakatsuji, H., Caricato, M., Li, X., Hratchian, H. P., Izmaylov, A. F., Bloino, J., Zheng, G., Sonnenberg, J. L., Hada, M., Ehara, M., Toyota, K., Fukuda, R., Hasegawa, J., Ishida, M., Nakajima, T., Honda, Y., Kitao, O., Nakai, H., Vreven, T., Montgomery, J. A., Jr. Vreven, T., Peralta, J. E., Ogliaro, F., Bearpark, M., Heyd, J. J., Brothers, E., Kudin, N., Staroverov, V. N., Kobayashi, R., Normand, J., Raghavachari, K., Rendell, A., Burant, J. C., Iyengar, S. S., Tomasi, J., Cossi, M., Rega, N., Millam, J. M., Klene, M., Knox, J. E., Cross, J. B., Bakken, V., Adamo, C., Jaramillo, J., Gomperts, R., Stratmann, R. E., Yazyev, O., Austin, A. J., Cammi, R., Pomelli, C., Ochterski, J. W., Martin, L. R., Morokuma, K., Zakrzewski, V. G., Voth, G. A., Salvador, P., Dannenberg, J. J., Dapprich, S., Daniels, A. D., Farkas, O., Foresman, J. B., Ortiz, J. V., Cioslowski, J. & Fox, D. J. (2009). *Gaussian Inc*. Wallingford.
- Govindarajan, M., Periandy, S., & Carthigayen, K. (2012). FT-IR and FT-Raman spectra, thermo dynamical behavior, HOMO and LUMO, UV, NLO properties, computed frequency estimation analysis and electronic structure calculations on α -bromotoluene. *Spectrochimica Acta Part A: Molecular and Biomolecular Spectroscopy*, 97, 411-422.
- Gürsoy-Kol, Ö., & Yüksek, H. (2010). Synthesis and invitro antioxidant evaluation of some novel 4,5-dihydro-1H-1,2,4-triazol-5-one derivatives, *E-Journal of Chemistry*, 7(1), 123-136.
- Jamróz, M. H. (2004). *Vibrational Energy Distribution Analysis*. VEDA 4 Program.
- Kido, J., Kimura, M., & Nagai, K. (1995). Multilayer white light-emitting organic electroluminescent device. *Science*, 267(5202), 1332-1334.
- Koç, E., Yüksek, H., Beytur, M., Akyıldırım, O., Akçay, M., & Beytur, C. (2020). Heterosiklik 4, 5-dihidro-1H-1, 2, 4-triazol-5-on Türevinin Antioksidan Özelliğinin Erkek Ratlarda (Wistar albino) İn vivo Olarak Belirlenmesi. *Bitlis Eren Üniversitesi Fen Bilimleri Dergisi*, 9(2), 542-548.
- Lee, S. Y. (1998). Molecular Structure and Vibrational Spectra of Biphenyl in the Ground and the lowest Triplet States. Density Functional Theory Study, *Bulletin of the Korean Chemical Society*, 19(1), 93-98.
- Mecca, C. Z., Fonseca, F. L., & Bagatin, I. A. (2016). Fluorescence in complexes based on quinolines-derivatives: a search for better fluorescent probes. *Spectrochimica Acta Part A: Molecular and Biomolecular Spectroscopy*, 168, 104-110.
- Mulliken, R. S. (1955). Electronic population analysis on LCAO-MO molecular wave functions. I. *The Journal of Chemical Physics*, 23(10), 1833-1840.
- Qin, J.C., Yang, Z.Y., Fan, L. & Wang, B.D. (2015). Fluorescent sensor for selective detection of Al⁽³⁺⁾ based on quinoline-coumarin conjugate, *Spectrochimica Acta Part A*, 140, 21-26.
- Rani, A. U., Sundaraganesan, N., Kurt, M., Cinar, M., & Karabacak, M. (2010). FT-IR, FT-Raman, NMR spectra and DFT calculations on 4-chloro-N-methylaniline. *Spectrochimica Acta Part A: Molecular and Biomolecular Spectroscopy*, 75(5), 1523-1529.
- Subramanian, N., Sundaraganesan, N., & Jayabharathi, J. (2010). Molecular structure, spectroscopic (FT-IR, FT-Raman, NMR, UV) studies and first-order molecular hyperpolarizabilities of 1, 2-bis (3-methoxy-4-hydroxybenzylidene) hydrazine by density functional method. *Spectrochimica Acta Part A: Molecular and Biomolecular Spectroscopy*, 76(2), 259-269.
- Sun, Y., Giebink, N. C., Kanno, H., Ma, B., Thompson, M. E., & Forrest, S. R. (2006). Management of singlet and triplet excitons for efficient white organic light-emitting devices. *Nature*, 440(7086), 908-912.

- Sztanke, K., Maziarka, A., Osinka, A. & Sztanke, M. (2003). Synthesis, antibacterial, antifungal and anti-HIV activities of Schiff and Mannich bases derived from isatin derivatives and N-[4-(4'-chlorophenyl)thiazol-2-yl] thiosemicarbazide. *European Journal of Pharmaceutical Sciences*, 21(13), 3648-3666.
- Turhan-Irak Z., Beytur, M. (2019). 4-Benzilidenamino-4,5-dihidro-1H-1,2,4-triazol-5-on Türevlerinin Antioksidan Aktivitelerinin Teorik Olarak İncelenmesi, *Journal of the Institute of Science and Technology*, 9(1), 512-521.
- Turhan-Irak , Z., & Gümüş, S. (2017). Heterotricyclic compounds via click reaction: A computational study. *Noble International Journal of Scientific Research*, 1(7), 80-89.
- Uğurlu, G., & Beytur, M. (2020). Theoretical Studies on The Structural, Vibrational, Conformational Analysis and Nonlinear Optic (NLO) Property of 4-(Methoxycarbonyl) Phenylboronic Acid. *Indian Journal of Chemistry-Section A*, 59(10), 1504-1512.
- Vosko, S. H., Wilk, L., & Nusair, M. (1980). Accurate spin-dependent electron liquid correlation energies for local spin density calculations: a critical analysis. *Canadian Journal of Physics*, 58(8), 1200-1211.
- Wade, L.G. (2006). *Organic Chemistry* (6nd ed). Pearson Prentice Hall.
- Wolinski, K., Hinton, J. F., & Pulay, P. (1990). Efficient implementation of the gauge-independent atomic orbital method for NMR chemical shift calculations. *Journal of the American Chemical Society*, 112(23), 8251-8260.
- Yang, D., Duan, Y., Yang, Y., Hu, N., Wang, X., Sun, F., & Duan, Y. (2015). Application of exciplex in the fabrication of white organic light emitting devices with mixed fluorescent and phosphorescent layers. *Journal of Luminescence*, 166, 77-81.
- Yüksek, H. (1992). 3-Alkil(aril)-4-amino-4,5-dihidro-1,2,4-triazol-5-on'ların bazı reaksiyonlarının incelenmesi (Doktora Tezi) KTÜ Fen Bilimleri Enstitüsü.
- Zhao, J., Wang, Z., Wang, R., Chi, Z., & Yu, J. (2017). Hybrid white organic light-emitting devices consisting of a non-doped thermally activated delayed fluorescent emitter and an ultrathin phosphorescent emitter. *Journal of Luminescence*, 184, 287-292.

Author Information

Murat BEYTUR

Kafkas University
Kars, Turkey

Contact e-mail: muratbeytur83@gmail.com

Haydar YUKSEK

Kafkas University
Kars, Turkey

To cite this article:

Beytur, M. & Yüksek, H. (2021). Investigation of theoretical and experimental properties of 2-[3-(n-propyl)-4,5-dihydro-1h-1,2,4-triazol-5-one-4-yl]-phenoxyacetic acid. *The Eurasia Proceedings of Science, Technology, Engineering & Mathematics (EPSTEM)*, 15, 1-9.

The Eurasia Proceedings of Science, Technology, Engineering & Mathematics (EPSTEM), 2021

Volume 15, Pages 10-20

ICBAST 2021: International Conference on Basic Science and Technology

Quantum Chemical Calculations of 2-Methoxy-4-[(3-*p*-Methylbenzyl-4,5-Dihydro-1*H*-1,2,4-Triazol-5-One-4-YL)Azomethine] Phenyl-2-Methylbenzoate Molecule

Gul KOTAN

Kafkas University

Haydar YUKSEK

Kafkas University

Abstract: 2-Methoxy-4-[(3-*p*-methylbenzyl-4,5-dihydro-1*H*-1,2,4-triazol-5-one-4-yl) azomethine] phenyl-2-methylbenzoate was optimized by using Density Functional Theory (DFT/B3LYP, B3PW91) methods (Frisch et al., 2009; Wolinski et al., 1990). ¹H-NMR and ¹³C-NMR isotropic shift values were calculated by the method of GIAO using the program package Gaussian G09 (Wolinski et al., 1990). Theoretical and experimental values were inserted into the graphic according to equation of $\delta_{exp} = a + b \cdot \delta_{calc}$. Experimental data obtained from the literature (Yüksek et al., 2018). The standard error values were found via SigmaPlot program with regression coefficient of a and b constants. Furthermore, the veda4f program was used in defining of IR data theoretically (Jamróz, 2004). Theoretically calculated IR data are multiplied with appropriate adjustment factors (Merrick et al., 2007) and the data obtained according to DFT(B3LYP, B3PW91) method are formed using theoretical infrared spectrum. Also, dipole moments, the HOMO-LUMO energy, ΔE_g , total energy of the molecule, bond lengths and Mulliken charges, the molecular surfaces such as molecular electrostatic potential (MEP) and MEP contour maps, the total density, the electron density and the electrostatic potential were calculated with same method and functions.

Keywords: 1,2,4-Triazol-5-one, DFT, Gaussian G09, HOMO-LUMO.

Introduction

Schiff bases are formed by the condensation of activated carbonyl and amino groups. These compounds contain an imine group (Puchtler, 1981). Organic compounds derived from 1*H*-1,2,4-Triazol-5-one have great importance in the synthesis of organic substances, pharmaceutical chemistry, medicine, food industry, antibacterial, antioxidant, and anti-inflammatory materials (Fan, et al., 2018; Chu, et al., 2019; Samuel, et al., 2017; Yüksek, et al., 2011; Yüksek, et al., 2020; Murtaza, et al., 2017). Besides, many heterocyclic compounds with 1,2,4 triazole derivatives; It has many biological activities such as antioxidant, antifungal, antimalarial, anti-analgesic, anticancer, anti convulsant, anti-viral (Zhang, et al., 2017; Ikizler, et al., 1998; Hashem, et al., 2007; Pandey, et al., 2012; Uddin, et al., 2020; Nilkanth, et al., 2020; Jarrahpour, et al., 2015; Kotan, et al., 2020). Recently, the properties such as electronic, geometric, spectroscopic, conductivity and thermodynamics of Schiff bases and many organic compounds containing 1,2,4-triazole have been investigated theoretically and have taken their place in the literature (Kotan, et al., 2021; Beytur, et al., 2021; Ulaş, et al., 2021). In article in the literature, the molecular structure analysis, other all theoretical properties have been studied effectively with the Density Function Theory (DFT) method. In this study, all theoretical calculations were performed with the DFT (B3LYP and B3PW91) method and the 6-311G(d,p) basis set of Gaussian 09W program (Frisch, et al.,

- This is an Open Access article distributed under the terms of the Creative Commons Attribution-Noncommercial 4.0 Unported License, permitting all non-commercial use, distribution, and reproduction in any medium, provided the original work is properly cited.

- Selection and peer-review under responsibility of the Organizing Committee of the Conference

2009) and the obtained results were evaluated. The scaled values (Merrick, et al., 2007) of infrared vibration frequencies were reached by using the Veda 4f program (Jamróz, 2004).

Table 1. $^1\text{H}/^{13}\text{C}$ -NMR(DMSO) isotropic chemical shifts (δ /ppm)

No	Exp.	B3LY		B3LY		Differ		Differ	
		P/ Vacuu m	Differ/ Vacuu m	P/ DMSO	Differ P	B3PW 91/ Vacuu m	B3PW9 1/ Vacuu m	B3PW 91 /DMS O	Differ B3PW 91/DM SO
C1	146.33	152.25	-5.92	153.18	-6.85	146.53	-0.20	147.39	-1.06
C2	151.24	152.64	-1.4	153.62	-2.38	147.61	3.63	148.51	2.73
C3	153.53	152.08	1.45	152.79	0.74	147.96	5.57	148.63	4.90
C4	128.66	133.11	-4.45	132.51	-3.85	128.00	0.66	127.34	1.32
C5	112.99	125.99	-13	126.08	-13.09	122.02	-9.03	122.03	-9.04
C6	121.25	126.2	-4.95	126.67	-5.42	122.18	-0.93	122.72	-1.47
C7	152.42	160.9	-8.48	161.53	-9.11	155.48	-3.06	156.16	-3.74
C8	139.7	145.8	-6.1	145.82	-6.12	140.36	-0.66	140.42	-0.72
C9	128.66	133.66	-5	133.98	-5.32	129.61	-0.95	129.90	-1.24
C10	30.74	34.58	-3.84	34.37	-3.63	30.43	0.31	30.18	0.56
C11	130.7	138.42	-7.72	138.39	-7.69	133.18	-2.48	133.20	-2.50
C12	128.09	133.04	-4.95	133.18	-5.09	128.94	-0.85	129.80	-1.71
C13	128.9	132.43	-3.53	132.86	-3.96	128.55	0.35	128.99	-0.09
C14	135.66	142.08	-6.42	143.37	-7.71	136.94	-1.28	138.35	-2.69
C15	128.9	132.83	-3.93	133.06	-4.16	128.88	0.02	129.12	-0.22
C16	127.99	131.87	-3.88	131.65	-3.66	127.90	0.09	127.68	0.31
C17	20.53	21.53	-1	21.14	-0.61	18.35	2.18	17.94	2.59
C18	56.22	59.09	-2.87	59.81	-3.59	55.08	1.14	55.74	0.48
C19	164.69	170.39	-5.7	171.45	-6.76	165.11	-0.42	166.11	-1.42
C20	126.43	130.84	-4.41	130.34	-3.91	125.79	0.64	125.26	1.17
C21	132.72	136.63	-3.91	136.92	-4.20	132.42	0.30	132.75	-0.03
C22	126.26	129.21	-2.95	129.89	-3.63	125.29	0.97	126.00	0.26
C23	133.02	137.41	-4.39	138.89	-5.87	133.38	-0.36	134.91	-1.89
C24	131.86	135.72	-3.86	136.19	-4.33	131.85	0.01	132.33	-0.47
C25	139.77	151.45	-11.68	151.44	-11.67	146.15	-6.38	146.16	-6.39
C26	21.06	25.21	-4.15	24.77	-3.71	21.87	-0.81	21.00	0.06
H27	11.92	7.61	4.31	8.14	3.78	7.71	4.21	8.25	3.67
H28	9.65	10.71	-1.06	10.68	-1.03	10.93	-1.28	10.89	-1.24
H29	7.73	8.83	-1.1	8.91	-1.18	9.01	-1.28	9.10	-1.37
H30	7.3	7.86	-0.56	8.08	-0.78	8.02	-0.72	8.18	-0.88
H31	7.44	7.68	-0.24	7.86	-0.42	7.86	-0.42	8.04	-0.60
H32	4.05	4.46	-0.41	4.53	-0.48	4.59	-0.54	4.67	-0.62
H33	4.05	4.58	-0.53	4.72	-0.67	4.75	-0.70	4.90	-0.85
H34	7.19	8.12	-0.93	8.31	-1.12	8.28	-1.09	8.48	-1.29
H35	7.07	7.93	-0.86	8.10	-1.03	8.07	-1.00	8.26	-1.19
H36	7.07	7.95	-0.88	8.10	-1.03	8.10	-1.03	8.26	-1.19
H37	7.19	8.19	-1	8.20	-1.01	8.36	-1.17	8.38	-1.19
H38	2.21	3.14	-0.93	3.16	-0.95	3.23	-1.02	3.26	-1.05
H39	2.21	2.69	-0.48	2.79	-0.58	2.80	-0.59	2.91	-0.70
H40	2.21	2.91	-0.7	2.99	-0.78	3.01	-0.80	3.10	-0.89
H41	3.87	4.15	-0.28	4.19	-0.32	4.48	-0.61	4.66	-0.79
H42	3.87	5	-1.13	5.08	-1.21	5.07	-1.20	5.15	-1.28
H43	3.87	4.41	-0.54	4.58	-0.71	4.21	-0.34	4.25	-0.38
H44	8.09	9.31	-1.22	9.36	-1.27	9.48	-1.39	9.54	-1.45
H45	7.68	8.07	-0.39	8.26	-0.58	8.24	-0.56	8.43	-0.75
H46	7.71	8.2	-0.49	8.43	-0.72	8.37	-0.66	8.61	-0.90
H47	7.46	8.06	-0.6	8.25	-0.79	8.22	-0.76	8.42	-0.96
H48	2.61	2.7	-0.09	3.44	-0.83	3.61	-1.00	3.56	-0.95
H49	2.61	3.79	-1.18	2.89	-0.28	3.92	-1.31	3.77	-1.16
H50	2.61	3.49	-0.88	3.63	-1.02	2.83	-0.22	3.03	-0.42

In addition, ^{13}C NMR and ^1H NMR chemical shift values were determined by DFT (B3LYP/B3PW91) method and 6-311G(d,p) base set according to GIAO method (Wolinski, et. al., 1990). The results of these spectral calculations and the experimental results from the literature (Yüksek, et al., 2018) were compared. Also, all theoretical calculations of the molecule have been done.

Method

In this study, the Gaussian 09W package program, which is a very comprehensive program, was used. First of all, with the B3LYP/6-311G(d,p) basis set of DFT, the most stable low-energy optimized structure of atoms and molecules has been established. Each atom of molecule was then given a number. From this optimized structure, spectroscopic, thermodynamic, geometric, electronic properties of the molecule were calculated (Frisch et al., 2009). IR vibration frequency values were calculated with the Veda 4f program (Jamróz., 2004). The ^1H -NMR and ^{13}C -NMR isotropic shift values were calculated by the GIAO method using the Gaussian G09 package program (Wolinski et al., 1990). These values were compared with the experimental values (Yüksek, et al., 2018) and the difference values were found, and these values were $\delta_{\text{exp}} = a + b \cdot \delta_{\text{calc}}$ plotted according to the equation. The regression coefficient was found using the Sigmaplot program. The HOMO-LUMO energy, total energy, bond angle, bond length, Mulliken atomic charges, dipole moment of the target molecule was calculated. In addition, MEP surface maps were visualized.

Results and Discussion

Computational Details

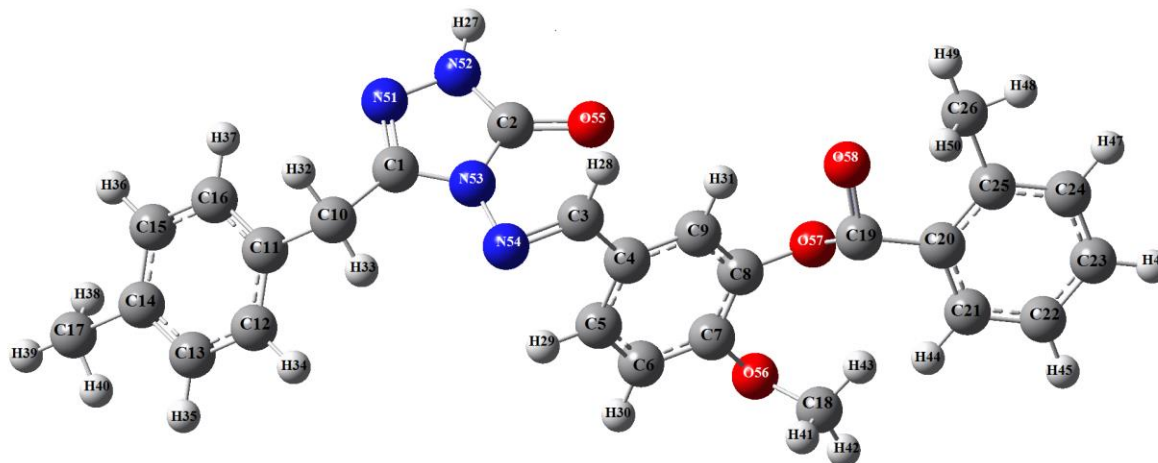


Figure 1. The Gaussview structure of the molecule.

The Relation between R Values of the Compound

There is such a relationship between R^2 -values of the compound. B3LYP(DMSO): ^1H : 0.8702, ^{13}C : 0.9951; B3PW91(DMSO)6-311G(d,p) ^1H : 0.8674, ^{13}C : 0.9955; B3LYP(vacuum): ^1H : 0.8433, ^{13}C : 0.9948; B3PW91(vacuum)6-311G(d,p) ^1H : 0.8403, ^{13}C : 0.9953. These values for compound were seen in the Table 2. Theoretical and experimental carbon/proton chemical shifts ratios between according to R^2 linear a correlation were observed (Figure 2).

Table 2. The correlation data for chemical shifts

	^{13}C -NMR/ R^2	^1H -NMR/ R^2
B3LYP(DMSO)	0.9951	0.8702
B3PW91(DMSO)	0.9955	0.8674
B3LYP	0.9948	0.8433
B3PW91	0.9953	0.8403

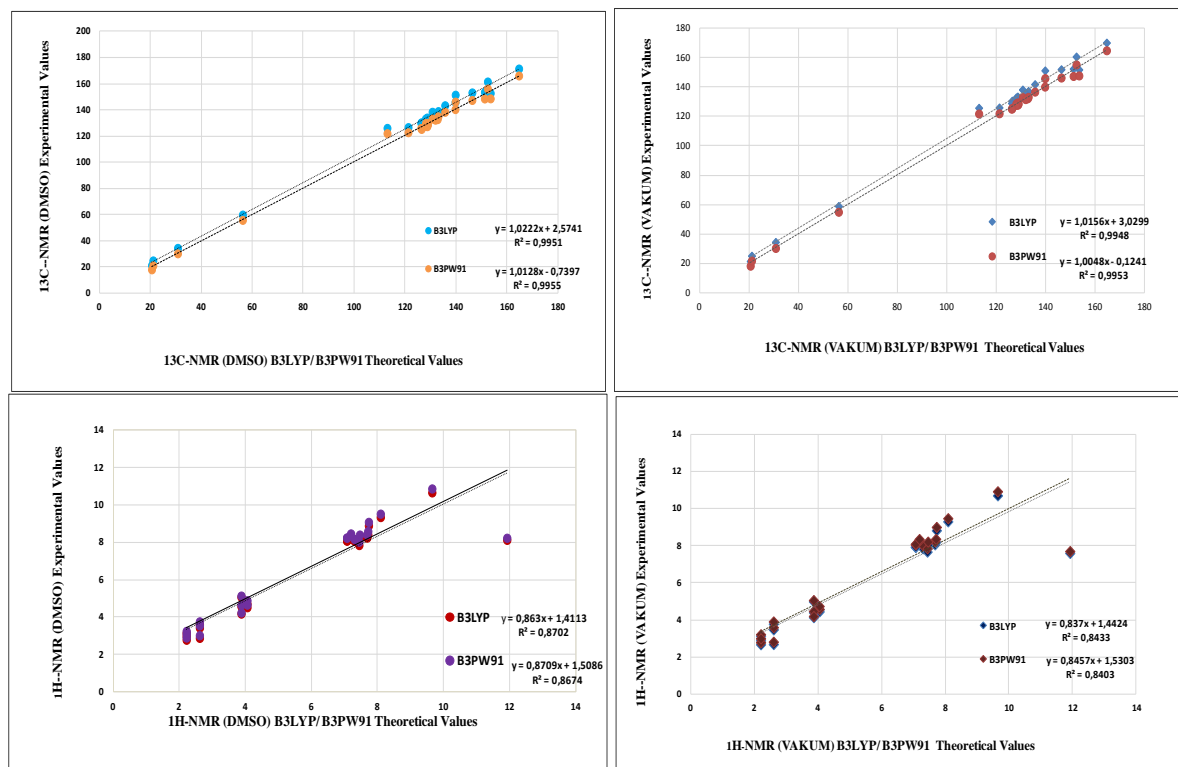


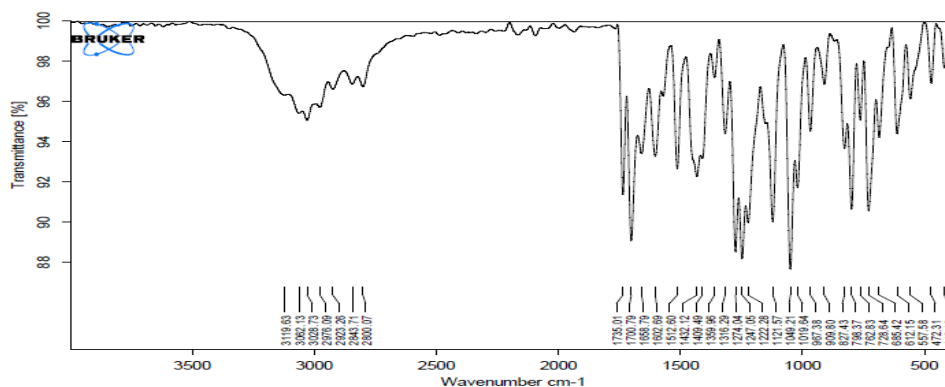
Figure 2. The experimental and theoretical ¹³C/ ¹H-NMR correlation graphs for DFT/(B3LYP, B3PW91) methods chemical shifts

The Vibration Frequency of the Compound

Theoretically IR values were calculation Veda 4f program and scala values were obtain. The calculated harmonic vibrational frequency values were scaled with 0.9671 for B3LYP 3-21 G level, 0.9688 for 6-311G(d,p) level (Merrick et al., 2007). The positive frequency in the data was found. IR spectrums were drawn with obtained values according to DFT method. Theoretically IR values were compare with experimentally IR values and found corresponding with each other of values.

Table 3. Significant vibrational frequencies (cm⁻¹)

Experimental IR	Scaled B3LYP	Scaled B3PW91	Experimental IR
v (NH)	3169	3514	3565
v (C=O)	1739. 1700	1708. 1664	1737. 1750
v (C=N)	1589	1577	1613
v (COO)	1231	1248	1259



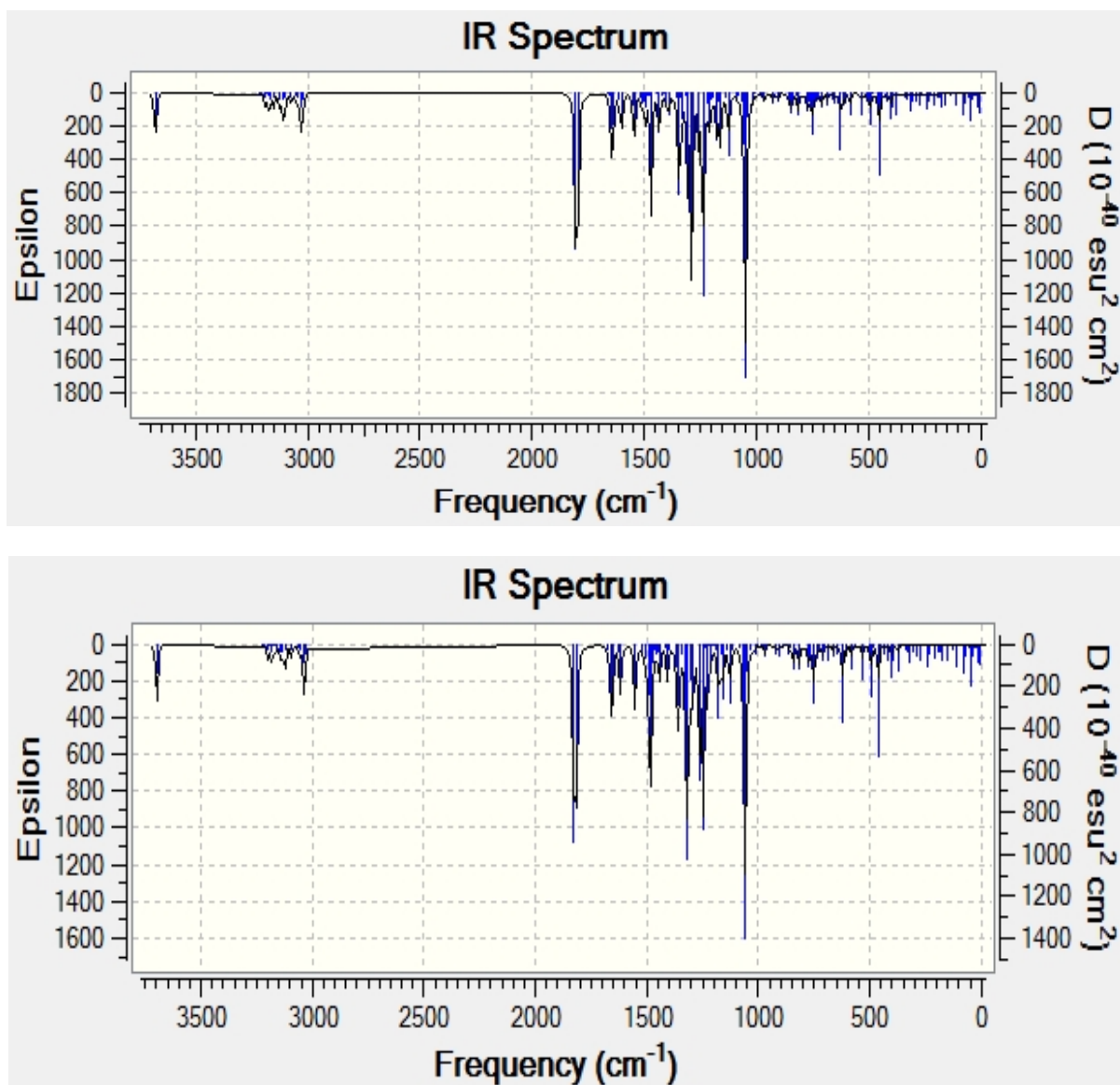


Figure 3. Experimental and theoretical IR spectrums simulated with DFT/(B3LYP, B3PW91)

Molecular Geometry

The bond angle and length are geometric parameters of the structure. To calculate these two parameters, 6-311G(d,p) basis set and B3LYP and B3PW91 functions are used. According to this calculations result, the highest bond length is between C(1)-C(10) atoms that this values are 1.49/1.48 Å for B3LYP/ B3PW91 6-311G(d,p). Besides, respectively, the bond lengths in the triazole ring N51-N52, N51-C1, C2-O55, C2-N52, N53-C1 are calculated 1.37/1.36; 1.29/1.29; 1.21/1.21; 1.36/1.36, 1.38/ 1.38 Å for B3LYP 3-21G(d,p)/ 6-311G(d,p) basis sets (table 4). In the literature, the N-N, N=C, C=O bond lengths are measured as 1.40 , 1.28, 1.21 Å (Sudha et al. 2018). The calculated bond length values are consistent with literature values.

The highest bond angle is between N(52)-C(2)-O(55) atoms, which is 129.86/129.84° for B3LYP/ B3PW91 6-311G(d,p) basis sets (table 5). The calculated Mulliken atomic charges (Mulliken, 1955) calculated by using the B3LYP, B3PW91 method with 6-311G(d,p) basis sets. The electronegative oxygen (O) and nitrogen (N) atoms have negative atomic charge values. The carbon atoms surrounded by electronegative atoms have negative atomic charge values. The C1 atom surrounded by two electronegative atoms (N51, N53) and C2 atom which is surrounded by three electronegative atoms (N52, N53, O55) have negative charges values. All hydrogen atoms of the compound (H27-50) have positive atomic charge values (table 6).

Table 4. The calculated bond lengths with B3LYP/B3PW91 6-311G(d,p)

Bond Length	B3LYP	B3PW91	Bond Length	B3LYP	B3PW91
1 C(1)-N(51)	1.297	1.296	35 C(20)-C(21)	1.404	1.401
2 C(1)-N(53)	1.387	1.383	36 C(23)-H(46)	1.084	1.085
3 C(1)-C(10)	1.492	1.487	37 C(23)-C(24)	1.390	1.388
4 N(51)-N(52)	1.379	1.369	38 C(24)-H(47)	1.084	1.085
5 N(52)-H(27)	1.005	1.005	39 C(24)-C(25)	1.398	1.396
6 N(52)-C(2)	1.369	1.365	40 C(25)-C(26)	1.508	1.502
7 C(2)-O(55)	1.216	1.214	41 C(26)-H(48)	1.091	1.092
8 C(2)-N(53)	1.419	1.414	42 C(26)-H(49)	1.091	1.091
9 N(53)-N(54)	1.371	1.363	43 C(26)-H(50)	1.091	1.092
10 N(54)-C(3)	1.285	1.284	44 C(8)-C(9)	1.389	1.387
11 C(3)-H(28)	1.086	1.088	45 C(9)-C(4)	1.396	1.394
12 C(3)-C(4)	1.461	1.457	46 C(10)-H(32)	1.093	1.094
13 C(4)-C(5)	1.405	1.402	47 C(10)-H(33)	1.091	1.092
14 C(4)-C(9)	1.396	1.394	48 C(10)-C(11)	1.522	1.517
15 C(5)-H(29)	1.082	1.083	49 C(11)-C(12)	1.394	1.392
16 C(5)-C(6)	1.379	1.377	50 C(12)-H(34)	1.085	1.085
17 C(6)-H(30)	1.083	1.084	51 C(12)-C(13)	1.393	1.391
18 C(6)-C(7)	1.405	1.402	52 C(13)-H(35)	1.085	1.086
19 C(7)-O(56)	1.357	1.351	53 C(13)-C(14)	1.396	1.394
20 O(56)-C(18)	1.433	1.425	54 C(14)-C(17)	1.509	1.504
21 C(18)-H(41)	1.089	1.090	55 C(17)-H(38)	1.095	1.095
22 C(18)-H(42)	1.090	1.091	56 C(17)-H(39)	1.092	1.092
23 C(18)-H(43)	1.093	1.093	57 C(17)-H(40)	1.093	1.093
27 C(7)-C(8)	1.401	1.399	58 C(14)-C(15)	1.399	1.397
28 C(8)-O(57)	1.396	1.390	59 C(15)-H(36)	1.085	1.086
29 O(57)-C(19)	1.380	1.373	60 C(15)-C(16)	1.390	1.388
30 C(19)-O(58)	1.203	1.201	61 C(16)-H(37)	1.085	1.086
31 C(19)-C(20)	1.487	1.483	62 C(16)-C(11)	1.398	1.395
32 C(21)-C(22)	1.387	1.385			
33 C(22)-H(45)	1.083	1.084			
34 C(22)-C(23)	1.392	1.390			

Table 5. The calculated bond angles with B3LYP/B3PW91 6-311G(d,p)

Bond Angles	B3LYP	B3PW91	Bond Angles	B3LYP	B3PW91
N(51)-C(1)-N(53)	111.440	111.370	C(4)-C(5)-H(29)	119.157	119.118
N(51)-N(52)-C(2)	114.366	114.511	H(29)-C(5)-C(6)	120.495	120.560
N(51)-N(52)-H(27)	120.514	120.497	C(4)-C(5)-C(6)	120.348	120.321
H(27)-N(52)-C(2)	125.101	124.977	C(5)-C(6)-H(30)	121.362	121.367
N(52)-C(2)-O(55)	129.862	129.840	H(30)-C(6)-C(7)	117.095	117.063
O(55)-C(2)-N(53)	128.893	128.963	C(5)-C(6)-C(7)	121.542	121.569
N(52)-C(2)-N(53)	101.245	101.196	C(6)-C(7)-O(56)	115.798	115.862
N(51)-C(1)-C(10)	124.504	124.651	C(7)-O(56)-C(18)	120.475	120.156
C(1)-C(10)-H(32)	106.336	106.336	O(56)-C(18)-H(41)	105.398	105.525
C(1)-C(10)-H(33)	109.020	108.990	O(56)-C(18)-H(42)	111.480	111.480
C(1)-C(10)-C(11)	113.862	113.635	O(56)-C(18)-H(43)	110.935	111.599
C(10)-C(11)-C(12)	120.942	120.965	O(56)-C(7)-C(8)	126.160	126.112
C(11)-C(12)-H(34)	119.560	119.553	C(7)-C(8)-O(57)	120.043	119.978
H(34)-C(12)-C(13)	119.566	119.585	C(8)-O(57)-C(19)	118.791	118.560
C(12)-C(13)-H(35)	119.388	119.406	O(57)-C(19)-O(58)	122.003	122.124
H(35)-C(13)-C(14)	119.513	119.479	O(57)-C(19)-C(20)	126.651	126.631
C(13)-C(14)-C(17)	121.265	121.266	C(19)-C(20)-C(21)	119.444	119.395
C(13)-C(14)-C(15)	117.797	117.778	C(20)-C(21)-H(44)	118.798	118.774
C(14)-C(17)-H(38)	111.067	111.440	H(44)-C(21)-C(22)	120.094	120.132
C(14)-C(17)-H(39)	111.415	111.414	C(21)-C(22)-H(45)	120.098	120.120
C(14)-C(17)-H(40)	111.398	110.981	H(45)-C(22)-C(23)	120.629	120.643
C(14)-C(15)-H(36)	119.427	119.412	C(22)-C(23)-H(46)	120.281	120.280
H(36)-C(15)-C(16)	119.345	119.354	H(46)-C(23)-C(24)	119.753	119.747
C(15)-C(16)-H(37)	119.823	119.875	C(23)-C(24)-H(47)	119.358	119.413

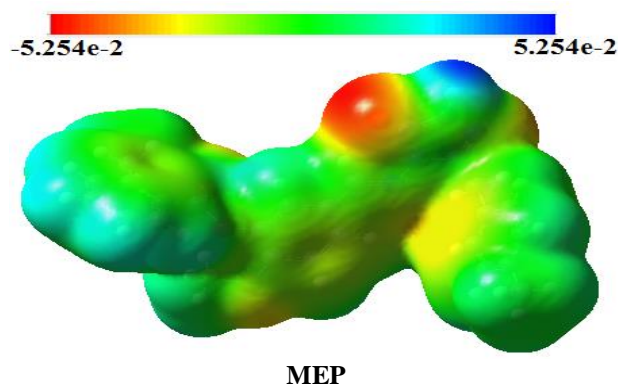
H(37)-C(16)-C(11)	119.459	119.411	H(47)-C(24)-C(25)	118.530	118.468
N(53)-N(54)-C(3)	118.850	118.752	C(24)-C(25)-C(26)	118.555	118.614
N(54)-C(3)-H(28)	121.955	121.928	C(25)-C(26)-H(48)	111.773	111.759
H(28)-C(3)-C(4)	117.627	117.746	C(25)-C(26)-H(49)	111.494	111.435
C(3)-C(4)-C(5)	123.074	123.061	C(25)-C(26)-H(50)	109.913	109.945

Table 6. The calculated mulliken charges datas B3LYP/B3PW91 6-311G(d,p)

Atom	DFT	B3PW91	Atom	DFT	B3PW91
C1	0.354	0.393	H29	0.108	0.121
C2	0.533	0.576	H30	0.106	0.118
C3	0.129	0.157	H31	0.102	0.115
C4	-0.175	-0.217	H32	0.150	0.169
C5	0	0.003	H33	0.136	0.155
C6	-0.102	-0.119	H34	0.083	0.094
C7	0.208	0.218	H35	0.082	0.092
C8	0.125	0.114	H36	0.084	0.094
C9	0.084	0.007	H37	0.098	0.112
C10	-0.157	-0.195	H38	0.127	0.130
C11	-0.120	-0.139	H39	0.109	0.123
C12	-0.060	-0.070	H40	0.115	0.143
C13	-0.076	-0.082	H41	0.124	0.135
C14	-0.098	-0.110	H42	0.124	0.139
C15	-0.075	-0.082	H43	0.117	0.133
C16	-0.036	-0.033	H44	0.115	0.126
C17	-0.258	-0.288	H45	0.10	0.110
C18	0.134	-0.175	H46	0.101	0.111
C19	0.415	0.435	H47	0.091	0.101
C20	-0.202	-0.233	H48	0.094	0.145
C21	-0.012	-0.014	H49	0.136	0.109
C22	-0.094	-0.105	H50	0.127	0.155
C23	-0.067	-0.073	N51	-0.228	-0.241
C24	-0.075	-0.084	N52	-0.313	-0.332
C25	-0.070	-0.078	N53	-0.382	-0.417
C26	-0.206	-0.245	N54	-0.209	-0.231
H27	0.249	0.258	O55	-0.390	-0.406
H28	0.140	0.158	O56	-0.361	-0.363

MEP Surface Analysis

By looking at the molecular electrostatic potential map, we can identify the electronegative and electropositive regions of the molecule. In the MEP map, the red regions were seen in the nucleophilic regions and the blue regions were seen in the electrophilic regions. In the MEP shape of this structure, the carbonyl group is around red, while the N-H acidic proton is blue around.



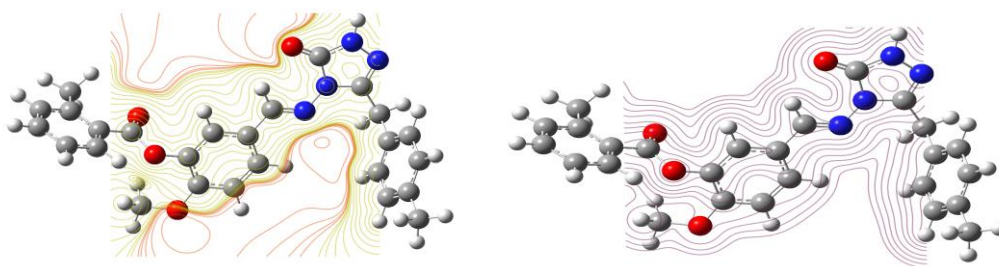


Figure 4. The calculated MEP and surface contour map of the molecule

Frontier Molecular Orbital Analysis

Frontier molecular orbitals (FMO) designated kinetic stability, the electronic transitions, electric and optical properties (Fukui, 1982). The HOMO-LUMO energy values was calculated as 4.17/4.20 eV for B3LYP and B3PW91 functionals in the 6-311G (d,p) basis set (figure 5). With the HOMO-LUMO energy gap electron affinity (A), global hardness (η), electronegativity (χ), chemical potential (μ), softness (S), ionization potential (I), chemical potential (Pi), electrophilic index(ω), Nucleophilic index (IP) for the compound was calculated and we are seen in table 7.

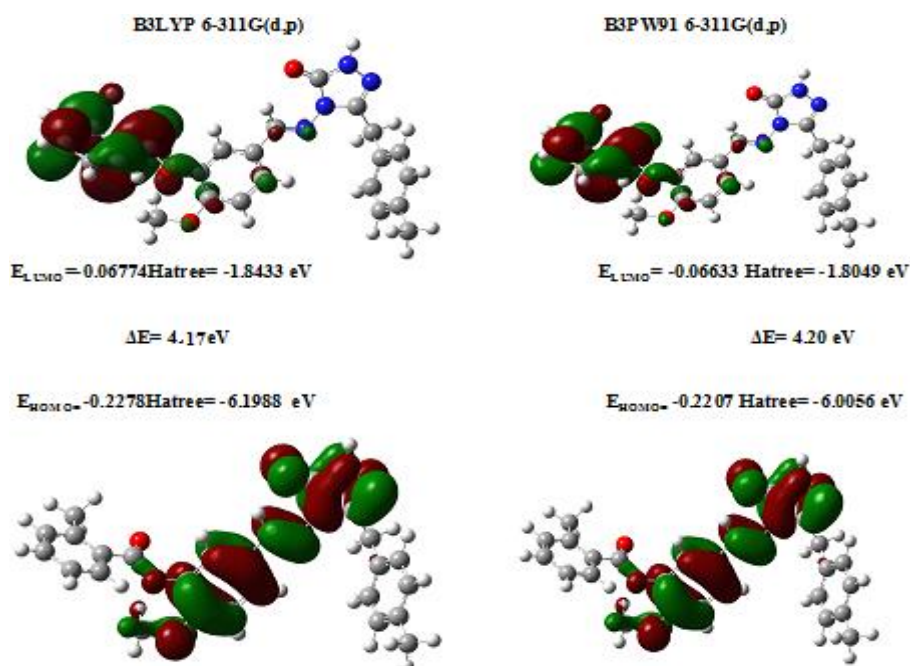


Figure 5. HOMO-LUMO energy of the molecule 6-311G(d,p)

Table 7. The calculated electronic structure parameters of the molecule

		B3LYP 3-21G(d,p)		B3LYP 6-311G(d,p)	
		Hatree	ev	Hatree	ev
	LUMO	-0.0599	-1.62992	-0.06774	-1.84325
	HOMO	-0.2191	-5.96186	-0.2278	-6.1986
A	elektron ilgisi	0.0599	1.62992	0.06774	1.84325
I	İyonlaşma potansiyeli	0.2191	5.96186	0.2278	6.1986
ΔE	energy gap	0.1592	4.33194	0.16006	4.35534
χ	electronegativity	0.1395	3.79589	0.14777	4.02093
Pi	chemical potential	-0.1395	-3.79589	-0.14777	-4.02093
ω	electrophilic index	0.000774518	0.02108	0.000873766	0.02378
IP	Nucleophilic index	-0.0111042	-0.30215	-0.01182603	-0.32179
S	molecular softness	12.5628	341.843	12.4953	340.006
η	molecular hardness	0.0796	2.16597	0.08003	2.17767

Table 8. The calculated dipole moments datas of the molecule

	μ_x	μ_y	μ_z	μ_{Toplam}
B3LYP	-1.6296	1.5316	-0.6621	2.3323
B3PW91	-2.5397	1.9737	-0.8065	3.3160

Table 9. The calculated total energy datas of the molecule

Energy(a.u.)	B3LYP	B3PW91
	-1525.48470748	-1524.88006830

Thermodynamics Properties

Thermodynamics parameters were calculated with the (B3LYP/ B3PW91) functionals of DFT method at 298.150 K and under 1 atm pressure and were summarized in the Table 10.

Table 10. The calculated thermodynamics parameters of the molecule

Parameters	B3LYP	B3PW91
Rotational temperatures (Kelvin)		
A	0.01000	0.01002
B	0.00226	0.00227
C	0.00203	0.00204
Rotational constants (GHZ)		
A	0.20833	0.20877
B	0.04710	0.04727
C	0.04225	0.04257
Thermal Energies E(kcal/mol)		
Translational	0.889	0.889
Rotational	0.889	0.889
Vibrational	304.170	305.163
Total	305.948	306.940
Thermal Capacity CV(cal/mol-K)		
Translational	2.981	2.981
Rotational	2.981	2.981
Vibrational	110.899	110.650
Total	116.861	116.612
Entropy S(cal/mol-K)		
Translational	44.242	44.242
Rotational	37.892	37.879
Vibrational	129.652	128.917
Total	211.786	211.038
Zero-point correction (Hartree/Particle)	0.456549	0.458187
Thermal correction to Energy	0.487559	0.489140
Thermal correction to Enthalpy	0.488503	0.490085
Thermal correction to Gibbs Free Energy	0.387876	0.389814
Sum of electronic and zero-point Energies	-1525.028158	-1524.421882
Sum of electronic and thermal Energies	-1524.997149	-1524.390928
Sum of electronic and thermal Enthalpies	-1524.996205	-1524.389984
Sum of electronic and thermal Free Energies	-1525.096831	-1524.490254
Zero-point vibrational energy (Kcal/mol)	286.48894	287.51650

Conclusion

All quantum chemical calculations of 2-Methoxy-4-[(3-*p*-methylbenzyl-4,5-dihydro-1*H*-1,2,4-triazol-5-one-4-yl) azomethine] phenyl-2-methylbenzoate compound with B3LYP, B3PW91/6-311G(d,p) sets were theoretically investigated. As a result of the comprehensive and comparative calculations based on the optimized structure. The R^2 values for the ^{13}C -NMR data of the molecule are 0.9955 in the B3PW91 6-311G (d,p) basic set and in the DMSO solvent environment and the closest value to 1 when compared to the other sets. As can be seen from the graphs, a deviation was observed in the ^1H -NMR chemical shift results. The reason for this is the

N-H acidic proton in the structure. IR vibration frequencies were calculated theoretically with two different methods and the values compared with the experimental values, and it was concluded that the values calculated with the comprehensive set B3PW91/6-311G(d,p) were more compatible with the experimental. No negative values were found in the theoretical IR data, which showed us that the molecule was stable. Among the energy values of the HOMO-LUMO orbitals of the molecule, the highest ΔE_g value is 4.20 eV obtained with B3PW91/6-311G((d,p) and this result tells us that the structure is stable. In addition, electron affinity using the HOMO-LUMO orbital energies, ionization potential, molecular hardness-softness, nucleophilic properties were calculated. The thermodynamic values of the molecule were found and, the geometric parameters were calculated and the bond lengths were compared with the values in the literature. The obtained data were found to be compatible with each other and with the experimental data. In addition, molecular surface maps were created and nucleophilic and electrophilic regions of the molecule were determined from the MEP map.

Scientific Ethics Declaration

The authors declare that the scientific ethical and legal responsibility of this article published in EPSTEM journal belongs to the authors.

References

- Beytur, M., & Avinca, I. (2021). Molecular, Electronic, Nonlinear Optical and Spectroscopic Analysis of Heterocyclic 3-Substituted-4-(3-methyl-2-thienylmethyleneamino)-4, 5-dihydro-1H-1, 2, 4-triazol-5-ones: Experiment and DFT Calculations. *Heterocyclic Communications*, 27(1), 1-16.
- Chu, X. M., Wang, C., Wang, W. L., Liang, L. L., Liu, W., Gong, K. K., & Sun, K. L. (2019). Triazole derivatives and their antiplasmodial and antimalarial activities. *European Journal of Medicinal Chemistry*, 166, 206-223.
- Fan, Y. L., Cheng, X. W., Wu, J. B., Liu, M., Zhang, F. Z., Xu, Z., & Feng, L. S. (2018). Antiplasmodial and antimalarial activities of quinolone derivatives: an overview. *European Journal of Medicinal Chemistry*, 146, 1-14.
- Frisch, M.J., Trucks, G.W., Schlegel, H.B., Scuseria, G.E., Robb, M.A., Cheeseman, J.R., Scalmani, G., Barone, V., Mennucci, B., Petersson, G.A., Nakatsuji, H., Caricato, M.; Li, X., Hratchian, H.P., Izmaylov, A.F., Bloino, J., Zheng, G., Sonnenberg, J.L., Hada, M., Ehara, M., Toyota, K., Fukuda, R., Hasegawa, J., Ishida, M., Nakajima, T., Honda, Y., Kitao, O., Nakai, H., Vreven, T., Montgomery, J.A., Jr. Vreven, T., Peralta, J.E., Ogliaro, F., Bearpark, M., Heyd, J.J., Brothers, E., Kudin, N., Staroverov, V.N., Kobayashi, R., Normand, J., Raghavachari, K., Rendell, A., Burant, J.C., Iyengar, S.S., Tomasi J., Cossi, M., Rega, N., Millam, J.M., Klene, M., Knox, J.E., Cross J.B., Bakken, V., Adamo, C., Jaramillo, J., Gomperts, R., Stratmann, R.E., Yazyev, O., Austin, A.J., Cammi, R., Pomelli, C., Ochterski, J.W., Martin; L.R., Morokuma, K., Zakrzewski, V.G., Voth, G.A., Salvador, P., Dannenberg, J.J., Dapprich, S.; Daniels A.D., Farkas, O.; Foresman, J.B., Ortiz, J.V., Cioslowski, J., and Fox, D.J. (2009). *Gaussian Inc.* Wallingford.
- Fukui, K. (1982). Role of frontier orbitals in chemical reactions. *Science*, 218(4574), 747-754.
- Hashem, A. I., Youssef, A. S., Kandeel, K. A., & Abou-Elmagd, W. S. (2007). Conversion of some 2 (3H)-furanones bearing a pyrazolyl group into other heterocyclic systems with a study of their antiviral activity. *European Journal of Medicinal Chemistry*, 42(7), 934-939.
- Ikizler, A. A., Ikizler, A., Yüksek, H., & Serdar, M. (1998). Antitumor activities of some 4, 5-dihydro-1H-1, 2, 4-triazol-5-ones. *Model. Measur. Control, Ser. C, 1*, 25-33.
- Jamróz, M. H. (2004). *Vibrational Energy Distribution Analysis*. VEDA 4 Program.
- Jarrahpour, A., Shirvani, P., Sharghi, H., Aberi, M., Sinou, V., Latour, C., & Brunel, J. M. (2015). Synthesis of novel mono-and bis-Schiff bases of morpholine derivatives and the investigation of their antimalarial and antiproliferative activities. *Medicinal Chemistry Research*, 24(12), 4105-4112.
- Kotan, G., & Kardaş, F. Structural and theoretical study based on DFT calculations of 3-Methyl-4-[3-ethoxy-(2-p-metilbenzenesulfonyloxy)-benzylidenamino]-4, 5-dihydro-1H-1, 2, 4-triazol-5-one. *International Journal of Chemistry and Technology*, 5(1), 42-51.
- Kotan, G., Gökce, H., Akyıldırım, O., Yüksek, H., Beytur, M., Manap, S., & Medetalibeyoğlu, H. (2020). Synthesis, Spectroscopic and Computational Analysis of 2-[(2-Sulfanyl-1 H-benzo [d] imidazol-5-yl) iminomethyl] phenyl Naphthalene-2-sulfonate. *Russian Journal of Organic Chemistry*, 56(11), 1982-1994.
- Merrick, J. P., Moran, D., Radom, L. (2007). An Evaluation of Harmonic Vibrational Frequency Scale Factors. *Journal of Physical Chemistry*, 111(45), 11683-11700.

- Mulliken, R. S. (1955). Electronic population analysis on LCAO–MO molecular wave functions. I. *The Journal of Chemical Physics*, 23(10), 1833-1840.
- Murtaza, S., Akhtar, M. S., Kanwal, F., Abbas, A., Ashiq, S., & Shamim, S. (2017). Synthesis and biological evaluation of schiff bases of 4-aminophenazone as an anti-inflammatory, analgesic and antipyretic agent. *Journal of Saudi Chemical Society*, 21, 359-S372.
- Nilkanth, P. R., Ghorai, S. K., Sathiyarayanan, A., Dhawale, K., Ahamad, T., Gawande, M. B., & Shelke, S. N. (2020). Synthesis and Evaluation of Anticonvulsant Activity of Some Schiff Bases of 7- Amino- 1, 3- dihydro- 2H- 1, 4- benzodiazepin- 2- one. *Chemistry & Biodiversity*, 17(9), 2000342.
- Pandey, A., Rajavel, R., Chandraker, S., & Dash, D. (2012). Synthesis of Schiff bases of 2-amino-5-aryl-1, 3, 4-thiadiazole and its analgesic, anti-inflammatory and anti-bacterial activity. *E-Journal of Chemistry*, 9(4), 2524-2531.
- Puchtler, H., & Meloan, S. N. (1981). On Schiff's bases and aldehyde-Fuchsin: A review from H. Schiff to RD Lillie. *Histochemistry*, 72(3), 321-332.
- Sudha, N., Abinaya, B., Arun Kumar, R., & Mathammal, R. (2018). Synthesis, Structural, Spectral, Optical and Mechanical Study of Benzimidazolium Phthalate crystals for NLO Applications. *Journal of Lasers Optics & Photonics*, 5(2), 1-6.
- Uddin, N., Rashid, F., Ali, S., Tirmizi, S. A., Ahmad, I., Zaib, S., ... & Haider, A. (2020). Synthesis, characterization, and anticancer activity of Schiff bases. *Journal of Biomolecular Structure and Dynamics*, 38(11), 3246-3259.
- Ulaş, Y. (2021). Synthesis, Spectroscopic Characterization (FT-IR, NMR, UV), NPA, NBO, NLO, Thermochemical Analysis and Molecular Docking Studies of 2-((4-hydroxyphenyl)(piperidin-1-yl) methyl) phenol. *Journal of Computational Biophysics and Chemistry*, 20(3), 323-335.
- Wolinski, K., Hinton, J. F., & Pulay, P. (1990). Efficient implementation of the gauge-independent atomic orbital method for NMR chemical shift calculations. *Journal of the American Chemical Society*, 112(23), 8251-8260.
- Yüksek, H., Gürsoy-Kol, O., Kemer, G., Ocak, Z., & Anil, B. (2011). Synthesis and in-vitro antioxidant evaluation of some novel 4-(4-substituted) benzylidenamino-4, 5-dihydro-1H-1, 2, 4-triazol-5-ones.
- Yüksek, H., Kutanis, O., Özdemir, G., Beytur, M., Kara, S., Gürsoy Kol, Ö., Alkan, M. (2018). Synthesis, In Vitro Antioxidant and Antimicrobial Activities of Some Novel 2-Methoxy-4-[(3-substitue-4,5-dihydro-1H-1,2,4-triazol-5-one-4-yl)azomethine]phenyl 2-methylbenzoate Derivatives. *Res J Pharm Biol Chem Sci*, 9(4), 501-512 .
- Yüksek, H., Özdemir, G., Manap, S., Yılmaz, Y., Kotan, G., Gürsoy-Kol, Ö., & Alkan, M. (2020). Synthesis and Investigations of Antimicrobial, Antioxidant Activities of Novel Di-[2-(3-alkyl/aryl-4, 5-dihydro-1H-1, 2, 4-triazol-5-one-4-yl)-azomethinephenyl] Isophthalates and Mannich Base Derivatives. *ACTA Pharmaceutica Scientia*, 58(1).
- Zhang, S., Xu, Z., Gao, C., Ren, Q.C., Chang, L., Lv, Z.S., Feng, L.S., 2017. Triazole derivatives and their anti-tubercular activity. *European Journal of Medicinal Chemistry*, 138, 501-513.

Author Information

Gul KOTAN

Kafkas University,
Kars, Turkey

Contact e-mail: gulkemer@hotmail.com

Haydar YUKSEK

Kafkas University
Kars, Turkey

To cite this article:

Kotan, G. & Yüksek, H. (2021). Quantum chemical calculations of 2-methoxy-4-[(3-p-methylbenzyl-4,5-dihydro-1h-1,2,4-triazol-5-one-4-yl)azomethine] phenyl-2-methylbenzoate molecule. *The Eurasia Proceedings of Science, Technology, Engineering & Mathematics (EPSTEM)*, 15, 10-20.

The Eurasia Proceedings of Science, Technology, Engineering & Mathematics (EPSTEM), 2021

Volume 15, Pages 21-27

ICBAST 2021: International Conference on Basic Science and Technology

Synthesis of Novel ABA-Type Amphiphilic Copolymers Including 2-Hydroxypropyl Propionate and N-Isobutoxymethyl B-Alanine by Peg-Dialkoxide Initiated Hydrogen-Transfer Polymerization

Efkan CATIKER
Ordu University**Temel OZTURK**
Giresun University**Bedrettin SAVAS**
Kafkas University**Mehmet ATAKAY**
Hacettepe University**Bekir SALIH**
Hacettepe University

Abstract: Novel ABA-type amphiphilic copolymers were prepared using end-groups activated poly (ethylene glycol) (PEG) as an initiator of hydrogen-transfer polymerization (HTP). For this purpose, PEG with 1450 Da (PEG-1450) was treated with the equivalent amount of sodium hydride to synthesize PEG with dialkoxide end-groups, namely PEG-dialkoxide. Using the PEG-dialkoxide as a macroinitiator, base-catalysed HTP of 2-hydroxypropyl acrylate (HPA), and N-isobutoxymethyl acrylamide (BMA) were performed to achieve the novel ABA-type block copolymers. The copolymers were obtained with relatively high yields. Characterization of the ABA-type amphiphilic copolymers was carried out using FTIR and MALDI mass spectrometry. FTIR spectra of the copolymers exhibited some characteristic bands assigning to the functional groups arising from the mechanism of HTP. Molar mass distributions of the copolymers from the MALDI mass study pointed out that chain extensions by mass in each copolymer were almost equal. Hence, the MALDI mass spectra of the copolymers revealed that chain extensions of PEGs by HPA, and BMA units were successfully fulfilled.

Keywords: ABA-type amphiphilic copolymer, Hydrogen-transfer polymerization, Macroinitiator, Poly(ethylene glycol).

Introduction

Many novel macromolecules via the extension of polymeric chains (Matyjaszewski, 2003) or coupling reactions (He et.al., 2012; Çatiker et.al., 2020; Çatiker et.al., 2019) have been reported by using the approach. Telechelics are generally synthesized via living radical polymerization (Frey et. al., 2018) and controlled living radical polymerization (Lunn et.al., 2017) because they yield narrow molar mass distribution. Block copolymers can be easily generated by using telechelics (Iijima et.al., 1997; Verso et. al., 2008; Boutevin et.al., 2006; Tasdelen et.al.,2011). Amphiphilic block copolymers are the most common block copolymer systems that self-assemble into different morphologies depending upon the nature of their chemical content (Levit M., et.al., 2020; Lee et. al., 2010) size of the blocks (Burguière et.al., 2002; LaRue et.al., 2008) and physical conditions (temperature, solvent, pH, electrical field, etc.) (Akiba et.al., 2010 November; Karayianni et. al., 2016; Wang et.al., 2017; Yorulmaz-Avşar et.al., 2019). Poly(ethylene glycol) (PEG) is the most common hydrophilic segment (Danafar

et.al., 2014; Quadir et.al., 2014) preferred in block copolymers possibly due to its unique physical and biocompatible properties. Polymers based on PEG are attractive materials for biomedical, industrial, and chemical applications, as PEG has these unique characters (Francolini et.al., 2020; Zarrintaj et.al., 2020). PEG units are helpful for hydrophobic polymers to gain hydrophilicity (Zhu et.al., 2012). Hydrogen transfer polymerization (HTP) is a useful route that can insert functional groups into the backbone of a macromolecule. However, it is necessary to use a monomer with a loose proton(s) and vinyl group to obtain the product via HTP (Çatiker et.al., 2018; Iwamura et.al., 2019). The PEG-1450 was treated with the equivalent amount of sodium hydride to sodium PEG-dialkoxide salt as shown ref. (Çatiker et.al., 2020). Using the salt as a macroinitiator, HTP of 2-hydroxypropyl acrylate (HPA), and N-isobutoxymethyl acrylamide (BMA) were carried out to yield PEG based ABA-type amphiphilic copolymers. Structural characterization of the copolymers was achieved using FTIR and MALDI-MS spectrometry.

Experimental

Materials

2-hydroxypropyl acrylate (Sigma), N-isobutoxymethyl acrylamide (Sigma), sodium hydride (Merck, 60 % dispersion in oil), PEG-1450 (Sigma-Aldrich), 2,5-dihydroxybenzoic acid (DHB) (Sigma-Aldrich, 98 %), and formic acid (Sigma-Aldrich, ≥ 99 %) were obtained commercially and used without purification. Tetrahydrofuran (Sigma-Aldrich, 99 %) was distilled over sodium mirror.

Instrumentation

FTIR spectra of the copolymers were achieved with Shimadzu IRAffinity 1 spectrometer in the range of 600-4000 cm^{-1} . MALDI-MS analyses were performed using a Bruker Rapiflex MALDI-TOF/TOF mass spectrometer (Bruker Daltonics, Bremen, Germany) equipped with a smartbeam™ 3D laser. The data were acquired in positive ion mode for each sample. DHB solution (20 mg/mL in 1:1, ACN:THF containing 1.0% (v/v) formic acid) was used as the matrix.

Preparation of Sodium PEG-dialkoxide

Sodium PEG-1450 dialkoxide was obtained by a reaction between PEG-1450 and equimolar NaH at about 45 °C as the ref. (Çatiker et.al., 2020). Briefly, a certain amount of PEG-1450 and NaH (two times of PEG-1450 as moles) were placed in a round bottom glass balloon under argon flux. The mixture was stirred at 45 °C (slightly above the melting temperature of PEG-1450) under argon flux until hydrogen gas evolution has stopped. The dark brown waxy paste was obtained and then directly used as a macroinitiator for HTP.

Synthesis of the ABA-type Amphiphilic Copolymers by HTP

Poly (2-hydroxypropyl propionate-b-ethylene glycol-b-2-hydroxypropyl propionate) [P(HPP-EG-HPP)] and poly (N-isobutoxymethyl β -alanine-b-ethylene glycol-b-N-isobutoxymethyl β -alanine) [P(BMBA-EG-BMBA)] were synthesized by HTP of 2-hydroxypropyl acrylate (HPA) and N-isobutoxymethyl acrylamide (BMA) using the sodium PEG-1450 dialkoxide as a macroinitiator. Reaction parameters were outlined in Table 1. The specified amounts of the monomers given in Table 1 were added into the separate balloons containing the sodium PEG-dialkoxide as an initiator of HTP. After nitrogen purging, the reaction mixture was stirred until the mixture becomes too viscous, or solid. Then, cold excess THF was poured into the reaction mixture to extract the purities. The product was filtered and washed with cold THF to remove possible unreacted PEG and monomer (HPA or BMA). The percentage yields of the ABA-type block copolymer were determined gravimetrically and calculated as 71.3 wt. % and 93.1 wt. %.

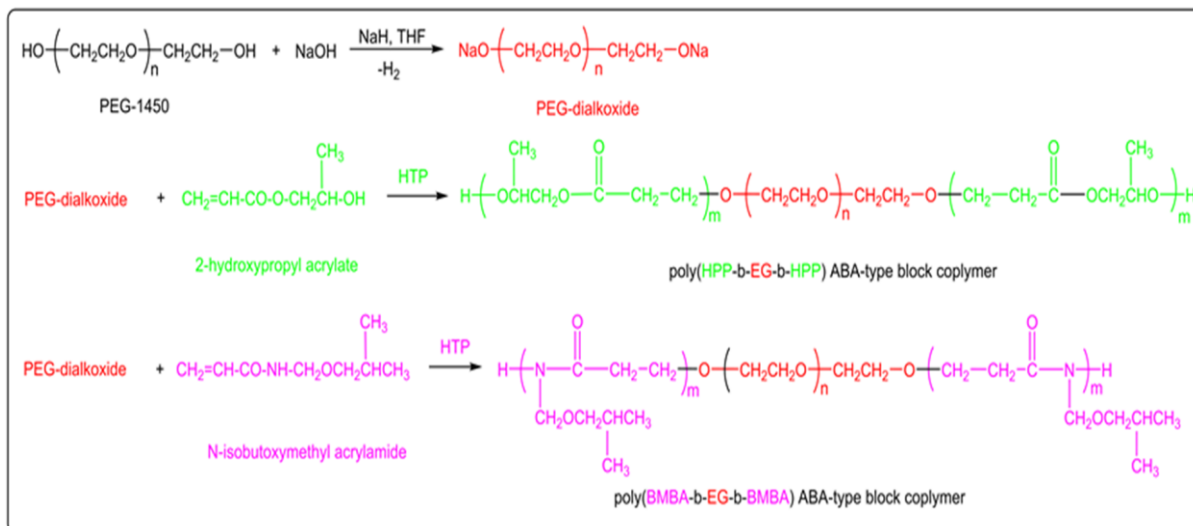
Table 1. Synthesis condition of the ABA-type triblock copolymers through HTP.

Initiator (g)	Monomer (mL)	Yield % (wt.)	Average Molar Mass (Da)
~ 0.45 (PEG-dialkoxide)	0.40 mL (HPA)	71.3	~ 3000
~ 0.45 (PEG-dialkoxide)	0.40 mL (BMA)	93.1	~ 2500

Results and Discussion

Synthesis of the ABA-type Block Copolymers

PEG-1450 was treated with sodium hydride to obtain PEG-dialkoxide salts. Line 1 in Scheme 1 shows the reaction pathway for the PEG-dialkoxide macroinitiator. Line 2 and 3 in Scheme 1 show the reaction outlines for P(HPP-EG-HPP) and P(BMBA-EG-BMBA) ABA-type block copolymers. The copolymers obtained from HTP were extracted with THF to remove unreacted PEG units and by-products. Then, the insoluble fractions were dried under vacuum at 40 °C.



Scheme 1. Reaction pathways in the synthesis of PEG-dialkoxide, and novel ABA-type block copolymers.

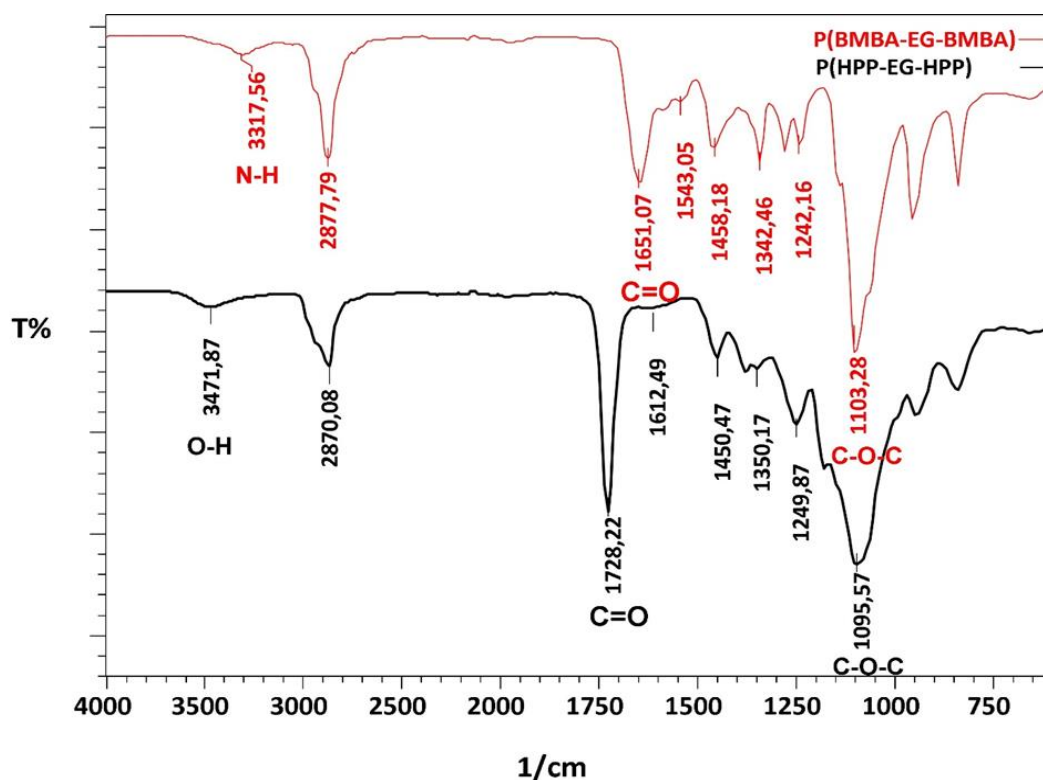


Figure 1. FTIR spectra of the ABA-type amphiphilic copolymers.

Characterization of the ABA-type Amphiphilic Copolymers

FTIR spectra of the ABA-type amphiphilic copolymers were comparatively given in Figure 1. FTIR spectrum of P(HPP-EG-HPP) has characteristic PEG bands as well as ester (1728 cm^{-1}) band in the HPP units. For the FTIR spectrum of P(BMBA-EG-BMBA), the characteristic secondary amide (I) (Çatiker et.al., 2018) at about 1650 cm^{-1} ($\text{C}=\text{O}$ stretching vibration) and ether about 1095 cm^{-1} (asymmetric C-O stretching vibration) show the existence of both repeating units in the products. The FTIR spectra of both THF-insoluble copolymer samples include the characteristic bands of PEG, normally known as very soluble in THF. This may be attributed to the formation of covalent bonding between the PEG units, and the chain extensions by HTP. The weak bands at 3472 and 3318 cm^{-1} belong to the OH and NH stretching vibrations in P(HPP-EG-HPP) and P(BMBA-EG-BMBA), respectively. The weakness of the bands shows the chain extensions are limited.

MALDI mass spectrum of the P(HPP-EG-HPP) in Figure 2 was acquired and examined to show molar mass distribution. The unimodal mass distribution centered at about m/z 3000 Da may be accepted as another proof of the successful chain extension.

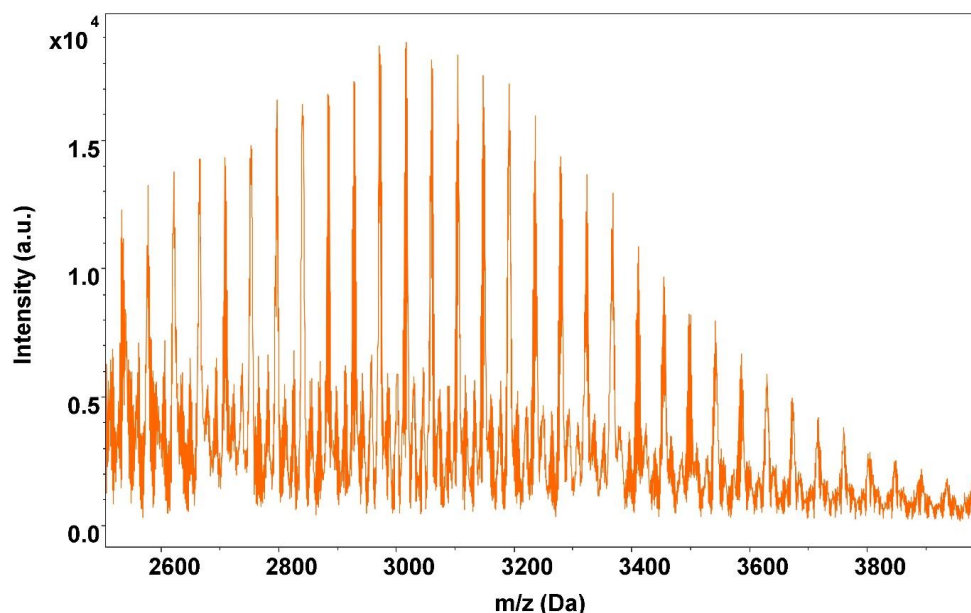


Figure 2. Wide-range MALDI mass spectra of P(HPP-EG-HPP)

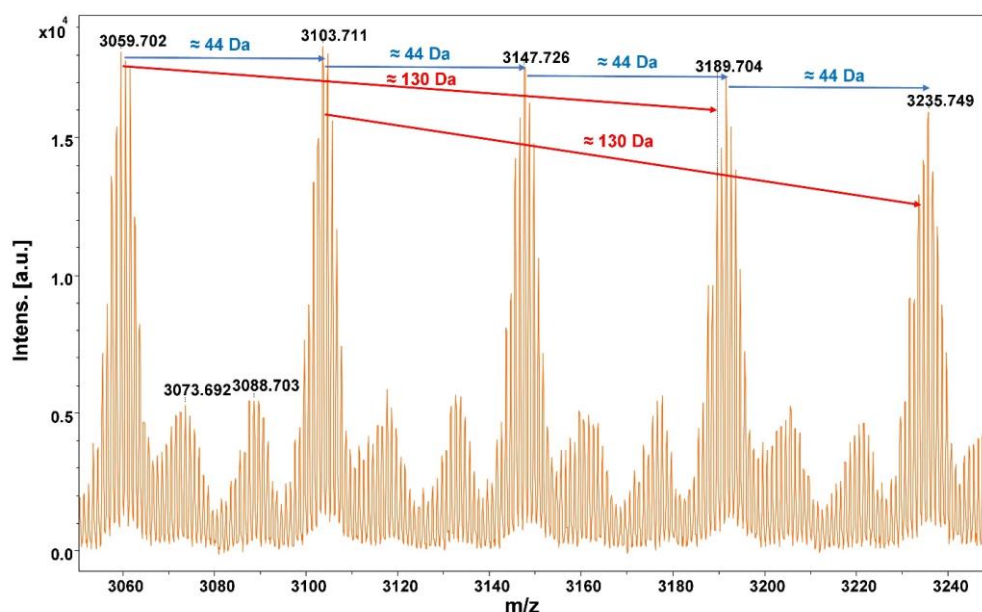


Figure 3. An expanded view of m/z the 3050-3250 region of MALDI-MS spectrum of P(HPP-EG-HPP).

Figure 3 shows an expanded view of m/z the 3050-3250 region of MALDI-MS spectrum of P(HPP-EG-HPP). The indisputable proof of the copolymer formation can be seen when the differences between consecutive signals are about m/z 130 and m/z 44 corresponding to the masses of HPP ($C_6H_{10}O_3$) and EG (C_2H_4O) repeating units of the copolymer, respectively. MALDI-TOF-MS analyzes of the copolymer sample show that the ABA-type poly(HPP-EG-HPP) copolymer has been synthesized successfully by confirming the targeted chemical structure with high mass accuracy.

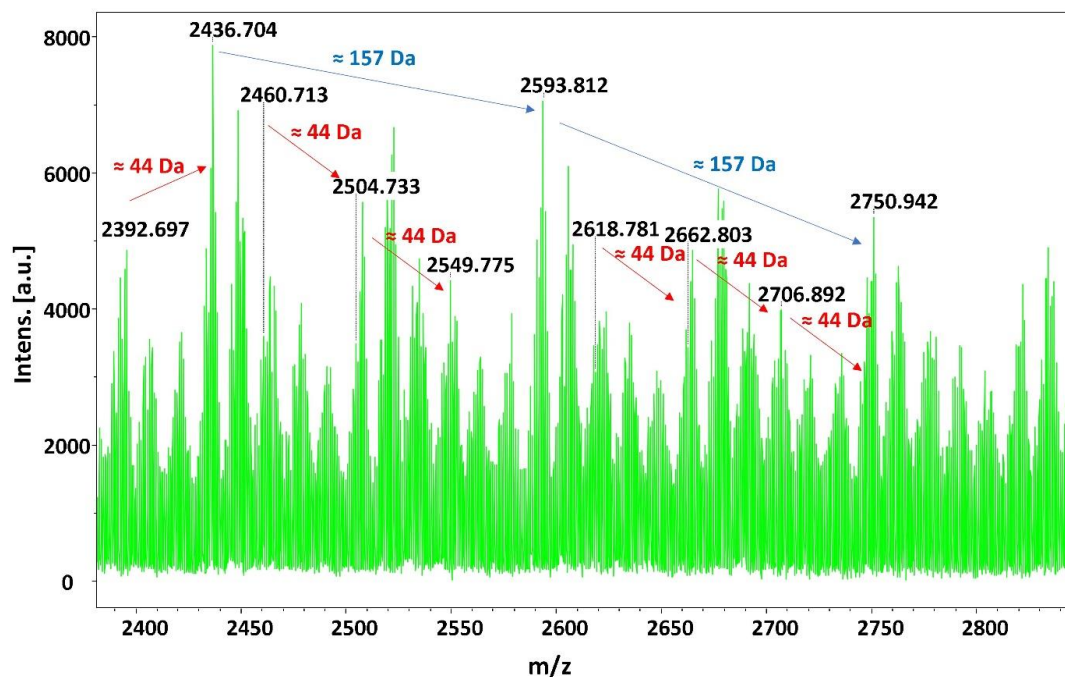


Figure 4. An expanded view of m/z the 2380-2900 region of MALDI mass spectrum of P(BMBA-EG-BMBA) block copolymer.

An expanded view of the m/z 2380-2900 region of the MALDI spectrum of P(BMBA-EG-BMBA) block copolymer was also illustrated in Figure 4. The differences between consecutive signals are about m/z 157 and m/z 44 corresponding to the masses of BMBA ($C_8H_{15}NO_2$) and EG (C_2H_4O) units in the copolymer, respectively. MALDI-TOF-MS analyzes of the ABA-type poly(BMBA-EG-BMBA) copolymer shows that chain extension of the PEG-1450 dialkoxide was fulfilled via HTP of isobutoxymethyl acrylamide.

Conclusion

The synthesis strategy given in the study to yield ABA-type triblock copolymers is simple and efficient. Results of the FTIR and MALDI mass methods prove indisputably the formation of novel ABA-type amphiphilic block copolymers. By a selection of appropriate lengths of PEG and the monomers capable of being involved in HTP, it may be possible to obtain well-defined ABA-type triblock copolymers for specific applications.

Scientific Ethics Declaration

The authors declare that the scientific ethical and legal responsibility of this article published in EPSTEM journal belongs to the authors.

References

Akiba, I., Akino, Y., Masunaga, H., & Sakurai, K. (2010, November). Self-assembly of amphiphilic block copolymers containing poly (n-octadecyl acrylate) block in aqueous solution. In *IOP Conference Series: Materials Science and Engineering*, 14(1), 012009. IOP Publishing.

- Boutevin, B., David, G., & Boyer, C. (2006). Telechelic oligomers and macromonomers by radical techniques. *Oligomers-Polymer Composites-Molecular Imprinting*, 31-135.
- Burguière, C., Chassenieux, C., & Charleux, B. (2003). Characterization of aqueous micellar solutions of amphiphilic block copolymers of poly (acrylic acid) and polystyrene prepared via ATRP. Toward the control of the number of particles in emulsion polymerization. *polymer*, 44(3), 509-518. [https://doi.org/10.1016/S0032-3861\(02\)00811-X](https://doi.org/10.1016/S0032-3861(02)00811-X).
- Çatıker, E., Güven, O., & Salih, B. (2018). Novel hydrophobic macromonomers for potential amphiphilic block copolymers. *Polymer Bulletin*, 75(1), 47-60.
- Çatıker, E., Öztürk, T., Atakay, M., & Salih, B. (2019). Synthesis and characterization of novel ABA type poly (Ester-ether) triblock copolymers. *Journal of Polymer Research*, 26(5), 1-9. <https://doi.org/10.1007/s10965-019-1778-5>.
- Çatıker, E., Öztürk, T., Atakay, M., & Salih, B. (2020). Synthesis and characterization of the ABA-type poly (ester-ether-ester) block copolymers. *Journal of Macromolecular Science, Part A*, 57(8), 600-609. <https://doi.org/10.1080/10601325.2020.1745080>.
- Danafar, H., Rostamizadeh, K., Davaran, S., & Hamidi, M. (2014). PLA-PEG-PLA copolymer-based polymersomes as nanocarriers for delivery of hydrophilic and hydrophobic drugs: preparation and evaluation with atorvastatin and lisinopril. *Drug Development and Industrial Pharmacy*, 40(10), 1411-1420.
- Francolini, I., Hall-Stoodley, L., & Stoodley, P. (2020). Biofilms, Biomaterials, and Device-Related Infections. In *Biomaterials Science* (pp. 823-840). Academic Press.
- Frey, H., & Ishizone, T. (2018). Living Anionic Polymerization–Part II: Further Expanding the Synthetic Versatility for Novel Polymer Architectures. *Macromolecular Chemistry and Physics*, 219(1), 1700567. <https://doi.org/10.1002/macp.201700567>.
- He, Y., He, W., Wei, R., Chen, Z., & Wang, X. (2012). Synthesizing amphiphilic block copolymers through macromolecular azo-coupling reaction. *Chemical Communications*, 48(7), 1036-1038. <https://doi.org/10.1039/c1cc16362k>.
- Iijima, M., Nagasaki, Y., Kato, M., & Kataoka, K. (1997). A potassium alcoholate-initiated polymerization of 2-(trialkylsiloxyethyl) methacrylate. *Polymer*, 38(5), 1197-1202. [https://doi.org/10.1016/S0032-3861\(96\)00623-4](https://doi.org/10.1016/S0032-3861(96)00623-4).
- Iwamura, T., Ashizawa, K., Adachi, K., & Takasaki, M. (2019). Anionic hydrogen- transfer polymerization of N- isopropylacrylamide under microwave irradiation. *Journal of Polymer Science Part A: Polymer Chemistry*, 57(24), 2415-2419.
- Karayianni, M., & Pispas, S. (2016). Self-assembly of amphiphilic block copolymers in selective solvents. In *Fluorescence Studies of Polymer Containing Systems* (pp. 27-63). Springer.
- LaRue, I., Adam, M., Zhulina, E. B., Rubinstein, M., Pitsikalis, M., Hadjichristidis, N., ... & Sheiko, S. S. (2008). Effect of the soluble block size on spherical diblock copolymer micelles. *Macromolecules*, 41(17), 6555-6563.
- Lee, R. S., & Huang, Y. T. (2010). Tuning the hydrophilic–hydrophobic balance of block-graft copolymers by click strategy: synthesis and characterization of amphiphilic PCL-b-(P₄N 3 CL-g-PBA) copolymers. *Polymer Journal*, 42(4), 304-312. <https://doi.org/10.1038/pj.2010.6>.
- Levit, M., Zashikhina, N., Vdovchenko, A., Dobrodumov, A., Zakharova, N., Kashina, A., ... & Korzhikova-Vlakh, E. (2020). Bio-inspired amphiphilic block-copolymers based on synthetic glycopolymer and poly (amino acid) as potential drug delivery systems. *Polymers*, 12(1), 183.
- Lunn, D. J., Discekici, E. H., Read de Alaniz, J., Gutekunst, W. R., & Hawker, C. J. (2017). Established and emerging strategies for polymer chain- end modification. *Journal of Polymer Science Part A: Polymer Chemistry*, 55(18), 2903-2914. <https://doi.org/10.1002/pola.28575>.
- Matyjaszewski, K. (2003). The synthesis of functional star copolymers as an illustration of the importance of controlling polymer structures in the design of new materials. *Polymer international*, 52(10), 1559-1565. <https://doi.org/10.1002/pi.1339>.
- Quadir, M. A., Morton, S. W., Deng, Z. J., Shopsowitz, K. E., Murphy, R. P., Epps III, T. H., & Hammond, P. T. (2014). PEG–polypeptide block copolymers as pH-responsive endosome-solubilizing drug nanocarriers. *Molecular Pharmaceutics*, 11(7), 2420-2430.
- Tasdelen, M. A., Kahveci, M. U., & Yagci, Y. (2011). Special Issue on Controlled/Living Polymerization. *Prog. Polym. Sci*, 36, 455-602.
- Verso, F. L., & Likos, C. N. (2008). End-functionalized polymers: Versatile building blocks for soft materials. *Polymer*, 49(6), 1425-1434. <https://doi.org/10.1016/j.polymer.2007.11.051>.
- Wang, G., Liu, Y., Xia, N., Zhou, W., Gao, Q., & Liu, S. (2017). The non-equilibrium self-assembly of amphiphilic block copolymers driven by a pH oscillator. *Colloids and Surfaces A: Physicochemical and Engineering Aspects*, 529, 808-814.

- Yorulmaz-Avsar, S., Kyropoulou, M., Di Leone, S., Schoenenberger, C. A., Meier, W. P., & Palivan, C. G. (2019). Biomolecules turn self-assembling amphiphilic block co-polymer platforms into biomimetic interfaces. *Frontiers in Chemistry*, 6, 645.
- Zarrintaj, P., Saeb, M. R., Jafari, S. H., & Mozafari, M. (2020). Application of compatibilized polymer blends in biomedical fields. In *Compatibilization of Polymer Blends* (pp. 511-537). Elsevier.
- Zhu, X., Fryd, M., Tran, B. D., Ilies, M. A., & Wayland, B. B. (2012). Modifying the hydrophilic–hydrophobic interface of PEG-b-PCL to increase micelle stability: preparation of PEG-b-PBO-b-PCL triblock copolymers, micelle formation, and hydrolysis kinetics. *Macromolecules*, 45(2), 660-665.

Author Information

Efkan CATIKER

Ordu University
52200 Ordu, Turkey.

Temel OZTURK

Giresun University
28200 Giresun, Turkey.

Bedrettin SAVAS

Kafkas University
36100 Kars, Turkey.
bdrtt.svs.36@gmail.com

Mehmet ATAKAY

Hacettepe University
06800 Ankara, Turkey.

Bekir SALIH

Hacettepe University
06800 Ankara, Turkey.

To cite this article:

Catiker, E., Ozturk, T., Savas, B., Atakay, M. & Salih, B. (2021). Synthesis of novel aba-type amphiphilic copolymers including 2-hydroxypropyl propionate and n-isobutoxymethyl β -alanine by peg-dialkoxide initiated hydrogen-transfer polymerization. *The Eurasia Proceedings of Science, Technology, Engineering & Mathematics (EPSTEM)*, 15, 21-27.

The Eurasia Proceedings of Science, Technology, Engineering & Mathematics (EPSTEM), 2021

Volume 15, Pages 28-34

ICBAST 2021: International Conference on Basic Science and Technology

Investigation of Conformation, Vibration and Electronic Properties of 2-Methoxythiophene Molecule by Theoretical Methods

Guventurk UGURLU
Kafkas University

Abstract: In this study, the structural parameters, vibrational frequency, the electronic energy, the dipole moment, the highest occupied molecular orbital (HOMO) energy, the lowest unoccupied molecular orbital (LUMO) energy, the polarizability, hyperpolarizability and the potential energy curves (PEC) of 2-methoxythiophene molecule were calculated at Hartree-Fock (HF) and Density Functional Theory (DFT) with B3LYP (Becke 3 Parameter Lee-Yang-Parr) model using the 6-311++(d,p) basis set in gas phase. The potential energy curves of the molecule were performed as a function the θ [C3-C2-O-C6] torsion angle varying from 0-360° at 10° intervals. The dipole moment value of the molecule was calculated as 1.99 Debye by the DFT/B3LYP/6-311++G(d,p) method and as 2.24 Debye by the HF/6-311++G(d,p) method, respectively. The obtained vibrational wave numbers were scaled with appropriate scale factors and the assigning of these vibrational wavenumbers was made according to the potential energy distribution (PED) using the VEDA 4f program. Also, by using HOMO-LUMO energies, energy gap values, ionization energy, electron affinity, chemical potential, electronegativity, hardness and softness indices were obtained. The approximate geometry of the molecules in three dimensions was drawn in the GaussView 5.0 molecular imaging program, and all theoretical calculations were used with the Gaussian 09W package.

Keywords: 2- methoxythiophene, Vibration analysis, Potential energy curve (PEC), Hartree-Fock, Dipole moment

Introduction

Thiophene and its substituted thiophene units are one of the important compounds in both organic synthesis and materials, and are versatile compounds used in various fields such as organic synthesis and materials science. The studies on thiophene having unique electronic and optical properties due to its small band gap and high polarizability continue to increase rapidly. The monomer of the thiophenes has been used as building blocks in the fields of dyes, pharmaceuticals, agrochemicals. Poly- and oligo thiophenes, which are thiophene forms, are used in material chemistry. They have received much attention for their conductivity (Li et al. 2009; Nejati et al. 2011; Schon et al. 2001) and optical nature affected by external stimuli (Shiraki et al. 2010; Yao et al. 2013) and application in field-effect transistors (Bao et al. 1999; Kline et al. 2006), electroluminescent devices (Mehes et al. 2016; Shao et al. 2014), and solar cells (Yan et al. 2019; Briseno et al. 2010). Also, they have become very important materials in practical applications like field effect transistors (Yang et al. 2016), photovoltaic (Kim et al. 2016), chemical sensors (Kim et al. 2016), thermal emission detectors, electrochromic materials (Lv et al. 2016). In the study on the 2-Methoxythiophene molecule, crystal structure of the molecule was determined experimentally using X-ray structure analysis and spectroscopic methods (Blake et al., 1999). The same studies, intramolecular and intermolecular geometry of the molecule with thiophenes with oxygen-containing substituents were examined.

The physical and chemical properties of a substance are strongly related to both its geometrical and electronic structures. In this work, molecular structure, dipole moment, relative energies, rotational barriers, polarizability,

- This is an Open Access article distributed under the terms of the Creative Commons Attribution-Noncommercial 4.0 Unported License, permitting all non-commercial use, distribution, and reproduction in any medium, provided the original work is properly cited.

- Selection and peer-review under responsibility of the Organizing Committee of the Conference

first static hyper polarizability, potential energy curve, the electronic structure and HOMO-LUMO energies of above-mentioned molecule have been studied. Also, by using HOMO-LUMO energies, energy gap values, ionization energy, electron affinity, chemical potential, electronegativity, hardness and softness indices were obtained. The molecular structure using numbering scheme of 2-Methoxythiophene is given in Figure 1.

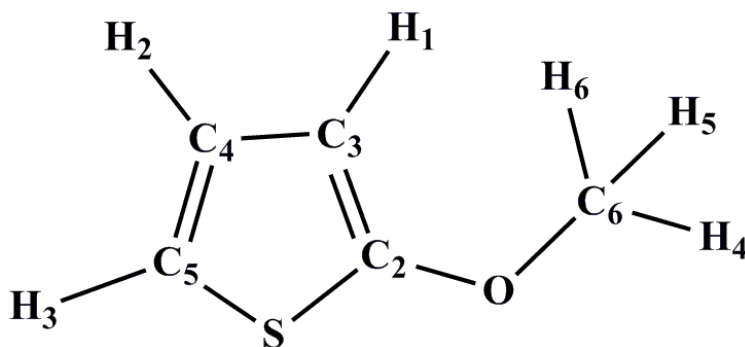


Figure 1. Molecular structure of 2-Methoxythiophene molecule numbering scheme

Method

Quantum-mechanical calculations on the title molecule was performed by the aid of Gaussian 09W program package and Gauss view 5.0 molecular visualization programs (Frisch et al., 2010; Dennington et al., 2009) in the gas phase. The structural parameters, vibrational frequency, the electronic energy, the dipole moment (μ), the highest occupied molecular orbital (HOMO) energy, the lowest unoccupied molecular orbital (LUMO) energy, the polarizability (α), hyperpolarizability (β) and the potential energy curves (PEC) of 2-methoxythiophene molecule were calculated at Hartree-Fock (HF) and Density Functional Theory (DFT) with B3LYP (Becke 3 Parameter Lee-Yang-Parr) (Becke et al., 1988; Lee et al., 1988; Becke, 1993) model using the 6-311++(d,p) basis set in gas phase. In order to obtain the best stable structures, Conformational analysis of the molecule was performed as a function of dihedral angle which was varied between 0 and 360° with increments of 10° both HF/6-311++G (d,p) and B3LYP/6-311++G(d,p) level of theory

Results and Discussion

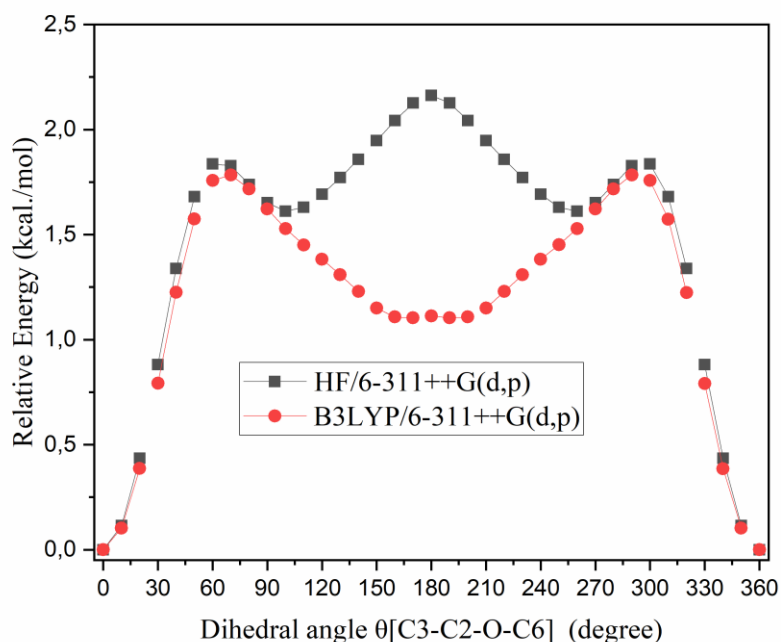


Figure 2. The potential energy curves of 2-Methoxythiophene molecule

Conformational Analysis and Torsional Barriers

The dihedral angle was defined as: θ [C3-C2-O-C6]. The dihedral angle θ is the C2-O single bond about which internal rotation forms clearly different conformations. The potential energy curves of the title molecule performed at both HF/6-311++G (d,p) and B3LYP/6-311G++ (d, p) level is shown Figure 2. The minimum of potential energy curves (PEC) was referred to as zero. Rotational barriers at 0° [$\Delta E_0 = E(\theta = 0^\circ) - E(\text{equilibrium})$], at 90° [$\Delta E_{90} = E(\theta = 90^\circ) - E(\text{equilibrium})$] and at 180° [$\Delta E_{180} = E(\theta = 180^\circ) - E(\text{equilibrium})$] were calculated by using the energies of the respective optimized structures. The low-energy conformers were obtained at 0 and 360° conformer. Maxima energy conformer were seen at 180° dihedral angle at HF/6-311++G (d,p) level of theory, but B3LYP/6-311G++ (d, p) level of theory, at 60 and 300° were seen.

Molecular Structure

The equilibrium state structures of 2-Methoxythiophene molecule obtained by the HF/6-311++ G (d,p) and DFT/6-311++G (d,p) methods are compiled. The calculated values of the electronic, dipole moment, polarizability, hyperpolarizability, HOMO, LUMO energy and energy gap (ΔE_g) at the ground-state equilibrium geometry of studied molecules are listed in Table 1.

Table 1. The electronic, HOMO, LUMO energy, dipole moment, polarizability, hyperpolarizability, and energy gap (ΔE_g) of 2-Methoxythiophene molecule

Electronic Energy (a.u)	B3LYP/6-311++G(d, p)					
	μ (D)	α (a.u)	β (a.u)	E_{HOMO} (a.u)	E_{LUMO} (a.u)	ΔE_g (eV)
-667.623428555	1.99	79,19	234,66	-0.217313	-0.011980	5,587
-665.258401234	HF/6-311++G(d, p)					
	2.24	72,51	176,01	-0.309299	0.037053	9,425

The X-ray crystal structures for studied molecule is available in the literature and (Blake et al., 1999) and the calculated parameter studied molecule of both at the B3LYP/6-311++G (d, p) and the HF/6-311++ G (d,p) methods in the ground state are tabulated in the Table 2 and findings here. As seen from Table 2, it is found that, in the title molecule, dihedral angle between the thiophene and methoxy group is planar and belong to Cs symmetry group.

Table 2. Selected structural parameters of 2-Methoxythiophene molecule

Atoms	Bond length (Å)		
	Exp ^a .	DFT	HF
S-C5	1.715(2)	1.7455	1.7376
S-C2	1.7232(17)	1.7491	1.7349
C2-O	1.350(2)	1.3488	1.3302
C2-C3	1.298(2)	1.3686	1.3478
C3-C4	1.440(3)	1.4342	1.4418
C4-C5	1.353(3)	1.3603	1.3400
O-C6	1.433(2)	1.4262	1.4046
Bond angle (°)			
C5-S-C2	91.35(9)	90.7238	90.8151
O-C2-C3	130.79(16)	131.3881	131.1727
O-C2-S	116.20(12)	116.4168	116.3542
C3-C2-S	113.01(13)	112.1951	112.4725
C2-C3-C4	109.11(16)	111.826	111.5949
C5-C4-C3	114.43(17)	113.6329	113.5237
C4-C5-S	112.10(15)	111.6222	111.5938
C2-O-C6	114.42(15)	116.1677	117.5966
Dihedral angle (°)			
C3-C2-O-C6	--	0,01	0,00
C1-C2-O-C6	--	-179.99	-179.99

(^a ref. Blake et al., 1999)

The electron affinity (A), global hardness (η)/softness (S), electronegativity (χ), chemical potential (μ), ionization potential (I), chemical potential (Pi) calculated by using HOMO-LUMO energies calculated the B3LYP/6-311++G (d, p) for the compound were given in Table 3.

Table 3. Electronic properties of 2-Methoxythiophene molecule

property	a.u	eV	kcal/mol	kJ/mol	
LUMO	-0,01198	-0,32598	-7,51749	-31,4535	
HOMO	-0,217313	-5,91324	-136,365	-570,555	
A	Electron affinity	0,01198	0,32598	7,51749	31,4535
I	Ionization potential	0,217313	5,91324	136,365	570,555
ΔE	Energy gap	0,205333	5,58725	128,847	539,102
χ	Electronegativity	0,1146465	3,11961	71,941	301,004
Pi	Chemical potential	-0,1146465	-3,11961	-71,941	-301,004
ω	Electrophilic index	0,000674715	0,01836	0,42339	1,77146
IP	Nucleophilic index	-0,01177035	-0,32028	-7,38593	-30,9031
S	Molecular softness	9,7403	265,04	6112,05	25573,1
η	Molecular hardness	0,1026665	2,79363	64,4235	269,551

Molecular electrostatic potential (MEP) surface values of the optimized geometry of 2-Methoxythiophene molecule by the HF/6-311++ G (d,p) and DFT/6-311++G (d,p) methods and the highest occupied molecular orbital (HOMO) energy, the lowest unoccupied molecular orbital (LUMO) obtained B3LYP/6-311++G (d, p) level of theory are presented Figure 3.

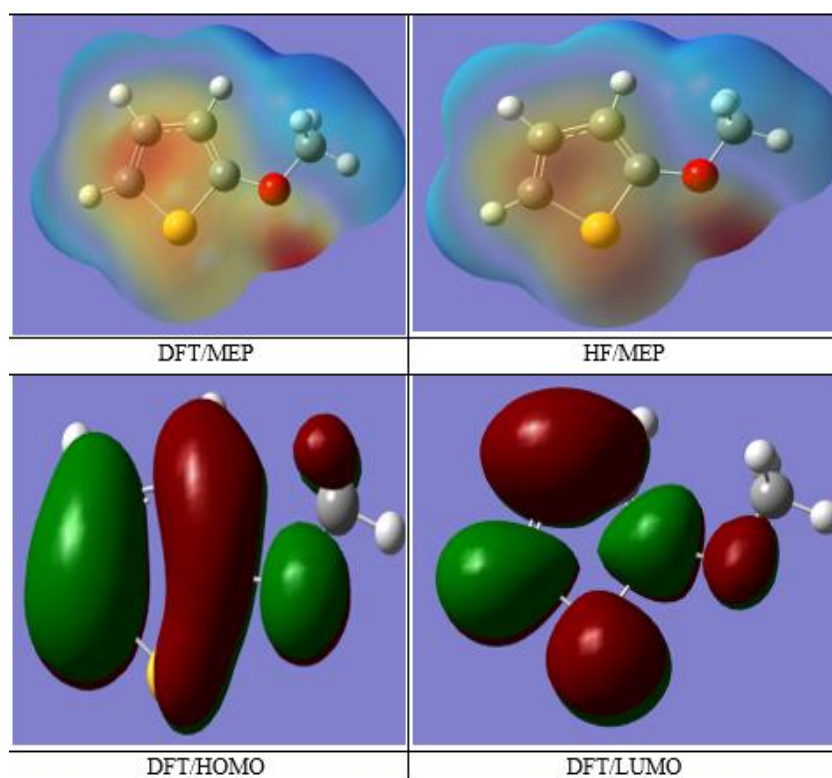


Figure 3. (a)The optimized geometry, (b) Molecular electrostatic (MEP) potential surface (PES) and HOMO-LUMO surface of 2-Methoxythiophene molecule

Vibrational Frequencies

2-Methoxythiophene molecule consist of 13 atoms having 33 normal modes of vibrations. The calculated vibrational wavenumbers, FT-IR and FT-Raman intensity of the title compounds are given in Table 4. Also, the calculated vibrational assignments of the normal modes were performed on the basis of the Potential Energy Distribution (PED) and it has been calculated using the Vibrational Energy Distribution Analysis VEDA 4

program (Jamroz, 2004). The molecular structure of the molecule belongs to Cs point group symmetry and It is seen, that the group Cs has two species, A' and A''.

Table 4. Electronic properties of 2-Methoxythiophene molecule

C	DFT/6-		Intensity		HF/6-		Intensity		Assignments with PED ($\geq 10\%$)
	Uns	Sc.	IR	Ram.	Uns	Sc.	IR	Ram.	
A'	325	311	0,9	139,2	340	308	2,1	123,9	C3H (26)C5H (69)
A'	322	308	3,5	97,7	337	306	5,3	81,8	C3H (70)C4H (21)
A'	319	306	7,8	104,6	335	303	10,2	86,8	C4H (75)C5H (21)
A'	314	301	15,5	103,3	329	298	29,1	99,0	C6H11(46)C6H12(46)
A	307	294	34,2	58,4	323	293	41,9	40,2	C6H11(50)C6H12(50)
A'	301	288	52,2	157,0	317	287	48,8	123,4	C6H13(91)
A'	158	155	110,4	9,7	173	157	118,1	4,3	C2C3(60)OC2(13)HC4C5(17)
A'	151	148	114,8	86,4	166	150	171,1	104,3	C5C4(46)HC6H(12)
A'	150	147	10,1	4,0	162	147	12,7	4,5	OC2(10)HC6H(68)HC6OC2(22)
A	148	146	10,4	11,8	161	146	9,0	10,8	HC6H(74)HC6OC2(12)HC6OC2
A'	146	143	60,0	27,4	159	144	79,5	24,3	C5C4(14)HC6H(70)
A'	138	136	4,7	6,2	149	135	4,1	7,2	C4C3(19)C2C3C4(14)HC5S(35)
A'	126	124	7,0	1,5	138	125	12,1	1,3	HC4C5(55)HC5S(12)
A'	122	120	234,2	2,1	135	123	283,7	3,0	C5C4(10)OC2(35) OC6(11)
A'	120	118	1,4	5,2	131	118	9,5	5,2	HC6H(20)HC6OC2(31)HC6OC2
A	116	114	0,7	3,0	128	116	2,5	2,7	HC6H(27)HC6OC2(25)HC6OC2
A'	110	109	15,5	14,2	120	108	13,1	18,3	HC3C4(26)HC5S(47)
A'	106	104	16,6	2,0	113	102	45,2	6,4	C4C3(48)HC3C4(30)
A'	102	100	28,3	3,3	111	101	1,4	2,4	OC6(72)C2C3C4(12)
A	889	874	0,0	1,0	102	931	0,0	2,6	HC3C2C1(47)HC4C5S(28)HC5SC
A'	844	830	18,2	7,2	904	820	21,0	5,5	C1S(29)C2C3C4(21)C5C4C3(30)
A	780	767	20,4	0,8	899	815	24,2	2,0	HC3C2C1(12)HC4C5S(60)C2C3C
A'	745	732	6,4	7,7	811	735	8,3	7,3	C5C4C3(11)SC5C4(33)
A'	724	712	6,5	12,4	778	705	10,0	12,2	C1S(49)C5C4C3(34)
A	674	662	81,4	0,0	770	698	99,7	0,0	HC3C2C1(37)HC5SC2(53)
A	558	548	3,8	1,1	620	562	0,9	1,8	HC5SC2(29)C2C3C4C5(47)OC3S
A'	551	542	7,8	3,0	595	539	7,5	2,8	C1S(18)SC5C4(43)
A	505	496	2,4	0,5	558	506	2,4	0,9	SC5C4C3(49)OC3SC2(31)
A'	401	394	2,5	7,9	433	392	2,2	5,0	C2C3C4(28)OC2S(25)C6OC2(31)
A	278	273	0,3	0,3	304	275	0,2	0,3	C2C3C4C5(21)SC5C4C3(29)OC3S
A'	234	230	3,0	1,0	253	229	3,2	1,0	OC2S(50)C6OC2(42)
A	202	198	0,1	1,3	223	202	0,2	0,8	HC6OC2 (56)OC3SC2(16)
A	82	81	4,7	0,5	93	84	5,5	0,6	C6OC2C3(78)

Conclusion

In this study, the structural parameters, vibrational frequency, the electronic energy, the dipole moment (μ), the highest occupied molecular orbital (HOMO) energy, the lowest unoccupied molecular orbital (LUMO) energy, the polarizability (α), hyperpolarizability (β) and the potential energy curves (PEC) of 2-methoxythiophene molecule were calculated at Hartree-Fock (HF) and Density Functional Theory (DFT) with B3LYP model using the 6-311++(d,p) basis set in gas phase. The calculated geometric parameters (bond lengths and bond-dihedral angles) of the molecule were compared with the experimental values in the literature (Blake et al., 1999) and they were found to be in good agreement. The vibrational frequencies and spectrums were obtained with the same methods and levels. All vibrational frequencies were found as positive. It is shown that titled compound was stable conclusions here.

The energy band gap, electron affinity (A), global hardness (η)/softness (S), electronegativity (χ), chemical potential (μ), ionization potential (I), chemical potential (Pi) properties of title molecule are calculated by using

the highest occupied molecular orbital (HOMO) energy, the lowest unoccupied molecular orbital (LUMO) energy.

Scientific Ethics Declaration

The authors declare that the scientific ethical and legal responsibility of this article published in EPSTEM journal belongs to the authors.

References

- Bao, Z., & Lovinger, A. J. (1999). Soluble regioregular polythiophene derivatives as semiconducting materials for field-effect transistors. *Chemistry of Materials*, 11(9), 2607-2612.
- Becke, A. D. (1988). Density-functional exchange-energy approximation with correct asymptotic behavior. *Physical review A*, 38(6), 3098.
- Becke, A. D., 1993. Density-functional thermochemistry .3. the role of exact exchange. *The Journal of Chemical Physics* 98(7), 5648-5652.
- Blake, A. J., Clark, B. A., Gierens, H., Gould, R. O., Hunter, G. A., McNab, H., ... & Sommerville, C. C. (1999). Intramolecular and intermolecular geometry of thiophenes with oxygen-containing substituents. *Acta Crystallographica Section B: Structural Science*, 55(6), 963-974.
- Briseno, A. L., Holcombe, T. W., Boukai, A. I., Garnett, E. C., Shelton, S. W., Fréchet, J. J., & Yang, P. (2010). Oligo- and polythiophene/ZnO hybrid nanowire solar cells. *Nano Letters*, 10(1), 334-340.
- Dennington, R., Keith T., Millam, J. (2009). Semichem, In *GaussView* (Version 5). Shawnee Mission.
- Frisch, M. J., Trucks G W, Schlegel H B, Scuseria G E, Robb M A, Cheeseman J R, Scalmani G, Barone V, Mennucci B, Petersson G A, Nakatsuji H, Caricato M, Li X, Hratchian H P, Izmaylov A F, Bloino J, Zheng G, Sonnenberg J L, Hada M, Ehara M, Toyota K, Fukuda R, Hasegawa J, Ishida, M, Nakajima T, Honda Y, Kitao O, Nakai H, Vreven T, Montgomery J A, Vreven T J, Peralta J E, Ogliaro F, Bearpark M, Heyd J. J, Brothers E, Kudin N, Staroverov V N, Kobayashi R, Normand J, Raghavachari K, Rendell A, Burant J C, Iyengar S S, Tomasi J, Cossi M, Rega N, Millam J M, Klene, M, Knox J E, Cross J B, Bakken V, Adamo C, Jaramillo J, Gomperts R, Stratmann R E, Yazyev O, Austin A J, Cammi R, Pomelli C J, Ochterski W, Martin L R, Morokuma K, Zakrzewski V G, Voth G A, Salvador P, Dannenberg J J, Dapprich S, Daniels A D, Farkas O, Foresman J B, Ortiz J V, Cioslowski J, Fox D J, (2009). *Gaussian Inc.* Wallingford.
- Jamroz, M. H. (2004) *Vibrational Energy Distribution Analysis*. VEDA Computer Program.
- Kim, J., Park, S. Y., Han, G., Chae, S., Song, S., Shim, J. Y., ... & Suh, H. (2016). Conjugated polymers containing 6-(2-thienyl)-4H-thieno [3, 2-b] indole (TTI) and isoindigo for organic photovoltaics. *Polymer*, 95, 36-44.
- Kim, D. M., Cho, S. J., Cho, C. H., Kim, K. B., Kim, M. Y., & Shim, Y. B. (2016). Disposable all-solid-state pH and glucose sensors based on conductive polymer covered hierarchical AuZn oxide. *Biosensors and Bioelectronics*, 79, 165-172.
- Kline, R. J., McGehee, M. D., & Toney, M. F. (2006). Highly oriented crystals at the buried interface in polythiophene thin-film transistors. *Nature Materials*, 5(3), 222-228.
- Lee, C., Yang, W., & Parr, R. G. (1988). Development of the Colle-Salvetti correlation-energy formula into a functional of the electron density. *Physical review B*, 37(2), 785.
- Li, X. G., Li, J., Meng, Q. K., & Huang, M. R. (2009). Interfacial synthesis and widely controllable conductivity of polythiophene microparticles. *The Journal of Physical Chemistry B*, 113(29), 9718-9727.
- Lv, X., Yan, S., Dai, Y., Ouyang, M., Yang, Y., Yu, P., & Zhang, C. (2015). Ion diffusion and electrochromic performance of poly (4, 4', 4''-tris [4-(2-bithienyl) phenyl] amine) based on ionic liquid as electrolyte. *Electrochimica Acta*, 186, 85-94.
- Méhes, G., Pan, C., Bencheikh, F., Zhao, L., Sugiyasu, K., Takeuchi, M., ... & Adachi, C. (2016). Enhanced electroluminescence from a thiophene-based insulated molecular wire. *ACS Macro Letters*, 5(7), 781-785.
- Nejati, S., & Lau, K. K. (2011). Chemical vapor deposition synthesis of tunable unsubstituted polythiophene. *Langmuir*, 27(24), 15223-15229.
- Schon, J.H., Dodabalapur, A., Bao, Z., Kloc, C.H., Schenker, O., Batlogg, B. (2001). Gate-induced superconductivity in a solution-processed organic polymer film. *Nature*. 410,189-92.
- Shao, M., Keum, J., Chen, J., He, Y., Chen, W., Browning, J. F., ... & Xiao, K. (2014). The isotopic effects of deuteration on optoelectronic properties of conducting polymers. *Nature communications*, 5(1), 1-11.

- Shiraki, T., Dawn, A., Tsuchiya, Y., & Shinkai, S. (2010). Thermo-and solvent-responsive polymer complex created from supramolecular complexation between a helix-forming polysaccharide and a cationic polythiophene. *Journal of the American Chemical Society*, 132(39), 13928-13935.
- Yan, W., Jiang, D., Liu, Q., Kang, Q., & Zhou, F. (2019). Solar cells constructed with polythiophene thin films grown along tethered thiophene–dye conjugates via photoelectrochemical polymerization. *ACS Applied Materials & Interfaces*, 11(20), 18755-18762.
- Yang, F., Li, C., Zhang, J., Feng, G., Wei, Z., & Li, W. (2016). Methylated conjugated polymers based on diketopyrrolopyrrole and dithienothiophene for high performance field-effect transistors. *Organic Electronics*, 37, 366-370.
- Yao, Z., Hu, X., Huang, B., Zhang, L., Liu, L., Zhao, Y., & Wu, H. C. (2013). Halochromism of a polythiophene derivative induced by conformational changes and its sensing application of carbon dioxide. *ACS applied materials & interfaces*, 5(12), 5783-5787.

Author Information

Guventurk UGURLU

Kafkas University

Kars 36100 Turkey

Contact e-mail: gugurlu@kafkas.edu.tr

To cite this article:

Ugurlu, G. (2021). Investigation of conformation, vibration and electronic properties of 2- methoxythiophene molecule by theoretical methods. *The Eurasia Proceedings of Science, Technology, Engineering & Mathematics (EPSTEM)*, 15, 28-34.

The Eurasia Proceedings of Science, Technology, Engineering & Mathematics (EPSTEM), 2021

Volume 15, Pages 35-41

ICBAST 2021: International Conference on Basic Science and Technology

Theoretical and Experimental Properties of 3-Ethyl-4-(3-Acetoxy-4-Methoxy-Benzylidenamino)-4,5-Dihydro-1*H*-1,2,4-Triazol-5-One

Songul ULUFER BULUT
Kafkas University

Murat BEYTUR
Kafkas University

Haydar YUKSEK
Kafkas University

Abstract: In the theoretical study, the 3-ethyl-4-(3-acetoxy-4-methoxy-benzylidenamino)-4,5-dihydro-1*H*-1,2,4-triazol-5-one has been optimized using B3LYP/6-311G(d) basis set. ¹H-NMR and ¹³C-NMR isotropic shift values were calculated by the method of GIAO using the program package Gaussian G09. Experimental and theoretical values were inserted into the graphic according to equation of $\delta_{\text{exp}_a+b} = \delta_{\text{calc}}$. The standard error values were found via SigmaPlot program with regression coefficient of a and b constants. IR absorption frequencies of this compound were calculated with same method. Theoretically calculated IR data are multiplied with appropriate adjustment factors and the data obtained according to DFT method are formed using theoretical infrared spectrum. The veda4f program was used in defining IR data which were calculated theoretically. The thermodynamic parameters, HOMO and LUMO energies, electronic properties, Mulliken atomic charges of titled compound has been investigated by using Gaussian 09W program. The spectroscopic data of this compound has been calculated by using 6-311G(d) basis set with density functional method (DFT/B3LYP) and compared with experimental values.

Keywords: Schiff base, B3LYP, Spectroscopic, Thermodynamic, Mulliken

Introduction

Heterocyclic compounds are defined as cyclic compounds consisting of carbon and heteroatom within a ring. They exhibit a variety of chemical and biological applications as a result of their structural diversity (Bahçeci et al., 2016; Koç et al., 2019; Bahçeci et al., 2017; Beytur et al., 2019; Çiftçi et al., 2018; Beytur et al., 2021; Beytur, 2020; Turhan Irak et al., 2019; Uğurlu et al., 2020; Boy et al, 2021). The optimized molecular structure, vibrational frequencies, UV-Vis spectroscopic parameters, atomic charges and frontier molecule orbitals (HOMO and LUMO) of the titled compound have been calculated by using DFT/B3LYP method with 6-311G(d) basis set. All quantum chemical calculations were carried out by using Gaussian 09W (Frisch et al., 2009; Wolinski et al., 1990) program package and the GaussView molecular visualization program (Frisch et al., 2003). The molecular structure and vibrational calculations of the molecule were computed by using Becke-3-Lee Yang Parr (B3LYP) (Becke, 1993; Lee et al., 1988) density functional method with 6-311G(d) basis set in ground state. IR absorption frequencies of analyzed molecule were calculated. Then, they were compared with experimental data, which are shown to be accurate. Infrared spectrum was composed by using the data obtained from both methods. The assignments of fundamental vibrational modes of the title molecule were performed on the basis of total energy distribution (TED) analysis by using VEDA 4f program (Jamróz, 2004).

- This is an Open Access article distributed under the terms of the Creative Commons Attribution-Noncommercial 4.0 Unported License, permitting all non-commercial use, distribution, and reproduction in any medium, provided the original work is properly cited.

- Selection and peer-review under responsibility of the Organizing Committee of the Conference

© 2021 Published by ISRES Publishing: www.isres.org

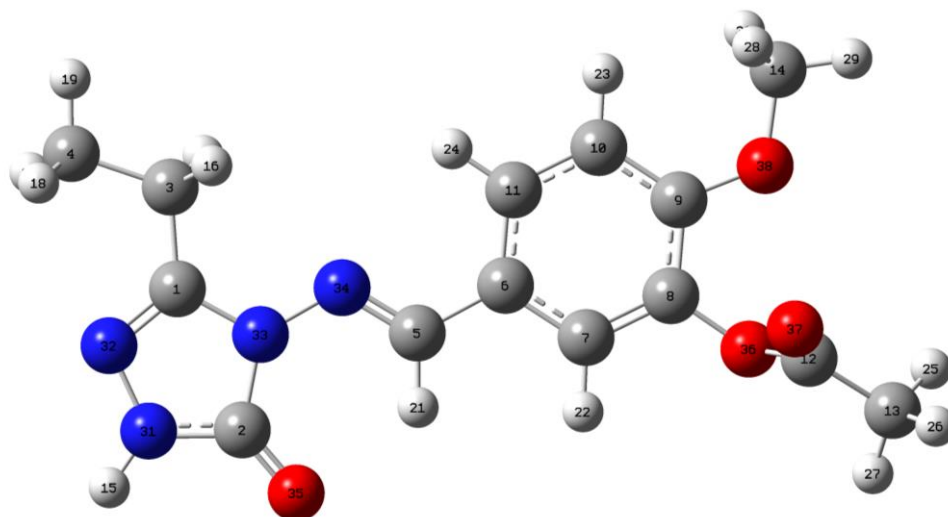


Figure 1. The optimized molecular structure of titled molecule with DFT 6–311G(d,p) level.

Table 1. The calculated and experimental ^{13}C and ^1H NMR isotropic chemical shifts of the molecule.

No	Experim.	DFT/6311(d)/DMSO	Diff./DMSO
1C		153,83	-153,83
2C		153,81	-153,81
3C		21,96	-21,96
4C		7,67	-7,67
5C		151,70	-151,70
6C		130,76	-130,76
7C		129,84	-129,84
8C		145,67	-145,67
9C		159,97	-159,97
10C		113,83	-113,83
11C		126,30	-126,30
12C		174,08	-174,08
13C		20,30	-20,30
14C		54,33	-54,33
15H	11,74	6,74	5,00
16H	2,55	2,49	0,06
17H	2,60	2,50	0,10
18H	1,20	0,98	0,22
19H	1,20	0,92	0,28
20H	1,20	0,99	0,21
21H	9,49	9,42	0,07
22H	7,10	6,75	0,35
23H	6,98	6,62	0,36
24H	7,51	7,83	-0,32
25H	2,45	2,10	0,35
26H	2,30	1,36	0,94
27H	2,4	2,01	0,39
28H	3,86	3,34	0,52
29H	3,86	3,76	0,10
30H	3,86	3,47	0,39

Method

The molecular structure of the title compound in the ground state (in vacuo) is computed by performing the density functional theory (DFT) by a hybrid functional B3LYP functional (Becke's three parameter hybrid functional using the LYP correlation functional) methods (Becke, 1993; Lee et. al., 1988) at 6-311G(d) level.

Results and Discussion

NMR spectral analysis

In nuclear magnetic resonance (NMR) spectroscopy, the isotropic chemical shift analysis allows us to identify relative ionic species and to calculate reliable magnetic properties which provide the accurate predictions of molecular geometries (Rani et al., 2010; Subramanian et al., 2010; Wade, 2006). In this framework, the optimized molecular geometry of the molecule was obtained by using B3LYP method with 6-311G(d) basis level in DMSO solvent. By considering the optimized molecular geometry of the title compound the ^1H and ^{13}C NMR chemical shift values were calculated at the same level by using Gauge-Independent Atomic Orbital (GIAO) method (Table 1). Theoretical and experimental (Bahçeci et al., 2017) values were plotted according to $\delta_{\text{exp}} = a \cdot \delta_{\text{calc}} + b$, Eq. a and b constants regression coefficients with a standard error values were found using the SigmaPlot program.

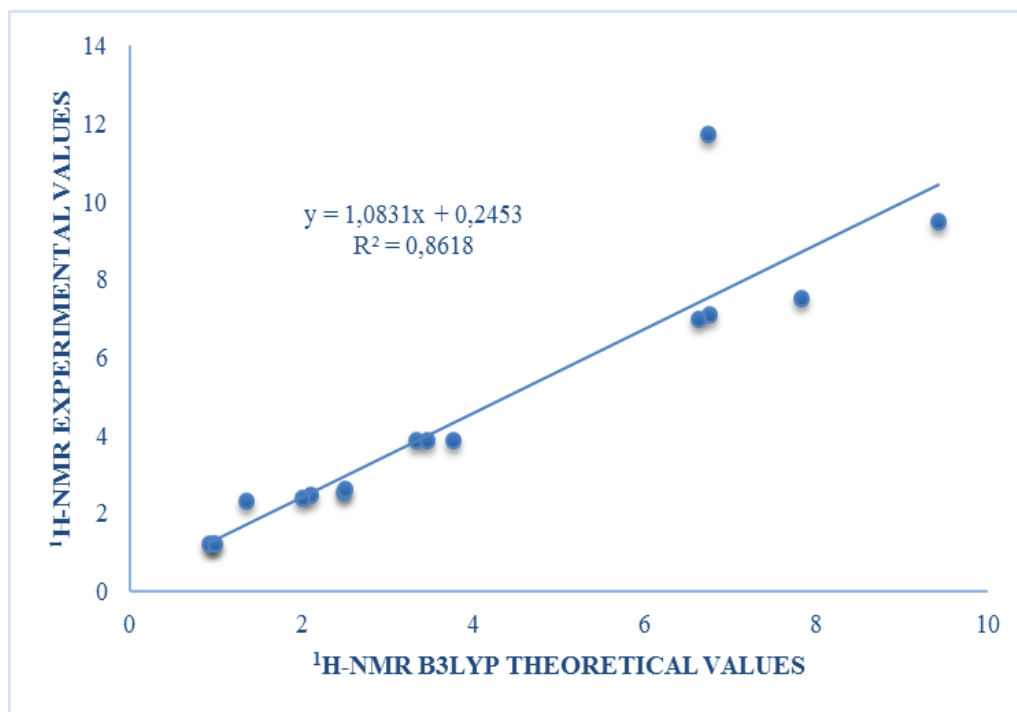


Figure 2. The correlation graphics for ^1H -NMR (DMSO) chemical shifts of the molecule

Vibrational frequencies

The 3-ethyl-4-(3-acetoxy-4-methoxy-benzylidenamino)-4,5-dihydro-1H-1,2,4-triazol-5-one has 38 atoms and the number of the normal vibrations are 108. The observed and calculated vibrational frequencies, the calculated IR intensities and assignments of selected vibrational frequencies for title compound are summarized in Table 2.

Table 2. The calculated frequencies values of the molecule.

Selected Vibrational Types	Experimental	scaled DFT
ν O_{36}C_8 , $\text{O}_{36}\text{C}_{12}$ (10)	1270	1208
ν O_{36}C_8 , $\text{O}_{36}\text{C}_{12}$ (22)	1270	1308
ν N_{32}C_1 , N_{34}C_5 (48)	1605	1644
ν N_{32}C_1 , N_{34}C_5 (31)	1605	1649
ν N_{32}C_1 , N_{34}C_5 (37)	1605	1671
ν O_{35}C_2 (73)	1710	1806
ν $\text{O}_{37}\text{C}_{12}$ (88)	1760	1850
ν $\text{N}_{31}\text{H}_{15}$ (100)	3190	3691

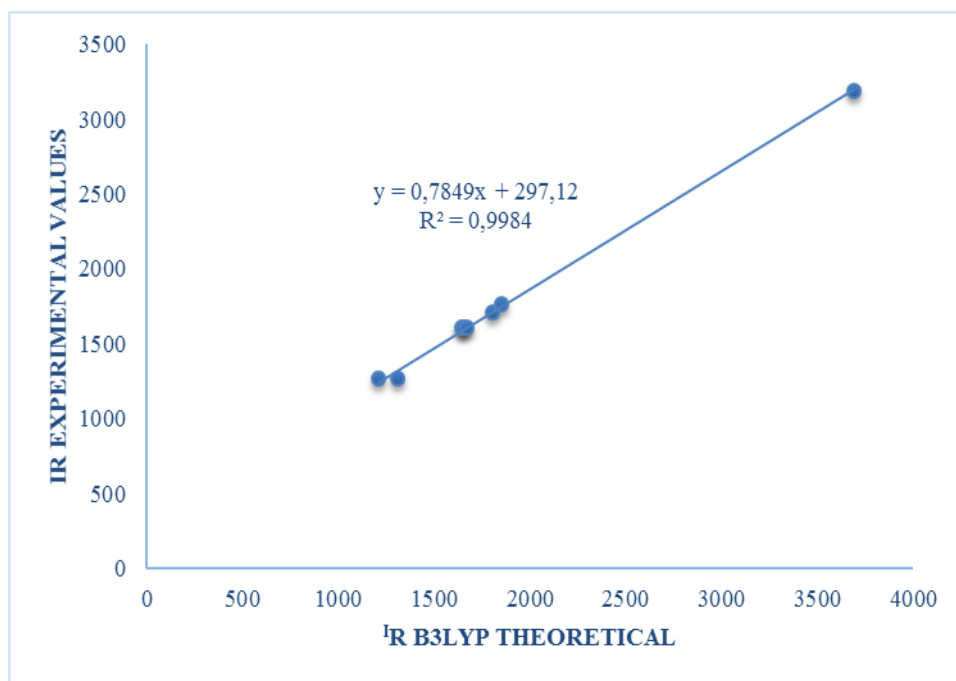
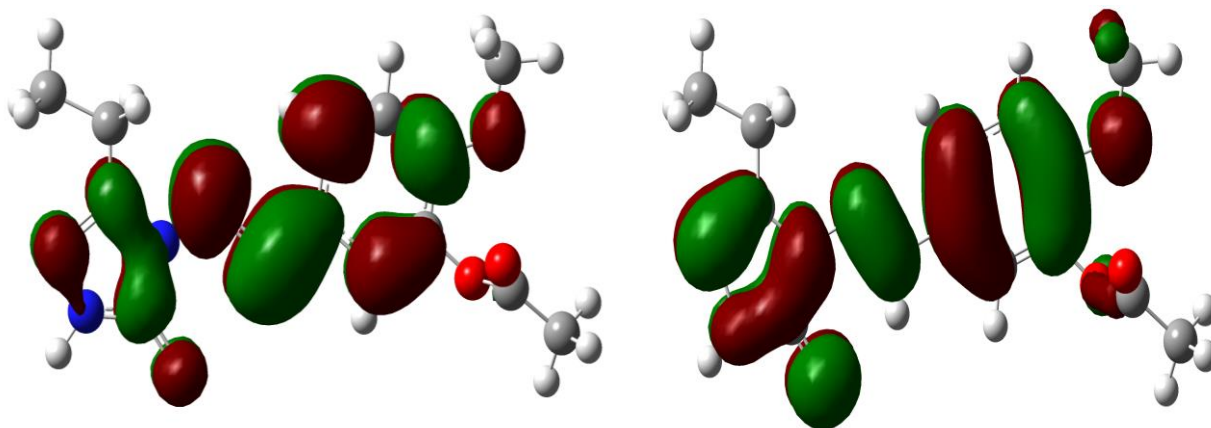


Figure 3. The correlation graphic for vibrational frequencies of the titled compound.

Electronic Properties



E_{LUMO} (B3LYP): -37.234 Kcal/mol

E_{LUMO} (B3LYP): -136.82 Kcal/mol

Figure 3. The calculated HOMO-LUMO energies of the molecule according to DFT/B3LYP/6-31G(d) level

Table 3. Electronic properties of the molecule

	DFT (kcal/mol)
Ionization Potential	136.82
Electron Affinity	37.27
Electronegativity	87.05
Chemical hardness	99.55

Table 4. The calculated dipole moment values of the molecule

Dipole Moment	B3LYP (a.u.)
μ_x	1.6480
μ_y	3.0189
μ_z	-1.1653
μ_{Toplam}	3.6315

Table 5. Mulliken atomic charges of the molecule

Atoms	DFT	Atoms	DFT	Atoms	DFT
1C	0.4347	14C	-0.4626	27H	0.2375
2C	0.5819	15H	0.3700	28H	0.2210
3C	-0.4685	16H	0.2321	29H	0.2337
4C	-0.6179	17H	0.2312	30H	0.2128
5C	-0.0602	18H	0.2200	31N	-0.4961
6C	-0.0146	19H	0.2083	32N	-0.2064
7C	-0.2260	20H	0.2198	33N	-0.3734
8C	0.2083	21H	0.2580	34N	-0.2106
9C	0.2731	22H	0.2099	35O	-0.3945
10C	-0.2712	23H	0.2182	36O	-0.3552
11C	-0.1566	24H	0.2104	37O	-0.3158
12C	0.3912	25H	0.2409	38O	-0.3334
13C	-0.6885	26H	0.2387		

Table 6. The thermodynamic properties of the titled compound

Rotational temperatures (Kelvin)	B3LYP
A	0.0290
B	0.0052
C	0.0046
Rotational constants (GHZ)	
A	0.6041
B	0.1092
C	0.0948
Zero-point vibrational energy (Kcal/Mol)	186.0992
Thermal correction to Energy	0.3182
Thermal correction to Enthalpy	0.3191
Thermal correction to Gibbs Free Energy	0.2432
Sum of electronic and zero-point Energies	-1062.9562
Sum of electronic and thermal Energies	-1062.9346
Sum of electronic and thermal Enthalpies	-1062.9336
Sum of electronic and thermal Free Energies	-1063.0095
Thermal Energies E(Kcal/mol)	
Translational	0.889
Rotational	0.889
Vibrational	197.886
Total	199,663
Thermal Capacity CV(Cal/Mol-Kelvin)	
Translational	2.981
Rotational	2.981
Vibrational	72.515
Total	78.477
Entropy S (Cal/Mol-Kelvin)	
Translational	43.033
Rotational	35.196
Vibrational	81.502
Total	159.732

Conclusion

The ^1H and ^{13}C NMR chemicals shifts, vibrational frequencies, HOMO and LUMO analyses and atomic charges of 3-ethyl-4-(3-acetoxy-4-methoxy-benzylidenamino)-4,5-dihydro-1H-1,2,4-triazol-5-one have been calculated by using DFT/B3LYP method. ^1H NMR chemical shifts parameters were obtained theoretically are in a very good agreement with the experimental data. Mulliken atomic charges of the titled compound have been investigated by the same basis set. Thermodynamic properties of analyzed molecule were calculated.

Scientific Ethics Declaration

The authors declare that the scientific ethical and legal responsibility of this article published in EPSTEM journal belongs to the authors.

References

- Becke, A. D. (1993). Density functional thermochemistry. III. The role of exact exchange, *The Journal of Chemical Physics*, 98, 5648-5652.
- Bahçeci, Ş., Yıldırım, N., Gürsoy-Kol, Ö., Manap, S., Beytur, M., & Yüksek, H. (2016). Synthesis, characterization and antioxidant properties of new 3-alkyl (aryl)-4-(3-hydroxy-4-methoxybenzylidenamino)-4, 5-dihydro-1H-1, 2, 4-triazol-5-ones. *Rasayan Journal of Chemistry*, 9(3), 494-501.
- Bahçeci, Ş., Yıldırım, N., Alkan, M., Gürsoy-Kol Ö., Manap, S., Beytur, M. & Yüksek, H. (2017). Investigation of antioxidant, biological and acidic properties of new 3-alkyl(aryl)-4-(3-acetoxy-4-methoxybenzylidenamino)-4,5-dihydro-1H-1,2,4-triazol-5-ones, *The Pharmaceutical and Chemical Journal*. 4 (4), 91-101.
- Beytur, M. (2020). Fabrication of platinum nanoparticle/boron nitride quantum dots/6-methyl-2-(3-hydroxy-4-methoxybenzylidenamino)-benzothiazole (ils) nanocomposite for electrocatalytic oxidation of methanol. *Journal of the Chilean Chemical Society*, 65(3), 4929-4933.
- B Beytur, M., & Avinca, I. (2021). Molecular, electronic, nonlinear optical and spectroscopic analysis of heterocyclic 3-substituted-4-(3-methyl-2-thienylmethyleneamino)-4, 5-dihydro-1h-1, 2, 4-triazol-5-ones: experiment and dft calculations. *Heterocyclic Communications*, 27(1), 1-16.
- Beytur, M., Irak, Z. T., Manap, S., & Yüksek, H. (2019). Synthesis, characterization and theoretical determination of corrosion inhibitor activities of some new 4, 5-dihydro-1H-1, 2, 4-triazol-5-one derivatives. *Heliyon*, 5(6), e01809.
- Boy, S. Türkan, F. Beytur, M. Aras, A. Akyıldırım O., Sedef Karaman, H., & Yüksek, H. (2017). Synthesis, design, and assessment of novel morpholine-derived Mannich bases as multifunctional agents for the potential enzyme inhibitory properties including docking study, *Bioorganic Chemistry*, 107, 104524.
- Çiftçi, E., Beytur M., Calapoğlu M., Gürsoy Kol Ö., Alkan M., Toğay, V.A., Manap S., Yüksek H. (2018). Synthesis, characterization, antioxidant and antimicrobial activities and DNA damage of some novel 2-[3-alkyl (aryl)-4,5-dihydro-1h-1,2,4-triazol-5-one-4-yl]-phenoxyacetic acids in human lymphocytes. *Research Journal of Pharmaceutical, Biological and Chemical Sciences*, 9(5), 1760-1771.
- Koç, E., Yüksek, H., Beytur, M., Akyıldırım, O., Akçay, M., & Beytur, C. (2020). Heterosiklik 4, 5-dihidro-1H-1, 2, 4-triazol-5-on Türevinin Antioksidan Özelliğinin Erkek Ratlarda (Wistar albino) İn vivo Olarak Belirlenmesi. *Bitlis Eren Üniversitesi Fen Bilimleri Dergisi*, 9(2), 542-548.
- Frisch, A., Nielson, A. B., & Holder, A. J. (2003). *Gaussview User Manual*. Inc. Wallingford.
- Frisch, M. J., Trucks, G., Schlegel, H. B., Scuseria, G. E., Robb, M. A., Cheeseman, J. R., Scalmani, G., Barone, V., Mennucci, B., Petersson, G. A., Nakatsuji, H., Caricato, M., Li, X., Hratchian, H. P., Izmaylov, A. F., Bloino, J., Zheng, G., Sonnenberg, J. L., Hada, M., Ehara, M., Toyota, K., Fukuda, R., Hasegawa, J., Ishida, M., Nakajima, T., Honda, Y., Kitao, O., Nakai, H., Vreven, T., Montgomery, J. A., Jr. Vreven, T., Peralta, J. E., Ogliaro, F., Bearpark, M., Heyd, J. J., Brothers, E., Kudin, N., Staroverov, V. N., Kobayashi, R., Normand, J., Raghavachari, K., Rendell, A., Burant, J. C., Iyengar, S. S., Tomasi, J., Cossi, M., Rega, N., Millam, J. M., Klene, M., Knox, J. E., Cross, J. B., Bakken, V., Adamo, C., Jaramillo, J., Gomperts, R., Stratmann, R. E., Yazyev, O., Austin, A. J., Cammi, R., Pomelli, C., Ochterski, J. W., Martin, L. R., Morokuma, K., Zakrzewski, V. G., Voth, G. A., Salvador, P., Dannenberg, J. J., Dapprich, S., Daniels, A. D., Farkas, O., Foresman, J. B., Ortiz, J. V., Cioslowski, J. & Fox, D. J. (2009). *Gaussian Inc.* Wallingford.
- Jamróz, M. H. (2004). *Vibrational energy distribution analysis: VEDA 4 program*.
- Lee, S. Y. (1998). Molecular structure and vibrational spectra of biphenyl in the ground and the lowest triplet states. *Bulletin of the Korean Chemical Society*, 19(1), 93-98.
- Rani, A. U., Sundaraganesan, N., Kurt, M., Cinar, M., & Karabacak, M. (2010). FT-IR, FT-Raman, NMR spectra and DFT calculations on 4-chloro-N-methylaniline. *Spectrochimica Acta Part A: Molecular and Biomolecular Spectroscopy*, 75(5), 1523-1529.
- Subramanian, N., Sundaraganesan, N., & Jayabharathi, J. (2010). Molecular structure, spectroscopic (FT-IR, FT-Raman, NMR, UV) studies and first-order molecular hyperpolarizabilities of 1, 2-bis (3-methoxy-4-hydroxybenzylidene) hydrazine by density functional method. *Spectrochimica Acta Part A: Molecular and Biomolecular Spectroscopy*, 76(2), 259-269.

- Turhan-Irak, Z., & Beytur, M. (2019). 4-Benzilidenamino-4, 5-dihidro-1H-1, 2, 4-triazol-5-on türevlerinin antioksidan aktivitelerinin teorik olarak incelenmesi. *Journal of the Institute of Science and Technology*, 9(1), 512-521.
- Uğurlu, G., & Beytur, M. (2020). Theoretical studies on the structural, vibrational, conformational analysis and nonlinear optic (NLO) property of 4-(Methoxycarbonyl) phenylboronic acid. *Indian Journal of Chemistry-Section A*, 59(10), 1504-1512.
- Wade, Jr. L.G. (2006). *Organic chemistry* (6nd ed.). Pearson Prentice Hall.
- Wolinski, K., Hinton, J. F., & Pulay, P. (1990). Efficient implementation of the gauge-independent atomic orbital method for NMR chemical shift calculations. *Journal of the American Chemical Society*, 112(23), 8251-8260

Author Information

Songul ULUFER- BULUT

Kafkas University
Kars, Turkey
Contact e-mail: sngulufer@gmail.com

Murat BEYTUR

Kafkas University
Kars, Turkey

Haydar YUKSEK

Kafkas University
Kars, Turkey

To cite this article:

Ulufur-Bulut, S., Beytur, M. & Yuksek, H. (2021). Theoretical and experimental properties of 3-ethyl-4-(3-acetoxy-4-methoxy-benzylidenamino)-4,5-dihydro-1h-1,2,4-triazol-5-one. *The Eurasia Proceedings of Science, Technology, Engineering & Mathematics (EPSTEM)*, 15, 35-41.

The Eurasia Proceedings of Science, Technology, Engineering & Mathematics (EPSTEM), 2021

Volume 15, Pages 42-53

ICBAST 2021: International Conference on Basic Science and Technology**Theoretical (6-311G(d,p)/ 3-21G) and Spectroscopic (¹³C/ ¹H-NMR, FT-IR) Analyses of 3-Propyl-4-[3-(2-Methylbenzyloxy)-Benzylideneamino]-4,5-Dihydro-1*h*-1,2,4-Triazol-5-One Molecule****Songul ULUFER BULUT**
Kafkas University**Gul KOTAN**
Kafkas University**Haydar YUKSEK**
Kafkas University

Abstract: The molecule was studied with the method Density Functional Theory (DFT) using two different the basis sets (6-311G(d,p)/ 3-21G) in the Gaussian 09W program. First, the most stable three-dimensional shape of the molecule was determined with the GaussView5.0 program (Dennington et al., 2009). Based on the structure of this optimized molecule, spectroscopic properties (FT-IR, ¹³C/ ¹H-NMR), the electronic properties (electron affinity (A), ionization potential (I), electronegativity (χ), chemical hardness and softness, electrophilic and nucleophilic index), HOMO-LUMO energies and ΔE_g energy, the geometric properties (bond length and angle) ve the thermodynamic properties (thermal energy (E), thermal capacity (CV), entropy (S)) were calculated with DFT/ 6-311G(d,p) and 3-21G. In addition, the total energy of the molecule, mulliken atomic charge values, dipole moment, molecular electron potential (MEP), total density and contour surface maps were determined. The electrophilic and nucleophilic regions of the structure were confirmed. Theoretical calculations of ¹³C/ ¹H-NMR isotropic shift values were performed in gas phase and solvent (DMSO) according to GIAO method and regression analyzes were by compare with experimental values of computational data. R² values were calculated and regression graphs were created. FT-IR (Infrared) vibration frequency values were calculated from the Veda4f program. The theoretical vibration frequency values were compared with the experimental IR values. Experimental data obtained from the literature.

Keywords: 1,2,4-Triazole-5-one, Giau, Mep, Homo-Lumo.

Introduction

Compounds containing the 4,5-dihydro-1*H*-1,2,4-triazol-5-one ring are antimicrobial (Turan-Zitouni et.al., 2005; Bayrak et.al., 2010), antitumor, anti-HIV (Ikizler et.al, 1998), antifungal (Sancak et.al.,2010), anticarcinogenic (Guzeldemirci et. al., 2010), inflammation preventive (Aytac et.al.,2009), antiviral (Hashem et.al., 2007), antioxidant (Gürsoy-Kol et.al., 2016), with biological properties (Chohan et.al., 2010), with pharmacological properties (Kucukguzel et.al., 2000), antimycobacterial (Klimeová et.al., 2004) have been reported in many different studies. Quantum chemical calculations have been used commonly to theoretically estimate the structure, electronic properties, thermodynamics, spectroscopy of molecular systems. (Yüksek et.al., 2005) Theoretical calculations investigated for the molecule were calculated with the Gaussian 09 quantum chemistry program (Frisch et.al., 2009) on an equipped computer. Assential calculations were carried out using the Density Functional Theory DFT method with the restricted B3LYP (Kohn et.al., 1996; Becke

- This is an Open Access article distributed under the terms of the Creative Commons Attribution-Noncommercial 4.0 Unported License, permitting all non-commercial use, distribution, and reproduction in any medium, provided the original work is properly cited.

- Selection and peer-review under responsibility of the Organizing Committee of the Conference

© 2021 Published by ISRES Publishing: www.isres.org

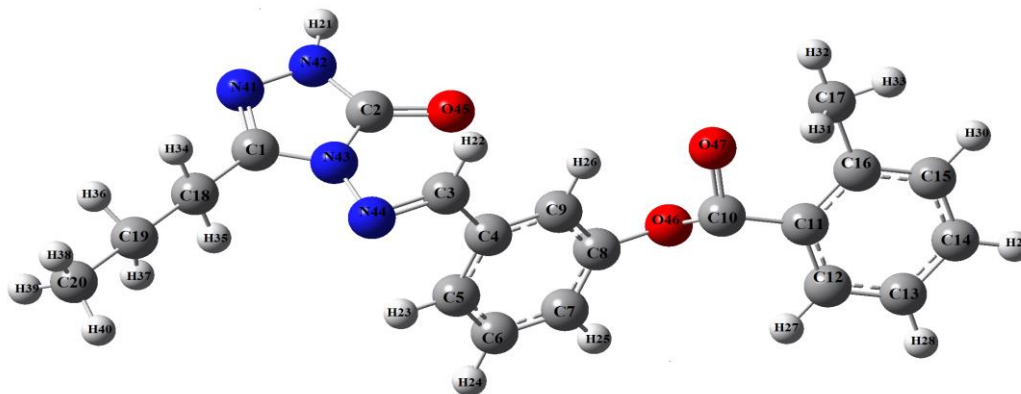


Figure 1. The Gaussview structure of the molecule.

Table 1. $^1\text{H}/^{13}\text{C}$ -NMR(DMSO) isotropic chemical shifts (δ /ppm)

No	Deneysel	B3LYP 3-21G/DMSO	Fark/DM SO	B3LYP/6-311G/DMSO	Fark/DM SO
C1	146.93	134.70	12.23	153.21	-6.28
C2	152.66	133.71	18.95	153.76	-1.10
C3	151.26	135.39	15.87	153.80	-2.54
C4	135.22	117.53	17.69	139.83	-4.61
C5	120.69	104.81	15.88	124.31	-3.62
C6	130.27	112.28	17.99	133.90	-3.63
C7	125.08	106.36	18.72	127.88	-2.80
C8	151.03	138.43	12.60	157.70	-6.67
C9	128.13	107.23	20.90	130.42	-2.29
C10	165.19	151.77	13.42	168.33	-3.14
C11	126.25	111.24	15.01	129.95	-3.70
C12	131.89	115.09	16.80	136.54	-4.65
C13	125.47	109.90	15.57	129.77	-4.30
C14	133.08	116.84	16.24	138.65	-5.57
C15	130.84	115.30	15.54	136.02	-5.18
C16	140.20	127.13	13.07	151.59	-11.39
C17	21.23	22.78	-1.55	25.07	-3.84
C18	26.62	25.14	1.48	30.52	-3.90
C19	18.85	19.28	-0.43	23.17	-4.32
C20	13.46	10.90	2.56	12.14	1.32
H21	11.88	6.71	5.17	8.06	3.82
H22	9.77	10.05	-0.28	10.88	-1.11
H23	7.77	7.70	0.07	9.00	-1.23
H24	7.60	7.10	0.50	8.45	-0.85
H25	8.12	6.78	1.34	8.18	-0.06
H26	7.79	8.38	-0.59	8.31	-0.52
H27	7.43	8.14	-0.71	9.38	-1.95
H28	7.62	6.96	0.66	8.26	-0.64
H29	7.47	7.12	0.35	8.44	-0.97
H30	7.45	7.01	0.44	8.29	-0.84
H31	2.61	2.86	-0.25	3.53	-0.92
H32	2.61	2.85	-0.24	3.67	-1.06
H33	2.61	2.07	0.54	2.94	-0.33
H34	2.66	1.93	0.73	2.98	-0.32
H35	2.66	2.88	-0.22	3.93	-1.27
H36	1.69	1.60	0.09	2.59	-0.90
H37	1.69	1.39	0.30	2.41	-0.72
H38	0.95	0.74	0.21	1.52	-0.57
H39	0.95	0.67	0.28	1.49	-0.54
H40	0.95	0.70	0.25	1.71	-0.76

et.al., 1993; Becke et.al., 1988) level of theory, using 6-31G(d,p) basis sets, for all atoms (Kotan et.al., Beytur et al., 2019). In this study, IR absorption frequencies of analyzed molecules were calculated Then, they were compared with experimental data (Ulufer, 2002), which are shown to be accurate.

Method

In this study, the Gaussian 09W package program, which is a very comprehensive program, was used. First of all, with the B3LYP/6-311G(d,p) and 3-21G(d,p) basis sets of Density Functional Theory, the most stable low-energy optimized structure of atoms and molecules has been established. Each atom was then given a number. From this optimized structure, all geometric, electronic, thermodynamic and spectroscopic theoretical values of the molecule were calculated (Frisch et al., 2009). IR vibration frequency values were calculated with the Veda 4f program (Jamróz., 2004). The $^1\text{H-NMR}$ and $^{13}\text{C-NMR}$ isotropic shift values were calculated by the GIAO method using the Gaussian G09 package program (Wolinski et al., 1990). These values were compared with the experimental values (Ulufer, 2002) and the difference values were found, and these values were $\delta_{\text{exp}}=a+b \cdot \delta_{\text{calc}}$. plotted according to the equation. The regression coefficient and standard error values of constants a and b were found using the Sigmaplot program. The dipole moment, HOMO-LUMO energy, total energy, bond angle, bond length, mulliken atomic charges of the target molecule were calculated. In addition, MEP surface maps were determined.

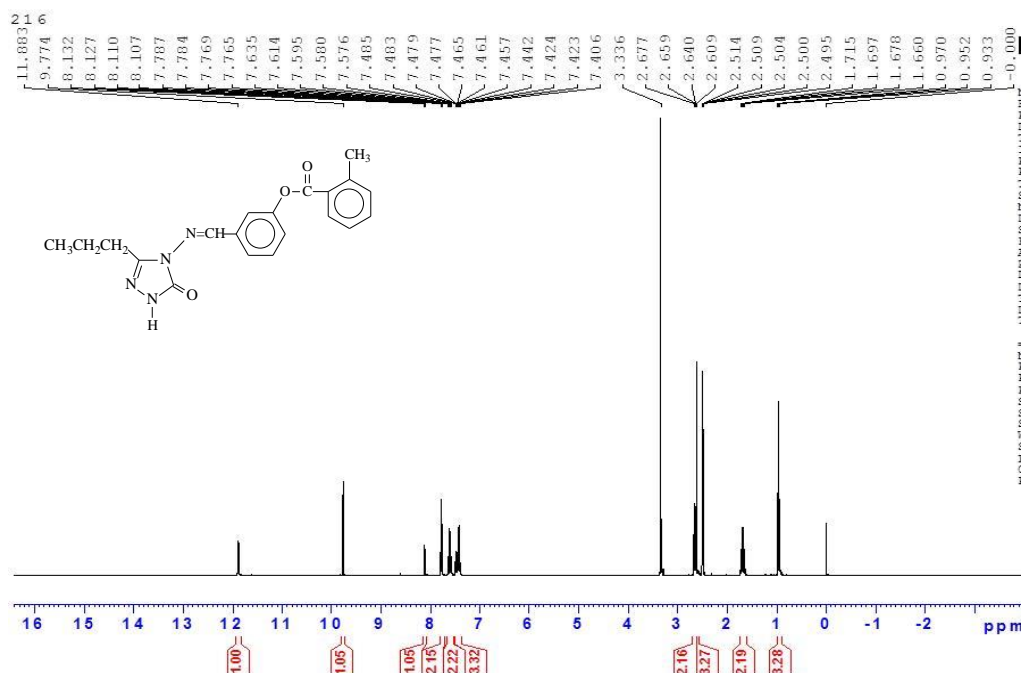
Results and Discussion

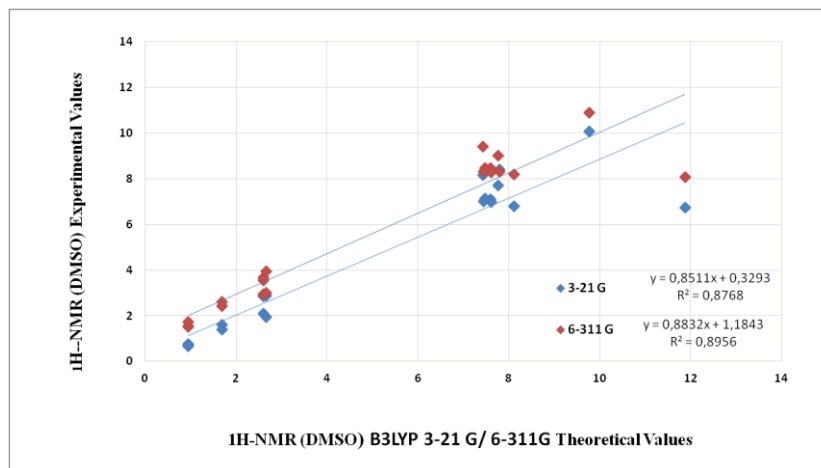
Computational Details

The Relation between R Values of the Compound

There is such a relationship between R^2 -values of the compound. B3LYP/3-21G(d,p) (DMSO): ^1H : 0,8768, ^{13}C : 0,9946; B3LYP/6-311G(d,p) (DMSO): ^1H : 0,8956, ^{13}C : 0,9978. These values for compound were seen in the table 2. Theoretical and experimental carbon/proton chemical shifts ratios between according to a, b values, R^2 linear a correlation were observed.

	$^{13}\text{C-NMR} / R^2$	$^1\text{H-NMR} / R^2$
3-21G(d,p)	0.9946	0.8768
6-311G(d,p)	0.9978	0.8956





216

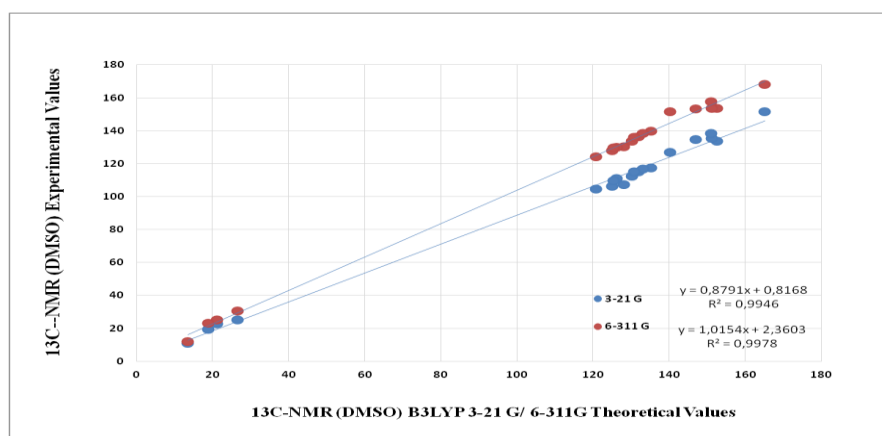
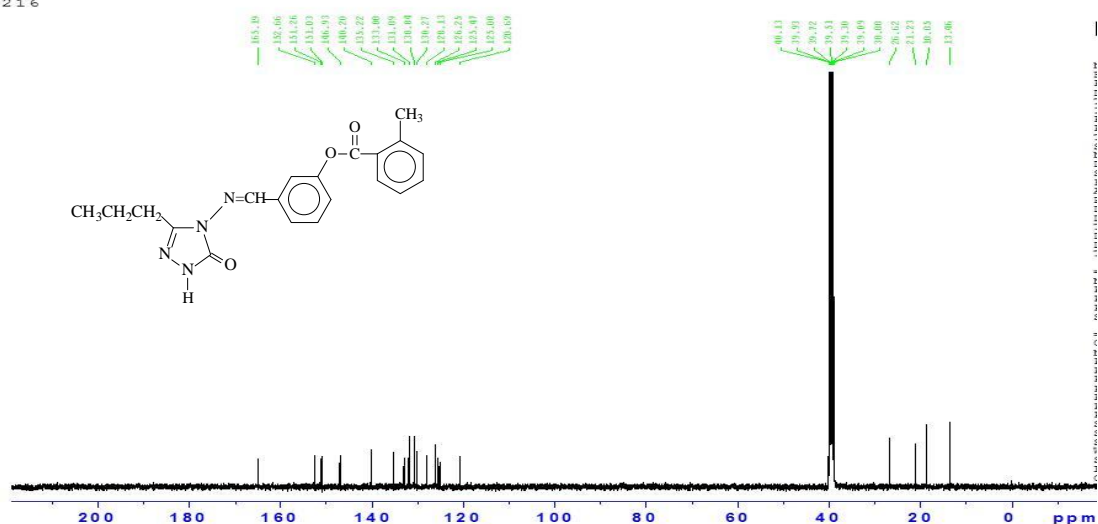


Figure 2. The experimental and theoretical $^{13}\text{C}/^1\text{H}$ -NMR correlation graphs for B3LYP 6-311G(d,p) and B3LYP 3-21G(d,p) DMSO chemical shifts

The Vibration Frequency of the Compound

Theoretically IR values were calculation veda 4f program and scale values were obtain. The calculated harmonic vibrational frequency values were scaled with 0.9671 for B3LYP 3-21 G level, 0.9688 for 6-311G(d,p) level (Merrick et al., 2007). The positive frequency in the data was found. IR spectrums were drawn

with obtained values according to DFT method. Theoretically IR values were compare with experimentally IR values and found corresponding with each other of values.

Table 3. Significant vibrational frequencies (cm^{-1})

Experimental IR	Scaled B3LYP 3-21G	Scaled B3LYP 6-311G	Experimental IR
ν (NH)	3169	3514	3565
ν (C=O)	1739. 1700	1708. 1664	1737. 1750
ν (C=N)	1589	1577	1613
ν (COO)	1231	1248	1259

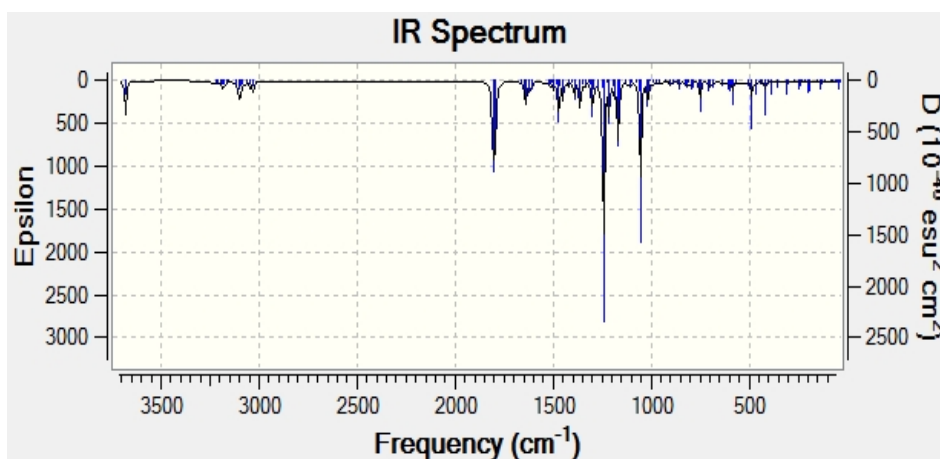
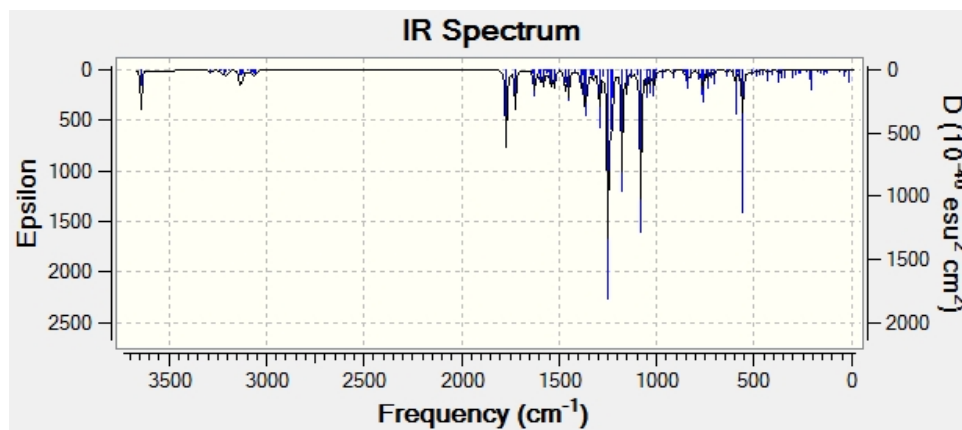
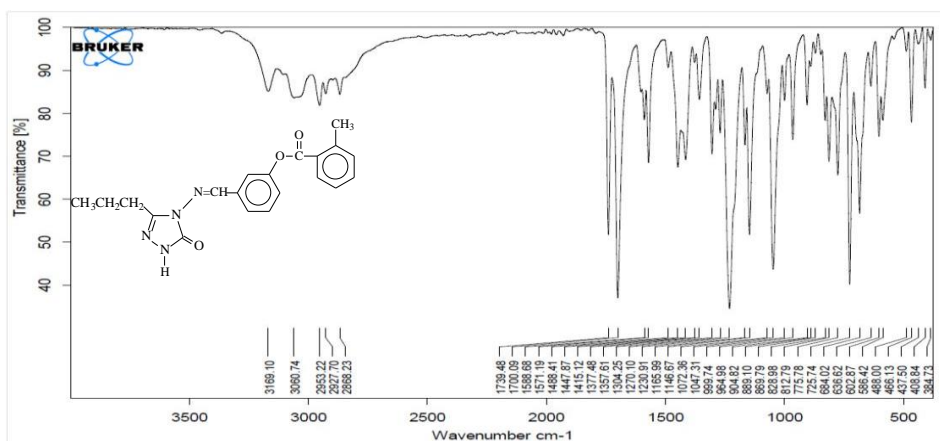


Figure 3. Experimental and theoretical IR spectrums simulated with B3LYP 3-21G(d,p) and B3LYP 6-311G(d,p)

Molecular Geometry

The molecular geometric parameters such as bond angles, Mulliken atomic charges, bond lengths calculated by using the and B3LYP functional in DFT method with 3-21G(d,p)/ 6-311G(d,p) basis set and data are summarized in Table 4-6. According to this result, the highest bond length is between C(18)-C(19) atoms that this values are 1.555/1.544 Å for B3LYP 3-21G(d,p)/ 6-311G(d,p). Besides, respectively, the bond lengths in the triazole ring N41-N42, N41-C1, C2-O45, C2-N43, N43-C1 are calculated 1.43/1.38; 1.31/1.29; 1.23/1.21; 1.43/1.42, 1.39/ 1.39 Å for B3LYP 3-21G(d,p)/ 6-311G(d,p) basis sets (table 4). In the literature, the N-N, N=C, C=O bond lengths are measured as 1.404, 1.280, 1.212 Å (Sudha et al. 2018).

The calculated bond length values are consistent with literature values. The highest bond angle is between H(21)-N(42)-C(2) atoms, which is 126.510/125.116° for B3LYP 3-21G(d,p)/ 6-311G(d,p) basis sets (table 5). The calculated Mulliken atomic charges (Mulliken, 1955) calculated by using the B3LYP method with 3-21G(d,p) and 6-311G(d,p) basis sets. The electronegative oxygen (O) and nitrogen (N) atoms have negative atomic charge values. The carbon atoms surrounded by electronegative atoms have negative atomic charge values. The C1 atom surrounded by two electronegative atoms (N41, N43) and C2 atom which is surrounded by three electronegative atoms (N42, N43, O45) have negative charges values. All hydrogen atoms of the compound (H22-H40) have positive atomic charge values (table 6).

Table 4. The calculated bond lengths with B3LYP 3-21G/ B3LYP 6-311G(d,p)

Bond Length	B3LYP 3-21G	B3LYP 6-311G	Bond Length	B3LYP 3-21G	B3LYP 6-311G
1 C(1)-N(41)	1.316	1.296	27 C(6)-C(7)	1.394	1.395
2 C(1)-N(43)	1.397	1.391	28 C(7)-H(25)	1.081	1.082
3 C(1)-C(18)	1.482	1.490	29 C(7)-C(8)	1.397	1.389
4 N(41)-N(42)	1.438	1.380	30 C(8)-O(46)	1.409	1.392
5 N(42)-H(21)	1.008	1.005	31 C(8)-C(9)	1.395	1.390
6 N(42)-C(2)	1.376	1.368	32 C(9)-H(26)	1.077	1.081
7 C(2)-O(45)	1.237	1.215	33 O(46)-C(10)	1.399	1.378
8 C(2)-N(43)	1.433	1.420	34 C(10)-O(47)	1.229	1.203
9 N(43)-N(44)	1.410	1.369	35 C(10)-C(11)	1.480	1.488
10 C(18)-H(34)	1.093	1.092	36 C(11)-C(12)	1.404	1.403
11 C(18)-H(35)	1.094	1.093	37 C(11)-C(16)	1.415	1.416
12 C(18)-C(19)	1.555	1.544	38 C(12)-H(27)	1.079	1.080
13 C(19)-H(36)	1.094	1.093	39 C(12)-C(13)	1.389	1.387
14 C(19)-H(37)	1.096	1.095	40 C(13)-H(28)	1.083	1.083
15 C(19)-C(20)	1.541	1.530	41 C(13)-C(14)	1.396	1.392
16 C(20)-H(38)	1.095	1.093	42 C(14)-H(29)	1.084	1.083
17 C(20)-H(39)	1.096	1.094	43 C(14)-C(15)	1.393	1.392
18 C(20)-H(40)	1.094	1.093	44 C(15)-H(30)	1.084	1.084
19 N(44)-C(3)	1.297	1.284	45 C(15)-C(16)	1.401	1.399
20 C(3)-H(22)	1.084	1.086	46 C(16)-C(17)	1.518	1.508
21 C(3)-C(4)	1.465	1.466	47 C(17)-H(31)	1.093	1.091
22 C(4)-C(5)	1.403	1.403	48 C(17)-H(32)	1.093	1.091
23 C(4)-C(9)	1.403	1.400	49 C(17)-H(33)	1.093	1.091
24 C(5)-H(23)	1.081	1.082			
25 C(5)-C(6)	1.391	1.386			
26 C(6)-H(24)	1.083	1.083			

MEP Surface Analysis

Electrophilic and nucleophilic regions of the molecule were determined by drawing the MEP map of the molecule with the 3-21G(d,p) and 6-311G(d,p) basic sets of B3LYP method. Different values of electrostatic energy are indicated by different colors. Red means there is very negative electrostatic energy, blue means there is very positive electrostatic energy. When the MEP map is examined, the region of N41, N46, O45 and O47 atoms and are in red, the region of H21 acidic proton atom is in blue, while the around of C-H atoms are in yellow-green.

Table 5. The calculated bond angles with B3LYP 3-21G/ B3LYP 6-311G(d,p)

bond angle	B3LYP 3-21G	B3LYP 6-311G	bond angle	B3LYP 3-21G	B3LYP 6-311G
N(41)-C(1)-N(43)	112.039	111.165	C(5)-C(6)-H(24)	120.150	120.008
N(41)-N(42)-H(21)	119.515	120.460	C(5)-C(6)-C(7)	120.358	120.530
H(21)-N(42)-C(2)	126.510	125.116	H(24)-C(6)-C(7)	119.493	119.462
N(42)-C(2)-O(45)	101.250	130.065	C(6)-C(7)-H(25)	121.563	121.519
O(45)-C(2)-N(43)	127.934	128.755	H(25)-C(7)-C(8)	118.556	119.202
N(43)-C(1)-C(18)	125.203	108.324	C(7)-C(8)-O(46)	113.865	116.550
C(1)-C(18)-H(34)	107.770	106.623	O(46)-C(8)-C(9)	125.611	122.292
C(1)-C(18)-H(35)	108.687	108.559	C(8)-C(9)-H(26)	119.801	120.225
C(1)-C(18)-C(19)	111.816	114.179	C(8)-O(46)-C(10)	125.652	120.495
H(34)-C(18)-H(35)	109.318	107.958	O(46)-C(10)-O(47)	122.921	122.433
H(34)-C(18)-C(19)	109.937	110.061	O(47)-C(10)-C(11)	110.229	126.390
H(35)-C(18)-C(19)	109.268	109.261	C(11)-C(12)-H(27)	118.461	118.795
C(18)-C(19)-H(36)	108.054	108.942	H(27)-C(12)-C(13)	120.779	120.062
C(18)-C(19)-H(37)	108.236	107.580	C(12)-C(13)-H(28)	120.122	120.094
C(19)-C(20)-H(38)	110.738	111.651	H(28)-C(13)-C(14)	120.403	120.619
C(19)-C(20)-H(39)	110.470	111.194	C(13)-C(14)-H(29)	120.173	120.292
C(19)-C(20)-H(40)	110.817	111.651	H(29)-C(14)-C(15)	119.809	119.778
H(38)-C(20)-H(39)	107.841	107.392	C(14)-C(15)-H(30)	119.705	119.350
H(39)-C(20)-H(40)	108.331	107.780	H(30)-C(15)-C(16)	118.630	118.527
H(38)-C(20)-H(40)	108.548	107.844	C(11)-C(12)-C(13)	120.760	121.143
C(1)-N(43)-C(2)	109.324	108.324	C(12)-C(13)-C(14)	119.475	119.287
N(43)-N(44)-C(3)	117.283	119.222	C(16)-C(17)-H(31)	111.133	111.684
N(44)-C(3)-H(22)	122.331	122.094	C(16)-C(17)-H(32)	111.136	111.550
H(22)-C(3)-C(4)	117.887	117.792	C(16)-C(17)-H(33)	109.644	109.908
C(3)-C(4)-C(5)	119.627	122.481	H(31)-C(17)-H(32)	106.312	105.889
C(3)-C(4)-C(9)	117.901	117.927	H(31)-C(17)-H(33)	109.268	108.853
C(4)-C(5)-H(23)	118.869	119.110	H(32)-C(17)-H(33)	109.274	108.825
C(4)-C(5)-C(6)	119.627	120.005			
C(4)-C(9)-C(8)	119.226	119.558			
H(23)-C(5)-C(6)	119.998	120.885			

Table 6. The calculated mulliken charges datas B3LYP 3-21G/ B3LYP 6-311G(d,p)

Atom	3-21G B3LYP	6-311G B3LYP	Atom	3-21G B3LYP	6-311G B3LYP
C1	0.660	0.342	H25	0.206	0.106
C2	0.948	0.534	H26	0.245	0.112
C3	0.109	0.133	H27	0.213	0.111
C4	-0.055	-0.173	H28	0.193	0.098
C5	-0.174	-0.015	H29	0.196	0.100
C6	-0.183	-0.103	H30	0.191	0.098
C7	-0.192	-0.056	H31	0.226	0.131
C8	0.301	0.152	H32	0.225	0.133
C9	-0.211	-0.010	H33	0.184	0.093
C10	0.710	0.436	H34	0.221	0.133
C11	-0.113	-0.215	H35	0.227	0.138
C12	-0.165	-0.003	H36	0.212	0.129
C13	-0.185	-0.094	H37	0.193	0.111
C14	-0.173	-0.067	H38	0.201	0.113
C15	-0.179	-0.076	H39	0.188	0.104
C16	0.029	-0.071	H40	0.189	0.109
C17	-0.587	-0.206	N41	-0.342	-0.216
C18	-0.429	-0.199	N42	-0.594	-0.313
C19	-0.384	-0.239	N43	-0.626	-0.374
C20	-0.554	-0.287	N44	-0.319	-0.207
H21	0.353	0.250	O45	-0.521	-0.387
H22	0.263	0.144	O46	-0.601	-0.374
H23	0.208	0.108	O47	-0.490	-0.325
H24	0.196	0.100			

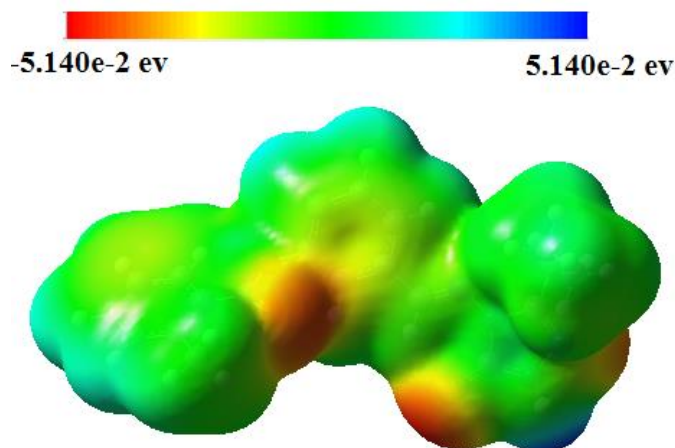


Figure 4. The calculated MEP molecular surface of the molecule

Frontier Molecular Orbital Analysis

Frontier molecular orbitals (FMO) designated kinetic stability, the electronic transitions, electric and optical properties (Fukui, 1982). HOMO-LUMO energy values of compound was calculated with three computational levels and these values are 4.33/4.35 eV for B3LYP 3-21G(d,p) and 6-311G (d,p) basis sets (figure 4). Using HOMO-LUMO energy gap electron affinity (A), global hardness (η), electronegativity (χ), chemical potential (μ), softness (S), ionization potential (I), chemical potential (Pi), electrophilic index(ω), Nucleophilic index (IP) for the compound was calculated and are showed in table 7.

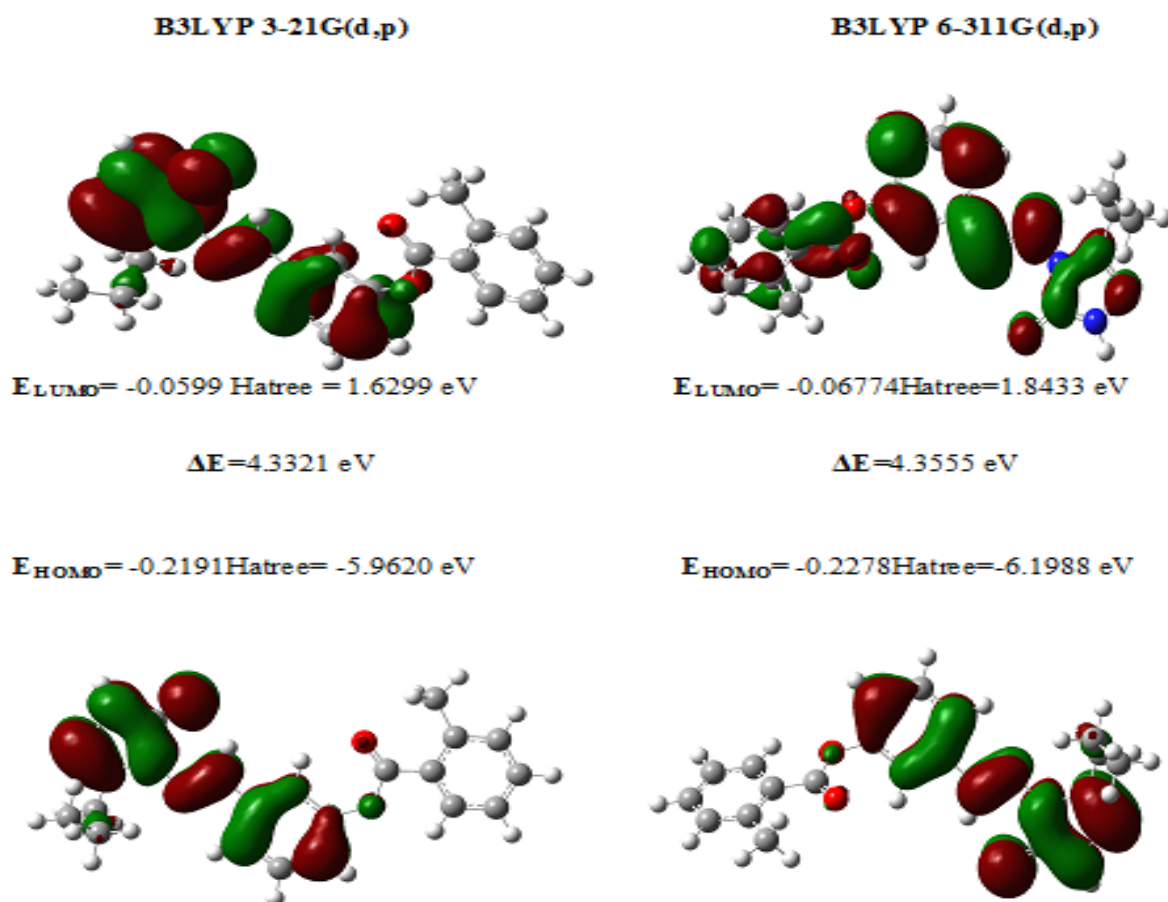


Figure 5. HOMO-LUMO energy of the molecule 6-311G(d,p)

Table 7. The calculated electronic structure parameters of the molecule

		B3LYP 3-21G(d,p)		B3LYP 6-311G(d,p)	
		Hatree	ev	Hatree	ev
	LUMO	-0.0599	-1.62992	-0.06774	-1.84325
	HOMO	-0.2191	-5.96186	-0.2278	-6.1986
A	elektron ilgisi	0.0599	1.62992	0.06774	1.84325
I	İyonlaşma potansiyeli	0.2191	5.96186	0.2278	6.1986
ΔE	energy gap	0.1592	4.33194	0.16006	4.35534
χ	electronegativity	0.1395	3.79589	0.14777	4.02093
Pi	chemical potential	-0.1395	-3.79589	-0.14777	-4.02093
ω	electrophilic index	0.000774518	0.02108	0.000873766	0.02378
IP	Nucleophilic index	-0.0111042	-0.30215	-0.01182603	-0.32179
S	molecular softness	12.5628	341.843	12.4953	340.006
η	molecular hardness	0.0796	2.16597	0.08003	2.17767

Table 8. The calculated dipole moments datas of the molecule

	μ_x	μ_y	μ_z	μ_{Toplam}
3-21G	0.1418	1.0885	-0.0173	1.0979
6-311G	0.5782	1.3859	0.1582	1.5100

Table 9. The calculated total energy datas of the molecule

Energy(a.u.)	B3lyp 3-21G	B3lyp 6-311G
	-1212.1405	-1219.1562

Table 10. The calculated thermodynamics parameters of the molecule

Rotational temperatures (Kelvin)	B3LYP/3-21G	B3LYP/6-311G
A	0.02219	0.02099
B	0.00307	0.00308
C	0.00275	0.00288
Rotational constants (GHZ)		
A	0.46236	0.43735
B	0.06401	0.06409
C	0.05740	0.05997
Thermal Energies E(kcal/mol)		
Translational	0.889	0.889
Rotational	0.889	0.889
Vibrational	249.967	247.611
Total	251.744	249.389
Thermal Capacity CV(cal/mol-K)		
Translational	2.981	2.981
Rotational	2.981	2.981
Vibrational	85.689	87.156
Total	91.651	93.118
Entropy S(cal/mol-K)		
Translational	43.570	43.570
Rotational	36.491	36.501
Vibrational	92.706	98.410
Total	172.767	178.482
Zero-point correction (Hartree/Particle)	0.377112	0.372743
Thermal correction to Energy	0.401180	0.397426
Thermal correction to Enthalpy	0.402125	0.398370
Thermal correction to Gibbs Free Energy	0.320037	0.313568
Sum of electronic and zero-point Energies	-1211.763415	-1218.783521
Sum of electronic and thermal Energies	-1211.739346	-1218.758837
Sum of electronic and thermal Enthalpies	-1211.738402	-1218.757893
Sum of electronic and thermal Free Energies	-1211.820489	-1218.842695
Zero-point vibrational energy (Kcal/mol)	236.64133	233.89962

Thermodynamics Properties

Thermodynamics parameters were calculated with (B3LYP) functional in the both two basis set of DFT method at 298.150 K and under 1 atm pressure (Table 10).

Conclusion

In this work, spectroscopic, electronic and geometric parameters of molecule are calculated by B3LYP functional of DFT method with the 3-21G(d,p) and 6-311G (d,p) basis sets at the program package Gaussian G09W. FT-IR vibrational frequencies and spectrums were obtained. The FT-IR data was found positive. This result showed that the structure of the compound was stable. The chemical shifts in the calculations FT-IR and $^1\text{H}/^{13}\text{C}$ -NMR vibrational frequencies are found to be compatible with the experimental data. Theoretical and experimental carbon chemical shifts ratios between according to R^2 linear a correlation was observed, but there is a slight deviation in the H-NMR correlation graph. The reason for this deviation is the N-H acidic proton (H21) in the molecule. Obtained spectroscopic parameters are compared with experimental data and with each other. In addition, the lowest unoccupied molecular orbital (LUMO) and the highest occupied molecular orbital (HOMO), bond angles, bond lengths, mulliken charges, $E_{\text{LUMO}}-E_{\text{HOMO}}$ energy gap (ΔE_g), electronic parameters, thermodynamics properties, dipole moments, total energy were calculated with different basis sets such as 3-21 G(d,p)/ 6-311G(d,p) basis set. Result, obtained all data basis set were compared and these values were consistent with each other. The closest results to the experimental values are the results obtained with the 6-311 G(d,p) base set.

Scientific Ethics Declaration

The authors declare that the scientific ethical and legal responsibility of this article published in EPSTEM journal belongs to the authors.

References

- Aytac, S. P., Tozkoparan, B., Kaynak, F. B., Aktay, G., Goktas, O., & Unuvar, S. (2009). Synthesis of 3,6-disubstituted 7H-1,2,4-triazolo[3,4-b]-1,3,4-thiadiazines as novel analgesic/anti-inflammatory compounds. *European Journal of Medicinal Chemistry*, 44(11): 4528-4538.
- Bayrak, H., Demirbas, A., Demirbas, N., & Karaoglu, S. A. (2010). Cyclization of some carbothioamide derivatives containing antipyrine and triazole moieties and investigation of their antimicrobial activities. *European Journal of Medicinal Chemistry*, 45(11): 4726-4732.
- Becke, A. D. (1993). Density functional thermochemistry. III. The role of exact exchange, *The Journal of Chemical Physics*, 98, 5648-5652.
- Becke, A.D. (1988). Density-functional exchange-energy approximation with correct asymptotic behavior. *Physical Review A: General physics*, 38(6), 3098-3100.
- Beytur, M., Irak, Z. T., Manap, S., & Yükses, H. (2019). Synthesis, characterization and theoretical determination of corrosion inhibitor activities of some new 4, 5-dihydro-1H-1, 2, 4-Triazol-5-one derivatives. *Helikon*, 5(6), e01809.
- Frisch, M. J., Trucks, G., Schlegel, H. B., Scuseria, G. E., Robb, M. A., Cheeseman, J. R., Scalmani, G., Barone, V., Mennucci, B., Petersson, G. A., Nakatsuji, H., Caricato, M., Li, X., Hratchian, H. P., Izmaylov, A. F., Bloino, J., Zheng, G., Sonnenberg, J. L., Hada, M., Ehara, M., Toyota, K., Fukuda, R., Hasegawa, J., Ishida, M., Nakajima, T., Honda, Y., Kitao, O., Nakai, H., Vreven, T., Montgomery, J. A., Jr. Vreven, T., Peralta, J. E., Ogliaro, F., Bearpark, M., Heyd, J. J., Brothers, E., Kudin, N., Staroverov, V. N., Kobayashi, R., Normand, J., Raghavachari, K., Rendell, A., Burant, J. C., Iyengar, S. S., Tomasi, J., Cossi, M., Rega, N., Millam, J. M., Klene, M., Knox, J. E., Cross, J. B., Bakken, V., Adamo, C., Jaramillo, J., Gomperts, R., Stratmann, R. E., Yazyev, O., Austin, A. J., Cammi, R., Pomelli, C., Ochterski, J. W., Martin, L. R., Morokuma, K., Zakrzewski, V. G., Voth, G. A., Salvador, P., Dannenberg, J. J., Dapprich, S., Daniels, A. D., Farkas, O., Foresman, J. B., Ortiz, J. V., Cioslowski, J. & Fox, D. J. (2009). *Gaussian Inc.* Wallingford.
- Fukui, K. (1982). Role of frontier orbitals in chemical reactions. *science*, 218(4574), 747-754.
- Guzeldemirci, N. U, Kucukbasmaci, O., (2010). Synthesis and antimicrobial activity evaluation of new 1,2,4-triazoles and 1,3,4-thiadiazoles bearing imidazo[2,1-b]thiazole moiety, *European Journal of Medicinal Chemistry*, 45(1): 63-68.

- Gürsoy-Kol, Ö., Yüksek, H., Manap, S., Tokalı, F.S., (2016). Synthesis, Characterization, and antioxidant activities of novel 1-(Morpholine-4-yl-methyl)-3-alkyl(aryl)-4-[4-(dimethylamino)-benzylidenamino]-4,5-dihydro-1H-1,2,4-triazol-5-ones. *Journal of the Turkish Chemical Society Section A: Chemistry*, 3(3), 105-120.
- Hashem, A. I., Youssef, A. S. A., Kandeel, K. A., & Abou-Elmalgd, W. S. I., (2007). Conversion of some 2(3H)-furanones bearing a pyrazolyl group into other heterocyclic systems with a study of their antiviral activity. *European Journal of Medicinal Chemistry*, 42(7), 934-939.
- Ikizler, A. A., Ikizler, A. Yüksek, H., & Serdar, M., (1998). Antitumor activities of some 4,5-dihydro-1H-1,2,4-triazol-5-ones. *Modelling, Measurement & Control C*, 57(1): 25-33
- Jamróz, M. H. (2004). *Vibrational energy distribution analysis: VEDA 4 program*
- Klimeová, V., Zahajská, L., Waisser, K., Kaustová, J., Möllmann, U., (2004). Synthesis and antimycobacterial activity of 1,2,4-triazole 3-benzylsulfanyl derivatives. *Il Farmaco*, 59(4), 279-288
- Kohn, W., Becke, A. D., & Parr, R. G. (1996). Density functional theory of electronic structure. *The Journal of Physical Chemistry*, 100(31), 12974-12980.
- Kotan, G., & Yüksek, H. (2016). Theoretical and Spectroscopic Studies of (E)-3-Benzyl-4-((4-Isopropylbenzylidene)-Amino)-1-(Morpholinomethyl)-1H-1.2.4-triazol-5(4H)-one molecule. *Journal of the Turkish Chemical Society Section A: Chemistry*, 3(3), 381-392.
- Küçükgülzel, Ş. G., Rollas, S., Erdeniz, H., Kiraz, M., Ekinci, A. C., & Vidin, A. (2000). Synthesis, characterization and pharmacological properties of some 4-arylhydrazono-2-pyrazoline-5-one derivatives obtained from heterocyclic amines. *European journal of medicinal chemistry*, 35(7), 761-771.
- Merrick, J. P., Moran, D., Radom, L. (2007). An evaluation of harmonic vibrational frequency scale factors. *Journal of Physical Chemistry*, 111(45), 11683-11700.
- Mulliken, R. S. (1955). Electronic population analysis on LCAO-MO molecular wave functions. *The Journal of Chemical Physics*, 23(10), 1833-1840.
- Sancak, K., Unver, Y., Kazak, C., Dugdu, E., Arslan, B., (2010). Synthesis and characterisations of some new 2,4-dihydro-[1,2,4]-triazol-3-one derivatives and X-ray crystal structures of 4-(3-phenylallylideneamino)-5-thiophen-2-yl-methyl-2,4-dihydro-[1,2,4]triazol-3-one. *Turkish Journal of Chemistry*, 34(5): 771-780.
- Sudha, N., Abinaya, B., Arun Kumar, R., & Mathammal, R. (2018). Synthesis, Structural, Spectral, Optical and Mechanical Study of Benzimidazolium Phthalate crystals for NLO Applications. *Journal of Lasers Optics & Photonics*, 5(2), 1-6.
- Turan-Zitouni, G., Kaplancıklı, Z. A., Yıldız, M. T., Chevallet, P., & Kaya, D. (2005). Synthesis and antimicrobial activity of 4-phenyl/cyclohexyl-5-(1-phenoxyethyl)-3-[N-(2-thiazolyl) acetamido] thio-4H-1, 2, 4-triazole derivatives. *European Journal of Medicinal Chemistry*, 40(6), 607-613.
- Ulufur, S., Gürsoy Kol, Ö., Yüksek, H., Bazı yeni 4-[3-(2-metilbenzoksi)-benzilidenamino]-4,5-dihidro-1H-1,2,4-triazol-5-on bileşiklerinin sentezi ve antioksidan özelliklerinin incelenmesi (Bildiri Özeti), 2. *Ulusal Organik Kimya Kongresi*, Ankara.
- Wolinski, K., Hinton, J. F., & Pulay, P. (1990). Efficient implementation of the gauge-independent atomic orbital method for NMR chemical shift calculations. *Journal of the American Chemical Society*, 112(23), 8251-8260
- Yüksek, H., Gürsoy, O., Cakmak, I., & Alkan, M. (2005). Synthesis and GIAO NMR calculations for some new 4, 5- dihydro- 1H- 1, 2, 4- triazol- 5- one derivatives: comparison of theoretical and experimental 1H and 13C chemical shifts. *Magnetic Resonance in Chemistry*, 43(7), 585-587.
- Chohan, Z. H., Sumrra, S. H., Youssoufi, M. H., & Hadda, T. B. (2010). Metal based biologically active compounds: Design, synthesis, and antibacterial/antifungal/cytotoxic properties of triazole-derived Schiff bases and their oxovanadium (IV) complexes. *European Journal of Medicinal Chemistry*, 45(7), 2739-2747.

Author Information

Songul ULUFER-BULUT

Kafkas University
Kars, Turkey
Contact e-mail: snugulufur@gmail.com

Haydar YUKSEK

Department of Chemistry
Kars, Turkey

Gul KOTAN

Kafkas University,
Kars, Turkey

To cite this article:

Ulufer-Bulut, S., Yuksek, H. & Kotan, G. (2021). Theoretical (6-311G(d,p)/ 3-21G) and spectroscopic (¹³C/¹H-NMR, FT-IR) analyses of 3-propyl-4-[3-(2-methylbenzoxylideneamino)-4,5-dihydro-1H-1,2,4-triazol-5-one] molecule. *The Eurasia Proceedings of Science, Technology, Engineering & Mathematics (EPSTEM)*, 15, 42-53.

The Eurasia Proceedings of Science, Technology, Engineering & Mathematics (EPSTEM), 2021

Volume 15, Pages 54-62

ICBAST 2021: International Conference on Basic Science and Technology

In Silico Calculations of 2-Methoxy-6-[(3-methyl-5-oxo-4,5-dihydro-1H-1,2,4-triazol-4-yl)-iminomethyl] Phenyl Benzoate

Murat BEYTUR
Kafkas University

Haydar YUKSEK
Kafkas University

Abstract: Schiff's bases are significant compound for organic chemistry. In the last year, computational properties of Schiff bases were examined on a computer. In this study, we investigated theoretical features of 2-methoxy-6-[(3-methyl-5-oxo-4,5-dihydro-1H-1,2,4-triazol-4-yl)-iminomethyl] phenyl benzoate with B3LYP/6-311G(d) basis set. All quantum chemical calculations were carried out using the Gaussian09W program package and the Gauss View molecular visualization program. The IR vibrational frequency values of the titled compound were calculated using B3LYP/6-311G(d) basis set. The vibrational spectral analysis was carried out using infrared spectroscopy in the range 4000-400 cm^{-1} for titled compound. The IR vibrational frequency values were defined using the veda4f software. The $^1\text{H-NMR}$ and $^{13}\text{C-NMR}$ spectral values of the titled compound were calculated utilizing the B3LYP/6-311G(d) basis set. To determine the $^1\text{H-NMR}$ and $^{13}\text{C-NMR}$ isotropic shift values, the gauge independent atomic orbital (GIAO) methodology was used. The UV-vis spectral calculations in the ethanol solvent of the titled compound were performed via the same basis set. TD-DFT computations in ethanol solvent were used to identify the UV-Vis spectral analyses. In addition, dipole moments, LUMO-HOMO, total energy, and electronic properties; $E_{\text{LUMO}}-E_{\text{HOMO}}$ energy gap (ΔE_g), electronegativity (χ), electron affinity (A), global hardness (η), softness (σ), ionization potential (I), thermodynamics properties; (thermal energies (E), thermal capacity (CV), entropy (S) were calculated.

Keywords: Schiff base, Gaussian09W, GIAO, UV-vis, HOMO-LUMO

Introduction

Heterocyclic organic compound having three nitrogen atoms in the five-membered ring have been extensively studied for their applicability in various areas such as biological, chemical and pharmaceutical applications (Alkan et al., 2007; Aytac et al., 2009; Aktaş-Yokuş et al., 2017; Boy et al., 2021; Çiftçi et al., 2018; Gürsoy-Kol et al., 2010; Turhan-Irak et al., 2019). There has recently been an increase in studies on heterocyclic organic compound in relation to corrosion inhibitors, optical sensors, theoretical, highly selective polymer membrane electrodes, highly thermal stability, modern technology (nonlinear optical materials), various coordination complexes, homogenous catalysis and biological probes (Bahçeci et al., 2016; Bahçeci et al., 2017; Beytur et al., 2019; Koç et al., 2019; Beytur et al., 2021; Beytur, 2020; Uğurlu et al., 2020). Also, several articles reporting the synthesis of some *N*-arylidenamino-4,5-dihydro-1H-1,2,4-triazol-5-one compounds and derivatives have been published (Yüksek et al., 2004; Turhan-Irak, 2017).

In this paper, the optimized molecular structure, vibrational frequencies, spectroscopic parameters, atomic charges and frontier molecule orbitals (HOMO and LUMO) of the 2-methoxy-6-[(3-methyl-5-oxo-4,5-dihydro-1H-1,2,4-triazol-4-yl)-iminomethyl] phenyl benzoate have been calculated by using DFT/B3LYP method with 6-311G(d) basis set. All quantum chemical calculations were carried out by using Gaussian 09W (Frisch et al.,

- This is an Open Access article distributed under the terms of the Creative Commons Attribution-Noncommercial 4.0 Unported License, permitting all non-commercial use, distribution, and reproduction in any medium, provided the original work is properly cited.

- Selection and peer-review under responsibility of the Organizing Committee of the Conference

2009; Wolinski et. al., 1990) program package and the GaussView molecular visualization program (Frisch, Nielson & Holder, 2003) (Figure 1). The molecular structure and vibrational calculations of the molecule were computed by using Becke-3-Lee Yang Parr (B3LYP) (Becke, 1993; Lee et al.,1998) density functional method with 6-311G(d) basis set in ground state. IR absorption frequencies of analyzed molecule were calculated by two methods. Then, they were compared with experimental data (Gürbüz et al., 2021), which are shown to be accurate. The assignments of fundamental vibrational modes of the title molecule were performed on the basis of total energy distribution (TED) analysis by using VEDA 4f program (Jamróz, 2004). Furthermore, molecular structure, HOMO and LUMO energy analysis, total energy, and electronic properties; $E_{\text{LUMO}}-E_{\text{HOMO}}$ energy gap (ΔE_g), electronegativity (χ), electron affinity (A), global hardness (η), softness (σ), ionization potential (I), thermodynamics properties; (thermal energies (E), thermal capacity (CV), entropy (S) were calculated.

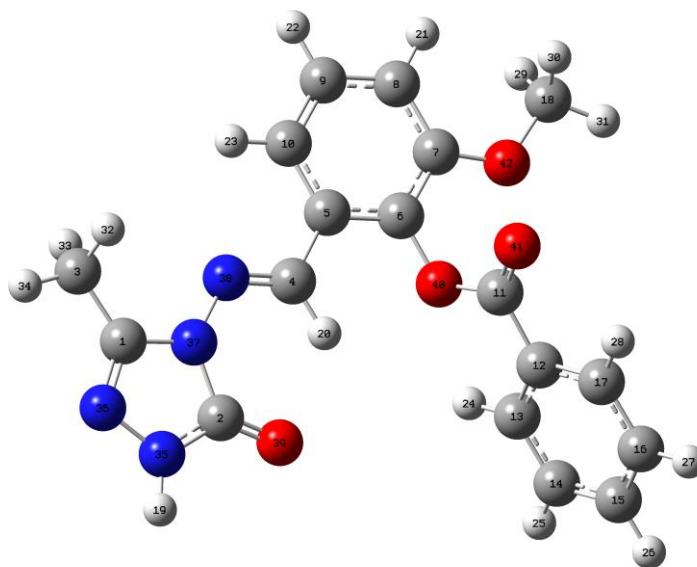


Figure 1. The optimized molecular structure (Gaussview Appearance) of 2-methoxy-6-[(3-methyl-5-oxo-4,5-dihydro-1H-1,2,4-triazol-4-yl)-iminomethyl]phenyl benzoate with DFT/B3LYP 6-311G(d) level.

Method

The molecular structure of the title compound in the ground state is computed by performing both the density functional theory (DFT) (Becke, 1993; Lee, 1998) at 6-311G(d) level. Density functionals for all studies reported in this paper have been in the following form

$$E_{XC} = (1 - a_0)E_X^{LSDA} + a_0E_X^{HF} + a_X\Delta E_X^{B88} + a_C E_C^{LYP} + (1 - a_C)E_C^{VWN}$$

where the energy terms are the Slater exchange, the Hartree-Fock exchange, Becke's exchange functional correction, the gradient corrected correlation functional of Lee, Yang and Parr, and the local correlation functional of Vosko, Wilk and Nusair (Vosko et al., 1980). The theoretical geometric structure of the title compound is given in Figure 1. Molecular geometry is restricted and the optimized geometrical parameters of the title compound in this study are carried out by using Gaussian 09W program package (Frisch et al., 2009) and the visualization parts were done with GaussView program (Dennington et al., 2009) on personal computer employing 6-311G(d) basis set. Additionally, harmonic vibrational frequencies for the title compound are calculated with these selected methods and then scaled by 0.9516 and 0.9905, respectively (Avcı et. al., 2008) and these results were compared with the experimental data (Gürbüz et al., 2021).

Results and Discussion

Analysis of Vibrational Modes

The number of potentially active fundamentals of non-linear molecule which have N atoms is equal to (3N-6) apart from three translational and three rotational degrees of freedom. The title molecule contains 42 atoms and

Table 1. The calculated frequencies values of the 2-methoxy-6-[(3-methyl-5-oxo-4,5-dihydro-1H-1,2,4-triazol-4-yl)-iminomethyl] phenyl benzoate.

Selected Vibrational Types	Experimental	Scaled DFT
τ HNNC (50)		442
τ HCCC (10), τ CCOC (23)		522
δ OCN (12), δ CCO (12), δ COC (20)		563
τ OCCC (35), τ CCCC (22)		592
δ OCN (16), δ CCC (12)		639
τ HCCC (14), τ ONNC (24)		688
τ HCCN (21), τ ONNC (41)	712	719
ν NC (16), CC (10), δ CNN (36)		762
τ HCCC (30), τ ONNC (36), τ CCCC (11)	783	776
δ OCO (15), δ COC (12), τ CCOC (11)		837
ν OC (26), δ HCC (11), δ CCC (22)		1025
ν NC (13), ν NN (52)		1060
ν CC (17), ν OC (15), δ HCC (19)		1069
δ HCC (11), τ HCCN (49), τ HCCC (14)		1073
ν NC (34), NN (17), δ OCN (12)		1182
ν NN (10), δ NCN (14), δ CNN (11), τ HCCN (19)		1217
ν CC (10), ν OC (17)	1259	1257
ν NN (12), τ HCCN (21)		1301
δ HCC (72), τ HCCN (13)		1333
ν NC (15), δ HCN (14), τ HCCN (33)		1355
δ HNN (64), τ HCCN (12)		1377
ν NC (14), δ HCN (11), τ HCCN (16)		1441
τ HCOC (12), τ CCCC (12)		1458
ν NC (47), ν CC (13)	1592	1588
ν NC (58)	1608	1600
ν OC (75), ν NC (11)	1700	1739
ν OC (87)	1744	1742
ν CH (95)		2899
ν CH (90)		2958
ν CH (100)		3066
ν CH (94)		3085
ν CH (96)		3096
ν NH (100)	3190	3549

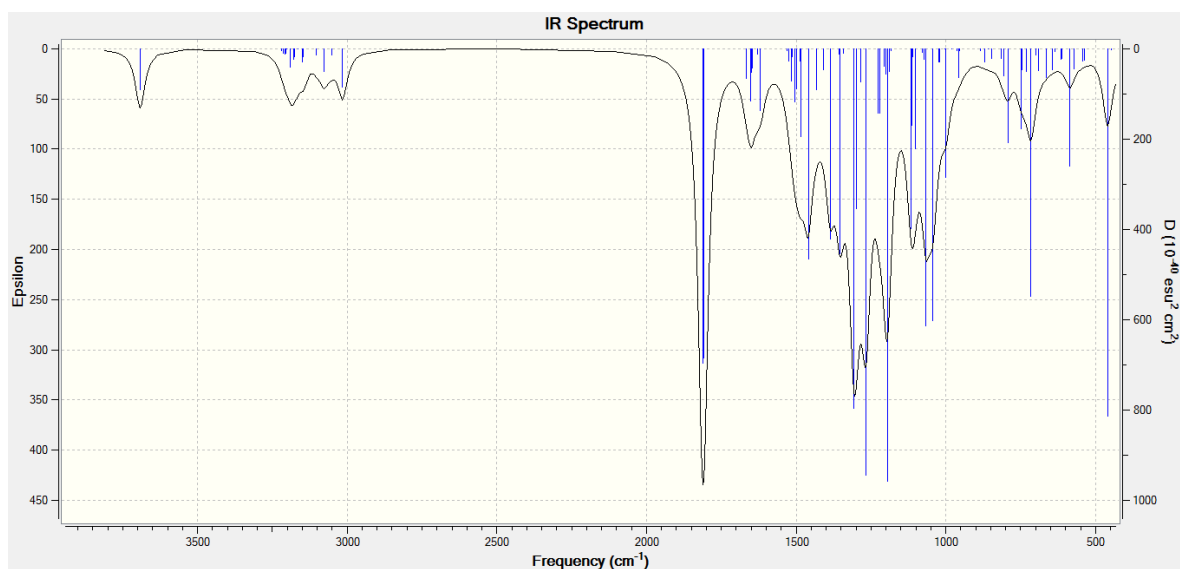


Figure 2. IR spectra simulated with DFT/B3LYP/6-311G(d) level of the 2-methoxy-6-[(3-methyl-5-oxo-4,5-dihydro-1H-1,2,4-triazol-4-yl)-iminomethyl]phenyl benzoate

120 normal vibration modes have C1 symmetry (Table 1). Experimentally (Gürbüz et al., 2021), the investigated 2-methoxy-6-[(3-methyl-5-oxo-4,5-dihydro-1H-1,2,4-triazol-4-yl)-iminomethyl] phenyl benzoate, as expected the IR spectra data, the N-H stretching vibration at 3190 cm^{-1} and two C=O peak at 1744 and 1700 cm^{-1} range was observed. In addition, C=N stretching vibration at 1608 and 1592 cm^{-1} and COO stretching vibrations at 1259 cm^{-1} are occurred. Theoretically and experimentally (Gürbüz et al., 2021), the calculated vibrational frequencies for the compound are summarized in Table 1. Furthermore, the experimental IR (Gürbüz et al., 2021) and simulated spectra by using B3LYP/6-311G(d) levels of the titled compound under investigation are given in Figure 2.

NMR Spectral Analysis

The isotropic chemical shift analysis allows us to identify relative ionic species and to calculate reliable magnetic properties in nuclear magnetic resonance (NMR) spectroscopy which provide the accurate predictions of molecular geometries (Wade, 2006; Rani, et al., 2010; Subramanian et al., 2010). For this purpose, the optimized molecular geometry of the 2-methoxy-6-[(3-methyl-5-oxo-4,5-dihydro-1H-1,2,4-triazol-4-yl)-iminomethyl] phenyl benzoate was obtained by using B3LYP method with 6-311G(d) basis level in DMSO solvent. By considering the optimized molecular geometry of the titled compound, the ^1H and ^{13}C NMR chemical shift values were calculated at the same level by using Gauge-Independent Atomic Orbital method (Table 2). Theoretically and experimentally values (Gürbüz et al., 2021) were plotted according to $\delta_{\text{exp}} = a \cdot \delta_{\text{calc}} + b$, Eq. a and b constants regression coefficients with a standard error values were found using the SigmaPlot program. The correlation graphics are given Figure 3 and the linear correlation data of the 2-methoxy-6-[(3-methyl-5-oxo-4,5-dihydro-1H-1,2,4-triazol-4-yl)-iminomethyl] phenyl benzoate by considering the results are given in Table 2. Therefore, the (R^2) values (DFT) for ^1H NMR (DMSO) and ^{13}C NMR (DMSO) chemical shifts in different solvents has been found as 0.8252 and 0.9971 for the compound (Figure 3). In our study, the ^1H -NMR spectrum of the titled compound was observed belong to H19 proton peak at 11.76 ppm because acidic show feature (Yüksek, 1992; Yüksek et al., 2005; Yüksek et al., 2006, Gürbüz et al., 2021). H20 protons were observed at 9.90 ppm. Theoretically, DMSO solvent these values for the mentioned proton atoms were found as 6.61 and 9.73 ppm, respectively. In Table 2, the biggest ^{13}C chemical shift value of the molecule are observed at 164.28 ppm for the C11 carbon atom double bounded to the oxygen in carbonyl group (Anderson et al., 2004). DMSO solvent the calculated ppm values (DFT) for C11 carbon atom were theoretically found as 168.64 ppm. Additionally, due to the electronegative property of nitrogen atoms in molecule, the experimental NMR chemical shift values for C1 and C2 carbon atom the bounded to nitrogen atoms in 1,2,4-triazol ring and C3 carbon atom with sp^2 hybrid are observed at 148.84, 152.03, and 144.62 ppm, respectively.

Table 2. The calculated and experimental ^1H and ^{13}C NMR isotropic chemical shifts of the 2-methoxy-6-[(3-methyl-5-oxo-4,5-dihydro-1H-1,2,4-triazol-4-yl)-iminomethyl] phenyl benzoate

No	Experim.	DFT/6311(d) DMSO	Diff./ DMSO	No	Experim.	DFT/6311(d) DMSO	Diff./ DMSO
1C	148.84	150.27	-1.43	19H	11.76	6.61	5.15
2C	152.03	153.29	-1.26	20H	9.90	9.73	0.17
3C	11.32	12.43	-1.11	21H	7.36	6.63	0.73
4C	144.62	147.85	-3.23	22H	7.43	7.15	0.28
5C	128.65	132.85	-4.20	23H	7.65	7.52	0.13
6C	139.49	146.77	-7.28	24H	8.17	8.10	0.07
7C	151.63	157.65	-6.02	25H	7.57	7.40	0.17
8C	115.84	115.76	0.08	26H	7.79	7.56	0.23
9C	127.64	130.06	-2.42	27H	7.6	7.4	0.20
10C	118.74	118.08	0.66	28H	8.17	7.88	0.29
11C	164.28	168.64	-4.36	29H	3.81	3.44	0.37
12C	127.67	131.79	-4.12	30H	3.81	3.29	0.52
13C	130.42	134.05	-3.63	31H	3.81	3.66	0.15
14C	129.56	131.98	-2.42	32H	2.11	2.05	0.06
15C	134.76	138.43	-3.67	33H	2.11	2.1	0.01
16C	129.56	131.70	-2.14	34H	2.11	1.7	0.41
17C	130.42	134.52	-4.10				
18C	56.71	54.02	2.69				

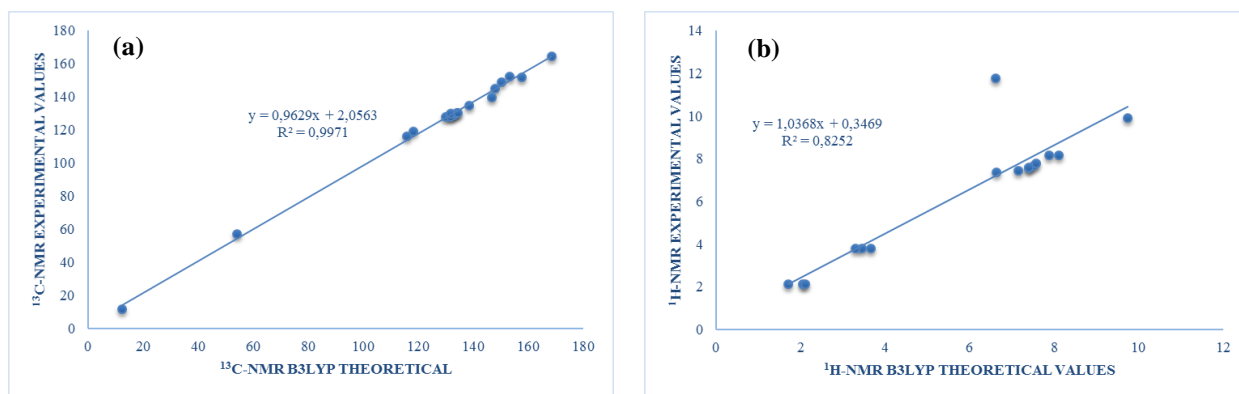


Figure 3. The correlation graphics for ^{13}C -NMR (DMSO) (a) and ^1H -NMR (DMSO) (b), chemical shifts of the 2-methoxy-6-[(3-methyl-5-oxo-4,5-dihydro-1H-1,2,4-triazol-4-yl)-iminomethyl]phenyl benzoate.

UV-visible Spectroscopy

The title molecule allow strong $\pi \rightarrow \pi^*$ and $\sigma \rightarrow \sigma^*$ transitions in UV-vis region with high extinction coefficients (Silverstein, et al., 1991). The absorption wavelengths (λ) excitation energies, and oscillator strengths (f) of UV-vis absorption spectroscopy of the titled compound has been calculated in ethanol solvents by using TD-DFT/B3LYP method (Figure 4 and Table 3).

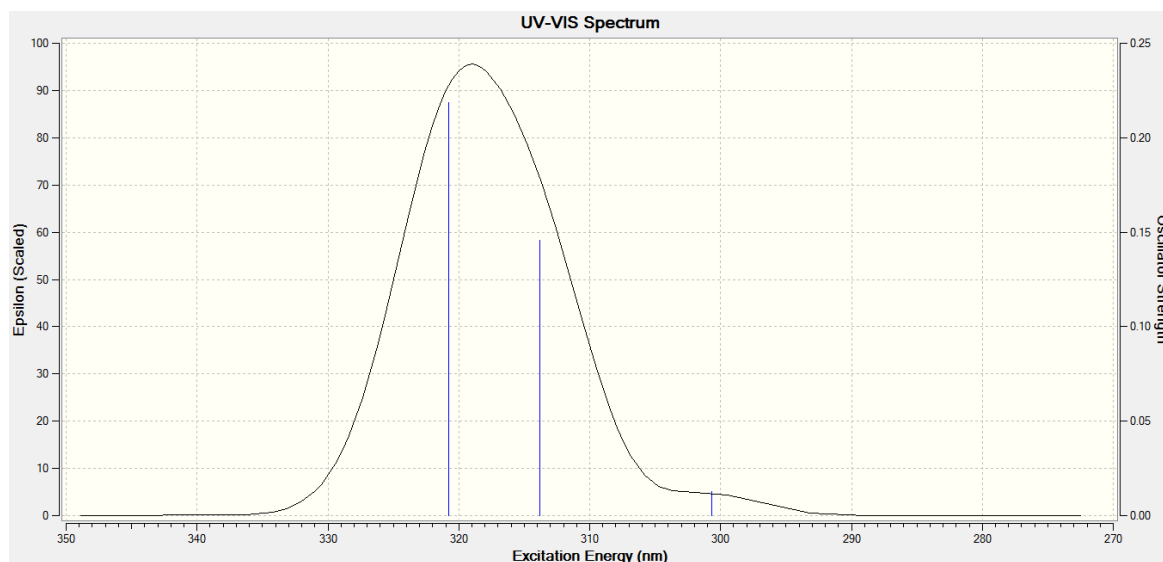


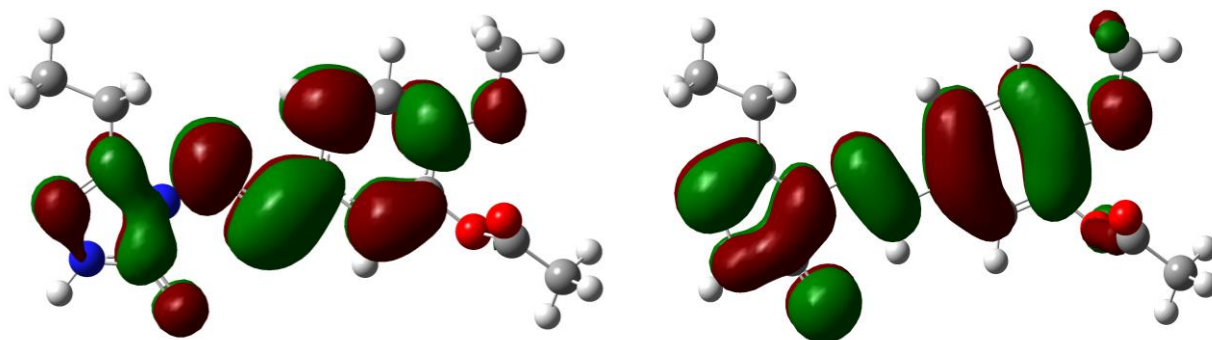
Figure 4. Simulated UV-Visible spectra with DFT/B3LYP/6-311G(d) level of the 2-methoxy-6-[(3-methyl-5-oxo-4,5-dihydro-1H-1,2,4-triazol-4-yl)-iminomethyl]phenyl benzoate.

Table 3. The experimental and calculated absorption wavelength (λ), excitation energies and oscillator strengths (f) the -methoxy-6-[(3-methyl-5-oxo-4,5-dihydro-1H-1,2,4-triazol-4-yl)-iminomethyl] phenyl benzoate.

λ (nm)Exp/B3LYP	Uyarma Enerjisi (eV) B3LYP	f (osilatör gücü) B3LYP
296/320.76	3.8653	0.2186
256/313.82	3.9208	0.1456
214/300.66	4.1237	0.0127

Frontier Molecular Orbital Analysis

The energies of two important molecular orbitals of the title molecule; the second highest and highest occupied MO's (HOMO), the lowest and the second lowest unoccupied MO's (LUMO) (Figure 5) were calculated by using DFT/B3LYP method with 6-311G(d) level and are presented in Table 4. The energy gap of the title molecule was calculated at DFT/B3LYP level, which reveals the chemical reactivity and proves the occurrence



E_{LUMO} (B3LYP): -2.1042 eV

E_{LUMO} (B3LYP): -6.0168 eV

Figure 5. The calculated HOMO-LUMO energies of the molecule according to DFT/B3LYP/6-31G(d) level

Table 4. The calculated HOMO-LUMO energies of the 2-methoxy-6-[(3-methyl-5-oxo-4,5-dihydro-1H-1,2,4-triazol-4-yl)-iminomethyl]phenyl benzoate according to DFT/B3LYP/6-311G(d) levels

Electronic properties	B3LYP	Electronic properties	B3LYP
I; Ionization Potential (eV)	6.1159	χ ; Electronegativity (eV)	3.9307
A; Electron Affinity (eV)	1.7456	Total Energy (a.u.)	-1215.7066
η ; Chemical Hardness (eV)	4.3703	ΔE ; Energy Gap (eV)	4.3703
S; Molecular Softness (eV)	2.1852	Pi; chemical potential	-3.9307

Table 5. The thermodynamic properties of the -methoxy-6-[(3-methyl-5-oxo-4,5-dihydro-1H-1,2,4-triazol-4-yl)-iminomethyl] phenyl benzoate

Rotational temperatures (Kelvin)	B3LYP
A	0.0117
B	0.0067
C	0.0045
Rotational constants (GHZ)	
A	0.2435
B	0.1396
C	0.0937
Zero-point vibrational energy (Kcal/Mol)	201.6304
Thermal correction to Energy	0.3444
Thermal correction to Enthalpy	0.3453
Thermal correction to Gibbs Free Energy	0.2656
Sum of electronic and zero-point Energies	-1215.3853
Sum of electronic and thermal Energies	-1215.3622
Sum of electronic and thermal Enthalpies	-1215.3613
Sum of electronic and thermal Free Energies	-1215.4410
Thermal Energies E(Kcal/mol)	
Translational	0.889
Rotational	0.889
Vibrational	214.329
Total	216.106
Thermal Capacity CV(Cal/Mol-Kelvin)	
Translational	2.981
Rotational	2.981
Vibrational	80.719
Total	86.680
Entropy S (Cal/Mol-Kelvin)	
Translational	43.470
Rotational	35.866
Vibrational	88.472
Total	167.808

of eventual charge transfer. The HOMO is located almost over the carbon atoms, oxygen atoms and also slightly delocalized in hydrogen atom and the LUMO is mainly delocalized in carbon atoms of benzene ring. The energy gap (energy difference between HOMO and LUMO orbital) is a critical parameter in determining molecular electrical transport properties (Fukui, 1982).

Conclusion

In this paper, the structure of the -methoxy-6-[(3-methyl-5-oxo-4,5-dihydro-1H-1,2,4-triazol-4-yl)-iminomethyl] phenyl benzoate is characterized by using FT-IR, ^1H , ^{13}C NMR and Uv-Vis spectroscopic methods. The molecular structures, vibrational frequencies, ^1H and ^{13}C NMR chemicals shifts, UV-vis spectroscopies, HOMO and LUMO analyses and atomic charges of -methoxy-6-[(3-methyl-5-oxo-4,5-dihydro-1H-1,2,4-triazol-4-yl)-iminomethyl] phenyl benzoate obtained have been calculated by using DFT/B3LYP method. By considering the results of experimental works it can be easily stated that the ^1H and ^{13}C NMR chemical shifts, and vibrational frequencies spectroscopic parameters obtained theoretically are in a very good agreement with the experimental data. Also, the electronic structure of titled compound is determined electronic structure identifiers such as the Energy of the Highest Occupied Molecular Orbital, Energy of the Lowest Unoccupied Molecular Orbital, molecular hardness, chemical softness, electronegativity, chemical potential, electrophilicity index, nucleophilicity index and dipole moment. Finally, in this study, the thermodynamic properties of the compound were calculated theoretically.

Scientific Ethics Declaration

The authors declare that the scientific ethical and legal responsibility of this article published in EPSTEM journal belongs to the authors.

References

- Aktaş-Yokuş, Ö., Yüksek, H. Manap, S. Aytemiz, F. Alkan, M. Beytur, M. & Gürsoy-Kol, Ö. (2017). In-vitro biological activity of some new 1, 2, 4-triazole derivatives with their potentiometric titrations, *Bulgarian Chemical Communications*, 49(1), 98-106.
- Alkan, M., Yuksek, H., Islamoglu, F., Bahceci, S., Calapoglu, M., Elmastas, M., Aksit, H., & Ozdemir, M. (2007). A study on 4-acylamino-4,5-dihydro-1H-1,2,4-triazol-5-ones, *Molecules*, 12 (8), 1805-1816.
- Anderson, R. J., Bendell, D. J., & Groundwater, P. W. (2004). *Organic spectroscopic analysis* (Vol. 22). Royal Society of Chemistry.
- Avcı, D., & Atalay, Y. (2009). Theoretical analysis of vibrational spectra and scaling- factor of 2- aryl- 1, 3, 4- oxadiazole derivatives. *International Journal of Quantum Chemistry*, 109(2), 328-341.
- Aytac, S. P., Tozkoparan, B., Kaynak, F. B., Aktay, G., Goktas, O., & Unuvar, S. (2009). Synthesis of 3,6-disubstituted 7H-1,2,4-triazolo[3,4-b]-1,3,4-thiadiazines as novel analgesic/anti-inflammatory compounds, *European Journal of Medicinal Chemistry*, 44(11), 4528-4538.
- Bahçeci, Ş. Yıldırım, N. Alkan, M. Gürsoy-Kol Ö., Manap, S., Beytur, M. & Yüksek, H. (2017). Investigation of Antioxidant, Biological and Acidic Properties of New 3-Alkyl(Aryl)-4-(3-acetoxy-4-methoxybenzylidenamino)-4,5-dihydro-1H-1,2,4-triazol-5-ones, *The Pharmaceutical and Chemical Journal*, 4(4), 91-101.
- Bahçeci, Ş., Yıldırım, N., Gürsoy-Kol, Ö., Manap, S., Beytur, M., & Yüksek, H. (2016). Synthesis, characterization and antioxidant properties of new 3-alkyl (aryl)-4-(3-hydroxy-4-methoxybenzylidenamino)-4, 5-dihydro-1H-1, 2, 4-triazol-5-ones. *Rasayan Journal of Chemistry*, 9(3), 494-501.
- Becke, A. D. (1993). Density functional thermochemistry. III. The role of exact Exchange, *The Journal of Chemical Physics*, 98, 5648-5652.
- Beytur, M. (2020). Fabrication of platinum nanoparticle/boron nitride quantum dots/6-methyl-2-(3-hydroxy-4-methoxybenzylidenamino)-benzothiazole (ils) nanocomposite for electrocatalytic oxidation of methanol. *Journal of the Chilean Chemical Society*, 65(3), 4929-4933.
- Beytur, M., & Avinca, I. (2021). Molecular, Electronic, Nonlinear Optical and Spectroscopic Analysis of Heterocyclic 3-Substituted-4-(3-methyl-2-thienylmethyleneamino)-4, 5-dihydro-1H-1, 2, 4-triazol-5-ones: experiment and dft calculations. *Heterocyclic Communications*, 27(1), 1-16.

- Beytur, M., Irak, Z. T., Manap, S., & Yüksek, H. (2019). Synthesis, characterization and theoretical determination of corrosion inhibitor activities of some new 4, 5-dihydro-1H-1, 2, 4-Triazol-5-one derivatives. *Heliyon*, 5(6), e01809.
- Boy, S. Türkan, F. Beytur, M. Aras, A. Akyıldırım O., Sedef Karaman, H., & Yüksek, H. (2017). Synthesis, design, and assessment of novel morpholine-derived Mannich bases as multifunctional agents for the potential enzyme inhibitory properties including docking study, *Bioorganic Chemistry*, 107, 104524.
- Çiftçi, E., Beytur M., Calapoğlu M., Gürsoy Kol Ö., Alkan M., Toğay, V.A., Manap S., Yüksek H. (2018). Synthesis, Characterization, Antioxidant and Antimicrobial Activities and DNA Damage of some novel 2-[3-alkyl (aryl)-4,5-dihydro-1h-1,2,4-triazol-5-one-4-yl]-phenoxyacetic acids in human lymphocytes, *Research Journal of Pharmaceutical, Biological and Chemical Sciences*, 9(5), 1760-1771.
- Dennington, R., Keith, T., & Millam, J. (2009). *GaussView*. Shawnee Mission.
- Frisch, A., Nielson, A. B., & Holder, A. J. (2003). *Gaussview User Manual*. Inc. Wallingford.
- Frisch, M. J., Trucks, G., Schlegel, H. B., Scuseria, G. E., Robb, M. A., Cheeseman, J. R., Scalmani, G., Barone, V., Mennucci, B., Petersson, G. A., Nakatsuji, H., Caricato, M., Li, X., Hratchian, H. P., Izmaylov, A. F., Bloino, J., Zheng, G., Sonnenberg, J. L., Hada, M., Ehara, M., Toyota, K., Fukuda, R., Hasegawa, J., Ishida, M., Nakajima, T., Honda, Y., Kitao, O., Nakai, H., Vreven, T., Montgomery, J. A., Jr. Vreven, T., Peralta, J. E., Ogliaro, F., Bearpark, M., Heyd, J. J., Brothers, E., Kudin, N., Staroverov, V. N., Kobayashi, R., Normand, J., Raghavachari, K., Rendell, A., Burant, J. C., Iyengar, S. S., Tomasi, J., Cossi, M., Rega, N., Millam, J. M., Klene, M., Knox, J. E., Cross, J. B., Bakken, V., Adamo, C., Jaramillo, J., Gomperts, R., Stratmann, R. E., Yazyev, O., Austin, A. J., Cammi, R., Pomelli, C., Ochterski, J. W., Martin, L. R., Morokuma, K., Zakrzewski, V. G., Voth, G. A., Salvador, P., Dannenberg, J. J., Dapprich, S., Daniels, A. D., Farkas, O., Foresman, J. B., Ortiz, J. V., Cioslowski, J. & Fox, D. J. (2009). *Gaussian Inc*. Wallingford.
- Gürbüz, A., Alkan, M., Manap, S., Özdemir, G., Yüksek, H. (2021). Synthesis and antimicrobial activities of novel 2-methoxy-6-[(3-alkyl-4,5-dihydro-1h-1,2,4-triazol-5-one-4-yl)-azomethin]-phenyl benzoates with their nonaqueous medium titrations. *World Journal of Pharmacy and Pharmaceutical Sciences*. 10(9), 65-80
- Gürsoy-Kol, O., & Yüksek, H. (2010). Synthesis and in vitro antioxidant evaluation of some novel 4, 5-dihydro-1H, 2, 4-triazol-5-one derivatives. *E-Journal of Chemistry*, 7(1), 123-136.
- Jamróz, M. H. (2004). *Vibrational Energy Distribution Analysis: VEDA 4 program*.
- Koç, E., Yüksek, H., Beytur, M., Akyıldırım, O., Akçay, M., & Beytur, C. (2020). Heterosiklik 4, 5-dihidro-1H-1, 2, 4-triazol-5-on türevinin antioksidan özelliğinin erkek ratlarda (wistar albino) in vivo olarak belirlenmesi. *Bitlis Eren Üniversitesi Fen Bilimleri Dergisi*, 9(2), 542-548.
- Lee, S. Y. (1998). Molecular structure and vibrational spectra of biphenyl in the ground and the lowest triplet states. *Bulletin of the Korean Chemical Society*, 19(1), 93-98.
- Rani, A. U., Sundaraganesan, N., Kurt, M., Cinar, M., & Karabacak, M. (2010). FT-IR, FT-Raman, NMR spectra and DFT calculations on 4-chloro-N-methylaniline. *Spectrochimica Acta Part A: Molecular and Biomolecular Spectroscopy*, 75(5), 1523-1529.
- Silverstein, R. M., & Bassler, G. C. (1962). Spectrometric identification of organic compounds. *Journal of Chemical Education*, 39(11), 546.
- Subramanian, N., Sundaraganesan, N., & Jayabharathi, J. (2010). Molecular structure, spectroscopic (FT-IR, FT-Raman, NMR, UV) studies and first-order molecular hyperpolarizabilities of 1, 2-bis (3-methoxy-4-hydroxybenzylidene) hydrazine by density functional method. *Spectrochimica Acta Part A: Molecular and Biomolecular Spectroscopy*, 76(2), 259-269.
- Turhan-Irak Z., & Gümüş, S. (2017). Heterotricyclic compounds via click reaction: A computational study. *Noble International Journal of Scientific Research*, 1(7), 80-89.
- Turhan-Irak, Z., & Beytur, M. (2019). 4-Benzilidenamino-4, 5-dihidro-1H-1, 2, 4-triazol-5-on türevlerinin antioksidan aktivitelerinin teorik olarak incelenmesi. *Journal of the Institute of Science and Technology*, 9(1), 512-521.
- Turhan-Irak, Z., & Gümüş, S. (2017). Heterotricyclic compounds via click reaction: A computational study. *Noble International Journal of Scientific Research*, 1(7), 80-89.
- Uğurlu, G., & Beytur, M. (2020). Theoretical studies on the structural, vibrational, conformational analysis and nonlinear optic (NLO) property of 4-(Methoxycarbonyl) phenylboronic acid. *Indian Journal of Chemistry-Section A*, 59(10), 1504-1512.
- Vosko, S. H., Wilk, L., & Nusair, M. (1980). Accurate spin-dependent electron liquid correlation energies for local spin density calculations: a critical analysis. *Canadian Journal of physics*, 58(8), 1200-1211.
- Wade, Jr. L.G. (2006). *Organic Chemistry* (6nd ed.). Pearson Prentice Hall.
- Wolinski, K., Hinton, J. F., & Pulay, P. (1990). Efficient implementation of the gauge-independent atomic orbital method for NMR chemical shift calculations. *Journal of the American Chemical Society*, 112(23), 8251-8260.

- Yüksek, H. (1992). 3-Alkil(aril)-4-amino-4,5-dihidro-1,2,4-triazol-5-on'ların bazı reaksiyonlarının incelenmesi (Doktora Tezi, KTÜ Fen Bilimleri Enstitüsü).
- Yüksek, H., Bahceci, S., Ocak, Z., Alkan, M., Ermis, B., Mutlu, T., Ocak, M., & Ozdemir, M. (2004). Synthesis of some 4,5-dihydro-1H-1,2,4-triazol-5-ones, *Indian journal of heterocyclic chemistry*, 13(4), 369-372.
- Yüksek, H., Kucuk, M., ALKAN, M., BAHCECI, Ş., Kolayli, S., Ocak, Z., ... & Ocak, M. (2006). Synthesis and antioxidant activities of some new 4-(4-hydroxybenzylidenamino)-4, 5-dihydro-1H-1, 2, 4-triazol-5-one derivatives with their acidic properties. *Asian Journal of Chemistry*, 18(1).
- Yüksek, H., Üçüncü, O., Alkan, M., Ocak, Z., & Bahceci, S. (2005). Synthesis and non-aqueous medium titrations of some new 4-benzylidenamino-4, 5-dihydro-1H-1, 2, 4-triazol-5-one derivatives. *Molecules*, 10(8), 961-970.

Author Information

Murat BEYTUR

Kafkas University

Kars, Turkey

Contact e-mail: muratbeytur83@gmail.com**Haydar YUKSEK**

Kafkas University

Kars, Turkey

To cite this article:

Beytur, M. & Yuksek, H. (2021). In silico calculations of 2-methoxy-6-[(3-methyl-5-oxo-4,5-dihydro-1h-1,2,4-triazol-4-yl)-iminomethyl] phenyl benzoate. *The Eurasia Proceedings of Science, Technology, Engineering & Mathematics (EPSTEM)*, 15, 54-62.

The Eurasia Proceedings of Science, Technology, Engineering & Mathematics (EPSTEM), 2021

Volume 15, Pages 63-68

ICBAST 2021: International Conference on Basic Science and Technology

Density Functional Theory Studies of Structural Nonlinear Optic and Electronic Properties of Chalcone (E)-3-(Furan-2-Yl)-1-Phenylprop-2-en-1-one Molecule

Guventurk UGURLU
Kafkas University

Abstract: In this study, the geometry optimization of Chalcone (E)-3-(Furan-2-yl)-1-Phenylprop-2-en-1-one molecule was performed at Density Functional Theory (DFT) with Becke-3-Lee-Yang-Parr (B3LYP) the hybrid functional using the 6-311++G(d,p) basis set in the gas phase. The highest occupied molecular orbital (HOMO) energy, the lowest unoccupied molecular orbital (LUMO) energy, the polarizability (α), and hyperpolarizability (β) values of title molecule were calculated DFT/B3LYP/6-311++G(d,p) method in the ground state. The ^1H and ^{13}C NMR spectroscopy values of the molecule were calculated at DFT/B3LYP method using different basis sets such as 6-31G, 6-31+G, 6-31G(d) and 6-311+(2d,p) and the calculated ^1H and ^{13}C NMR values were compared with the experimental values in the literature. The equilibrium state (ground state) dipole moment values of the molecule were calculated as 3.33 Debye by B3LYP/6-311++ G(d,p) method. The electronic energy, dipole moment, polarizability and hyperpolarizability of the title molecule are analyzed and reported. The calculated geometric parameters (bond lengths and bond-dihedral angles) of the molecule were compared with the experimental values in the literature and they were found to be in good agreement. The approximate geometry of the molecules in three dimensions was drawn in the GaussView 5.0 molecular imaging program, and all theoretical calculations were used with the Gaussian 09W package program.

Keywords: Chalcone (E)-3-(Furan-2-yl)-1-Phenylprop-2-en-1-one, Dipole moment, HOMO, LUMO, Polarizability

Introduction

Chalcones are found in various types of plants such as vegetables, fruits, tea and soy, and consist of two aromatic rings are linked by a three carbon α , β -unsaturated carbonyl system. Chalcones possess many biological activities such as antidiabetic (Hsieh et al. 2012; Maly et al. 2006), antiviral (de Campos-Buzzi et al. 2006; Kozłowski et al. 2007), antitumor (Kumar et al. 2003), antibacterial (Nielsen et al. 2004; Farooq et al. 2020), anti-inflammatory (Herencia et al. 1998) antifungal (Valla et al. 2006), as well as non-biological applications in solar dyes, chemosensors (Hu et al. 2013), photo-conductors (Girgis et al. 2018), and optoelectronic devices (Xiao et al. 2013). These compounds are an intermediate for the synthesis of diverse heterocyclic compounds like isoxazole (Kaur et al. 2013), pyrazolone (Reddy et al. 2016), thiazine (Badshah et al. 2016), indazole pyrimidine valuable in pharmaceutical industries. Crystal structure of Chalcone (E)-3-(Furan-2-Yl)-1-Phenylprop-2-en-1-one molecule (1) were determined experimentally using X-ray structure analysis and spectroscopic methods (Vázquez-Vuelvas et al., 2015) but molecular properties such as electronic energy, non-linear optic of title molecule have not been determined.

In this work, molecular structure, dipole moment, polarizability, first static hyper polarizability, the electronic structure and HOMO-LUMO energies of above-mentioned molecule have been studied. The calculated geometric parameters (bond lengths and bond-dihedral angles) of the molecule were compared with the

- This is an Open Access article distributed under the terms of the Creative Commons Attribution-NonCommercial 4.0 Unported License, permitting all non-commercial use, distribution, and reproduction in any medium, provided the original work is properly cited.

- Selection and peer-review under responsibility of the Organizing Committee of the Conference

© 2021 Published by ISRES Publishing: www.isres.org

experimental values in the literature and they were found to be in good agreement ^1H NMR and ^{13}C NMR chemical shifts calculations have been performed. Also, the energy band gap of Chalcone (E)-3-(Furan-2-yl)-1-Phenylprop-2-en-1-one molecule is calculated by using the highest occupied molecular orbital (HOMO) energy, the lowest unoccupied molecular orbital (LUMO) energy. The molecular structure using numbering scheme of the compound (1) is given in Figure 1

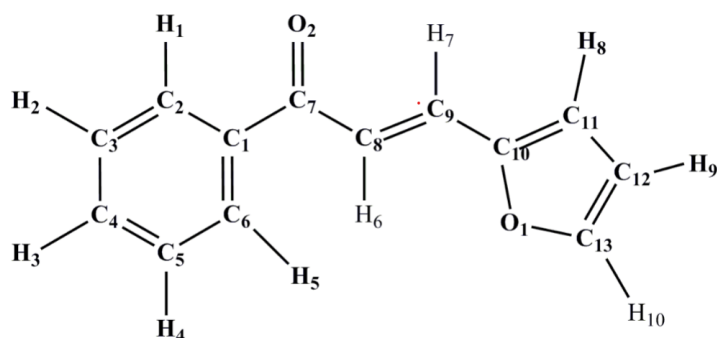


Figure 1. Molecular structure of Chalcone (E)-3-(Furan-2-yl)-1-Phenylprop-2-en-1-one molecule numbering scheme

Method

The quantum mechanics calculations on the isolated of Chalcone (E)-3-(Furan-2-yl)-1-Phenylprop-2-en-1-one molecule were performed by the aid of Gaussian 09W program package and Gauss view 5.0 molecular visualization programs (Frisch et al., 2010; Dennington et al., 2009) in the gas phase. The geometric parameters of 3-bromo-4-(2-pyridyl) thiophene molecule in the equilibrium state were optimized at DFT with Becke's three parameter hybrid functional (B3) (Becke, 1988) and combined with gradient corrected correlation functional of Lee–Yang–Parr (LYP) (Lee et al., 1988; Becke, 1993) and employing 6-311++G (d,p) basis set (Francl et al., 1982; Rassolov et al., 2001). After optimization, at optimized structures of the title compound obtained B3LYP/6-311++G (d,p) level of theory, dipole moment (μ), polarizability (α), hyperpolarizability (β) based on finite field approach and energy differences of $E_{\text{LUMO}} - E_{\text{HOMO}}$ were calculated in the same as level of theory. The ^1H and ^{13}C NMR chemical shifts were calculated by GIAO approach by using B3LYP level of theory with different basis sets.

Results and Discussion

Firstly, the geometric parameters of the title compound in the ground state were optimized at DFT-B3LYP level of theory using 6-311++G (d, p) as basis set. The optimized geometry of the title molecule performed at B3LYP/6-311G++ (d, p) level with atoms numbering is shown Figure 1. The optimized geometry and Molecular electrostatic potential (MEP) surface values of title molecule obtained B3LYP/6-311++G (d, p) level are presented Figure 2 (a) and (b)

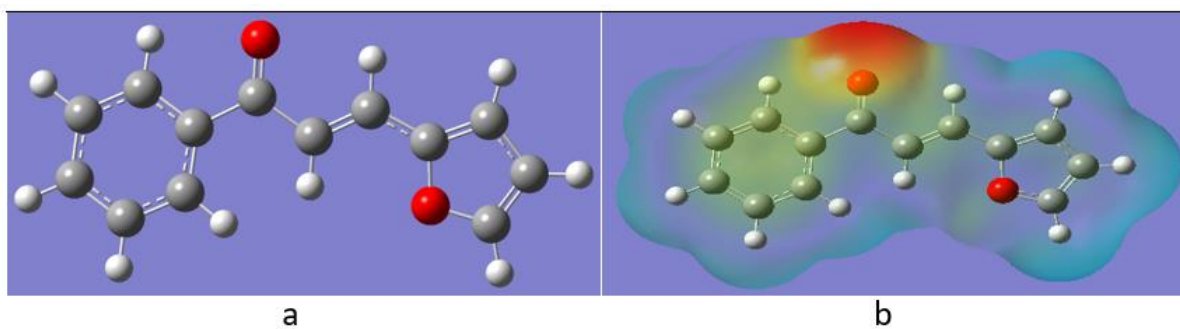


Figure 2. (a)The optimized geometry, (b) Molecular electrostatic (MEP) potential surface (PES) of Chalcone (E)-3-(Furan-2-yl)-1-Phenylprop-2-en-1-one molecule.

The calculated values of the electronic energy, dipole moment, polarizability, hyperpolarizability, using the highest occupied molecular orbital (HOMO) energy, the lowest unoccupied molecular orbital (LUMO) energy and energy gap (ΔE_g) at the ground-state equilibrium geometry of studied molecule are listed in Table 1. As seen from Table 1, the equilibrium state (ground state) dipole moment values of the molecule were calculated as 3.33 Debye by B3LYP/6-311++ G(d,p) method. The energy band gap was obtained as 3,83 eV by using HOMO and LUMO energy.

Table 1. The electronic, HOMO, LUMO energy, dipole moment, polarizability, hyperpolarizability, and energy gap (ΔE_g) of Chalcone (E)-3-(Furan-2-Yl)-1-Phenylprop-2-en-1-one molecule

DFT/B3LYP/6-311++G (d,p)						
Electronic Energy (a.u)	μ (D)	α (a.u)	β (a.u)	E_{HOMO} (a.u)	E_{LUMO} (a.u)	ΔE_g (eV)
-651.993113415	3.33	183,58	2289,05	-0.232847	-0.092067	3,830

The X-ray crystal structures for studied molecule is available in the literature and (Vázquez-Vuelvas et al., 2015) and the calculated parameter studied molecule of both at the B3LYP/6-311++G (d, p) method in the ground state are tabulated in the Table 2. and findings here. The polarizability, hyperpolarizability of title molecule are calculated as 183,58 a.u and 2289,05 a.u, respectively and studied molecule was found to have a high hyperpolarizability value.

Table 2. Selected structural parameters of Chalcone (E)-3-(Furan-2-Yl)-1-Phenylprop-2-en-1-one molecule

Atoms	Bond length (Å)		Atoms	Bond angle (°)	
	DFT	Exp ^a .		DFT	Exp ^a .
O1—C13	1.3568	1.3627(17)	C2-C1-C7	118.77	118.43 (11)
O1—C10	1.3739	1.3628(15)	C6-C1-C7	123.55	122.76 (12)
C1—C2	1.4028	1.3855 (19)	O2-C7-C8	121.14	120.74 (12)
C1—C6	1.4017	1.3857 (18)	O2-C7-C1	119.87	119.78 (12)
C1—C7	1.5032	1.4882 (17)	C8-C7-C1	118.98	119.44 (11)
O2—C7	1.2256	1.2218 (15)	C8-C9-C10	126.31	
C7—C8	1.4801	1.4664 (18)	C8-C9-H9	119.96	116,30
C9—C8	1.3485	1.3308 (17)	C10-C9-H9	117.96	116,30
C9—C10	1.4305	1.4236 (18)	C9-C8-C7	120.16	121.16 (12)
C10—C11	1.3740	1.3468 (18)	C9-C8-H8	119.86	119,40
C11—C12	1.4247	1.407 (2)	C7-C8-H8	119.96	119,40
C6—C5	1.3934	1.3840 (19)	C11-C10-C9	131.60	131.84 (12)
C12—C13	1.3625	1.327 (2)	O1-C10-C9	119.35	118.76 (11)
C2—C3	1.3891	1.377 (2)	C10-C11-C12	106.91	107.32 (12)
C5—C4	1.3931	1.364 (2)	C5-C6-C1	120.53	120.15 (14)
C4—C3	1.3963	1.366 (2)			
Dihedral angle (°)					
C2-C1-C7-O2	10.01	19.4 (2)	C9-C10-C11-C12	-179.94	-176.65 (14)
C6-C1-C7-O2	-169.05	-159.66 (14)	C6-C5-C4-C3	-0.43	-0.1 (2)
C2-C1-C7-C8	-169.00	-158.15 (13)	C5-C4-C3-C2	-0.40	-0.7 (3)
C6-C1-C7-C8	11.00	22.74 (19)	C10-C11-C12-	0.01	-0.29 (17)
C10-C9-C8-	-179.21	-176.31 (13)	C1-C2-C3-C4	0.50	0.7 (3)
O2-C7-C8-C9	2.77	-5.4 (2)	C8-C9-C10-O1	0.02	-3.2 (2)
C1-C7-C8-C9	-177.84	172.14 (12)	C11-C12-C13-O1	-0.02	-0.03 (18)
C6-C1-C2-C3	-0.49	0.0 (2)	C13-O1-C10-C11	-0.02	-0.50 (16)
C7-C1-C2-C3	-179.59	-179.11 (14)	C13-O1-C10-C9	179.94	177.07 (12)
C2-C1-C6-C5	0.03	-0.7 (2)	C8-C9-C10-C11	179.96	173.72 (14)
C7-C1-C6-C5	179.07	178.37 (13)	O1-C10-C11-C12	0.01	0.49 (16)
C1-C6-C5-C4	0.43	0.8 (2)	C10-O1-C13-C12	0.02	0.33 (17)

(^aref Vázquez-Vuelvas et al., 2015)

¹H and ¹³C NMR Chemical Shift

The ¹H NMR and ¹³C NMR chemical shifts of Chalcone (E)-3-(Furan-2-Yl)-1-Phenylprop-2-en-1-one molecule are calculated using the gauge-independent atomic orbital method (GIAO method) and the hybrid three-parameter B3LYP density functional in combination with different basis sets such as 6-31G, 6-31+G and 6-31+G(d) basis sets in gas phase and in solvents (DMSO). The calculated ¹H and ¹³C chemical shielding

values calculated B3LYP/6-31G, B3LYP/6-31+G and B3LYP/6-31+G(d) are given in the Table 3. Also, the value ^{13}C NMR chemical shifts are carried regression analyses and the results were indicated linear correlation. The calculated R^2 (6-31+G(d)) have been 0.9906 (gas phase) and 0.9962 (DMSO) for ^{13}C -NMR chemical shifts values. These results show that there is a good agreement between the experimental values and the theoretical values.

Table 3. The calculated ^1H -NMR and ^{13}C -NMR isotropic chemical shifts (ppm) for title molecule.

No	Exp ^a	DFT/B3LYP					
		6-31G		6-31+G		6-31G+(d)	
		GAS	DMSO	GAS	DMSO	GAS	DMSO
C7	189.95	181,48	183,24	183,54	185,92	178,64	181,17
C10	151.69	150,29	149,37	154,40	153,60	149,66	148,94
C13	144.98	140,91	143,81	143,39	146,80	139,50	143,16
C1	138.16	135,05	135,03	138,01	138,21	134,50	134,65
C4	132.82	127,43	129,44	129,08	131,64	126,74	129,32
C9	130.72	125,79	127,58	127,93	130,04	126,00	127,97
C2	128.47	125,67	125,19	127,66	127,40	125,92	125,26
C6	128.47	124,42	125,18	126,24	127,26	123,71	125,23
C3	128.47	123,55	124,91	125,17	127,11	123,21	124,90
C5	128.47	123,27	124,80	125,07	126,99	122,57	124,70
C8	119.30	115,41	118,99	117,70	120,57	113,78	118,01
C11	116.33	115,34	115,02	116,26	117,57	113,27	113,09
C12	112.74	111,08	112,67	111,62	113,67	108,01	109,91
R^2		0.9915	0.9958	0.9885	0.9939	0.9906	0.9962
H1	8.04	8,51	8,36	8,67	8,54	8,45	8,33
H7	8.04	7,89	7,92	8,03	8,10	7,69	7,75
H6	7.61	7,85	7,91	7,82	7,92	7,37	7,48
H10	7.58	7,82	8,06	7,98	8,25	7,96	8,22
H5	7.52	7,57	7,84	7,72	8,02	7,46	7,75
H2	7.52	7,51	7,69	7,54	7,74	7,45	7,62
H3	7.49	7,45	7,72	7,63	7,92	7,51	7,78
H4	7.47	7,44	7,69	7,55	7,82	7,43	7,68
H8	6.72	6,65	7,00	6,82	7,20	6,56	6,92
H9	6.51	6,51	6,79	6,66	6,96	6,41	6,66

Conclusion

In this work, the lowest unoccupied molecular orbital (LUMO) and the highest occupied molecular orbital (HOMO), bond lengths, electronic parameters, dipole moments and total energy values of Chalcone (E)-3-(Furan-2-Y1)-1-Phenylprop-2-en-1-one molecule were calculated by DFTB3LYP level with the 6-311++G(d,p) basis set. The ^1H NMR and ^{13}C NMR chemical shifts of Chalcone (E)-3-(Furan-2-Y1)-1-Phenylprop-2-en-1-one molecule are calculated using the gauge-independent atomic orbital method (GIAO method) and the hybrid three-parameter B3LYP density functional in combination with different basis sets such as 6-31G, 6-31+G and 6-31+G(d) basis sets in gas phase and in solvents (DMSO). As seen from Table 1, the value ^{13}C NMR chemical shifts are carried regression analyses and the results were indicated linear correlation. The calculated R^2 (6-31+G(d)) have been 0.9906 (gas phase) and 0.9962 (DMSO) for ^{13}C -NMR chemical shifts values.

Scientific Ethics Declaration

The authors declare that the scientific ethical and legal responsibility of this article published in EPSTEM journal belongs to the authors.

References

- Badshah, S. L., & Naeem, A. (2016). Bioactive thiazine and benzothiazine derivatives: green synthesis methods and their medicinal importance. *Molecules*, 21(8), 1054.
- Becke, A. D. (1988) Density-functional exchange-energy approximation with correct asymptotic behavior. *Physical Review A*, 38(6), 3098–3100.
- Becke, A. D. (1992). Density- functional thermochemistry. I. The effect of the exchange- only gradient correction. *The Journal of chemical physics*, 96(3), 2155-2160.
- de Campos- Buzzi, F., Pereira de Campos, J., Pozza Tonini, P., Corrêa, R., Augusto Yunes, R., Boeck, P., & Cechinel- Filho, V. (2006). Antinociceptive effects of synthetic chalcones obtained from xanthoxylone. *Archiv der Pharmazie: An International Journal Pharmaceutical and Medicinal Chemistry*, 339(7), 361-365.
- Dennington, R., Keith T., Millam, J. (2009). Semicem Inc, In *GaussView* (Version 5). Shawnee Mission.
- Farooq, S., Ngaini, Z., & Mortadza, N. A. (2020). Microwave- assisted Synthesis and Molecular Docking Study of Heteroaromatic Chalcone Derivatives as Potential Antibacterial Agents. *Bulletin of the Korean Chemical Society*, 41(9), 918-924.
- Francl, M. M., Pietro, W. J., Hehre, W. J., Binkley, J. S., Gordon, M. S., DeFrees, D. J., & Pople, J. A. (1982). Self- consistent molecular orbital methods. XXIII. A polarization- type basis set for second- row elements. *The Journal of Chemical Physics*, 77(7), 3654-3665.
- Frisch M J, Trucks G W, Schlegel H B, Scuseria G E, Robb M A, Cheeseman J R, Scalmani G, Barone V, Mennucci B, Petersson G A, Nakatsuji H, Caricato M, Li X, Hratchian H P, Izmaylov A F, Bloino J, Zheng G, Sonnenberg J L, Hada M, Ehara M, Toyota K, Fukuda R, Hasegawa J, Ishida, M, Nakajima T, Honda Y, Kitao O, Nakai H, Vreven T, Montgomery J A, Vreven T J, Peralta J E, Ogliaro F, Bearpark M, Heyd J. J, Brothers E, Kudin N, Staroverov V N, Kobayashi R, Normand J, Raghavachari K, Rendell A, Burant J C, Iyengar S S, Tomasi J, Cossi M, Rega N, Millam J M, Klene, M, Knox J E, Cross J B, Bakken V, Adamo C, Jaramillo J, Gomperts R, Stratmann R E, Yazyev O, Austin A J, Cammi R, Pomelli C J, Ochterski W, Martin L R, Morokuma K, Zakrzewski V G, Voth G A, Salvador P, Dannenberg J J, Dapprich S, Daniels A D, Farkas O, Foresman J B, Ortiz J V, Cioslowski J, Fox D J, (2009). *Gaussian Inc.* Wallingford.
- Girgis, A. S., Basta, A. H., El-Saied, H., Mohamed, M. A., Bedair, A. H., & Salim, A. S. (2018). Synthesis, quantitative structure–property relationship study of novel fluorescence active 2-pyrazolines and application. *Royal Society Open Science*, 5(3), 171964.
- Herencia, F., Ferrandiz, M. L., Ubeda, A., Dominguez, J., Charris, J. E., Lobo, G. M., & Alcaraz, M. J. (1998). Synthesis and anti-inflammatory activity of chalcone derivatives. *Bioorganic & Medicinal Chemistry Letters*, 8(10), 1169-1174.
- Hsieh, C. T., Hsieh, T. J., El-Shazly, M., Chuang, D. W., Tsai, Y. H., Yen, C. T., ... & Chang, F. R. (2012). Synthesis of chalcone derivatives as potential anti-diabetic agents. *Bioorganic & medicinal chemistry letters*, 22(12), 3912-3915.
- Hu, S., Zhang, S., Hu, Y., Tao, Q., & Wu, A. (2013). A new selective pyrazoline-based fluorescent chemosensor for Cu²⁺ in aqueous solution. *Dyes and Pigments*, 96(2), 509-515.
- Kaur, N., & Kishore, D. (2013). Application of chalcones in heterocycles synthesis: synthesis of 2-(isoxazolo, pyrazolo and pyrimido) substituted analogues of 1, 4-benzodiazepin-5-carboxamides linked through an oxyphenyl bridge. *Journal of Chemical Sciences*, 125(3), 555-560.
- Kozłowski, D., Trouillas, P., Calliste, C., Marsal, P., Lazzaroni, R., & Duroux, J. L. (2007). Density functional theory study of the conformational, electronic, and antioxidant properties of natural chalcones. *The Journal of Physical Chemistry A*, 111(6), 1138-1145.
- Kumar, S. K., Hager, E., Pettit, C., Gurulingappa, H., Davidson, N. E., & Khan, S. R. (2003). Design, synthesis, and evaluation of novel boronic-chalcone derivatives as antitumor agents. *Journal of Medicinal Chemistry*, 46(14), 2813-2815.
- Lee, C., Yang, W., & Parr, R. G. (1988). Development of the Colle-Salvetti correlation-energy formula into a functional of the electron density. *Physical Review B*, 37(2), 785.
- Nielsen, S. F., Boesen, T., Larsen, M., Schönning, K., & Kromann, H. (2004). Antibacterial chalcones— bioisosteric replacement of the 4'-hydroxy group. *Bioorganic & Medicinal Chemistry*, 12(11), 3047-3054.
- Rassolov, V. A., Ratner, M. A., Pople, J. A., Redfern, P. C., & Curtiss, L. A. (2001). 6- 31G* basis set for third- row atoms. *Journal of Computational Chemistry*, 22(9), 976-984.
- Xiao, D., Xi, L., Yang, W., Fu, H., Shuai, Z., Fang, Y., & Yao, J. (2003). Size-tunable emission from 1, 3-diphenyl-5-(2-anthryl)-2-pyrazoline nanoparticles. *Journal of the American Chemical Society*, 125(22), 6740-6745.

Vázquez-Vuelvas, O. F., Enríquez-Figueroa, R. A., García-Ortega, H., Flores-Alamo, M., & Pineda-Contreras, A. (2015). Crystal structure of the chalcone (E)-3-(furan-2-yl)-1-phenylprop-2-en-1-one. *Acta Crystallographica Section E: Crystallographic Communications*, 71(2), 161-164.

Author Information

Guventurk UGURLU

Kafkas University

Department of Physics, Kars 36100 Turkey

gugurlu@kafkas.edu.tr

To cite this article:

Ugurlu, G. (2021). Density functional theory studies of structural nonlinear optic and electronic properties of chalcone (E)-3-(Furan-2-Yl)-1-Phenylprop-2-en-1-one molecule. *The Eurasia Proceedings of Science, Technology, Engineering & Mathematics (EPSTEM)*, 15, 63-68.

The Eurasia Proceedings of Science, Technology, Engineering & Mathematics (EPSTEM), 2021

Volume 15, Pages 69-78

ICBAST 2021: International Conference on Basic Science and Technology

Experimental (FT-IR, $^{13}\text{C}/^1\text{H}$ -NMR) and DFT (B3LYP, B3PW91) Studies of 3-*n*-Propyl-4-[2-(4-Methoxybenzoxy)-3-Methoxy] Benzylidenamino-4,5-Dihydro-1*h*-1,2,4-Triazol-5-Ones Molecule

Gul KOTAN

Kafkas University

Muzaffer ALKAN

Kafkas University

Haydar YUKSEK

Kafkas University

Abstract: All theoretical calculations of 3-*n*-propyl-4-[2-(4-methoxybenzoxy)-3-methoxy] benzylidenamino-4,5-dihydro-1*H*-1,2,4-triazol-5-ones has been performed with B3LYP/B3PW91 functions of DFT method using the 6-311G(d,p) basis set (Frisch et al., 2009; Wolinski et al., 1990). Firstly, optimized to achieve the most stable form of the molecule. Then, the veda4f program was used in defining Infrared (IR) data (Jamróz, 2004). The standard error values were found via the Sigma plot with regression coefficient of a and b constants. The vibrational frequency values of this molecule have been calculated by using 6-311G(d,p) basis set with DFT (B3LYP/ B3PW91) methods. Then, these values are scaled with appropriate scale factors (Merrick et al., 2007). ^1H -NMR and ^{13}C -NMR spectral values according to GIAO method (Wolinski et al., 1990) was calculated using Gaussian G09W program package in DMSO solvent and in gas phase. Theoretical spectral values of molecule were compared with experimental values. Experimental data obtained from the literature (Alkan et al., 2014). In addition, electronic properties (electronegativity (χ), global hardness (η), electron affinity (A), ionization potential (I), softness (σ), thermodynamics properties (heat capacity CV^0 , entropy S^0 and enthalpy H^0), HOMO-LUMO energy, $E_{\text{LUMO}}-E_{\text{HOMO}}$ energy gap (ΔE_g), geometric properties (bond angles, bond lengths), dipole moments, Mulliken atomic charges, total energy of the molecule were calculated. Finally, the molecular surfaces such as the electron density, molecular electrostatic potential (MEP), contour and the total density maps were designated.

Keywords: B3LYP, B3PW91, DFT, HOMO-LUMO, MEP.

Introduction

The 1,2,4-triazole and its derivatives are important heterocyclic compounds. They are also present in the structure of Schiff bases, which contain a (-C=N-) azomethine group in their structure and, are generally synthesized by the condensation of primary amines with an aldehyde or ketone. The Schiff bases containing 1,2,4-triazole are very active in terms of showing biological activity. In particular, they show antitubercular (Amim, et al., 2017), antibacterial (Kotan, 2021), antitumor (Demirbaş, et al., 2002), antioxidant (Yüksek, et al., 2011; Manap, et al., 2020), analgesic (Rana, et al., 2012), antifungal (Dharmaraj, et al., 2001), anti-inflammatory (Shukla, et al., 2014) and anticancer properties (Uddin, et al., 2020). The Schiff bases are important molecules in the pharmaceutical and medicinal fields. In recent years, many theoretical studies for Schiff bases containing 1,2,4-triazole have been carried out (Kotan, et al., 2020; Yüksek, et al., 2017; Kotan, et

- This is an Open Access article distributed under the terms of the Creative Commons Attribution-Noncommercial 4.0 Unported License, permitting all non-commercial use, distribution, and reproduction in any medium, provided the original work is properly cited.

- Selection and peer-review under responsibility of the Organizing Committee of the Conference

© 2021 Published by ISRES Publishing: www.isres.org

al., 2021; Beytur, et al., 2021). Gaussian 09W program was used for quantum chemical calculations. First, the optimization process was carried out to reach the most stable state of the molecule, then the atoms of the molecule were numbered. From this optimized structure, all electronic, thermodynamic, spectroscopic and geometric theoretical values of the molecule were calculated (Frisch et al., 2009). IR vibration frequency values were calculated with the Veda 4f program (Jamróz., 2004) and the vibration frequency data were multiplied with definite scala factor (Merrich, et al., 2007) The ^1H - ^{13}C / NMR isotropic shift values were calculated by the GIAO method using the Gaussian G09 package program (Wolinski et al., 1990). These values were compared with the experimental values (Alkan, et al., 2002) and the difference values were found, and these values were $\delta_{\text{exp}} = a + b \cdot \delta_{\text{calc}}$. δ_{calc} plotted according to the equation. The bond length, HOMO-LUMO energy, total energy, bond angle, mulliken atomic charges, dipole moment of the molecule were calculated. In addition, MEP surface maps were determined.

Method

The 1,2,4-triazole and its derivatives are important heterocyclic compounds. They are also present in the structure of Schiff bases, which contain a (-C=N-) azomethine group in their structure and, are generally synthesized by the condensation of primary amines with an aldehyde or ketone. The Schiff bases containing 1,2,4-triazole are very active in terms of showing biological activity. In particular, they show antitubercular (Amim, et al., 2017), antibacterial (Kotan, 2021), antitumor (Demirbaş, et al., 2002), antioxidant (Yüksek, et al., 2011; Manap, et al., 2020), analgesic (Rana, et al., 2012), antifungal (Dharmaraj, et al., 2001), anti-inflammatory (Shukla, et al., 2014) and anticancer properties (Uddin, et al., 2020). The Schiff bases are important molecules in the pharmaceutical and medicinal fields. In recent years, many theoretical studies for Schiff bases containing 1,2,4-triazole have been carried out (Kotan, et al., 2020; Yüksek, et al., 2017; Kotan, et al., 2021; Beytur, et al., 2021). Gaussian G09W program was used for quantum chemical calculations. First, the optimization process was carried out to reach the most stable state of the molecule, then the atoms of the molecule were numbered. From this optimized structure, all electronic, thermodynamic, spectroscopic and geometric theoretical values of the molecule were calculated (Frisch et al., 2009). IR vibration frequency values were calculated with the Veda 4f program (Jamróz., 2004) and the vibration frequency data were multiplied with definite scala factor (Merrich, et al., 2007) The ^1H - ^{13}C / NMR isotropic shift values were calculated by the GIAO method using the Gaussian G09 package program (Wolinski et al., 1990). These values were compared with the experimental values (Alkan, et al., 2014) and the difference values were found, and these values were $\delta_{\text{exp}} = a + b \cdot \delta_{\text{calc}}$. δ_{calc} plotted according to the equation. The bond length, HOMO-LUMO energy, total energy, bond angle, Mulliken atomic charges, dipole moment of the molecule was calculated. In addition, MEP surface maps were determined.

Results and Discussion

Theoretical Study

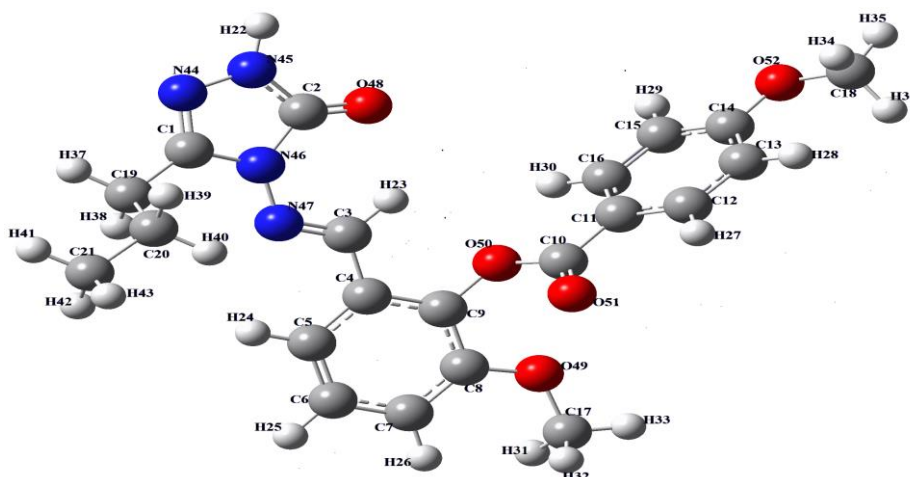


Figure 1. The minimized energy optimized structure of the molecule.

Table 1. $^1\text{H}/^{13}\text{C}$ -NMR(DMSO) isotropic chemical shifts (δ /ppm)

No	Experimental	B3LYP/Vacuum	Difference	B3PW91/Vacuum	Difference
C1	147.28	152.53	-5.25	146.91	0.37
C2	152.13	152.32	-0.19	147.29	4.84
C3	148.89	149.45	-0.56	145.22	3.67
C4	127.82	133.94	-6.12	129.05	-1.23
C5	118.58	118.90	-0.32	114.92	3.66
C6	127.42	128.80	-1.38	124.76	2.66
C7	115.65	113.57	2.08	109.72	5.93
C8	151.74	157.90	-6.16	152.42	-0.68
C9	139.71	148.41	-8.7	142.98	-3.27
C10	164.42	166.49	-2.07	161.58	2.84
C11	120.7	125.40	-4.7	120.48	0.22
C12	132.67	138.09	-5.42	134.19	-1.52
C13	114.82	109.64	5.18	105.91	8.91
C14	163.93	169.31	-5.38	163.6	0.33
C15	114.82	120.49	-5.67	116.52	-1.7
C16	132.67	136.93	-4.26	132.79	-0.12
C17	56.6	54.25	2.35	50.36	6.24
C18	56.1	54.25	1.85	50.69	5.41
C19	26.97	31.53	-4.56	27	-0.03
C20	19.17	25.35	-6.18	20.66	-1.49
C21	13.8	14.62	-0.82	11.18	2.62
H22	11.8	7.41	4.39	7.5	4.3
H23	9.9	11.19	-1.29	11.38	-1.48
H24	7.55	8.57	-1.02	8.76	-1.21
H25	7.39	7.92	-0.53	8.09	-0.7
H26	7.31	7.36	-0.05	7.54	-0.23
H27	8.1	9.00	-0.9	9.18	-1.08
H28	7.13	7.33	-0.2	7.52	-0.39
H29	7.13	7.76	-0.63	7.92	-0.79
H30	8.1	9.11	-1.01	9.28	-1.18
H31	3.8	4.58	-0.78	4.3	-0.5
H32	3.8	4.24	-0.44	4.21	-0.41
H33	3.8	4.14	-0.34	4.66	-0.86
H34	3.88	4.28	-0.4	4.35	-0.47
H35	3.88	4.26	-0.38	4.77	-0.89
H36	3.88	4.69	-0.81	4.33	-0.45
H37	2.48	2.95	-0.47	3.07	-0.59
H38	2.48	3.47	-0.99	3.57	-1.09
H39	1.6	2.03	-0.43	2.12	-0.52
H40	1.6	2.68	-1.08	2.77	-1.17
H41	0.88	1.59	-0.71	1.66	-0.78
H42	0.88	1.68	-0.8	1.76	-0.88
H43	0.88	1.87	-0.99	1.94	-1.06

The Relation between R Values of the Compound

There is such a relationship between R^2 -values of the compound. B3LYP(vacuum): ^1H : 0.8749, ^{13}C : 0.9945; B3PW91(vacuum)6-311G(d,p) ^1H : 0.8722, ^{13}C : 0.9955. These values for compound were seen in the table 2. Theoretical and experimental carbon/proton chemical shifts ratios between according to R^2 linear a correlation was observed (Figure 2).

Table 2. The correlation data for chemical shifts

	^{13}C -NMR/ R^2	^1H -NMR/ R^2
B3LYP/ Vakum	0.9945	0.8749
B3PW91/ Vakum	0.9955	0.8722

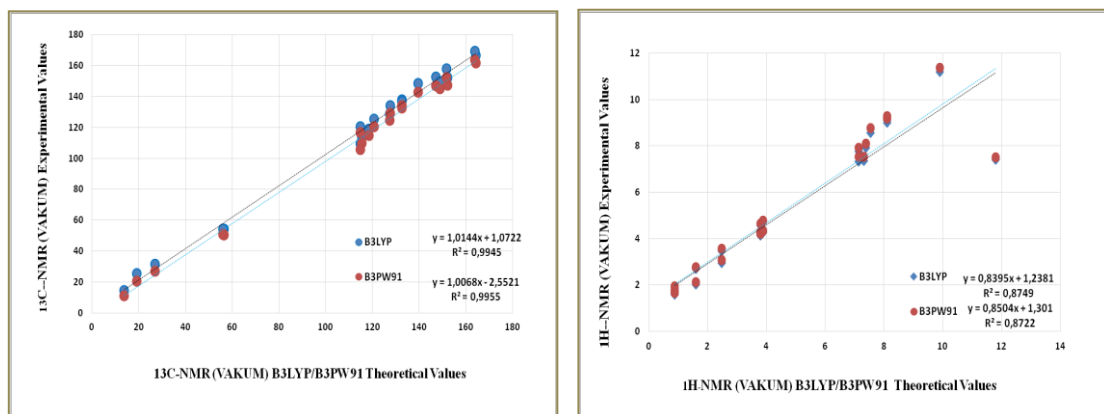


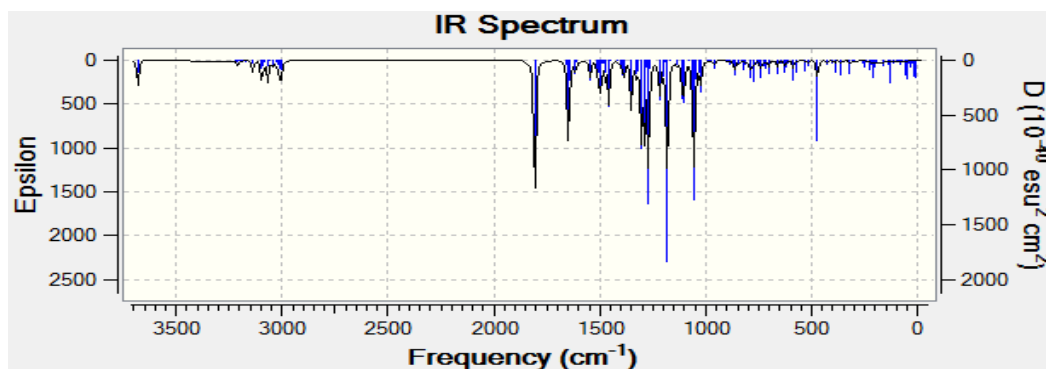
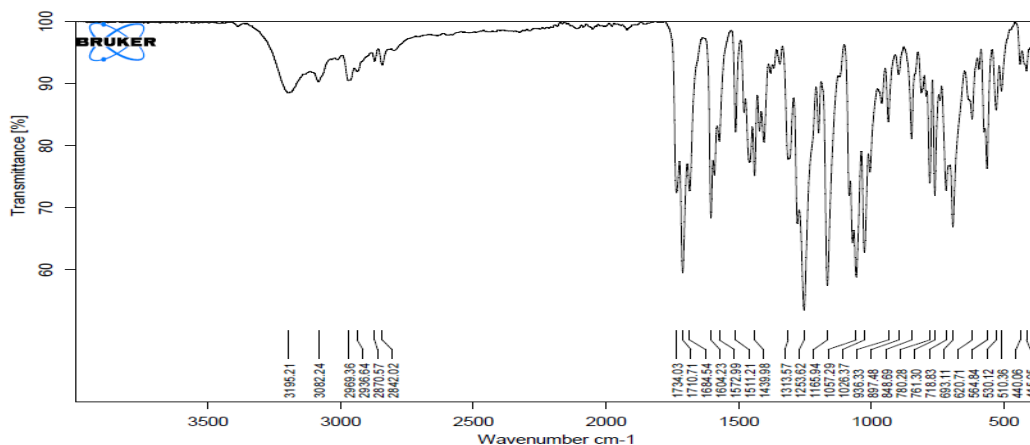
Figure 2. The experimental and theoretical ¹³C/¹H-NMR correlation graphs for DFT/(B3LYP, B3PW91) methods chemical shifts

The Infrared Analysis

The IR vibration frequencies were calculated theoretically with the Veda 4f program and the scaled values were obtained by multiplying 0.915 for B3LYP/ 6-311G(d,p) and 0.9905 for B3PW91/ 6-311G(d,p). The using these values were created theoretical IR spectrum graphs and were listed in Table 3.

Table 3. Significant vibrational frequencies (cm⁻¹)

vibrations	Scaled B3LYP	Scaled B3PW91	Experimental IR
v (NH)	3503	3664	3198
v (C=O)	1720,1718	1812, 1808	1735, 1708
v (C=N)	1580	1611	1603
v (COO)	1255	1245	1253



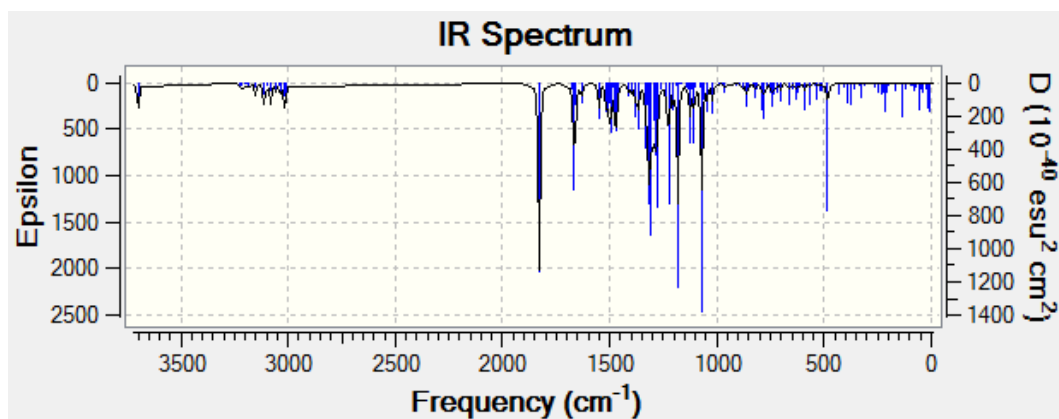


Figure 3. Experimental and theoretical IR spectrums simulated with DFT/(B3LYP, B3PW91)

Molecular Geometry

To calculate these two structure parameters, 6-311 G(d,p) basis set and B3LYP and B3PW91 functions are used. According to this calculations result, the highest bond length is between C(19)-C(20) atoms that this values are 1.54/1.54 Å for B3LYP/ B3PW91 6-311G(d,p). Besides, respectively, the bond lengths in the triazole ring N44-N45, N46-N47, N44-C1, C2-O48, C2-N46, N46-C1, N47=C3 are calculated 1.38/1.37; 1.37/1.36; 1.29/1.29; 1.21/1.21; 1.42/ 1.42; 1.28/ 1.28 Å for B3LYP 6-311G(d,p) basis sets (table 4).

Table 4. The calculated bond lengths with B3LYP/B3PW91 6-311G(d,p)

Bağ Açılıarı	B3LYP	B3PW91	Bağ Açılıarı	B3LYP	B3PW91
N(44)-C(1)-N(46)	111.27	111.18	H(26)-C(7)-C(8)	120.41	120.35
N(44)-N(45)-H(22)	120.48	120.46	C(7)-C(8)-O(49)	125.37	125.35
H(22)-N(45)-C(2)	125.07	124.95	O(49)-C(17)-H(31)	111.48	111.50
N(45)-C(2)-O(48)	129.98	129.99	O(49)-C(17)-H(32)	111.21	111.26
O(48)-C(2)-N(46)	128.45	128.90	O(49)-C(17)-H(33)	105.69	105.81
N(45)-C(2)-N(46)	101.16	101.10	C(7)-C(8)-C(9)	118.99	118.97
N(44)-C(1)-C(19)	124.77	124.93	C(8)-C(9)-O(50)	118.84	118.80
C(1)-C(19)-C(20)	113.60	113.51	C(9)-O(50)-C(10)	118.07	117.68
C(1)-C(19)-H(37)	106.65	106.65	O(50)-C(10)-O(51)	122.62	122.70
C(1)-C(19)-H(38)	109.02	108.94	O(50)-C(10)-C(11)	125.96	125.88
C(19)-C(20)-C(21)	113.60	112.17	C(10)-C(11)-C(16)	123.09	123.10
C(19)-C(20)-H(39)	108.74	108.75	C(10)-C(11)-C(12)	117.87	117.80
C(19)-C(20)-H(40)	109.08	109.04	C(11)-C(12)-H(27)	118.60	118.54
C(20)-C(21)-H(41)	111.32	111.34	H(27)-C(12)-C(13)	120.33	120.42
H(42)-C(20)-C(21)	111.68	111.30	C(12)-C(13)-H(28)	119.45	119.46
H(43)-C(21)-C(22)	111.05	111.10	H(28)-C(13)-C(14)	121.08	121.07
H(41)-C(21)-H(42)	107.67	107.63	C(13)-C(14)-O(52)	124.52	124.44
H(42)-C(21)-H(43)	107.64	107.66	C(13)-C(14)-C(15)	119.80	119.80
H(41)-C(21)-H(43)	107.69	107.60	C(14)-O(52)-C(18)	118.80	118.47
C(1)-N(46)-C(2)	108.29	108.28	O(52)-C(18)-H(34)	111.42	111.46
N(46)-N(47)-C(3)	119.92	118.92	O(52)-C(18)-H(35)	111.41	111.46
N(47)-C(3)-H(23)	122.29	122.30	O(52)-C(18)-H(36)	105.71	105.83
H(22)-C(3)-C(4)	118.22	118.40	H(34)-C(18)-H(36)	109.33	109.23
C(3)-C(4)-C(5)	122.21	122.15	H(35)-C(18)-H(36)	109.34	109.23
C(3)-C(4)-C(9)	119.08	119.07	H(34)-C(18)-H(35)	109.52	109.50
C(4)-C(5)-H(24)	118.62	118.54	C(14)-C(15)-H(29)	118.34	118.36
C(4)-C(5)-C(6)	120.16	120.13	H(29)-C(15)-C(16)	121.40	121.41
C(5)-C(6)-H(25)	119.98	119.99	C(15)-C(16)-H(30)	120.04	120.05
C(5)-C(6)-C(7)	120.93	120.91	H(30)-C(16)-C(11)	119.56	119.56
H(25)-C(6)-C(7)	119.08	119.08			
C(6)-C(7)-H(26)	119.69	119.71			

In the literature, the N-N, C=O N=C bond lengths are measured as 1.40, 1.21, 1.28, Å (Sudha et al. 2018). The calculated bond length values are consistent with literature values. The highest bond angle is between N(45)-

C(2)-O(48) atoms, which is 129.98/129.99⁰ for B3LYP/ B3PW91 6-311G(d,p) basis sets (table 5). The calculated Mulliken atomic charges (Mulliken, 1955) calculated by using the B3LYP, B3PW91 method with 6-311G(d,p) basis sets. The electronegative oxygen (O) and nitrogen (N) atoms have negative atomic charge values. The carbon atoms surrounded by electronegative atoms have negative atomic charge values. The C1 atom surrounded by two electronegative atoms (N44, N46) and C2 atom which is surrounded by three electronegative atoms (N45, N46, O48) have negative charges values. All hydrogen atoms of the compound (H22-43) have positive atomic charge values (table 6).

Table 5. The calculated bond angles with B3LYP/B3PW91 6-311G(d,p)

bond length	B3LYP	B3PW91	bond length	B3LYP	mPW1PW91
C(1)-N(44)	1.29	1.29	C(7)-C(8)	1.39	1.39
C(1)-N(46)	1.39	1.39	C(8)-O(49)	1.35	1.35
C(1)-C(19)	1.48	1.48	O(49)-C(17)	1.42	1.41
N(44)-N(45)	1.38	1.37	C(17)-H(31)	1.09	1.09
N(45)-H(22)	1.00	1.00	C(17)-H(32)	1.09	1.09
N(45)-C(2)	1.36	1.36	C(17)-H(33)	1.08	1.09
C(2)-N(46)	1.42	1.42	C(8)-C(9)	1.40	1.40
C(2)-O(48)	1.21	1.21	C(9)-O(50)	1.38	1.38
N(46)-N(47)	1.37	1.36	C(4)-C(9)	1.39	1.39
C(19)-H(37)	1.09	1.09	O(50)-C(10)	1.38	1.38
C(19)-H(38)	1.09	1.09	C(10)-O(51)	1.20	1.20
C(19)-C(20)	1.54	1.54	C(10)-C(11)	1.47	1.47
C(20)-H(39)	1.09	1.09	C(11)-C(12)	1.39	1.39
C(20)-H(40)	1.09	1.09	C(12)-H(27)	1.08	1.08
C(20)-C(21)	1.53	1.52	C(12)-C(13)	1.38	1.39
C(21)-H(41)	1.09	1.09	C(13)-H(28)	1.08	1.08
C(21)-H(42)	1.09	1.09	C(13)-C(14)	1.40	1.40
C(21)-H(43)	1.09	1.09	C(14)-C(15)	1.40	1.40
N(47)-C(3)	1.28	1.28	C(15)-H(29)	1.08	1.08
C(3)-H(23)	1.08	1.08	C(15)-C(16)	1.38	1.38
C(3)-C(4)	1.46	1.46	C(16)-H(30)	1.08	1.08
C(4)-C(5)	1.40	1.40	C(14)-O(52)	1.35	1.35
C(5)-H(24)	1.08	1.08	O(52)-C(18)	1.42	1.42
C(5)-C(6)	1.38	1.38	C(18)-H(34)	1.09	1.09
C(6)-H(25)	1.08	1.08	C(18)-H(35)	1.09	1.09
C(6)-C(7)	1.39	1.39	C(18)-H(36)	1.08	1.10
C(7)-H(26)	1.08	1.08			

Table 6. The calculated mulliken charges datas B3LYP/B3PW91 6-311G(d,p)

Atom	B3LYP	B3PW91	Atom	B3LYP	B3PW91	Atom	B3LYP	B3PW91
C1	0.337	0.379	C19	-0.179	-0.222	H37	0.130	0.149
C2	0.530	0.572	C20	-0.232	-0.278	H38	0.133	0.153
C3	0.143	0.172	C21	-0.297	-0.336	H39	0.116	0.134
C4	-0.143	-0.176	H22	0.249	0.257	H40	0.130	0.150
C5	-0.139	-0.033	H23	0.156	0.176	H41	0.105	0.119
C6	-0.032	-0.102	H24	0.103	0.116	H42	0.104	0.119
C7	-0.090	-0.119	H25	0.095	0.104	H43	0.112	0.127
C8	-0.107	0.225	H26	0.109	0.124	N44	-0.221	-0.244
C9	0.213	0.156	H27	0.111	0.121	N45	-0.313	0.333
C10	0.164	-0.171	H28	0.109	0.125	N46	-0.375	-0.409
C11	0.465	0.497	H29	0.107	0.119	N47	-0.209	-0.233
C12	-0.251	-0.290	H30	0.112	0.123	O48	0.385	-0.402
C13	-0.022	-0.024	H31	0.109	0.123	O49	-0.348	-0.390
C14	-0.138	-0.155	H32	0.118	0.132	O50	-0.387	-0.336
C15	0.189	0.197	H33	0.133	0.144	O51	-0.326	-0.343
C16	-0.095	-0.110	H34	0.116	0.130	O52	-0.341	-0.349
C17	-0.131	0.005	H35	0.133	0.144			
C18	0.005	-0.175	H36	0.115	0.128			

MEP Surface Analysis

The molecular electron potential map allows us to identify the electronegative and electropositive atoms of the molecule. When we look at the MEP map, we see different colors because of the electron distribution. The nucleophilic regions with high electron density are in red, and the regions with low electron density, that is, electrophilic regions, are in blue. The region where the carbonyl group and other oxygens are located in the molecule is red in color because of its high electron density, while the surrounding of the N-H acidic proton is blue and were shown in Figure 4.

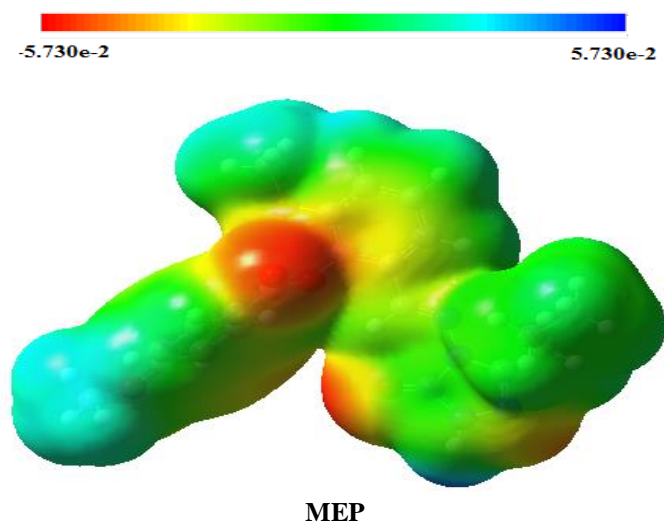


Figure 4. The calculated MEP and surface contour map of the molecule

Frontier molecular orbital analysis

Frontier molecular orbitals (FMO) identified optical and electric properties, kinetic stability, the electronic transitions (Fukui, 1982). The HOMO-LUMO energy values was calculated as 4.37/4.37 eV for B3LYP and B3PW91 functionals in the 6-311G(d,p) basis set (figure 5).

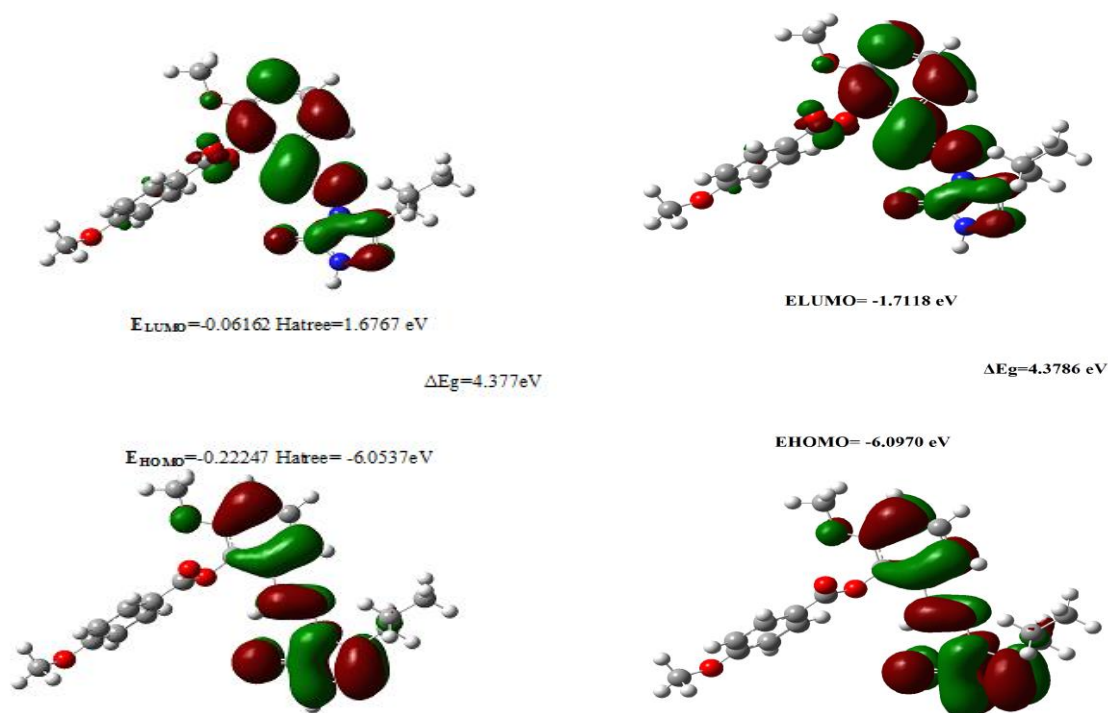


Figure 5. HOMO-LUMO energy of the molecule 6-311G(d,p)

Table 7. The calculated electronic structure parameters of the molecule

	B3LYP		B3PW91	
	Hatree	eV	Hatree	eV
LUMO	-1,6767	-45,6242	-1,7184	-46,7589
HOMO	-6,0537	-164,725	-6,097	-165,904
A elektron ilgisi	1,6767	45,6242	1,7184	46,7589
I İyonlaşma potansiyeli	6,0537	164,725	6,097	165,904
ΔE energy gap	4,377	119,101	4,3786	119,145
χ electronegativity	3,8652	105,175	3,9077	106,331
Pi chemical potential	-3,8652	-105,175	-3,9077	-106,331
ω electrophilic index	16,34784446	444,836	16,71543608	454,839
IP Nucleophilic index	-8,4589902	-230,175	-8,55512761	-232,791
S molecular softness	0,4569	12,4335	0,4568	12,4289
η molecular hardness	2,1885	59,5506	2,1893	59,5724

Table 8. The calculated dipole moments datas of the molecule

	μ_x	μ_y	μ_z	μ_{Toplam}
B3LYP	-1.9556	1.5362	0.3083	2.5059
B3PW91	2.0727	5.5753	-1.7611	6.2033

Table 9. The calculated total energy datas of the molecule

Energy(a.u.)	B3LYP	B3PW91
	-1408.9372	-1408.3805

Table 10. The calculated thermodynamics parameters of the molecule

Parameters	B3LYP	B3PW91
Rotational temperatures (Kelvin)		
A	0.00889	0.00897
B	0.00409	0.00410
C	0.00300	0.00301
Rotational constants (GHZ)		
A	0.18520	0.18695
B	0.08532	0.08553
C	0.06241	0.06273
Thermal Energies E(kcal/mol)		
Translational	0.889	0.889
Rotational	0.889	0.889
Vibrational	273.264	274.209
Total	275.041	275.986
Thermal Capacity CV(cal/mol-K)		
Translational	2.981	2.981
Rotational	2.981	2.981
Vibrational	99.719	99.395
Total	105.680	105.356
Entropy S(cal/mol-K)		
Translational	43.925	43.925
Rotational	37.031	37.014
Vibrational	114.189	113.691
Total	195.145	194.631
Zero-point correction (Hartree/Particle)	0.409861	0.411456
Thermal correction to Energy	0.438306	0.439812
Thermal correction to Enthalpy	0.439251	0.440756
Thermal correction to Gibbs Free Energy	0.346531	0.348281
Sum of electronic and zero-point Energies	-1408.527436	-1407.969093
Sum of electronic and thermal Energies	-1408.498990	-1407.940737
Sum of electronic and thermal Enthalpies	-1408.498046	-1407.939793
Sum of electronic and thermal Free Energies	-1408.590766	-1408.032268
Zero-point vibrational energy (Kcal/mol)	257.19173	258.19228

Thermodynamics Properties

Thermodynamics parameters were calculated with the (B3LYP/ B3PW91) functionals of DFT method at 298.150 K and under 1 atm pressure and were summarized in the Table 10.

Conclusion

In this theoretical study, which supports all the experimentally obtained parameters, all the theoretical properties of the substance recorded in the literature have been studied. As a result, the experimental spectroscopic values of the molecule and the theoretical values obtained with the B3LYP and B3PW91 functions were compared. We observed that in all spectral calculation results, the values of both functions are very close to each other and to the experimental one. We were also able to find electrophilic and nucleophilic regions from the MEP map. Finally, we visualized the HOMO-LUMO orbitals of the molecule and calculated the energy gaps between them.

Scientific Ethics Declaration

The authors declare that the scientific ethical and legal responsibility of this article published in EPSTEM journal belongs to the authors.

References

- Alkan, M., Gürbüz, A., Yüksek, H., Kol, Ö. G., & Zafer, O. (2014). Synthesis and non-aqueous medium titrations of some new 3-alkyl(aryl)-4-[2-(4-methoxybenzoxy)-3-methoxy]-benzylidenamino-4,5-dihydro-1H-1, 2, 4-triazol-5-ones. *Caucasian Journal Of Science*, 1(1), 138-148.
- Amim, R. S., Pessoa, C., CS Lourenco, M., VN de Souza, M., & A Lessa, J. (2017). Synthesis, Antitubercular and Anticancer Activities of p-nitrophenylethylenediamine-derived Schiff Bases. *Medicinal Chemistry*, 13(4), 391-397.
- Beytur, M., & Avinca, I. (2021). Molecular, Electronic, Nonlinear Optical and Spectroscopic Analysis of Heterocyclic 3-Substituted-4-(3-methyl-2-thienylmethyleneamino)-4, 5-dihydro-1H-1, 2, 4-triazol-5-ones: Experiment and DFT Calculations. *Heterocyclic Communications*, 27(1), 1-16.
- Demirbaş, N., Ugurluoğlu, R., & Demirbaş, A. (2002). Synthesis of 3-alkyl (Aryl)-4-alkylidenamino-4, 5-dihydro-1H-1, 2, 4-triazol-5-ones and 3-alkyl-4-alkylamino-4, 5-dihydro-1H-1, 2, 4-triazol-5-ones as antitumor agents. *Bioorganic & Medicinal Chemistry*, 10(12), 3717-3723.
- Dharmaraj, N., Viswanathamurthi, P., & Natarajan, K. (2001). Ruthenium (II) complexes containing bidentate Schiff bases and their antifungal activity. *Transition Metal Chemistry*, 26(1), 105-109.
- Frisch, M.J., Trucks, G.W., Schlegel, H.B., Scuseria, G.E., Robb, M.A., Cheeseman, J.R., Scalmani, G., Barone, V., Mennucci, B., Petersson, G.A., Nakatsuji, H., Caricato, M.; Li, X., Hratchian, H.P., Izmaylov, A.F., Bloino, J., Zheng, G., Sonnenberg, J.L., Hada, M., Ehara, M., Toyota, K., Fukuda, R., Hasegawa, J., Ishida, M., Nakajima, T., Honda, Y., Kitao, O., Nakai, H., Vreven, T., Montgomery, J.A., Jr. Vreven, T., Peralta, J.E., Ogliaro, F., Bearpark, M., Heyd, J.J., Brothers, E., Kudin, N., Staroverov, V.N., Kobayashi, R., Normand, J., Raghavachari, K., Rendell, A., Burant, J.C., Iyengar, S.S., Tomasi, J., Cossi, M., Rega, N., Millam, J.M., Klene, M., Knox, J.E., Cross J.B., Bakken, V., Adamo, C., Jaramillo, J., Gomperts, R., Stratmann, R.E., Yazyev, O., Austin, A.J., Cammi, R., Pomelli, C., Ochterski, J.W., Martin, L.R., Morokuma, K., Zakrzewski, V.G., Voth, G.A., Salvador, P., Dannenberg, J.J., Dapprich, S.; Daniels A.D., Farkas, O.; Foresman, J.B., Ortiz, J.V., Cioslowski, J., and Fox, D.J. (2009). *Gaussian Inc.* Wallingford.
- Fukui, K. (1982). Role of frontier orbitals in chemical reactions. *Science*, 218(4574), 747-754.
- Jamroz, M. H. (2004). *Vibrational energy distribution analysis*. VEDA 4 Program.
- Kotan, G., & Yüksek, H. (2021). 2-(3-Fenil-4, 5-dihidro-1H-1, 2, 4-triazol-5-on-4-il)-azometin benzoik asid Molekülünün Deneysel ve Kuantum Kimyasal Hesaplamaları. *Avrupa Bilim ve Teknoloji Dergisi*, (21), 649-659.
- Kotan, G., (2021). novel mannich base derivatives: synthesis, characterization, antimicrobial and antioxidant activities. *Letters in Organic Chemistry*, 18(10), 830-841.
- Kotan, G., Gökce, H., Akyıldırım, O., Yüksek, H., Beytur, M., Manap, S., & Medetalibeyoğlu, H. (2020). Synthesis, Spectroscopic and Computational Analysis of 2-[(2-Sulfanyl-1 H-benzo [d] imidazol-5-yl)

- iminomethyl] phenyl Naphthalene-2-sulfonate. *Russian Journal of Organic Chemistry*, 56(11), 1982-1994.
- Manap, S., Gürsoy-Kol, Ö., Alkan, M., & Yüksek, H. (2020). Synthesis, in vitro antioxidant and antimicrobial activities of some novel 3-substitued-4-(3-methoxy-4-isobutyryloxybenzylideneamino)-4, 5-dihydro-1H-1, 2, 4-triazol-5-one derivatives. *Indian Journal of Chemistry*, 59(2), 271-282.
- Merrick, J. P., Moran, D., Radom, L. (2007). An evaluation of harmonic vibrational frequency scale factors. *Journal of Physical Chemistry*, 111(45), 11683-11700.
- Mulliken, R. S. (1955). Electronic population analysis on LCAO–MO molecular wave functions. I. *The Journal of Chemical Physics*, 23(10), 1833-1840.
- Rana, K., Pandurangan, A., Singh, N., & Tiwari, A. (2012). A systemic review of schiff bases as an analgesic, anti-inflammatory. *International Journal of Current. Pharmaceutical Research*, 4(2), 5-11.
- Shukla, P. K., Soni, N., Verma, A., & Jha, A. K. (2014). Synthesis, characterization and in vitro biological evaluation of a series of 1, 2, 4-triazoles derivatives & triazole based schiff bases. *Der Pharma Chemica*, 6(3), 153-160.
- Sudha, N., Abinaya, B., Arun Kumar, R., & Mathammal, R. (2018). Synthesis, structural, spectral, optical and mechanical study of benzimidazolium phthalate crystals for NLO applications. *Journal of Lasers Optics & Photonics*, 5(2), 1-6.
- Uddin, N., Rashid, F., Ali, S., Tirmizi, S. A., Ahmad, I., Zaib, S., ... & Haider, A. (2020). Synthesis, characterization, and anticancer activity of Schiff bases. *Journal of Biomolecular Structure and Dynamics*, 38(11), 3246-3259.
- Wolinski, K., Hinton, J. F., & Pulay, P. (1990). Efficient implementation of the gauge-independent atomic orbital method for NMR chemical shift calculations. *Journal of the American Chemical Society*, 112(23), 8251-8260.
- Yüksek, H., Gursoy-Kol, O., Kemer, G., Ocak, Z., & Anil, B. (2011). Synthesis and in-vitro antioxidant evaluation of some novel 4-(4-substitued) benzylidenamino-4, 5-dihydro-1H-1, 2, 4-triazol-5-ones.
- Yüksek, H., Kotan, G., Medetalibeyoğlu, H., Gürbüz, A., & Alkan, M. (2017). B3LYP ve HF Temel Setleri Kullanılarak Bazı 3-Alkil-4-(2-asetoksi-3-metoksibenzilidenamino)-4, 5-dihidro-1H-1, 2, 4-triazol-5-on Bileşiklerinin Deneysel ve Teorik Özelliklerinin İncelenmesi/The Investigation of Experimental and Theoretical Properties of Some 3-Alkyl-4-(2-acetoxy-3-methoxybenzylidenamino)-4, 5-dihydro-1H-1, 2, 4-triazol-5-one Using B3LYP and HF Basis Sets. *Celal Bayar University Journal of Science*, 13(1), 193-204.

Author Information

Gul KOTAN

Kafkas University,
Kars Vocational School, Kars, Turkey
Contact e-mail: gulkemer@hotmail.com

Muzaffer ALKAN

Kafkas University,
Education Faculty, Kars, Turkey

Haydar YUKSEK

Kafkas University,
Department of Chemistry, Kars, Turkey

To cite this article:

Kotan, G., Alkan, M. & Yuksek, H. (2021). Experimental (FT-IR, 13C/1H-NMR) and DFT (B3LYP, B3PW91) studies of 3-n-propyl-4-[2-(4-methoxybenzoxy)-3-methoxy] benzylidenamino-4,5-dihydro-1h-1,2,4-triazol-5-ones molecule. *The Eurasia Proceedings of Science, Technology, Engineering & Mathematics (EPSTEM)*, 15, 69-78.

The Eurasia Proceedings of Science, Technology, Engineering & Mathematics (EPSTEM), 2021

Volume 15, Pages 79-87

ICBAST 2021: International Conference on Basic Science and Technology

The Investigation of Spectroscopic and Electronic Properties of 3-Ethyl-4-(4-cinnamoyloxybenzylidenamino)-4,5-dihydro-1H-1,2,4-triazol-5-one Compound Using Density Functional Theory and Hartree-Fock Basis Sets

Murat BEYTUR
Kafkas University

Haydar YUKSEK
Kafkas University

Abstract: In this study, we reported a combined experimental and theoretical study on 3-n-propyl-4-(3-cinnamoyloxybenzylidenamino)-4,5-dihydro-1H-1,2,4-triazol-5-one compound. The title compound was prepared and characterized by UV-Vis, FT-IR spectra, ^1H and ^{13}C NMR. UV-visible absorption spectra and the stimulation contributions in UV-visible transitions were obtained with TD-DFT/B3LYP and TD-FF methods and 6-311G(d) polarizer set based on optimized structure. Calculated absorption wavelengths (λ), oscillator power (f) and excitation energies were compared with experimental values. The calculated IR data of compound were calculated in gas phase by using of 6-31G(d) basis set of B3LYP and HF methods and are multiplied with appropriate scale factors. Theoretical infrared spectrums are formed from the data obtained according to B3LYP method. In the identification of calculated IR data was used the veda4f program. The molecular geometry, gauge including atomic orbital (GIAO), Experimental and theoretical values were inserted into the graphic according to equation of $\delta_{\text{exp}}=a+b \cdot \delta_{\text{calc}}$. The standard error values were found via SigmaPlot program with regression coefficient of a and b constants. Obtained results indicate that there is a good agreement between the experimental and theoretical data. Also, HOMO-LUMO analyses properties, Mulliken's atomic charges, dipole moment and total energy of the title compound in the ground state were investigated by using Hartree-Fock (HF) and density functional theory (DFT/B3LYP) methods with 6-31G(d) basic set.

Keywords: 1,2,4-Triazol-5-one, DFT, Hartree-Fock, HOMO-LUMO, Gaussian G09

Introduction

Intense studies have been carried out in recent years on many properties of heterocyclic compounds (Aktaş Yokuş et al., 2017; Bahçeci et al., 2016; Bahçeci et al., 2017; Beytur et al., 2019; Koç et al., 2019; Beytur et al., 2021; Beytur, 2020; Uğurlu et al., 2020). Triazole is an unsymmetrical heterocyclic organic compound having three nitrogen atoms in the five-membered ring. 1,2,4-Triazole and derivatives are reported to possess a broad spectrum of biological activities such as antimicrobial, antifungal, antitumor, anti-HIV, antiviral, anticancer, anti-inflammatory, analgesic and antioxidant properties (Alkan et al., 2007; Boy et al., 2021; Bayrak et al., 2010; Çiftçi et al., 2018; Gürsoy-Kol et al., 2010; Güzeldemirci et al., 2010; Hashem et al., 2007; Tozkoparan et al., 2007; Turhan-Irak et al., 2019). Also, several articles reporting the synthesis of some 1,2,4-triazol-5-one compounds and derivatives have been published (Bahçeci et al., 2002; Yüksek et al., 2005; Yüksek et al., 2006).

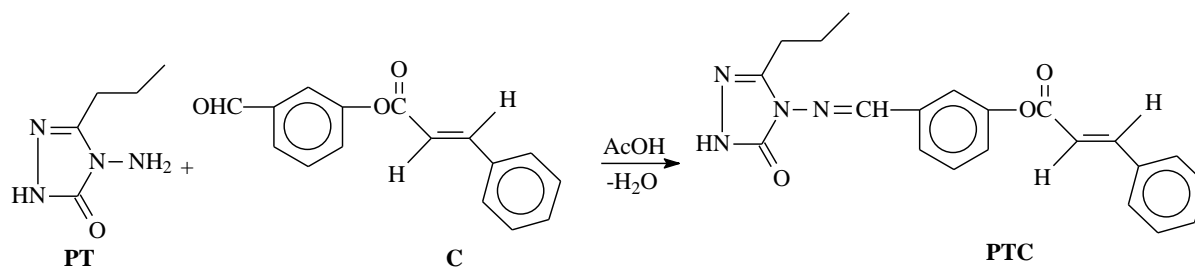
In this paper, 3-n-propyl-4-(3-cinnamoyloxybenzylidenamino)-4,5-dihydro-1H-1,2,4-triazol-5-one (**PTC**) was obtained from the reaction of compound (**PT**) with 4-cinnamoyloxybenzaldehyde (**C**) (Vasavado et al., 2003)

- This is an Open Access article distributed under the terms of the Creative Commons Attribution-Noncommercial 4.0 Unported License, permitting all non-commercial use, distribution, and reproduction in any medium, provided the original work is properly cited.

- Selection and peer-review under responsibility of the Organizing Committee of the Conference

© 2021 Published by ISRES Publishing: www.isres.org

which was synthesized by the reaction of 4-hydroxybenzaldehyde with cinnamoyl chloride by using triethylamine (Scheme 1).



Scheme 1. Synthesis method of compound PTC

Method

Synthesis

The compound **PT** (10 mmol) was dissolved in acetic acid (20 mL) and treated with 3-cinnamoyloxybenzaldehyde (**C**) (10 mmol). The mixture was refluxed for 2 hour. Several recrystallizations of the residue from ethanol gave pure compound 3-n-propyl-4-(3-cinnamoyloxybenzylideneamino)-4,5-dihydro-1H-1,2,4-triazol-5-one (PTC) was prepared. m.p. 195 °C; Yield 97 %. IR: (NH) 3166; C=CH 3064; C=O 1709; C=C 1633; C=N 1611; COO 1203; 1,3-disubstituted aromatic ring 846 and 721; monosubstituted aromatic ring 763 and 681 cm^{-1} . ^1H NMR (400 MHz, DMSO- d_6): δ 0.97 (t, 3H, $\text{CH}_2\text{CH}_2\text{CH}_3$; $J=7.60$ Hz), 1.70 (sext, 2H, $\text{CH}_2\text{CH}_2\text{CH}_3$; $J=7.60$ Hz), 2.67 (t, 2H, $\text{CH}_2\text{CH}_2\text{CH}_3$; $J=7.20$ Hz), 6.94 (d, 1H, =CH; $J=16.00$ Hz), 7.40-7.43 (m, 1H, ArH), 7.48-7.51 (m, 3H, ArH), 7.61 (t, 1H, ArH; $J=8.00$ Hz), 7.70-7.72 (m, 1H, ArH), 7.75-7.77 (m, 1H, ArH), 7.83-7.85 (m, 2H, ArH), 7.92 (d, 1H, =CH; $J=16.00$ Hz), 9.78 (s, 1H, N=CH), 11.90 (s, 1H, NH). ^{13}C -NMR (100 MHz, DMSO- d_6): δ 13.46 ($\text{CH}_2\text{CH}_2\text{CH}_3$), 18.84 ($\text{CH}_2\text{CH}_2\text{CH}_3$), 26.62 ($\text{CH}_2\text{CH}_2\text{CH}_3$), 116.99 and 146.76 (CH=CH), 128.70 (2C); 129.01 (2C); 130.96; 133.82 (Monosubstitued Ar-C), 120.26; 124.90; 125.55; 130.26; 135.21; 151.26 (1,3-Disubstitued Ar-C), 146.91 (Triazole C_3), 150.93 (N=CH), 152.66 (Triazole C_5), 164.84 (COO). UV [Etanol, λ_{max} , nm (ϵ , $\text{L}\cdot\text{mol}^{-1}\cdot\text{cm}^{-1}$): 286 (18657), 264 (18187), 224 (16199).

Computational Properties

The molecular structure of the title compound in the ground state is computed by performing both the Density Functional Theory (DFT) and Hartree-Fock (HF) (Becke, 1993; Lee, 1998) at 6-31G(d) level. The theoretical geometric structure of the compound **PTC** is given in Figure 1. Molecular geometry is restricted and the optimized geometrical parameters, of the title compound in this study are carried out by using Gaussian G09 program package (Frisch et al., 2009) and the visualization parts were done with GaussView program (Dennington et al., 2009) on personal computer employing 6-31G(d) basis set. Additionally, harmonic vibrational frequencies for the title compound are calculated with these selected methods and then scaled by 0.9516 and 0.9905, respectively (Avci and Atalay, 2008) and these results were compared with the experimental data.

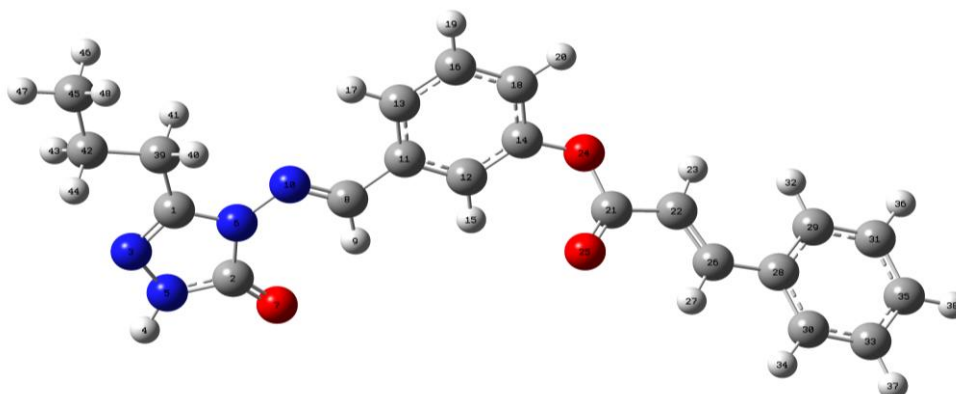


Figure 1. The optimized molecular structure of titled molecule PTC with DFT/HF 6-31G(d) level

Results and Discussion

UV-visible Spectroscopy

The title molecule allow strong $\pi \rightarrow \pi^*$ and $\sigma \rightarrow \sigma^*$ transitions in UV-vis region with high extinction coefficients (Silverstein, et al., 1991). The experimental absorption wavelengths of the compound **PTC** in ethanol solvent have been observed at 300, 262 and 214 nm. The absorption wavelengths (λ) excitation energies, and oscillator strengths (f) of UV-vis absorption spectroscopy of the compound **PTC** has been calculated in ethanol solvents by using TD-DFT/B3LYP and TD-HF method (Figure 2 and Table 1).

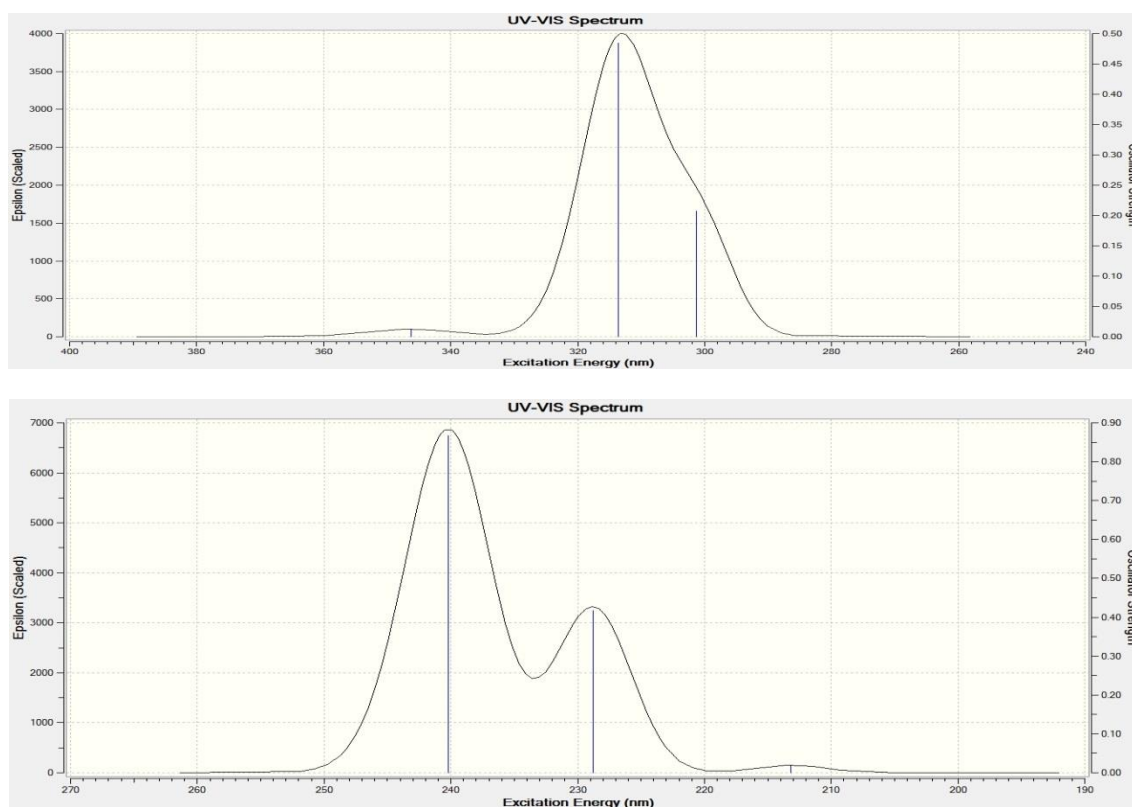


Figure 2. UV-Visible spectra experimental and simulated with DFT/B3LYP/6-31G(d) and HF/6-31G(d) levels of the compound PTC, respectively.

Table 1. The experimental and calculated absorption wavelength (λ), excitation energies and oscillator strengths (f) the compound PTC.

λ (nm)	Uyarma Enerjisi (eV) B3LYP/HF	f (osilatör gücü) B3LYP/HF
346.29/240.22	3.5804/5.1614	0.0125/0.8667
313.54/228.79	3.9543/5.4192	0.4849/0.4176
301.36/213.21	4.1142/5.8151	0.2077/0.0198

Analysis of Vibrational Modes

The vibrational spectra of substituted benzene derivatives have been greatly investigated by various spectroscopic, since the single substitution can have a tendency to put greater changes in vibrational wavenumbers of benzene (Turhan-Irak et. al., 2017; Beytur et al., 2019; Uğurlu et. al., 2020). In other words, molecular system of benzene is greatly affected by the nature of substituents. The number of potentially active fundamentals of non-linear molecule which have N atoms is equal to $(3N-6)$ apart from three translational and three rotational degrees of freedom. The molecule contains 48 atoms and 138 normal vibration modes have C1 symmetry (Table 2 and Figure 3).

Table 2. The calculated frequencies values of the titled compound (PTC).

Selected Vibrational Types	B3LYP	HF	Selected Vibrational Types	B3LYP	HF
τ HNNC, τ NNCN	630	640	ν NC, δ HCN, τ HCCN	1332	1351
τ CCOO, τ OCOC	665	676	δ NNC	1350	1385
τ HCCC, τ CCCC	671	680	δ HCH, τ HCCC	1462	1462
τ HCCC, τ OCOC	690	695	ν NC, ν CC	1589	1615
τ ONNC	693	713	ν NC, ν CC	1593	1620
δ OCO, δ COC	729	750	ν NC	1615	1670
τ HCCC, τ CCCC, τ OCOC	750	759	ν CC, δ HCC	1631	1703
δ CCC	754	771	ν OC	1740	1761
ν NC, δ CNN	774	781	ν OC, ν NC	1754	1788
τ HCCC, τ CCCC	784	805	ν CH	3075	3024
ν NN, δ NNC, δ NCC	818	828	ν CH	3105	3046
τ HCCN, τ HCCC	1098	1097	ν CH	3118	3048
ν CC, ν OC, δ OCO	1118	1103	ν NH	3540	3520
ν OC, δ HCC	1140	1108			

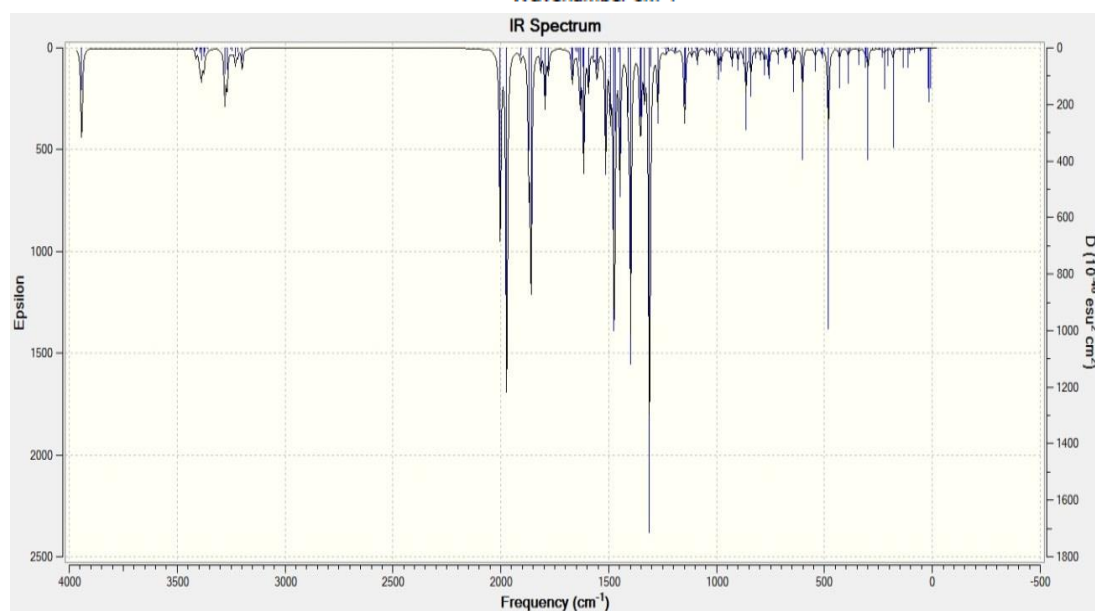
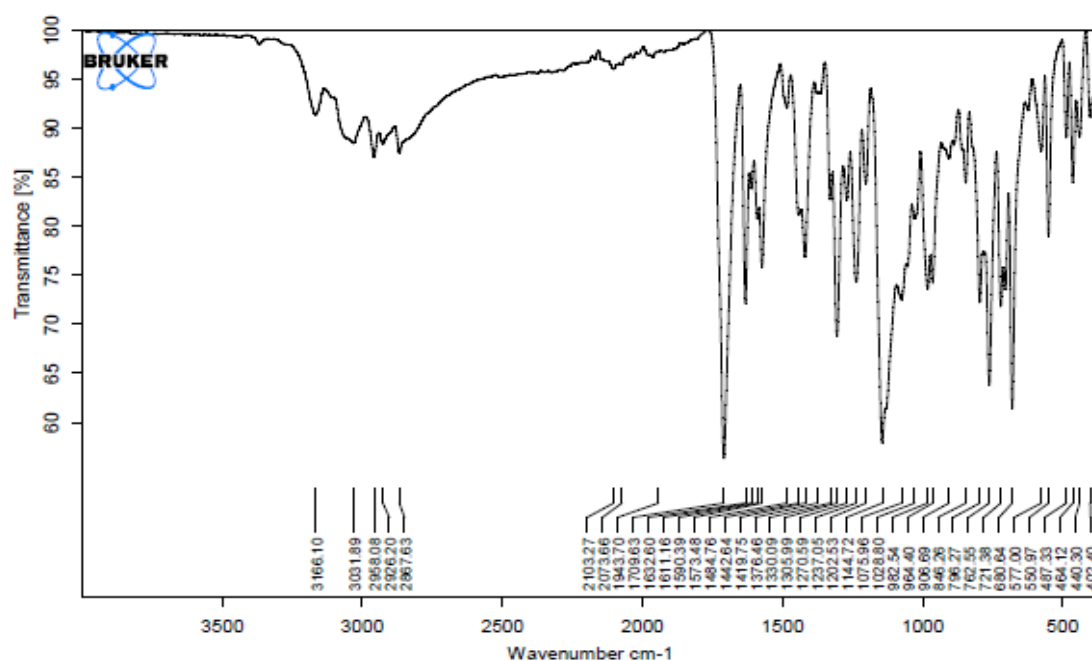


Figure 3. IR spectra experimental and simulated with DFT/B3LYP/6-31G(d) levels of the compound PTC.

NMR Spectral Analysis

In the NMR spectroscopy, the isotropic chemical shift analysis allows us to identify relative ionic species and to calculate reliable magnetic properties in nuclear magnetic resonance (NMR) spectroscopy which provide the accurate predictions of molecular geometries (Rani, et al., 2010; Subramanian et al., 2010; Wade, 2006). For this purpose, the optimized molecular geometry of the compound **PTC** was obtained by using B3LYP and HF methods with 6-31G(d) basis level in DMSO solvent. By considering the optimized molecular geometry of the compound **PTC** the ^1H and ^{13}C NMR chemical shift values were calculated at the same level by using Gauge-Independent Atomic Orbital method (Table 3). Theoretically and experimentally values were plotted according to $\delta_{\text{exp}} = a \cdot \delta_{\text{calc}} + b$, Eq. a and b constants regression coefficients with a standard error values were found using the SigmaPlot program. The correlation graphics are given Figure 4 and the linear correlation data of the compound **PTC** by considering the results are given in Table 3.

Table 3. The calculated and experimental ^{13}C and ^1H NMR isotropic chemical shifts of the compound **PTC** (with respect to TMS, all values in ppm).

Nucleus	Experimental	B3LYP	B3LYP/ DMSO	Different	Different /DMSO	HF	HF/ DMSO	Different	Different /DMSO
C1	146,91	151,37	152,81	-4,46	-5,90	145,62	147,56	1,29	-0,65
C2	152,66	151,83	152,62	0,83	0,04	145,39	146,10	7,27	6,56
C3	150,93	154,94	155,30	-4,01	-4,37	148,49	149,06	2,44	1,87
C4	135,21	139,59	139,02	-4,38	-3,81	130,57	130,05	4,64	5,16
C5	125,55	131,57	130,85	-6,02	-5,30	125,66	125,11	-0,11	0,44
C6	151,26	155,23	154,99	-3,97	-3,73	144,23	143,54	7,03	7,72
C7	124,40	126,41	127,50	-2,01	-3,10	121,15	122,09	3,25	2,31
C8	130,26	132,54	133,78	-2,28	-3,52	125,36	126,37	4,90	3,89
C9	120,26	124,64	124,89	-4,38	-4,63	119,23	119,72	1,03	0,54
C10	164,84	166,16	167,57	-1,32	-2,73	156,83	158,68	8,01	6,16
C11	116,99	120,07	119,32	-3,08	-2,33	108,25	107,41	8,74	9,58
C12	146,76	152,73	154,13	-5,97	-7,37	147,63	149,12	-0,87	-2,36
C13	133,82	137,76	136,93	-3,94	-3,11	128,15	127,06	5,67	6,76
C14	129,01	137,87	138,39	-8,86	-9,38	130,15	130,77	-1,14	-1,76
C15	128,70	132,51	132,86	-3,81	-4,16	124,54	124,51	4,16	4,19
C16	130,96	134,70	136,13	-3,74	-5,17	128,05	129,34	2,91	1,62
C17	128,70	132,24	132,75	-3,54	-4,05	124,30	124,42	4,40	4,28
C18	129,01	129,53	129,84	-0,52	-0,83	123,02	123,61	5,99	5,40
C19	26,62	39,01	38,61	-12,39	-11,99	24,03	23,69	2,59	2,93
C20	18,54	29,60	29,72	-11,06	-11,18	14,32	14,46	4,22	4,08
C21	13,46	25,93	25,42	-12,47	-11,96	13,02	12,55	0,44	0,91
H22	11,90	6,98	7,46	4,92	4,44	6,19	6,62	5,71	5,28
H23	9,78	10,14	10,08	-0,36	-0,30	9,58	9,55	0,20	0,23
H24	7,71	7,81	7,81	-0,10	-0,10	7,26	7,39	0,45	0,32
H25	7,41	7,23	7,47	0,18	-0,06	7,12	7,39	0,29	0,02
H26	7,61	7,67	7,93	-0,06	-0,32	7,38	7,67	0,23	-0,06
H27	7,76	8,30	8,40	-0,54	-0,64	8,12	8,26	-0,36	-0,50
H28	6,94	6,70	6,86	0,24	0,08	6,19	6,37	0,75	0,57
H29	7,92	8,06	8,10	-0,14	-0,18	7,96	8,01	-0,04	-0,09
H30	7,83	7,61	7,77	0,22	0,06	7,36	7,56	0,47	0,27
H31	7,50	7,72	7,90	-0,22	-0,40	7,35	7,53	0,15	-0,03
H32	7,49	7,66	7,88	-0,17	-0,39	7,42	7,66	0,07	-0,17
H33	7,50	7,72	7,92	-0,22	-0,42	7,32	7,59	0,18	-0,09
H34	7,85	8,19	7,38	-0,34	0,47	7,95	8,10	-0,10	-0,25
H35	2,67	3,07	3,17	-0,40	-0,50	2,18	2,30	0,49	0,37
H36	2,67	3,12	3,22	-0,45	-0,55	2,20	2,34	0,47	0,33
H37	1,70	2,33	2,28	-0,63	-0,58	1,52	1,45	0,18	0,25
H38	1,70	2,33	2,28	-0,63	-0,58	1,52	1,45	0,18	0,25
H39	0,97	1,46	1,53	-0,49	-0,56	0,75	0,83	0,22	0,14
H40	0,97	1,45	1,52	-0,48	-0,55	0,74	0,83	0,23	0,14
H41	0,97	1,67	1,67	-0,70	-0,70	1,06	1,06	-0,09	-0,09

Electronic Properties

The energies of two important molecular orbitals of the molecule; the second highest and highest occupied MO's (HOMO), the lowest and the second lowest unoccupied MO's (LUMO) were calculated by using DFT/B3LYP and HF methods with 6-31G(d) level and are presented in Figure 4. The energy gap of the title molecule was calculated at DFT/B3LYP and HF level, which reveals the chemical reactivity and proves the occurrence of eventual charge transfer. The HOMO is located almost over the carbon atoms, oxygen atoms and also slightly delocalized in hydrogen atom and the LUMO is mainly delocalized in carbon atoms of benzene ring. The energy gap (energy difference between HOMO and LUMO orbital) is a critical parameter in determining molecular electrical transport properties (Fukui, 1982). The HOMO-LUMO energy gap of the title molecule is found to 0.11445/0.3863 a.u. obtained at DFT/HF method with 6-31G(d) levels.

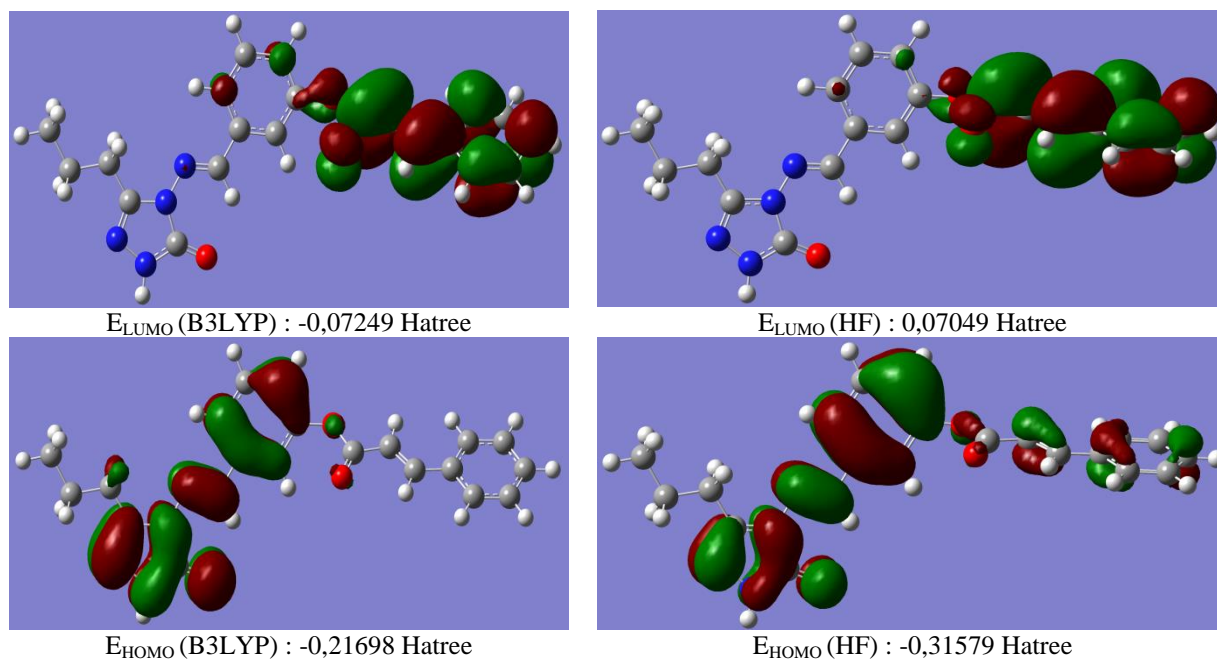


Figure 4. The calculated HOMO-LUMO energies of the molecule according to DFT/B3LYP/6-31G(d,p) and HF/B3LYP/6-311G(d,p) levels

Dipole moment and total energy

The energetic behavior of title molecule was investigated in vacum. Dipol moments and total energy values of title molecule were calculated by using B3LYP/6-31G(d), HF/6-31G(d) level. The calculated dipole moments and total energy values are given in Table 4.

Table 4. The calculated dipole moment values of the molecule

Dipole Moment	B3LYP (a.u.)	HF (a.u.)
μ_x	1.3544	2.5992
μ_y	3.1952	4.3845
μ_z	2.9544	3.8141
μ_{Toplam}	4.5576	6.3661

Mulliken's Atomic Charges

The Mulliken atomic charges at the HF/6-31 G(d) and B3LYP/6-31 G(d) level of compound 3 in gas phase are given in Table 7 (Mulliken, 1955). The electronegative N42, N43, N44, N45, O46, O47 and O48 atoms of compound PTC have negative atomic charge values. The Mulliken atomic charges (DFT/HF) of the mentioned atoms were calculated as -0.519 /-0.659, -0.338/-0.348, -0.428 /-0.637, -0.311/-0.312, -0.540/-0.656, -0.549/-0.707 and -0.479/-0.568 a.u., respectively. The C1, C2, C3, C6, C10 and C13 carbon atoms bounded to the mentioned electronegative atoms in the molecule under study have positive atomic charge values. The values of

the positive charges of the mentioned carbon atoms were found as 0.556/0.627, 0.825/1.059, 0.037/0.094, 0.350/0.406, 0.618/0.811 and 0.166/0.016 a.u., respectively. Therefore the C1 atom surrounded with two electronegative N43 and N44 atoms, the C2 atom surrounded with the electronegative N42, N45 and O46 atoms and the C10 atom surrounded with two electronegative O47 and O48 atoms have the highest positive charge values. In the compound PTC the atomic charges of all hydrogen atoms have positive values.

Table 4. Mulliken atomic charges of the molecule

	DFT	HF		DFT	HF		DFT	HF
C1	0.556	0.627	C17	-0.131	-0.204	H33	0.139	0.209
C2	0.825	1.059	C18	-0.170	-0.202	H34	0.137	0.212
C3	0.037	0.094	C19	-0.323	-0.352	H35	0.170	0.200
C4	0.117	-0.032	C20	-0.251	-0.312	H36	0.169	0.199
C5	-0.199	-0.231	C21	-0.447	-0.486	H37	0.154	0.181
C6	0.350	0.406	H22	0.355	0.418	H38	0.153	0.181
C7	-0.159	-0.223	H23	0.212	0.290	H39	0.144	0.159
C8	-0.142	-0.204	H24	0.167	0.236	H40	0.143	0.159
C9	-0.155	-0.190	H25	0.144	0.224	H41	0.149	0.171
C10	0.618	0.811	H26	0.139	0.212	N42	-0.519	-0.659
C11	-0.215	-0.347	H27	0.152	0.234	N43	-0.338	-0.348
C12	-0.146	-0.120	H28	0.153	0.222	N44	-0.428	-0.637
C13	0.166	0.016	H29	0.171	0.247	N45	-0.311	-0.312
C14	-0.186	-0.215	H30	0.143	0.216	O46	-0.540	-0.656
C15	-0.131	-0.203	H31	0.140	0.210	O47	-0.549	-0.707
C16	-0.123	-0.192	H32	0.139	0.210	O48	-0.479	-0.568

Conclusion

In this paper, 3-*n*-propyl-4-(3-cinnamoyloxybenzylidenamino)-4,5-dihydro-1H-1,2,4-triazol-5-one (PTC) was synthesized from the reaction of compound (PT) with 4-cinnamoyloxybenzaldehyde (C). The structure of the titled compound is characterized by using ¹H, ¹³C NMR, FT-IR and UV spectroscopic methods. The molecular structures, vibrational frequencies, ¹H and ¹³C NMR chemical shifts, UV-vis spectroscopies, HOMO and LUMO analyses and atomic charges of 3-ethyl-4-(4-cinnamoyloxybenzylidenamino)-4,5-dihydro-1H-1,2,4-triazol-5-one molecule (PTC) synthesized for the first time have been calculated by using DFT/B3LYP and HF methods. By considering the results of experimental works it can be easily stated that the ¹H and ¹³C NMR chemical shifts, vibrational frequencies, and UV spectroscopic parameters obtained theoretically are in a very good agreement with the experimental data.

Acknowledgment

This study was supported by Kafkas University Scientific Research Project (Proje Number: 2016-FM-25).

Scientific Ethics Declaration

The authors declare that the scientific ethical and legal responsibility of this article published in EPSTEM journal belongs to the authors

References

- Aktaş-Yokuş, Ö., Yüksek, H., Manap, S., Aytemiz, F., Alkan, M., Beytur, M., & Gürsoy-Kol, Ö. (2017). In-vitro biological activity of some new 1, 2, 4-triazole derivatives with their potentiometric titrations. *Bulgarian Chemical Communications*, 49(1), 98-106.
- Alkan, M., Yüksek, H., İslamoğlu, F., Bahçeci, S., Calapoğlu, M., Elmastaş, M., ... & Özdemir, M. (2007). A Study on 4-Acylamino-4, 5-dihydro-1H-1, 2, 4-triazol-5-ones. *Molecules*, 12(8), 1805-1816.
- Avcı, D., & Atalay, Y. (2009). Theoretical analysis of vibrational spectra and scaling- factor of 2- aryl- 1, 3, 4- oxadiazole derivatives. *International Journal of Quantum Chemistry*, 109(2), 328-341.

- Bahçeci Ş., Yüksek H., Ocak Z., Köksal C., Ozdemir M. (2002). Synthesis and non-aqueous medium titrations of some new 4,5-dihydro-1H-1,2,4-triazol-5-one derivatives. *Acta Chimica Slovenica*, 49, 783-794.
- Bahçeci, Ş. Yıldırım, N. Alkan, M. Gürsoy-Kol Ö., Manap, S., Beytur, M. & Yüksek, H. (2017). Investigation of Antioxidant, Biological and Acidic Properties of New 3-Alkyl(Aryl)-4-(3-acetoxy-4-methoxybenzylidenamino)-4,5-dihydro-1H-1,2,4-triazol-5-ones, *The Pharmaceutical and Chemical Journal*, 4(4), 91-101.
- Bahçeci, Ş., Yıldırım, N., Gürsoy-Kol, Ö., Manap, S., Beytur, M., & Yüksek, H. (2016). Synthesis, characterization and antioxidant properties of new 3-alkyl (aryl)-4-(3-hydroxy-4-methoxybenzylidenamino)-4, 5-dihydro-1H-1, 2, 4-triazol-5-ones. *Rasayan Journal of Chemistry*, 9(3), 494-501.
- Bayrak, H., Demirbas, A., Demirbas, N., & Karaoglu, S. A. (2010). Cyclization of some carbothioamide derivatives containing antipyrine and triazole moieties and investigation of their antimicrobial Beytur, M. (2020). Fabrication of platinum nanoparticle/boron nitride quantum dots/6-methyl-2-(3-hydroxy-4-methoxybenzylidenamino)-benzothiazole (ils) nanocomposite for electrocatalytic oxidation of methanol. *Journal of the Chilean Chemical Society*, 65(3), 4929-4933.
- Beytur, M., & Avinca, I. (2021). Molecular, Electronic, Nonlinear Optical and Spectroscopic Analysis of Heterocyclic 3-Substituted-4-(3-methyl-2-thienylmethyleneamino)-4, 5-dihydro-1H-1, 2, 4-triazol-5-ones: Experiment and DFT Calculations. *Heterocyclic Communications*, 27(1), 1-16.
- Beytur, M., Irak, Z. T., Manap, S., & Yüksek, H. (2019). Synthesis, characterization and theoretical determination of corrosion inhibitor activities of some new 4, 5-dihydro-1H-1, 2, 4-Triazol-5-one derivatives. *Heliyon*, 5(6), e01809.
- Boy, S. Türkan, F. Beytur, M. Aras, A. Akyıldırım O., Sedef Karaman, H., & Yüksek, H. (2021). Synthesis, design, and assessment of novel morpholine-derived Mannich bases as multifunctional agents for the potential enzyme inhibitory properties including docking study, *Bioorganic Chemistry*. 107, 104524.
- Çiftçi E., Beytur M., Calapoğlu M., Gürsoy Kol Ö., Alkan M., Toğay, V.A., Manap S., Yüksek H. (2018). Synthesis, characterization, antioxidant and antimicrobial activities and dna damage of some novel 2-[3-alkyl (aryl)-4,5-dihydro-1h-1,2,4-triazol-5-one-4-yl]-phenoxyacetic acids in human lymphocytes, *Research Journal of Pharmaceutical, Biological and Chemical Sciences*, 9(5), 1760-1771.
- Dennington, R., Keith, T., & Millam, J. (2009). *GaussView*. Shawnee Mission.
- Frisch, M. J., Trucks, G., Schlegel, H. B., Scuseria, G. E., Robb, M. A., Cheeseman, J. R., Scalmani, G., Barone, V., Mennucci, B., Petersson, G. A., Nakatsuji, H., Caricato, M., Li, X., Hratchian, H. P., Izmaylov, A. F., Bloino, J., Zheng, G., Sonnenberg, J. L., Hada, M., Ehara, M., Toyota, K., Fukuda, R., Hasegawa, J., Ishida, M., Nakajima, T., Honda, Y., Kitao, O., Nakai, H., Vreven, T., Montgomery, J. A., Jr. Vreven, T., Peralta, J. E., Ogliaro, F., Bearpark, M., Heyd, J. J., Brothers, E., Kudin, N., Staroverov, V. N., Kobayashi, R., Normand, J., Raghavachari, K., Rendell, A., Burant, J. C., Iyengar, S. S., Tomasi, J., Cossi, M., Rega, N., Millam, J. M., Klene, M., Knox, J. E., Cross, J. B., Bakken, V., Adamo, C., Jaramillo, J., Gomperts, R., Stratmann, R. E., Yazyev, O., Austin, A. J., Cammi, R., Pomelli, C., Ochterski, J. W., Martin, L. R., Morokuma, K., Zakrzewski, V. G., Voth, G. A., Salvador, P., Dannenberg, J. J., Dapprich, S., Daniels, A. D., Farkas, O., Foresman, J. B., Ortiz, J. V., Cioslowski, J. & Fox, D. J. (2009). *Gaussian Inc.* Wallingford
- Fukui, K. (1982). Role of frontier orbitals in chemical reactions. *science*, 218(4574), 747-754.
- Gürsoy-Kol, Ö., & Yüksek, H. (2010). Synthesis and invitro antioxidant evaluation of some novel 4,5-dihydro-1H-1,2,4-triazol-5-one derivatives, *E-Journal of Chemistry*, 7(1), 123-136.
- Güzeldemirci N.U., Kucukbasmaci O. (2010). Synthesis and antimicrobial activity evaluation of new 1,2,4-triazoles and 1,3,4-thiadiazoles bearing imidazo[2,1-b]thiazole moiety. *European Journal of Medicinal Chemistry*, 45(1), 63-68.
- Hashem A.I., Youssef A.S.A., Kandeel K.A., Abou-Elmalgd W.S.I. (2007). Conversion of some 2(3H)-furanones bearing a pyrazolyl group into other heterocyclic systems with a study of their antiviral activity, *European Journal of Medicinal Chemistry*, 42(7), 934-939.
- Koç, E., Yüksek, H., Beytur, M., Akyıldırım, O., Akçay, M., & Beytur, C. (2020). Heterosiklik 4, 5-dihidro-1H-1, 2, 4-triazol-5-on türevinin antioksidan özelliğinin erkek ratlarda (wistar albino) in vivo olarak belirlenmesi. *Bitlis Eren Üniversitesi Fen Bilimleri Dergisi*, 9(2), 542-548.
- Lee, S. Y. (1998). Molecular structure and vibrational spectra of biphenyl in the ground and the lowest triplet states. density functional theory study. *Bulletin of the Korean Chemical Society*, 19(1), 93-98.
- Mulliken, R. S. (1955). Electronic population analysis on LCAO-MO molecular wave functions. I. *The Journal of Chemical Physics*, 23(10), 1833-1840.
- Rani, A. U., Sundaraganesan, N., Kurt, M., Cinar, M., & Karabacak, M. (2010). FT-IR, FT-Raman, NMR spectra and DFT calculations on 4-chloro-N-methylaniline. *Spectrochimica Acta Part A: Molecular and Biomolecular Spectroscopy*, 75(5), 1523-1529.

- Silverstein, R. M., & Bassler, G. C. (1962). Spectrometric identification of organic compounds. *Journal of Chemical Education*, 39(11), 546.
- Subramanian, N., Sundaraganesan, N., & Jayabharathi, J. (2010). Molecular structure, spectroscopic (FT-IR, FT-Raman, NMR, UV) studies and first-order molecular hyperpolarizabilities of 1, 2-bis (3-methoxy-4-hydroxybenzylidene) hydrazine by density functional method. *Spectrochimica Acta Part A: Molecular and Biomolecular Spectroscopy*, 76(2), 259-269.
- Tozkoparan B., Kupeli E., Yesilada E., Ertan M. (2007). Preparation of 5-aryl-3-alkylthio-1,2,4-triazoles and corresponding sulfones with anti-inflammatory-analgesic activity. *Bioorganic & Medicinal Chemistry*, 15(4), 1808-1814.
- Turhan-Irak Z., Beytur, M. (2019). 4-benzilidenamino-4,5-dihidro-1h-1,2,4-triazol-5-on türevlerinin antioksidan aktivitelerinin teorik olarak incelenmesi. *Journal of the Institute of Science and Technology*, 9(1), 512-521.
- Turhan-Irak Z., Gümüş, S. (2017). Heterotricyclic compounds via click reaction: A computational study. *Noble International Journal of Scientific Research*, 1(7), 80-89.
- Uğurlu, G., & Beytur, M. (2020). Theoretical studies on the structural, vibrational, conformational analysis and nonlinear optic (NLO) property of 4-(Methoxycarbonyl) phenylboronic acid. *Indian Journal of Chemistry-Section A*, 59(10), 1504-1512.
- Vasavada, J. A., & Parekh, H. H. (2003). Synthesis and antimicrobial screening of cyclohexenones and oxazines. *ChemInform*, 34(39), 55-56.
- Wade, L.G. (2006). *Organic chemistry* (6nd ed). Pearson Prentice Hall.
- Yüksek H., Kolaylı S., Küçük M., Yüksek M.Ö., Ocak U., Şahinbaş E., Sivrikaya E., & Ocak M. (2006). Synthesis and antioxidant activities of some 4-benzilidenamino-4,5-dihidro-1h-1,2,4-triazol-5-one derivatives, *Indian Journal of Chemistry-Section B*, 45(3), 715-718.
- Yüksek, H., Üçüncü, O., Alkan, M., Ocak, Z., & Bahceci, S. (2005). Synthesis and non-aqueous medium titrations of some new 4-benzilidenamino-4, 5-dihidro-1H-1, 2, 4-triazol-5-one derivatives. *Molecules*, 10(8), 961-970.

Author Information

Murat BEYTUR

Kafkas University
Department of Chemistry, Kars, Turkey
Contact e-mail: muratbeytur83@gmail.com

Haydar YUKSEK

Kafkas University
Department of Chemistry, Kars, Turkey

To cite this article:

Beytur, M. & Yüksek, H. (2021). The investigation of spectroscopic and electronic properties of 3-ethyl-4-(4-cinnamoyloxybenzylidenamino)-4,5-dihidro-1h-1,2,4-triazol-5-one compound using density functional theory and hartree-fock basis sets. *The Eurasia Proceedings of Science, Technology, Engineering & Mathematics (EPSTEM)*, 15, 79-87.

The Eurasia Proceedings of Science, Technology, Engineering & Mathematics (EPSTEM), 2021

Volume 15, Pages 88-98

ICBAST 2021: International Conference on Basic Science and Technology

Review on Microbial Enhanced Oil Recovery and Controlling Its Produced Hydrogen Sulfide Effects on Reservoir and Transporting Pipelines

Ali HARATIAN

Amirkabir University of Technology

Soroosh EMAMI MEYBODI

Amirkabir University of Technology

Abstract: Using viable microbial cultures within hydrocarbon reservoirs so as to enhancement of oil recovery through metabolic activities is exactly what we recognize as Microbial enhanced oil recovery (MEOR). In similar with many other process in industries, there are some cons and pros following with MEOR. The creation of sulfides such as hydrogen sulfide as a result of injecting the sulfate-containing seawater into hydrocarbon reservoirs in order to maintain the required reservoir pressure, leads to produce and growth of Sulfate Reducing Bacteria (SRB) approximately near the injection wells, turning the reservoir into sour, however SRB is not considered as the only microbial process stimulating the formation of sulfides. Along with SRB, thermochemical sulfate reduction or thermal redox reaction (TSR) is also known to be highly effective at resulting in having extremely concentrated zones of H_2S in the reservoir fluids eligible to cause corrosion. Owing to extent of the topic, more information on formation of H_2S are going to be put finger on. Besides, confronting the undesirable production of sulfide species in the reservoirs can lead to serious operational, environmental and financial problems in particular the transporting pipelines. Consequently, conjuring up reservoir souring control strategies on the way production of oil and gas is the only way to prevent possible damages in terms of environment, finance and man power which requires determining the compound's reactivity, origin and partitioning behavior. This article is going to provide a comprehensive review on progress made in this field and the possible advent of new strategies in this technologically advanced world of petroleum industry.

Keywords: Corrosion, Hydrogen sulfide, NRB, Reservoir souring, SRB

Introduction

Deployment of microorganisms in purpose of enhancing oil recovery is not considered as a newly developed assessment in this field (Rashedi, 2014; Chilingarian et. al., 1989; Patel et. al., 2015; Nmegbu, 2014). In 1926, the effect of bacteria on mineral oil were tested and reported by Beckmann, consequently he observed the high efficiency of bacterial enzymes in order to be used for enhance oil recovery methods (Chilingarian et. al., 1989; Zobell, 1973; Nerurkar et. al., 2012). In oil microbiological studies, six principles were targeted respectively: Beginning of the rebirth of organic compounds in sediments and oils, the degradation of hydrocarbons, hydrocarbons enhanced recovery from reservoirs, modification of hydrocarbon products at initial production or reproduction, reduction of disturbing microorganisms and eventually biological purging of product or crude oil (Rashedi, 2014; Zobell, 1973). Putting effort into enhancing oil recovery in microbial way is done by injecting sulfate-containing seawater into reservoir for maintaining the requiring pressure of oil reservoirs in order to recover oil from depleted wells (Ekemini et. al., 2019; Basafa et. al., 2019; Nmegbu et. al., 2014). Regarding the injection of seawater, resuscitation of thiosulfate into sulfide could be expecting in the reservoirs (Little, 2013). H_2S is a toxic, corrosive, hazardous and explosive gas, procreating remarkable operational and health risks

- This is an Open Access article distributed under the terms of the Creative Commons Attribution-Noncommercial 4.0 Unported License, permitting all non-commercial use, distribution, and reproduction in any medium, provided the original work is properly cited.

- Selection and peer-review under responsibility of the Organizing Committee of the Conference

© 2021 Published by ISRES Publishing: www.isres.org

which makes those in charge of enhancing oil recovery unable to avoid financial and environmental damages (Kögler et. al., 2021).

The idea behind this biological damage could be announced the creation and spread of SRB known as sulfate-reducing bacteria which by making physical and chemical changes at oil in reservoirs, increases the production of oil along with some unwanted influences on reservoir leading to souring which has no outcome except acidifying the atmosphere dominant over the reservoir and corrosion of transporting pipelines (Rashedi, 2014). As a matter of fact, the reduction of sulfate to sulfide is the main cause of chemically and biologically mediated reactions resulting in formation of various reduced sulfur compounds, consequently the souring of reservoir takes place (Holubnyak et. al., 2011; Basafa et. al., 2019; Patel et. al., 2015; Quraishi et. al., 2021).

Along with sulfides, other species such as Sulfite, Thiosalts and polysulfide are all along with sulfide in reservoir (Basafa et. al., 2019). The average oxidation state of these Sulfur species only ranges between Sulfate-Sulfur (+ 6) and Sulfidic-Sulfur (- 2) which means they are usually referred to as intermediate sulfur species (fig.1) (Basafa et. al., 2019; Little, 2013). As is obvious, these intermediate sulfur species could affect the treatment approaches for sourd reservoirs due to having implications in microbial and chemical process. Appearing in different oxidation–reduction is what can be done by reduced sulfur species leading to react with other species in reservoir (Basafa et. al., 2019; Little, 2013).

As a result, in order to get by these possible damages, some strategies must be used to reduce and finally stop the extent of sulfide species. In this paper, some of the most effective strategies to stop spreading the sulfide are going to be reviewed and discussed which are expected to be using biocides, NRB and a newly researched way, using molybdate as Inhibitor of biogenic hydrogen sulfide produce by Sulfate-Reducing Bacteria (SRB) (Al-Tamimi et. al., 2017).

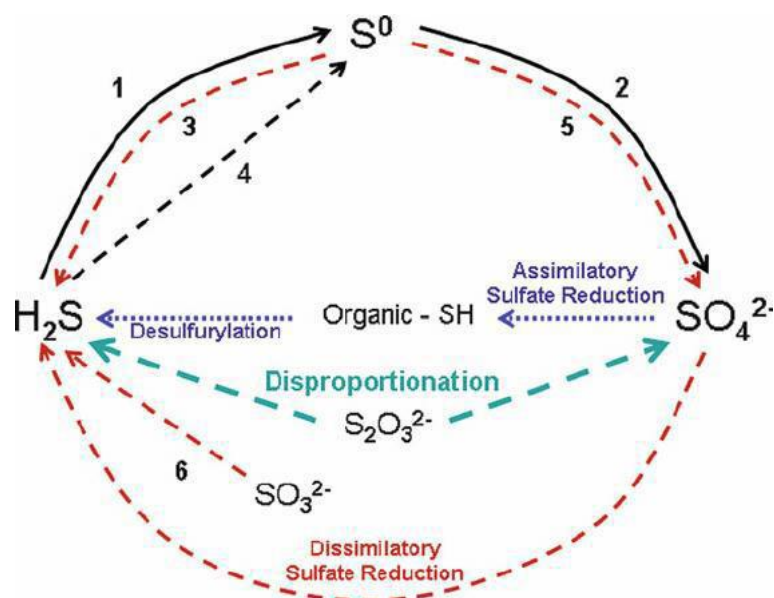


Figure 1. The biological sulfur cycle with roles of bacteria identified. Solid lines indicate aerobic reactions, dashed lines indicate anaerobic reactions, and dotted lines indicate both aerobic and anaerobic activity (Barton et. al., 2017).

Controlling these harmful process requires knowing some primitive information about souring and consequently corrosion like their being a function of pressure, pH, composition and reservoir temperature, hence while the conditions at reservoir changes within unit operations and other reasons, these specific compounds could degrade to corrosion leading to turning up of some problematic situation such as health and manpower hazards, equipment’s damage and decline of effectiveness of produced water and other treatment systems (Basafa et. al., 2019; Ibrahim et. al., 2012)

In this case, the injection of nitrate into an oil reservoir to boost the growth of nitrate reducing bacteria (NRB), could be considered as a cost-effective and ordinary strategy to inhibit microbial sulfate reduction by several mechanisms (Kögler et. al., 2021). Besides, employment of biocides, chemical compounds used to disinfect, decontaminate and sterilize materials (Surfaces or objects) in order to eliminate microbiological degradation

processes, as an inhibitor is getting common in oil industries (Okoro, 2014). As stated earlier, another inhibition method exists known as Inhibition of microbial sulfate reduction by molybdate which has received much less attention in compare with the other strategies even with having more advantages in various fields related to reservoirs (Jesus et. al., 2015). The objective of this study is to evaluate the efficiency of implementing the stated souring control strategies in different situation in purpose of managing the activity of sulfur reducing bacteria (SRB) and other process namely TSR so as to prevent the taking place of corrosion with transporting pipelines and other supplements used to get to oil and gas and The reader is directed to recent reviews discussing these topics (Gieg et. al., 2011; Jesus et. al., 2015; Sugai et. al., 2015).

Discussion

Reservoir Souring and Thermochemical Sulfate Reduction

The highly concentrated Aggregation of hydrogen sulfide present in many oil and gas fields is thought to levitate from the oxidation of petroleum hydrocarbons by sulfate-reduction reactions occurring at temperatures above 250C. However sulfate derived from seawater or the dissolution of solid calcium sulfide is able to be reduced by a great amount of chemical and organic compounds known as polar aromatic, saturated hydrocarbons and alcohols (Lin et. al., 2020; Goldstein et. al., 1991). This thermal-related reaction is known as thermochemical sulfur reduction(TSR) considered to be responsible for bulk of these reduction-related reactions leading to get the reservoirs soured, significantly in deep and high temperatures (Goldstein et. al., 1991). Thermochemical Sulfate Reduction is fully known in the field and experiments have been led to survey the reactions engaged with this process, any possible products, and the impact of temperature, various types of oxidants, the presence of different sulfur species and metal cations, and the effect of pH on the rate of Thermochemical Sulfate Reduction (Goldstein et. al., 1991; Basafa et. al., 2019; Singhapetcharat et. al., 2018).

Besides Thermolysis aquathermolysis of aromatic thiophene-type organosulfur compounds similar to thiophene and aliphatic organic sulfides such as tetrahydrothiophene in heavy oil are also in ability to produces H_2S . The amount of H_2S produced by thermal way of decomposition of oil is symmetric to the sulfur content of the oil and is usually measured at a number less than 5% in reservoir (Basafa et. al., 2019). The most available sulfur species present at bitumen are sulfide, Polysulfide, Thiols, disulfides, benzothiophenes, dibenzothiophenes and thiophenes while disulfides and Thiols are the most reactive ones, on the other hand the Benzothiophenic compounds are considered as the most stable (Basafa et. al., 2019; Barton et. al., 2017; Nourani et. al., 2007; Sugai et. al., 2015). Some oxidative and reductive dissolution of metal sulfides under specific circumstances like acidic atmosphere may lead to production of sulfate ions and naturally H_2S during employment of steam injection and water flooding as an asset to enhance the pressure of reservoir (Basafa et. al., 2019).

Oxidative dissolution reaction:



Reductive dissolution reaction:



The MS in all Oxidative dissolutions and Reductive dissolutions is indicator of sulfide mineral where M is coined the metal base, O and R are oxidized and reduced compounds in the redox reaction, respectively. The acidic components all come from the injection of water or the bio degradation of injected biocides and scale inhibitors and corrosion. Pyrite and pyrrotite, known as some Iron sulfides, are common metal sulfide minerals associated with reservoirs forming under reducing conditions (Basafa et. al., 2019; Li et. al., 2011)

How things get done is that Pyrite is oxidized to sulfate and hydrogen reduces the pH of the environment surrounding. When PH values are lower than 7, Pyrite oxidation by dissolved oxygen may produce Tetrathionate and sulfate on the contrary, at higher pH values, more than 7, thiosulfate and sulfite are considered as the major reaction products (Basafa et. al., 2019; Goldstein et. al., 1991; Lin et. al., 2020; Correia et. al., 2021). The most favorable decomposition reactions for pyrite at low pH values to be exact less than 7 and under reducing conditions, generating H_2S are (Okoro et. al., 2015):



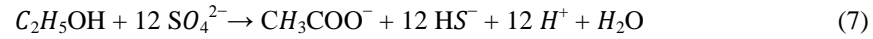


Under some conditions, pyrite is turned into sulfate and sulfide, as, in the presence of an oxidant, it is become to elemental sulfur (Okoro et. al., 2015):



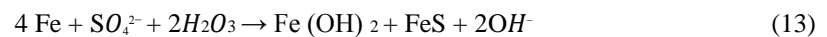
Sulfate Reducing Bacteria (SRB)

The turning up of SRB, is considered as a common problem during the injection of sea water into reservoir in order to increase the pressure of reservoir as a known method of enhanced oil recovery. SRB are anaerobic microbes having most accompaniment with microbial corrosion, reservoir plugging, deterioration of product quality, and decrease in the permeability of pores of underground petroleum reservoirs (Okoro et. al., 2015; Little, 2013). They are diverse groups of anaerobic microbes present everywhere and zero in on producing H_2S by using sulfate ion as the final electron receiver although enormous amount of different organic matters such as format, acetate, propionate, pyruvate, lactate, butyrate and ethanol can play the role as the electron donors for SRB (Little, 2013; Naresh et. al., 2015; Tatar, 2018). An outstanding amount of these bacteria, by using H_2 or some organic compounds are able to reduce nitrate, sulfite, thiosulfate and fumarate (Little, 2013). The following reaction was assumed to occur in the reservoir into which the water containing the SRB was injected (Suga et. al., 2020):



These bacteria have already departed from diverse zones including seawater containing a compactness of 25 mM. However, the amount of seawater's oxygen is above thermocline ranges from 5 to 10 ppm, anaerobic microbes settled at anaerobic microniches stay alive until the return of formation's normal conditions (Little, 2013; Ibrahim et. al., 2015).

If the rate of aerobic breathing at the biofilm is more than the rate of oxygen infiltration, the biofilm-iron area can turn into anaerobic and embark on creating an opportunity for production of sulfide species with help of sulfate reducing bacteria (Little, 2013). In fact, metabolic activity of SRB causes the accumulation of sulfide near the iron species. Due to studies done in the recent years, many mechanisms have been found to be related to SRB detrimental activities: Cathodic Depolarization due to Dehydrogenase enzyme, anodic Depolarization, formation of iron sulfides, sulfide-induced stress cracking or hydrogen blister. These reactions are discussed to be involved in sulfate reducing bacteria process (Little, 2013; Jesus et. al., 2015):



These reactions are known as Cathodic Depolarization, stating that sulfate reducing bacteria omit the accumulated hydrogen's hydrogenase (Hase+) at cathode (Little, 2013). In 1985, Hamilton studied H_2S reduction as a cathodic reaction and the role of FeS as a low hydrogen overvoltage. Afterwards, it was revealed that Desulfovibrio which doesn't form hydrogenase (Hase+) as a result of Cathodic Depolarization, can stimulate the corrosion rate (Hamilton et. al., 1985).

Regarding the investigation done in field of SRB corrosion, sulfate reducing bacteria mostly have been based on Desulfovibrio although it was revealed that the presence of Desulfobacterium is dominant at a marine environment and grows faster than Desulfovibrio species (Little, 2013).

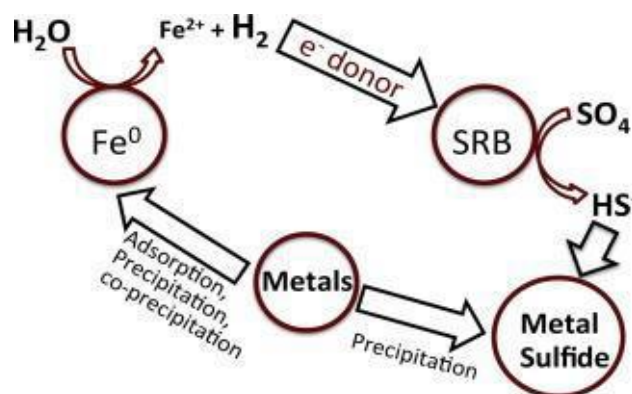


Figure 2. A general overview of SRB and other process involved in.

As a result, the SRB's bleaching activities to the reservoir and environment along with drilling equipment has to be stopped in the most proportional ways due to studies have been done during recent years. As far as the microbial enhanced oil recovery method keeps on going, the production of SRB is expected to be continued so taking advantages of MEOR method could be feasible by prompting big changes on the way controlling SRB activities (Basafa et. al., 2019; Ekemini et. al., 2019; Ibrahim et. al., 2015).

Sulfur Chemistries and The Catalyzers

When the reservoir fluids flow from injection well to production well, production of intermediate sulfur species could be expecting owing to microbial and chemical reactions occurring at reservoir (Basafa et. al., 2019). What makes these compounds complex is their dependence over some factors like PH, Temperature along with the presence of other sulfur species, metals, and microorganisms (Chen et. al., 2018).

		sulfur oxidation states					
		-2	-1	0	+2	+4	+6
compounds, ions & functional groups	R-S-R sulfides	R-S-S-R disulfides	S elemental sulfur	S=O sulfur monoxide	O=S=O sulfur dioxide	O O=S=O sulfur trioxide	
	R-S-H thiols	R-S-OH sulfenic acid	R-S-OH sulfenic acid	O R-S-R O sulfonates	O O-S-O sulfite	O O-S-O sulfate	
	+ R-S-R R sulfonium ion	O R-S-R sulfoxides	O R-S-R sulfonates	O R-S-OH sulfenic/ sulfoxylic* acid	O R-S-OH O sulfonic/ sulfurous* acid	O R-O-S-O-R O sulfate esters/ sulfuric* acid	
	S- sulfur atoms at polysulfide chain end	-S _n - sulfur atoms in polysulfide chains	-S _n - sulfur atoms in polysulfide chains	O R-S-OH sulfenic/ sulfoxylic* acid	O R-S-OH O sulfonic/ sulfurous* acid	O R-O-S-O-R O sulfate esters/ sulfuric* acid	
		S- sulfane sulfur in thiosulfate	S- sulfane sulfur in thiosulfate		O -S-O O sulfonate sulfur in thiosulfate		

*R = H

Figure 3. Most common inorganic and organic sulfur compounds ions and functional group

In terms of chemical views, these compounds are divided into three major groups; the first group are rich in acidic properties and include Carbonyl sulfide, Aryl, Carbon disulfide and Thiols (Rabbani, 2010). The second group is chemically neutral however they are not stable at high temperatures and this group has been made up of Sulfur and Polysulfur (Rabbani, 2010). The third group not only is neutral but also have shown resistance and stability at high temperatures. Thiophene is an example compound of the last discussed group. Major parts of these compounds under redox conditions, produce H₂S like the reaction of Thiocarbamat and reduction of Thioter (Rabbani, 2010):

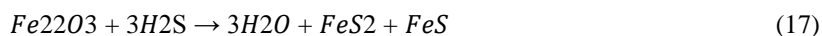


Non-organic sulfur compounds mostly flash around as Insoluble metal or soluble sulfate. There are some incomplete redox reactions involving H_2S , sulfur dioxide, or even sulfate which are likely the reason why the sulfur oxyanions are generated in places with low temperature. Partial re oxidation of H_2S to sulfur may occur in some aerobic environments, where molecular O_2 is present, and in high temperature anaerobic environments, excess sulfate may act as the role of the oxidant. Intermediate sulfur species are able to be reduced to sulfide. Some of the sulfate reducers can reduce the sulfur compounds like sulfite, Thiosalts and sulfur (Rabbani, 2010, Basafa et. al., 2019; Hiorth et. al., 2007). Electrochemical detection and Ion chromatography with a glassy carbon electrode chemically modified with palladium particles have shown the highly potential ability to catalyze sulfide oxidation over vast potential and pH ranges and thus, could discover dissolved ions in all aqueous solutions.

Hydrogen Embrittlement in Pipelines Transporting Sour Hydrocarbons

In order to achieve a good integrity management, knowledge of damage mechanisms is very important. In the recent years many studies have been done on hydrogen embrittlement (HE) and how effects on load carrying steel. As ASTM F2078 states, HE is defined as “a permanent loss of ductility in a metal or alloy caused by hydrogen in combination with stress, either externally applied or internal residual stress”. However, the interaction of Hydrogen with metals under stress is very complex and many different mechanisms are proposed (Gabetta et. al., 2018; Nmegbu et. al., 2014). Diffused Hydrogen, for instance, not only can be associated to embrittlement but also to enhanced ductility. Three conditions are required to cause cracking - potentially developing to failure: presence of water solution, Tensile stresses and material susceptibility (Gabetta et. al., 2018). In particular, the first two i.e. the nature of the flow wetting the pipe wall and the working factors of line pipe material when in service, commonly act as triggers for cracking, while the root cause remains the line pipe material susceptibility (Gabetta et. al., 2018; Nmegbu, 2014). Don't forget that the presence of H_2S and other sulfur species in hydrocarbons can be in charge of the general and localized corrosion. Laminations are a significant threat to the integrity of the pipeline and due to the presence of H_2S in the fluid, it is reported several laminar features (Gilliland, 1976).

In presence of wet H_2S in the fluid, however, it is possible to observe blisters. From blisters, cracks may propagate in the steel. An estimate of crack growth rate for these defects can be useful to assess the integrity of pipelines. H_2S has a great tendency to react with minerals rich in iron such as siderite ($FeCO_3$), hematite (Fe_2O_3), and magnetite (Fe_3O_4) as shown in the coming part (Hosseini noosheri, 2016):



As a matter of fact, Temperature, pressure, and pH influence the solubility of iron-rich minerals. So, that changes the amount of adsorbed hydrogen sulfide which has no outcome expect the reservoir souring and corrosion following with transport pipes embrittlement (Gilliland, 1976; Hosseini noosheri, 2016; Anon, 1988).

Souring Control Strategies and Treatments

Underestimating the spontaneous process leading to formation of H_2S and other intermediate sulfur species following with reservoir souring and other hazardous consequences like environmental, human and financial problems, can be considered as irreparable mistake in long term. Putting finger on seeking effective solutions in recent years, has ended up with some highly effective strategies to anticipate and stop the reservoir from destructive souring anymore. Controlling the microbial oilfield souring activities is done by several a number of various methods.

One of the most common ways of controlling the reservoir souring is injection of biocides to the top side and injection water mostly known as biocides treatments. The efficiency of biocides has been proved in both studies and operations. The possible obstacles on the way using the biocides are considered as high costs of using, the rate of toxic and eventually its efficiency at operational environments.

What is exactly done by biocides is inhibition of microbial growth and activity special in those reservoirs where souring is bounded to the zone surrounding the injecting well. The determination of these compounds effects at reservoir environment due to the sulfate reducing bacteria's desire to grow in biofilm environment and formation's matrix is extremely tough thus, biocide compounds are hardly able to contact them. Besides, another trouble flashing around in biocide treatment is the SRB's resistivity against the biocides during injecting the biocides (Rabbani, 2010; Hubert et al). As the surveys demonstrate, it could be inferred that deployment of these compounds is not usually considered cost-effective and has no outcome except wasting time and energy (Rabbani, 2010; Udosoh et. al., 2020). In order to make sure that the biocides efficiency is in the most proportional way, some qualitative tastings are required to be done (Little, 2013). By normal water treatments, the reduction of bacteria to less than 1000 at m liter could be possible in (Table 1).

Morris and his colleagues gathered comprehensive information from 33 places of natural gas stations about biocides and corrosion inhibitors (Little, 2013; Berben et. al., 2017) (Table 2). In the coming tables, normal water treatments and the active biocides and the numbers they have been used are respectively going to be shown in coming tables.

Table 1. Conventional water treatments.

Suggest	Technical Information	Precautions	Operating Range	Water Improvement
Injecting from some various points.	- PH, amount of ammonia FE and MN. Temperature of water.	- -	- PH 6.5 to 7.5 evacutaions restrictions approved By EPA.	Oxidizing biocide Chlorine.
2.5 times more effective than chlorine for controlling mud	PH, amount of Ammonia FE and MN. Temperature of water	Very volatile compounds	PH to 8.7 restrictions approved By EPA	Chlorine dioxide
-	-	-	-	Non-oxidizing biocide
Can be used at water no minerals	Suspended solids	Needs to fine sieve	Low flow	Ultraviolet light

Table 2. Active biocide components and the number of their usages

Active component	Number of uses
Glutaraldehyde	9
Quarter ammonium compounds (QAC)	3
Acrolein	1
Isothiazolin	1
Diamine acetates (Cocodiamine)	1
Carbamates	1
Methylene-bis-thiocyanate	1

According to Table 1, glutaraldehyde is a non-oxidizing biocide providing the cell's death by cell proteins denaturation (Little, 2013). Glutaraldehyde is soluble in water and insoluble in oils and is incompatible with alkaline substances or strong acids. Quaternary Ammonium compounds are able to dissolve the lipid and lead to cells vitals leak (Little, 2013). As an effective inhibitor, Quaternary Ammonium compounds form some protective films on inner surface and reduce the contacts with oxidizers. The rate of efficiency has a direct relation to consumption and the local conditions. The major usages of these compounds are at closed systems like extraction tubes and gas-liquid separators. Acrolein is a carbon compound including aldehyde and vinyl (Little, 2013). The biocide activity is resulted from both. As the researches indicate, vinyl is the most reactor and toxic. Acrolein is effective removal of sulfide which creates complex reactions and sulfuric compounds with H_2S and metal sulfides (Little, 2013; Gabetta et. al., 2018). Isothiazoline is a complex compound containing nitrogen and oxygen, mostly used at industrial complexes such as water-cooled air-conditioning systems and oil reservoir injecting systems however Isothiazoline gets inactive by H_2S thus is not effective at sour environment.

Diamine acetates have 2 Amine groups. The experiments done in purpose of determining the efficiency have shown the inefficiency of Diamine acetates at controlling microbial corrosion at fluids and on surface of carbon steel (Little, 2013). Biocides are highly hazardous to oilfield workers and the environment involved in and is hard to inject very deep into reservoir, making the treatment of SRB distant from all injection well challenges (Basafa et. al., 2019; Haiyan et. al., 2020).

An alternative treatment for reservoir souring is nitrate injecting at the injection well or at the production well in the produced water. In contrast with the biocide treatment, nitrate is able to flow readily into an oil-bearing formation, consequently shift the corrosive microbial activity from SRB to nitrate reducing bacteria (NRB). The idea behind injecting nitrate-containing seawater is to stimulate nitrate-reducing bacteria in charge of reduction of nitrate to nitrite (Basafa et. al., 2019). Based on researches done on nitrate and nitrite's effect on SRB, the general activities of sulfur reducing bacteria (SRB) stops while the density of nitrite reaches to a level of 2 ppm whereas a density of nitrate above 100 ppm had no remarkable impact on the growth rate of SRB (Rabbani, 2010) [figure 4]. Due to instability of nitrite behavior as a result of potential difference of redox occurred after adding nitrate to sulfate reducing bacteria (SRB) containing seawater (Rabbani, 2010). More importantly, the SRB are very sensitive to redox leading to their habitat only available in reduction environments. The ways the NRB is able to effect on SRB are divided into two ways: 1- direct inhibition as in presence of nitrate, 2- indirect inhibition based on difference at redox potential. Chemical reaction of nitrite with H_2S demonstrates that the high value of nitrite to nitrate, is considered necessary in order to have optimal inhibition sulfate-reducing-bacteria (SRB) in sour hydrocarbon reservoirs in particular at the time the formation's PH is close to 7 or even less than 7 (Rabbani, 2010; Fan et. al., 2018).

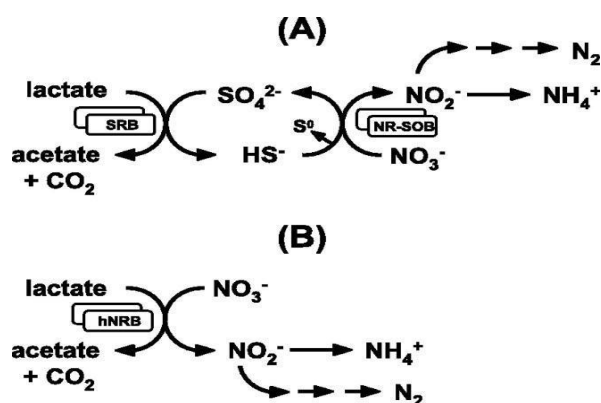


Figure 4. Impact of nitrate on the oil field sulfur cycle.

In comparison with other two strategies for controlling reservoir souring, using molybdate as an inhibitor to activity of sulfate-reducing bacteria, is less expensive along with having no significant side effects to subsurface environment, besides, most biocides are non-specific and cannot be used to stop sulfate reducing bacteria (SRB) if the growth of other microbial species is desirable. (Kögler et. al., 2021; Chilingar et. al., 1985). Deployment of Molybdate as a particular inhibition was first done by Peck in 1959 and already applied to prevent microbial sulfide genesis in sediments yet in recent years, its function as inhibitor to sulfate-reducing bacteria has been tested and proved. Molybdenum is an important chemical element for biological systems, including the anaerobic sulfate-reducing bacteria (Kögler et. al., 2021). It is used by these microbes in the synthesis of enzymes in charge of catalyzing reduction reactions, and it plays a key role in carbon, nitrogen, and sulfur cycles although the high concentration of molybdenum could be harmful for the environment due to its effect on development of microorganism (Kögler et. al, 2021). Looking over how this process is done, reveals that the molybdate ion can operate as a functional analog sulfate that can move into the bacteria so as to make it deprived of sulfur reducing compounds while the process of cellular respiration is being executed (Kögler et. al., 2021). Therefore, this acts as an ion specific metabolic inhibitor that limits sulfate reduction while is toxic to these microorganisms (Kögler et. al., 2021). In the studies done earlier, the most efficiency of molybdate has been proved to be resulted at 0.04 to 0.2 mM to fully stop the growth of pure cultures of SRB in a culture medium low in sulfate 5 mM (480 mg L⁻¹) (Kögler et. al., 2021; Guo et. al., 2015).

Conclusion

The presence of intermediate sulfur species within the reservoir formed as a result of detrimental microbial activities may lead to operational, personnel, financial and environment irreparable damages. Not only do these

sulfur compounds form toxic and corrosive compound of H_2S , but also impress the total reactivity and quality of the existing fluids in reservoir. Needless to say that as the rate of these corrosive and souring compounds rise in the reservoirs, the cost of final product decreases. In order to prevent more harms on the way microbial enhanced oil recovery scientists have come to obtain the ability to control the Phenomenon of reservoir souring resulting in corrosion by various strategies. Sulfate-reducing bacteria (SRB) is targeted as the common enemy of all strategies designed for coming over the activity of SRB and as stated earlier although the utilization of both biocides and nitrate-reducing bacteria have put the process of controlling the reservoir souring in a highly advanced way, but the comparisons between using molybdate and biocides and NRB as inhibitors to activity of SRB has brought out an awareness to the operators using these strategies as their inhibitors. Molybdate has been less impressed by the operators unlike its being cost-effective and providing less side effects.

Above all, the mentioned souring control strategies are all rich in pros and cons which made the able to be used at different and proportional circumstances compatible with the atmosphere dominant over the reservoir. On the whole, all available techniques in order to detect and get by the activity of SRB and other factors must be deployed in order to prevent further disorders in reservoirs leading to souring and corrosion and the production which is going to be delivered to the markets. All these methods must be done quick and reliable due to the rapid changes that could occur during the analysis of sulfur species.

Acknowledgements or Notes

The authors declare that they have no known financial source or personal relationships that could have appeared to influence this information reported in this paper.

Scientific Ethics Declaration

The authors declare that the scientific ethical and legal responsibility of this article published in EPSTEM journal belongs to the authors.

References

- Al-Tamimi, W. H., & Mehdi, K. H. (2017). Inhibition of biogenic hydrogen sulfide produce by Sulfate Reducing Bacteria isolated from oil fields in Basra by nitrate based treatment. *Journal of Petroleum Research and Studies*, 7(3), 88-106.
- Anon (1988). *Breakthrough in oil recovery technique*.
- Barton, L. L., Fardeau, M. L., & Fauque, G. D. (2014). Hydrogen sulfide: a toxic gas produced by dissimilatory sulfate and sulfur reduction and consumed by microbial oxidation. *The Metal-Driven Biogeochemistry of Gaseous Compounds in the Environment*, 14,237-277.
- Basafa, M., & Hawboldt, K. (2019). Reservoir souring: sulfur chemistry in offshore oil and gas reservoir fluids. *Journal of Petroleum Exploration and Production Technology*, 9(2), 1105-1118.
- Berben, T., Overmars, L., Sorokin, D. Y., & Muyzer, G. (2017). Comparative genome analysis of three thiocyanate oxidizing Thioalkalivibrio species isolated from soda lakes. *Frontiers in Microbiology*, 8(105), 254.
- Chen, Q., Sherwen, T., Evans, M., & Alexander, B. (2018). DMS oxidation and sulfur aerosol formation in the marine troposphere: a focus on reactive halogen and multiphase chemistry. *Atmospheric Chemistry and Physics*, 18(18), 13617-13637.
- Donaldson, E. C., Chilingarian, G. V., & Yen, T. F. (Eds.). (1985). *Enhanced oil recovery, i: fundamentals and analyses*. Elsevier.
- Donaldson, E. C., Chilingarian, G. V., & Yen, T. F. (Eds.). (1989). *Enhanced oil recovery, ii: processes and operations*. Elsevier.
- Donaldson, E. C., Chilingarian, G. V., & Yen, T. F. (Eds.). (1989). *Microbial enhanced oil recovery*. Newnes.
- Correia, J., Rodrigues, L. R., Teixeira, J. A., & Gudiña, E. J. (2021). Application of biosurfactants for microbial enhanced oil recovery (MEOR). *Biosurfactants for a Sustainable Future: Production and Applications in the Environment and Biomedicine*, 99-118. <http://dx.doi.org/10.1002/9781119671022.ch5>
- Ituen, E. B., Solomon, M. M., Umoren, S. A., & Akaranta, O. (2019). Corrosion inhibition by amitriptyline and amitriptyline based formulations for steels in simulated pickling and acidizing media. *Journal of Petroleum Science and Engineering*, 174, 984-996.

- Gabetta, G., Pagliari, F., & Rezgui, N. (2018). Hydrogen embrittlement in pipelines transporting sour hydrocarbons. *Procedia Structural Integrity*, 13, 746-752.
- Gieg, L. M., Jack, T. R., & Foght, J. M. (2011). Biological souring and mitigation in oil reservoirs. *Applied microbiology and biotechnology*, 92(2), 263-282. doi: 10.1007/s00253-011-3542-6.
- Gilliland (1976). *Oil Recovery Techniques MEOR*.
- Goldstein, T., & Aizenshtat, Z. (1994). Thermochemical sulfate reduction a review. *Journal of Thermal Analysis and Calorimetry*, 42(1), 241-290.
- Guo, Hu & Li, Yiqiang & Yiran, Zhao & Wang, Fuyong & Wang, Yansheng & Yu, Zhaoyan & Haicheng, She & Yuanyuan, Gu & Chuyi, Jin & Xian, Gao. (2015). Progress of microbial enhanced oil recovery in China. In *SPE Asia Pacific Enhanced Oil Recovery Conference*. OnePetro. <http://dx.doi.org/10.2118/174697-MS>
- Zhou, H., & Davarpanah, A. (2020). Hybrid chemical enhanced oil recovery techniques: A simulation study. *Symmetry*, 12(7), 1086. <http://dx.doi.org/10.3390/sym12071086>
- Hamilton, M. A., & Hunter, J. E. (1985). Analyzing utterances as the observational unit. *Human Communication Research*, 12(2), 285-294.
- Hiorth, A., Kaster, K., Lohne, A., Siqueland, O. K., Berland, H., Giske, N. H., & Stavland, A. (2007, September). Microbial enhanced oil recovery-mechanism. In *Proceedings of the International Symposium of the Society of Core Analysts, Calgary, Canada*.
- Holubnyak, Y. I., Bremer, J. M., Mibeck, B. A., Hamling, J. A., Huffman, B. W., Klapperich, R. J., ... & Harju, J. A. (2011, April). Understanding the souring at Bakken oil reservoirs. In *SPE International Symposium on Oilfield Chemistry*. OnePetro.
- Hosseini noosheri P. (2016). Further model development and application of UTCHEM for microbial enhanced oil recovery and reservoir souring. http://dx.doi.org/10.1007/978-94-007-2214-9_31
- Hubert, C., & Voordouw, G. (2007). Oil field souring control by nitrate-reducing *Sulfurospirillum* spp. that outcompete sulfate-reducing bacteria for organic electron donors. *Applied and Environmental Microbiology*, 73(8), 2644-2652.
- Ibrahim, A. M. (2015). The corrosion effect of sulfur-reducing bacteria on reinforced high strength concrete: Civil. *Diyala Journal of Engineering Sciences*, 8(4), 144-156.
- de Jesus, E. B., & de Andrade Lima, L. R. P. (2016). Simulation of the inhibition of microbial sulfate reduction in a two-compartment upflow bioreactor subjected to molybdate injection. *Bioprocess and Biosystems Engineering*, 39(8), 1201-1211.
- Kögler, F., Hartmann, F. S., Schulze-Makuch, D., Herold, A., Alkan, H., & Dopffel, N. (2021). Inhibition of microbial souring with molybdate and its application under reservoir conditions. *International Biodeterioration & Biodegradation*, 157, 105158.
- Li, J., Liu, J., Trefry, M. G., Park, J., Liu, K., Haq, B., ... & Volk, H. (2011). Interactions of microbial-enhanced oil recovery processes. *Transport in Porous Media*, 87(1), 77-104. <http://dx.doi.org/10.1007/s11242-010-9669-6>
- Little, B. J., & Lee, J. S. (2007). *Microbiologically influenced corrosion* (Vol. 2). John Wiley & Sons.
- Kumar, N., Chaurand, P., Rose, J., Diels, L., & Bastiaens, L. (2015). Synergistic effects of sulfate reducing bacteria and zero valent iron on zinc removal and stability in aquifer sediment. *Chemical Engineering Journal*, 260, 83-89.
- Nerurkar, A. S., Suthar, H. G., & Desai, A. J. (2012). Biosystem development for microbial enhanced oil recovery (MEOR). In *Microorganisms in Sustainable Agriculture and Biotechnology* (pp. 711-737). Springer. 10.1007/978-94-007-2214-9_31.
- Nmegbu, C. G. J. & Pepple, D. D. (2014). Modeling a well stimulation process using the meor technique. *International Journal of Research in Engineering and Technology*, 3(3), 153-159. <http://dx.doi.org/10.15623/ijret.2014.0303028>
- Nmegbu, C. G. J. & Spiff, J. (2014). Chemical flocculation of microorganisms in the reservoir during MEOR. *Int. J. Eng. Adv. Tech*, 3(5), 46-49.
- Nmegbu, C. G. (2014). Application of steady state analysis to microbial enhanced oil recovery (MEOR) undergoing layers in series. *International Journal of Advancements in Research & Technology*, 3(5), 201-206
- Nmegbu, Godwin. (2014). Modeling the pressure distribution in a reservoir undergoing MEOR for a 2-dimensional flow system. *International Journal of Emerging Technology and Advanced Engineering*, 4(6), 402-411.
- Nourani, M., Panahi, H., Biria, D., Azad, R. R., Haghghi, M., & Mohebbi, A. (2007, December). Laboratory studies of MEOR in micromodel as a fractured system. In *IPTC 2007: International Petroleum Technology Conference* (pp. cp-147). European Association of Geoscientists & Engineers. <http://dx.doi.org/10.2118/110988-MS>

- Okoro, C. C., Samuel, O., & Lin, J. (2016). The effects of Tetrakis-hydroxymethyl phosphonium sulfate (THPS), nitrite and sodium chloride on methanogenesis and corrosion rates by methanogen populations of corroded pipelines. *Corrosion Science*, 112, 507-516.
- Okoro, C. C. (2014). The level of inhibition of microbial functional group activities by some oxidizing agents commonly used as Biocides in oil field operations. *Microbiology Research Journal International*, 4(10), 1069-1083.
- Okoro, C. C., & Amund, O. (2015). Souring and corrosion potentials of onshore and offshore oil-producing facilities in the Nigerian oil-rich Niger delta. *Petroleum Science and Technology*, 33(17-18), 1563-1570.
- Patel, J., Borgohain, S., Kumar, M., Rangarajan, V., Somasundaran, P., & Sen, R. (2015). Recent developments in microbial enhanced oil recovery. *Renewable and Sustainable Energy Reviews*, 52, 1539-1558. <http://dx.doi.org/10.1016/j.rser.2015.07.135>
- Quraishi, Marzuqa & Bhatia, Shashi & Pandit, Soumya & Gupta, Piyush & Rangarajan, Vivek & Lahiri, Dibyajit & Varjani, Sunita & Mehariya, Sanjeet & Yang, Yung-Hun. (2021). Exploiting microbes in the petroleum field: Analyzing the credibility of microbial enhanced oil recovery (MEOR). *Energies*, 14(15), 4684. <http://dx.doi.org/10.3390/en14154684>.
- Rabbani, A. (2010). *Hydrogen sulfide and sour reservoir of oil and gas* (1st ed). Nashr Jahat.
- Rashedi, H. (2014). *Microbial enhanced oil recovery* (1st ed.).
- Lin, R., Chen, K., Miao, M., Zhang, L., Wang, X., Jiang, Y., ... & Pan, H. (2020). Reaction mechanism of H₂S generation during tetrahydrothiophene aquathermolysis reaction. *Energy & Fuels*, 34(3), 2781-2789.
- Phetcharat, T., Dawkrajai, P., Chitov, T., Wongpornchai, P., Saenton, S., Mhuantong, W., ... & Bovonsombut, S. (2018). Effect of inorganic nutrients on bacterial community composition in oil-bearing sandstones from the subsurface strata of an onshore oil reservoir and its potential use in Microbial Enhanced Oil Recovery. *Plos one*, 13(11), e0198050. <http://dx.doi.org/10.1371/journal.pone.0198050>
- Sugai, Y.; Owaki, Y.; Sasaki, K. (2020). Simulation study on reservoir souring induced by injection of reservoir brine containing sulfate-reducing bacteria. *Sustainability*, 12, 4603.
- Sugai, Yuichi & Komatsu, Keita & Sasaki, Kyuro & Mogensen, Kristian & Bennetzen, Martin. (2015). Fundamental study on applicability of MEOR to North Sea Oil. *Journal of the Japanese Association for Petroleum Technology*. 80. 465-469. 10.3720/japt.80.465. <http://dx.doi.org/10.3720/japt.80.465>
- Tatar, A. (2018). Microbial enhanced oil recovery. *Fundamentals of Enhanced Oil and Gas Recovery from Conventional and Unconventional Reservoirs*, 291-508. <http://dx.doi.org/10.1016/B978-0-12-813027-8.00010-2>
- Udosoh, N. E., & Nwaoha, T. C. (2020). Demonstration of MEOR as an alternative enhanced oil recovery technique in Nigeria offshore oilfield. *Journal of Mechanical and Energy Engineering*, 4(3), 277-284. <http://dx.doi.org/10.30464/jmee.2020.4.3.277>
- Fan, W., Jirui, H., Zhiming, W., Yunfei, M. A., & Dongying, W. A. N. G. (2018). An enhanced oil recovery technique by targeted delivery ASP flooding. *Petroleum Exploration and Development*, 45(2), 321-327. [http://dx.doi.org/10.1016/S1876-3804\(18\)30035-1](http://dx.doi.org/10.1016/S1876-3804(18)30035-1)
- ZoBell, C. E. (1973). Bacterial degradation of mineral oils at low temperatures.
- ZoBell, C. E. (1973). Microbial degradation of oil: Present status, problems and perspectives. *The Microbial Degradation of Oil Pollutants*, 3-16.

Author Information

Ali HARATIAN

University of Technology (Tehran Polytechnic),
Tehran, Iran
Contact e-mail: ali3023@aut.ac.ir

Soroosh EMAMI MEYBODI

University of Technology (Tehran Polytechnic),
Tehran, Iran

To cite this article:

Haratian, A. & Emami Meybodi, S. (2021). Review on microbial enhanced oil recovery and controlling its produced hydrogen sulfide effects on reservoir and transporting pipelines. *The Eurasia Proceedings of Science, Technology, Engineering & Mathematics (EPSTEM)*, 15, 88-98.